



Large Refreezing Lead off Point Barrow (February 27, 2017)

2016-17 FREEZE-UP STUDY
OF THE
ALASKAN BEAUFORT AND CHUKCHI SEAS

Coastal Frontiers Corporation
882A Patriot Drive
Moorpark, CA 93021-3544
(818) 341-8133

Vaudrey & Associates, Inc.
1685 El Caserio Court
San Luis Obispo, CA 93401
(805) 544-9399

2016-17 FREEZE-UP STUDY OF THE ALASKAN BEAUFORT AND CHUKCHI SEAS

FINAL REPORT

Prepared for:

U.S. Department of the Interior, Bureau of Safety and Environmental Enforcement
Washington, D.C.

Prepared by:

Coastal Frontiers Corporation
Moorpark, California
Vaudrey & Associates, Inc.
San Luis Obispo, California

November 2017

*This study was funded by the Bureau of Safety and Environmental Enforcement (BSEE), U.S. Department of the Interior, Washington, D.C., under Contract Number **E16PC00016**.*

This report has been reviewed by the Bureau of Safety and Environmental Enforcement (BSEE), and approved for publication. Approval does not signify that the contents necessarily reflect the views and policies of the Bureau, nor does mention of trade names or commercial products constitute endorsement or recommendation for use.

EXECUTIVE SUMMARY

This report describes an investigation of the ice conditions that prevailed in the Alaskan Beaufort and Chukchi Seas during the 2016-17 freeze-up season. The study was performed for the U.S. Department of the Interior, Bureau of Safety and Environmental Enforcement (“BSEE”), by Coastal Frontiers Corporation and Vaudrey & Associates, Inc.

The 2016-17 study was the eighth in a series of annual freeze-up investigations that began in 2009-10. It was designed to address five specific objectives:

1. Describe the ice conditions that evolve during the freeze-up and early winter seasons, including the development of the landfast ice zone and early shear zone;
2. Locate and map features of potential importance for offshore exploration and production activities, including ice movement lines, substantial leads and polynyas (linear and areal openings in the sea ice, respectively), first-year ridges and rubble fields, and multi-year ice floes;
3. Locate, map, and characterize ice pile-ups on natural shorelines and man-made structures;
4. Correlate significant changes in the ice canopy with the corresponding meteorological conditions;
5. Using the data acquired during the past eight years, characterize present-day freeze-up processes and compare them with those in the 1980s.

The study was conducted using publicly-available data, proprietary data, and aerial reconnaissance missions. The acquisition of publicly-available meteorological data, ice charts, and satellite imagery began in September 2016, and continued through March 2017. These data were supplemented with 20 high-resolution RADARSAT-2 images purchased from MacDonald Dettwiler and Associates Ltd. for the period from mid-October 2016 through late February 2017.

Four aerial reconnaissance missions were conducted in late February and early March, 2017, to supplement the remotely-sensed data obtained from the sources outlined above. The flights, consisting of two in the Beaufort Sea and two in the Chukchi, were used to document the conditions that prevailed at the end of the freeze-up season.

The principal study findings are summarized below:

Entire Study Area

1. **Overview:** Freeze-up in 2016-17 was distinguished by exceptionally warm air temperatures, stunted ice growth, uncharacteristically high frequencies of westerly winds, and an absence of multi-year ice.
2. **Air Temperatures:** For the fourth consecutive year, the air temperatures during the 2016-17 winter season were exceptionally warm. Those recorded at Barrow Airport were the highest in the past 47 years by a wide margin, while those at Deadhorse Airport ranked a close second among those recorded in the past eight years.
3. **First-Year Ice Growth:** The computed thickness of undeformed first-year ice at the end of the 2016-17 winter season was 148 cm in the Alaskan Beaufort Sea and 134 cm in the Chukchi Sea, based on accumulations of 6,144 and 5,194 FDD at Deadhorse and Barrow Airports, respectively. The thickness in the Beaufort tied that in 2014-15 and 2015-16 as the lowest value in the past eight years, while that in the Chukchi was 9 cm less than the prior minimum of 143 cm in 2013-14. The highest values in recent years, 176 cm in the Beaufort and 167 cm in the Chukchi, occurred in 2011-12.

Beaufort Sea

1. **Late Summer:** The ice cover in the Alaskan Beaufort Sea diminished slowly in June, July, and early August, reflecting the prevalence of cloudy skies and reduced solar insolation. The pace quickened appreciably in late August and early September, creating a large expanse of open water off the coast. The minimum ice extent, which occurred on September 10th, tied that in 2007 as the second lowest on record since the acquisition of satellite-based data began in 1979.
2. **Timing of Freeze-Up:** Freeze-up began in mid-October with the formation of ice in the semi-protected waters adjacent to the coast. Complete ice coverage in the nearshore region occurred on November 7th, followed by complete coverage in the entire Alaskan Beaufort Sea on November 23rd. During the past eight years, the average date for the occurrence of nearshore freeze-up has been October 26th with a standard deviation of eight days. The average date for the occurrence of basin-wide freeze-up has been November 9th with a standard deviation of nine days.
3. **Duration of Freeze-Up:** The duration of freeze-up was 39 days, consisting of 23 days from first ice to nearshore freeze-up and an additional 16 days from nearshore freeze-up to complete freeze-up in the basin. During the past eight years, the duration has averaged 36 days with a standard deviation of 11 days.

4. **Wind Regime:** Based on the daily average wind directions recorded at Deadhorse Airport, easterlies prevailed 65% of the time in October. Westerlies predominated in the four months that followed, with frequencies ranging from 65% in December to 77% in January. Over the entire five-month study period (October through February), westerlies outnumbered easterlies by a ratio of 64% to 36%, representing the highest frequency of westerly winds in the past eight years. The highest monthly average wind speed, a modest 12 kt (6 m/s), occurred in both January and February.
5. **Storm Events:** Storm events with daily average wind speeds exceeding 15 kt (8 m/s) occurred on 13 occasions encompassing 31 days. Seven of the events were easterlies, while six were westerlies. The westerly storms tended to be of longer duration, averaging 3.2 days/event versus 1.7 days/event for the easterlies. The total number of storm-days tied that in 2009-2010 as the lowest in the past eight years.
6. **Landfast Ice:** Landfast ice began to develop during the last week in October, and expanded to cover all of the coastal lagoons and a significant portion of Harrison Bay over the course of November. The expansion stalled in December, with gains during the first half of the month erased by losses during the second. The next major advance occurred in late January, when easterly winds propelled the ice edge to the vicinity of the 11-m isobath. After another period of minimal change, the ice edge moved to the 18-m isobath in late February in response to a strong easterly storm. This advance marked the first occasion during the 2016-17 freeze-up season when the ice reached its customary anchor points on Weller Bank and Stamukhi Shoal.
7. **Ice Pile-Ups:** Thirty-eight ice pile-ups formed in the central portion of the Alaskan Beaufort Sea during the 2016-17 freeze-up season. One was located on the Oooguruk Offshore Drillsite (ODS), one on the Spy Island Drillsite (SID), one on Northstar Production Island, two on Thetis Island (a natural barrier island in Harrison Bay), and 33 on natural barrier islands and shoals to the east of Prudhoe Bay. The dimensions of the pile-ups tended to be unexceptional by historical standards, with heights of 1 to 8 m, encroachment distances of 0 to 12 m, and block thicknesses of 20 to 40 cm. Several of the features extended alongshore for substantial distances, however, including a maximum length of 5.9 km on a spit that emanates from Point Brownlow.
8. **Multi-Year Ice:** With the exception of two small patches of second-year ice that drifted away from Point Barrow in October, multi-year ice remained absent from the nearshore region of the Alaskan Beaufort Sea throughout the five-month study period. The minimum separation between the ice and the coast, 170 nm (315 km), occurred off Barter Island at the end of February.

Chukchi Sea

- 1. Timing of Freeze-Up:** Ice began to form in Kasegaluk Lagoon, the Kuk River Inlet, and Peard Bay during the third week in October, but freeze-up proceeded slowly in the weeks that followed due to air temperatures that hovered near freezing. Complete coverage of these semi-enclosed basins and initial ice formation in the nearshore region occurred in early November. The pack ice, after advancing rapidly to the south during the first week in November, reached the vicinity of Point Barrow during the second week and began to coalesce with the nascent strip of coastal ice. On or about December 7th, a flash-freeze created an isolated patch of ice centered approximately 150 nm (278 km) west of Icy Cape. Freeze-up in the nearshore region took place three days later, on December 10th, in response to a cold spell that brought five days of air temperatures below -10°F (-23°C). Freeze-up in the entire Chukchi Sea north of Cape Lisburne followed on December 27th. During the past eight years, the average date for the occurrence of nearshore freeze-up has been November 23rd with a standard deviation of 12 days. The average date for the occurrence of basin-wide freeze-up has been December 9th with a standard deviation of ten days.
- 2. Duration of Freeze-Up:** The duration of freeze-up was 73 days, consisting of 56 days from first ice to nearshore freeze-up and an additional 17 days from nearshore freeze-up to complete freeze-up in the basin. During the past eight years, the duration has averaged 62 days with a standard deviation of nine days.
- 3. Wind Regime:** Easterly winds predominated in October, November, and December, with frequencies ranging from 58% to 77%. This pattern changed in January and February, when westerlies prevailed by narrow margins. Over the entire five-month period, easterlies outpaced westerlies by a margin of 61% to 39%. The highest average monthly speed, 12 kt (6 m/s), occurred in October and January.
- 4. Storm Events:** Fourteen storm events took place from October through February, consisting of eight easterlies and six westerlies. The easterlies produced 18 storm-days, for an average duration of 2.3 days/event. The westerlies produced 19 storm-days, averaging 3.2 days/event.
- 5. Landfast Ice:** The landfast ice zone reflected the influence of the wind regime, with stunted growth in November and December followed by substantial growth in January and early February. Landfast ice first appeared at the end of October, but remained narrow and discontinuous for the next two months in response to the predominance of easterly winds. The situation changed in January, when an increased frequency of westerly winds coupled with several westerly storms produced a continuous band of ice up to 10 nm (19 km) wide off Skull Cliff and 8 nm (15 km) wide between Icy Cape and Point Lay. During the second half of January, the ice grounded on Blossom Shoals, its

customary anchor point off Icy Cape. Additional expansion followed in early February, resulting in the maximum width observed during the study period, 20 nm (37 km) between Wainwright and the Nokotlek River mouth. Subsequently, at the end of February, a strong easterly storm dislodged the newly-accumulated ice and caused the landfast ice edge to retreat to the location it had occupied at the beginning of the month.

6. **Coastal Flaw Lead:** From December 2016 through February 2017, the distinctive flaw lead that forms off the Chukchi Sea coast in response to easterly winds opened on nine different occasions. The frequency of occurrence, which averaged 51% over the three-month period, increased from 42% in December to 52% in January and 61% in February. The maximum width, 50 nm (93 km), and maximum length, 250 nm (463 km), both occurred during a single event that began in late January and continued into early February. The lead persisted for periods that ranged from one to 15 days.
7. **Offshore Ice Cover:** When a reconnaissance flight was performed at the end of February, the ice on the west side of the flaw lead was found to be relatively uniform, consisting of first-year floes typically ranging from less than 500 m to 1 km in diameter. Deformation was modest relative to that noted in prior years, with ridge and rubble heights typically varying from 1 to 2 m and occasionally reaching 3 m.
8. **Ice Pile-Ups:** Sixty-three ice pile-ups occurred on the shoreline between Barrow and Point Lay during the 2016-17 freeze-up season. Fifty-two were located to the south of Point Belcher, while 11 were located to the north. Their dimensions were relatively small compared to those observed in past years, with heights of 1 to 5 m, encroachment distances of 0 to 10 m, and alongshore lengths of 50 m to 4 km. The block thicknesses were estimated to vary from 30 to 40 cm.
9. **Multi-Year Ice:** With the exception of the two small patches of second-year ice that drifted away from Point Barrow in October (discussed above for the Beaufort Sea), multi-year ice remained completely absent from the Chukchi Sea study area during the five-month study period.

Trends

1. **Air Temperatures:** Since the 1970s, progressively warmer winter seasons have caused the number of accumulated freezing-degree days at Barrow to decline at an average rate of 49 per year. The rate of warming has accelerated, with the greatest increase in temperature occurring during the early portion of freeze-up.
2. **Winds:** Since the early 1980s, the frequency of storm events during freeze-up has increased by about 50%. The frequency of mid-winter storms (January through April) also has increased, but only by about 13%.

3. **Timing of Freeze-Up:** Freeze-up in the nearshore region currently tends to occur during the fourth week in October in the Alaskan Beaufort Sea, and the fourth week in November in the northeastern Chukchi Sea. The former is about three weeks later than in the 1980s, while the latter is more than one month later than in the 1970s. The rate of change has accelerated in recent years, with the date of freeze-up currently trending later by 2.3 days/yr in the Beaufort and 4.3 days/year in the Chukchi. These high rates of change imply that the length of the open-water season will increase substantially in the years ahead.
4. **Duration of Freeze-Up:** The duration of freeze-up in the Alaskan Beaufort Sea, from first ice to complete cover, currently averages 36 days with a standard deviation of 11 days. In the Chukchi, the duration is substantially longer, averaging 62 days with a standard deviation of ten days. The duration in the Beaufort is increasing at a rate of 1.3 days/yr, while that in the Chukchi is increasing at 2.3 days/yr.
5. **First-Year Ice Growth:** Based on air temperature alone, the thickness of undeformed first-year ice attained during an average winter has decreased by 21 cm (12.3%) since the early 1980s. However, a significant increase in snowfall may be causing an even greater reduction in the ice thickness due to its insulating effect. Other temperature-related factors, including reduced ice production in leads, decreased consolidation of ridges and rubble fields, and reduced ice strength, serve to amplify the impact of reduced thickness on ice dynamics.
6. **Landfast Ice Development and Stability:** In the Alaskan Beaufort Sea, the extent of the landfast ice zone to the west of Prudhoe Bay is similar to that observed in the 1980s but the landfast ice develops more slowly. To the east of Prudhoe Bay, a stable, well-grounded shear zone is less likely to develop during freeze-up and early winter, and develops more slowly in those years when it does occur. In the Chukchi, the narrow, ephemeral nature of the landfast ice zone noted in the 1980s continues to prevail today.
7. **Coastal Flaw Lead:** Notwithstanding trends toward warmer air temperatures, increased storminess, and slower ice growth during freeze-up, the frequencies with which the flaw lead and extended flaw lead occur off the Chukchi Sea coast have remained unchanged since the 1990s.
8. **Multi-Year Ice in the Alaskan Beaufort Sea:** The probability of large multi-year ice floes invading the nearshore portion of the Alaskan Beaufort Sea is substantially less than in the 1980s. This change has resulted in part from a reduction in the amount of multi-year ice comprising the permanent polar pack and in part from an increase in the northerly retreat of the ice edge during the summer months, both of which have reduced the opportunities for pack floes to enter the nearshore area. In addition, warmer air temperatures, longer open-water seasons, and increased storminess have decreased the

likelihood that first-year ridges and rubble will survive the summer melt season to become second-year floes of any consequence. Nevertheless, as demonstrated in 2009-10, the possibility of multi-year ice invasions cannot be ruled out in the nearshore region of the Beaufort. The probability of an invasion currently is about 12% in any given freeze-up season, based on two such occurrences in the past 17 years.

9. ***Multi-Year Ice in the Chukchi Sea:*** The probability of multi-year ice entering the Chukchi Sea to the south and west of Point Barrow also has decreased since the 1980s, but to a lesser extent than in the Beaufort. Although the factors that have reduced the probability of invasions in the Beaufort apply to the Chukchi as well, their impact has been mitigated by the ability of the Multi-Year Gateway and Early-Season Entry to divert multi-year ice floes to the southwest. The probability of an invasion currently is about 65% in any given freeze-up season, based on 11 invasions in the past 17 years.

TABLE OF CONTENTS

EXECUTIVE SUMMARY i

TABLE OF CONTENTS viii

LIST OF TABLES x

LIST OF FIGURES xii

LIST OF PLATES xvii

1. INTRODUCTION 1

2. PRIOR STUDIES 9

 2.1. 1980s Freeze-Up Studies 9

 2.2. 2009-10 Freeze-Up Study 11

 2.3. 2010-11 Freeze-Up Study 13

 2.4. 2011-12 Freeze-Up Study 14

 2.5. 2012-13 Freeze-Up Study 16

 2.6. 2013-14 Freeze-Up Study 18

 2.7. 2014-15 Freeze-Up Study 20

 2.8. 2015-16 Freeze-Up Study 21

3. DATA ACQUISITION AND ANALYSIS 24

 3.1. Meteorological Data 24

 3.2. Ice Charts 26

 3.3. Satellite Imagery 29

 3.4. Drift Buoys 33

 3.5. Aerial Reconnaissance Missions 34

4. BEAUFORT SEA FREEZE-UP 41

 4.1. Overview 41

 4.2. Late Summer 2016 48

 4.3. Early Freeze-Up 51

 4.3.1. October 2016 51

 4.3.2. November 2016 54

 4.4. Late Freeze-Up 64

 4.4.1. December 2016 64

 4.4.2. January 2017 70

 4.4.3. February 2017 75

 4.5. Reconnaissance Flights 77

 4.5.1. Lagoon Ice 81

 4.5.2. Landfast Ice and Shear Zone 83

 4.5.3. Offshore Ice 85

 4.5.4. Leads 85

 4.5.5. Ice Pile-Ups 87

 4.5.6. Multi-Year Ice 87

 4.5.7. Ice Conditions in Camden Bay Prospects 89

 4.5.8. Ice Conditions in Harrison Bay Prospects 89

TABLE OF CONTENTS

(continued)

5.	CHUKCHI SEA FREEZE-UP	94
	5.1 Overview	94
	5.2 Early Freeze-Up	103
	5.2.1 October 2016	103
	5.2.2 November 2016	108
	5.3 Late Freeze-Up	111
	5.3.1 December 2016	111
	5.3.2 January 2017	119
	5.3.3 February 2017	125
	5.4 Reconnaissance Flights	131
	5.4.1 Lagoon Ice	132
	5.4.2 Landfast Ice	132
	5.4.3 Leads	134
	5.4.4 Offshore Ice	134
	5.4.5 Ice Pile-Ups	136
	5.4.6 Multi-Year Ice	136
	5.4.7 Ice Conditions in Chukchi Sea Prospects	136
	5.4.8 Katie’s Floeberg	138
6.	TRENDS	141
	6.1 Air Temperatures	141
	6.2 Winds	145
	6.3 Timing of Freeze-Up	151
	6.4 Duration of Freeze-Up	154
	6.5 First-Year Ice Growth	157
	6.6 Landfast Ice	160
	6.7 Coastal Flaw Lead	162
	6.8 Multi-Year Ice	163
7.	SUMMARY AND CONCLUSIONS	168
	7.1 Milestones	168
	7.2 Detailed Findings	169
8.	REFERENCES	175
	APPENDIX A DRAWINGS (Bound Separately)	
	APPENDIX B DIGITAL DATA (DVD)	

LIST OF TABLES

<u>Title</u>	<u>Page No.</u>
Table 1. Accumulated Freezing-Degree Days (<29°F) at Barrow and Deadhorse Airports in 2016-17	25
Table 2. IABP Drift Buoy Characteristics	34
Table 3. Abbreviations for Ice Features	37
Table 4. Beaufort Sea Wind Characteristics, October 2016 – February 2017	41
Table 5. Beaufort Sea Storm Characteristics, October 2015 – February 2017	42
Table 6. Beaufort Sea Computed Ice Thickness, September 2016 – May 2017	44
Table 7. Ice Pile-Ups on Beaufort Sea Coast during 2016-17 Freeze-Up Season	45
Table 8. Beaufort Sea Ice Drift, November 2016 – February 2017	47
Table 9. Minimum Arctic Sea Ice Extent, 2007-2016	50
Table 10. Significance of Color Bands in Plots of Meteorological Conditions	52
Table 11. Chukchi Sea Wind Characteristics, October 2016 – February 2017	95
Table 12. Chukchi Sea Storm Characteristics, October 2016 – February 2017	96
Table 13. Chukchi Sea Computed Ice Thickness, October 2016 – May 2017	97
Table 14. Ice Pile-Ups on Chukchi Sea Coast during 2016-17 Freeze-Up Season	98
Table 15. Chukchi Sea Ice Drift, November 2016 – February 2017	103
Table 16. Ice Cover in Chukchi Sea Prospects during Freeze-Up	115
Table 17. Accumulated Freezing-Degree Days (<29°F) at Barrow, 1970-71 through 2016-17	142
Table 18. Beaufort Sea Wind Directions, 2009-10 through 2016-17	146

LIST OF TABLES

(continued)

<u>Title</u>	<u>Page No.</u>
Table 19. Chukchi Sea Wind Directions, 2009-10 through 2016-17.....	146
Table 20. Beaufort Sea Storms, 2009-10 through 2016-17	148
Table 21. Chukchi Sea Storms, 2009-10 through 2016-17.....	148
Table 22. Timing of Freeze-Up in Alaskan Beaufort Sea, 2009 through 2016	152
Table 23. Timing of Freeze-Up in Chukchi Sea, 2009 through 2016.....	153
Table 24. Duration of Freeze-Up in Alaskan Beaufort Sea, 2009 through 2016....	155
Table 25. Duration of Freeze-Up in Chukchi Sea, 2009 through 2016	156
Table 26. Computed Ice Thickness at Barrow, 1970-71 through 2016-17.....	158

LIST OF FIGURES

<u>Title</u>	<u>Page No.</u>
Figure 1. Study Area.....	2
Figure 2. Geographic Points of Interest in Central Beaufort Sea	6
Figure 3. Geographic Points of Interest in Western Beaufort Sea.....	7
Figure 4. Geographic Points of Interest in Chukchi Sea	8
Figure 5. Meteorological Data Recorded at Deadhorse Airport in February 2017 ..	25
Figure 6. CIS Ice Stage of Development Chart of Beaufort Sea for November 28, 2016.....	27
Figure 7. NIC Ice Chart of Beaufort Sea for November 8, 2016	28
Figure 8. NIC Arctic Marginal Ice Zone Chart for November 24, 2016.....	29
Figure 9. CIS RADARSAT-2 Mosaic December 9-12, 2016	30
Figure 10. RADARSAT-2 Image of Chukchi Sea Acquired on January 31, 2017	31
Figure 11. AVHRR Image of Beaufort and Chukchi Seas Acquired on January 16, 2017	32
Figure 12. MODIS Image Acquired on October 25, 2016	33
Figure 13. On-Ice Drift Buoy Tracks during 2016-17 Freeze-Up Season	35
Figure 14. Beaufort Sea Drift Buoy Tracks, November 2016 – February 2017	48
Figure 15. Large Expanse of Open Water off Alaskan Beaufort Sea Coast on September 10, 2016.....	49
Figure 16. Sea Ice Minimum Extent on September 10, 2016.....	50
Figure 17. Average Sea Ice Extent in September, 1979-2016.....	51
Figure 18. Meteorological Conditions at Deadhorse Airport in October 2016.....	52
Figure 19. CIS RADARSAT-2 Mosaic of Beaufort Sea for October 31, 2016	53

LIST OF FIGURES

(continued)

<u>Title</u>	<u>Page No.</u>
Figure 20. Beaufort Sea Landfast Ice Edge in October 2016.....	55
Figure 21. CIS Stage-of-Development Ice Chart of Beaufort Sea for October 3, 2016.....	56
Figure 22. Meteorological Conditions at Deadhorse Airport in November 2016	57
Figure 23. CIS Stage-of-Development Ice Chart of Beaufort Sea for November 7, 2016.....	58
Figure 24. RADARSAT-2 Image of Beaufort Sea Acquired on November 15, 2016.....	59
Figure 25. Beaufort Sea Landfast Ice Edge in November 2016.....	60
Figure 26. Beaufort Sea Drift Buoy Tracks in November 2016.....	62
Figure 27. Beaufort Sea Drift Buoy Daily Average Speeds in November 2016.....	63
Figure 28. Meteorological Conditions at Deadhorse Airport in December 2016	64
Figure 29. Beaufort Sea Landfast Ice Edge in December 2016	66
Figure 30. RADARSAT-2 Image of Beaufort Sea Acquired on January 2, 2017	67
Figure 31. Beaufort Sea Drift Buoy Tracks in December 2016	68
Figure 32. Beaufort Sea Drift Buoy Daily Average Speeds in December 2016	69
Figure 33. Meteorological Conditions at Deadhorse Airport in January 2017	71
Figure 34. Beaufort Sea Landfast Ice Edge in January 2017	72
Figure 35. RADARSAT-2 Image of Beaufort Sea Acquired on February 2, 2017 ...	73
Figure 36. Beaufort Sea Drift Buoy Track in January 2017.....	74
Figure 37. Beaufort Sea Drift Buoy Daily Average Speed in January 2017.....	75
Figure 38. Meteorological Conditions at Deadhorse Airport in February 2017	76

LIST OF FIGURES

(continued)

<u>Title</u>	<u>Page No.</u>
Figure 39. Beaufort Sea Landfast Ice Edge in February 2017	78
Figure 40. RADARSAT-2 Image of Beaufort Sea Acquired on February 26, 2017 .	79
Figure 41. Beaufort Sea Drift Buoy Track in February 2017.....	80
Figure 42. Beaufort Sea Drift Buoy Daily Average Speed in February 2017.....	81
Figure 43. Frequency of Occurrence of Chukchi Sea Flaw Lead, December 2016 – February 2017	101
Figure 44. Chukchi Sea Drift Buoy Tracks, December 2016 – February 2017	102
Figure 45. Meteorological Conditions at Barrow Airport in October 2016.....	103
Figure 46. MODIS Image Acquired on October 28, 2016	104
Figure 47. RADARSAT-2 Image of Chukchi Sea Acquired on October 31, 2016 .	105
Figure 48. NIC Ice Chart for November 1, 2016	105
Figure 49. Chukchi Sea Landfast Ice Edge in October 2016	107
Figure 50. Meteorological Conditions at Barrow Airport in November 2016.....	108
Figure 51. NIC Ice Chart for November 8, 2016	109
Figure 52. RADARSAT-2 Image of Chukchi Sea Acquired on November 17, 2016.....	110
Figure 53. Chukchi Sea Landfast Ice in November 2016.....	112
Figure 54. Meteorological Conditions at Barrow Airport in December 2016.....	113
Figure 55. RADARSAT-2 Image of Chukchi Sea Acquired on December 7, 2016	114
Figure 56. Chukchi Sea Landfast Ice Edge in December 2016.....	117
Figure 57. Chukchi Sea Drift Buoy Track in December 2016.....	118

LIST OF FIGURES

(continued)

<u>Title</u>	<u>Page No.</u>
Figure 58. Chukchi Sea Drift Buoy Daily Average Speed in December 2016	119
Figure 59. Meteorological Conditions at Barrow Airport in January 2017.....	120
Figure 60. Chukchi Sea Landfast Ice Edge in January 2017.....	121
Figure 61. AVHRR Image of Chukchi Sea Acquired on January 3, 2017.....	122
Figure 62. RADARSAT-2 Image of Chukchi Sea Acquired on January 31, 2017..	123
Figure 63. Chukchi Sea Drift Buoy Track in January 2017	124
Figure 64. Chukchi Sea Drift Buoy Daily Average Speed in January 2017	125
Figure 65. Meteorological Conditions at Barrow Airport in February 2017	126
Figure 66. Chukchi Sea Landfast Ice in February 2017.....	127
Figure 67. RADARSAT-2 Image of Chukchi Sea Acquired on February 28, 2017	128
Figure 68. AVHRR Image of Chukchi Sea Acquired on February 28, 2017.....	129
Figure 69. Chukchi Sea Drift Buoy Track in February 2017	130
Figure 70. Chukchi Sea Drift Buoy Daily Average Speed in February 2017	131
Figure 71. MODIS Image of Chukchi Sea Acquired on March 14, 2017.....	140
Figure 72. Accumulated Freezing Degree Days (<29°F) at Barrow, 1970-71 through 2016-17.....	144
Figure 73. Differences between Recent Monthly Air Temperatures and Long-Term Average Values at Barrow.....	144
Figure 74. Frequency of Occurrence of Easterly Winds at Deadhorse and Barrow Airports	147
Figure 75. Storms per Winter at Barrow Airport, 2010-2017	150

LIST OF FIGURES

(continued)

<u>Title</u>	<u>Page No.</u>
Figure 76. Yearly Storm Count at Barrow during Open-Water and Freeze-Up Seasons, 1950-2004.....	150
Figure 77. Feedback Loop Leading to Delay in Onset of Freeze-Up.....	151
Figure 78. Timing of Freeze-Up in Alaskan Beaufort and Chukchi Seas, 2009-2016	154
Figure 79. Duration of Freeze-Up in Alaskan Beaufort and Chukchi Seas, 2009-2016	156
Figure 80. Computed Ice Thickness: Recent Winters vs. 1970s and 1980s.....	159
Figure 81. Annual Snowfall at Barrow during Freeze-Up (October – February), 1970-71 through 2016-17.....	160
Figure 82. AVHRR Image Acquired on March 12, 2001, Illustrating Multi-Year Gateway	165
Figure 83. RADARSAT-2 Image Acquired on November 16, 2015, Illustrating Early-Season Entry	166

LIST OF PLATES

<u>Title</u>	<u>Page No.</u>
Plate 1. Aero Commander 690 at Barrow Airport	36
Plate 2. Undeformed Ice in Stefansson Sound and 4-m Pile-Up on West End of Narwhal Island	82
Plate 3. Thermal Crack Extending South from Dinkum Sands into Stefansson Sound, along with 8-m Pile-Up	83
Plate 4. Shear Line with Low Shear Wall at Landfast Ice Edge 3.5 nm off Narwhal Island	84
Plate 5. 6-m Rubble in Shear Zone 2 nm off Narwhal Island	84
Plate 6. Newly-Grounded Rubble with Heights to 8 m on Stamukhi Shoal	85
Plate 7. 6-m Grounded Ridge Backed by Extensive Rubble Field on Weller Bank	86
Plate 8. Shear Line at Landfast Ice Edge 20 nm off Admiralty Bay	86
Plate 9. Flat First-Year Floes and Intermittent Ridges and Rubble with Heights to 2 m off Camden Bay	87
Plate 10. Multiple Small Leads off Harrison Bay	88
Plate 11. Large Refreezing Lead off Camden Bay	88
Plate 12. 5-m High Pile-Up that Encroached 12 m onto North Shore of Duchess Island	89
Plate 13. Flat First-Year Floes, Scattered 1-m Rubble, and Refreezing Lead in Central Portion of Camden Bay Prospects	90
Plate 14. Flat First-Year Floes with Scattered Rubble to 3 m in Southern Portion of Camden Bay Prospects	90
Plate 15. Intermittent Shear Line with 2-m Rubble at Landfast Ice Edge 2 nm off Mary Sachs Entrance	91

LIST OF PLATES

(continued)

<u>Title</u>	<u>Page No.</u>
Plate 16. First-Year Floes with Widely-Scattered 1-m Rubble near Southern Boundary of Harrison Bay Prospects.....	92
Plate 17. First-Year Floes with 2-m Rubble in Northern Portion of Harrison Bay Prospects.....	92
Plate 18. Well-Defined Shear Line with 4-m Shear Wall at Landfast Ice Edge in Southern Portion of Harrison Bay Prospects.....	93
Plate 19. Flat Ice in Kasegaluk Lagoon and 3-m Pile-Up that Encroached 10 m onto Barrier Island 14 nm East of Icy Cape.....	132
Plate 20. Narrow Strip of Landfast Ice and Flaw Lead off Barrow.....	133
Plate 21. Large Expanse of Landfast Ice Grounded on Blossom Shoals.....	133
Plate 22. Mixture of Young and First-Year Ice on Western Side of Flaw Lead 20 nm off Point Franklin.....	134
Plate 23. First-Year Ice with Ridges and Rubble to 2 m and Refreezing Leads in Central Portion of Burger Prospects.....	135
Plate 24. Large Refreezing Lead 60 nm Northwest of Point Barrow.....	135
Plate 25. 3-m Pile-Up that Encroached 5 m onto Barrier Island 15 nm Southwest of Kuk River Inlet.....	136
Plate 26. First-Year Ice with Ridges and Rubble to 2 m and Refreezing Lead in Central Portion of Hanna Shoal Prospects.....	137
Plate 27. Compact Ice Canopy with Ridges and Rubble to 2 m Located 10 nm East of Devil's Paw Prospects.....	137
Plate 28. Katie's Floeberg in 2016.....	139
Plate 29. First-Year Ice with Ridges and Rubble to 3 m and Refreezing Lead over Hanna Shoal.....	139

2016-17 FREEZE-UP STUDY OF THE ALASKAN BEAUFORT AND CHUKCHI SEAS

1. INTRODUCTION

This report describes an investigation of the ice conditions that prevailed in the Alaskan Beaufort and Chukchi Seas during the 2016-17 freeze-up season. The study was performed on behalf of the U.S. Department of the Interior, Bureau of Safety and Environmental Enforcement (“BSEE”), by Coastal Frontiers Corporation and Vaudrey & Associates, Inc.

As shown in Figure 1, the study area includes the southern portion of the Beaufort Sea from Barter Island on the east to Point Barrow on the west, and the northeastern portion of the Chukchi Sea bounded by the shoreline between Point Barrow and Point Lay, the 74°N parallel, and the 168°W meridian. The boundaries in the Beaufort Sea were selected to encompass all existing oil and gas developments, while those in the Chukchi were selected to encompass Hanna Shoal and lease tracts of recent interest, including the Burger and Crackerjack prospects.

Despite their proximity, the ice regimes in the Beaufort and Chukchi Seas differ markedly due to factors that include geography, meteorology, and oceanography. Whereas the Beaufort Sea coast is oriented east southeast-west northwest, the Chukchi coast trends northeast-southwest (Figure 1). As a result, the easterly winds that occur frequently in both basins tend to push the ice along the Beaufort Sea coast but away from the Chukchi coast. In the Beaufort, the alongshore winds coupled with flat nearshore slopes produce an extensive zone of grounded, landfast ice bordered by a compact, well-consolidated ice canopy farther offshore. In the Chukchi, the growth of landfast ice is limited not only by the prevalence of offshore winds but also by the relatively steep slopes that prevail off the coast. As a result, the landfast ice zone typically consists of a narrow strip of grounded ice that clings to the shoreline. A flaw lead frequently opens offshore of the landfast ice, and the ice canopy tends to be less consolidated and more mobile than in the Beaufort.

The pronounced difference in ice regimes that exists during the freeze-up and winter seasons also prevails during break-up and summer. Whereas the Beaufort Gyre transports pack ice from east to west in the Beaufort Sea, the Alaska Coastal Current carries warm water north from the Bering Sea and contributes to the retreat of the pack ice in the Chukchi (Figure 1).

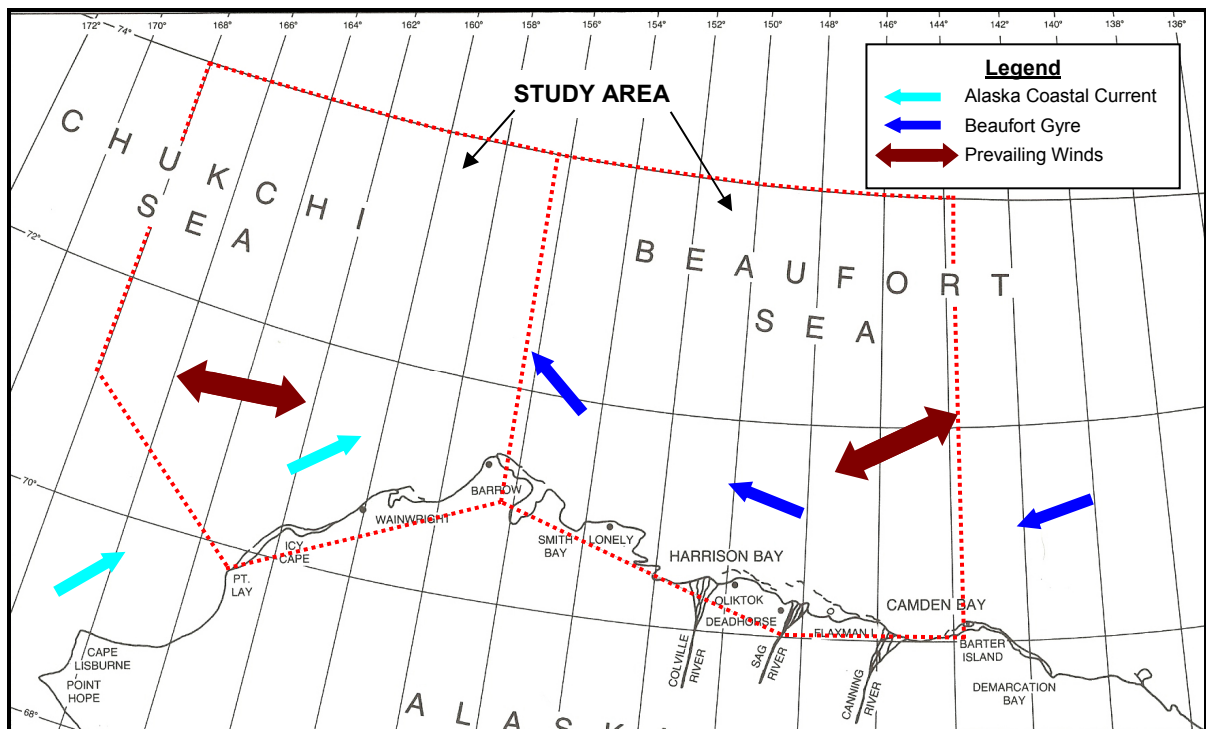


Figure 1. Study Area

During freeze-up, the ice cover in the study area consists primarily of thin, flexible sheets of newly-formed ice. It also may contain thicker, stronger multi-year floes that have moved into the region after surviving one or more summer melt seasons. Frequent storms tend to disturb the first-year ice before it attains sufficient thickness to resist displacement, allowing the multi-year floes to travel great distances and attain relatively high speeds in the absence of significant confinement by the first-year canopy. Potential concerns for oil and gas facilities include impact loads on fixed structures such as man-made islands and platforms, displacement of floating structures such as drillships, and ice gouging on the routes of subsea pipelines.

In addition to ice movements, the storms during freeze-up and early winter can produce significant pile-up events when the ice encounters fixed objects such as natural shorelines, shoals, and man-made islands. The storms also can cause substantial deformation of the first-year ice, leading to the formation of ridges and rubble fields.

The foregoing phenomena, along with the impairment of vessel navigation and, in the case of the Beaufort, the use of the ice sheet as a platform for transportation and construction, imply that an understanding of freeze-up is essential for the safe design and operation of offshore oil and gas facilities. To this end, six freeze-up studies were conducted as joint-industry projects from 1980-81 through 1985-86 (Vaudrey, 1981a;

1982a; 1983; 1984; 1985a; 1986). Each was largely observational in nature, and included aerial surveys undertaken at intervals of two to three weeks from early October until early December. In some instances, an additional aerial survey was conducted at the end of January to record late freeze-up ice movements. The primary objectives of these annual studies were twofold: (1) observe and record major ice movement events and their effects on man-made structures, and (2) document the size and distribution of multi-year ice floes, the locations of major first-year ridges and rubble fields, and the zonation of the nearshore ice.

Between 1986 and 2008, freeze-up processes in the Alaskan Beaufort and Chukchi Seas were investigated primarily through analyses of satellite imagery (Vaudrey, 1988a, 1989a, 1990, 1991, 1992; Eicken, *et al.*, 2006). The resulting information, although useful in its own right, lacked some of the detail provided by the earlier observational studies. Specifically, items such as the character of multi-year ice floes and the locations and characteristics of ice pile-ups could not be extracted from the satellite data. To remedy this shortcoming, a new series of freeze-up studies that combined remote sensing with on-site observations was initiated 2009-10. The studies have been conducted on an annual basis since that time. Each included an analysis of meteorological data, ice charts, and satellite imagery in concert with a series of aerial reconnaissance missions to document the conditions at the end of freeze-up (Coastal Frontiers and Vaudrey, 2010; 2011; 2012a; 2013; 2014; 2015; 2016). Four of the studies (2011-12, 2012-13, 2014-15, and 2015-16) also included reconnaissance flights in late November or early December to document the conditions that prevailed in the middle of the freeze-up period.

To expand the newly-acquired database on the nature and interannual variability of present-day freeze-up processes, a similar investigation was undertaken in 2016-17. As in each of the past freeze-up studies, the scope of work was designed to address five specific objectives:

1. Describe the ice conditions that evolve during the freeze-up and early winter seasons, including the development of the landfast ice zone and early shear zone;
2. Locate and map features of potential importance for offshore exploration and production activities, including ice movement lines, substantial leads and polynyas (linear and areal openings in the sea ice, respectively), first-year ridges and rubble fields, and multi-year ice floes;
3. Locate, map, and characterize ice pile-ups on natural shorelines and man-made structures;
4. Correlate significant changes in the ice canopy with the corresponding meteorological conditions;

5. Using the data acquired during the past eight years, characterize present-day freeze-up processes and compare them with those in the 1980s.

Although the methods were virtually identical to those used in the prior seven freeze-up studies, the scope of work was reduced in the interest of reserving funds for an investigation of break-up to follow in spring 2017. The following specific changes were made:

- The study period was reduced from six months (October through March) to five (October through February);
- The fixed-wing reconnaissance flights conducted in late November/early December were eliminated;
- The helicopter reconnaissance flight conducted in the central Beaufort Sea in February was eliminated.

If sufficient funding had been available, the scope of work for the prior freeze-up studies would have been retained without modification in 2016-17. The foregoing changes were judged to represent a reasonable trade-off for a much-needed study of break-up, however, in that they did not compromise the ability of the freeze-up study to address the five objectives outlined above.

The acquisition of publicly-available meteorological data, ice charts, and satellite imagery for the freeze-up study began in September 2016 and continued through February 2017. These data were supplemented with 20 high-resolution RADARSAT-2 images obtained from mid-October 2016 through the end of February 2017.

Aerial reconnaissance missions were conducted in late February and early March 2017 to document the ice conditions at the end of the freeze-up season (when processes such as nearshore rubble formation and ice encroachment onto the shoreline typically have slowed or ceased). The missions consisted of two fixed-wing flights in the Beaufort followed by two fixed-wing flights in the Chukchi.

The remainder of this report presents a detailed account of the 2016-17 Freeze-Up Study. To provide historical context, the findings of the thirteen prior studies (1980-81 through 1985-86 and 2009-10 through 2015-16) are summarized in Section 2. Data acquisition and analysis are discussed in Section 3, which covers the aerial reconnaissance missions as well as the data obtained from all other sources. Section 4 describes the progression of freeze-up in the Alaskan Beaufort Sea in 2016-17, while Section 5 provides analogous information for the Chukchi. In Section 6, trends in freeze-up are identified by

characterizing present-day processes and comparing them with those in the 1980s. Conclusions are presented in Section 7, followed by references in Section 8. Figures, tables, and plates are interspersed with the text, while three large-format drawings that display the observations made during the reconnaissance flights are provided in Appendix A. The digital data files that were used in conducting the study are compiled in Appendix B. The 2017 Break-Up Study, although performed under the same contract as the 2016-17 Freeze-Up Study, will be presented in a separate report.

The horizontal datum for all geographic coordinates provided in this report is the North American Datum of 1983 (NAD 83). Many of the graphical products also include a grid referenced to the Universal Transverse Mercator (UTM) Datum, NAD 83, with units of meters. UTM Zone 6N is used in the central Beaufort Sea, UTM Zone 5N in the western Beaufort Sea, and UTM Zone 4N in the Chukchi Sea.

The vertical datum is Mean Sea Level (MSL). MSL lies only 9 cm above Mean Lower Low Water (MLLW) at Barter Island, 11 cm at Prudhoe Bay, and 10 cm at Point Hope (National Ocean Service, 2017). For purposes of this report, the difference between MSL and MLLW (which represents the vertical datum for all National Ocean Service nautical charts of the region) is assumed to be negligible.

The International System of Units (SI) is used throughout the report, with three exceptions: (1) distances are provided in nautical miles (nm) to maintain consistency with the use of geographic coordinates; (2) wind speeds are provided in knots (kt), again to maintain consistency with the use of geographic coordinates; and (3) freezing degree days (“FDD”) are computed using the Fahrenheit rather than Celsius scale to provide greater resolution and maintain consistency with past freeze-up reports. In the case of nautical miles and knots, the corresponding values in SI units are provided in parentheses.

Throughout this report, the locations of ice features are referenced to geographic features that include bays, rivers, lagoons, points of land, natural and man-made islands, and coastal villages. For ease of reference, these geographic features are shown in Figures 2 (Central Beaufort Sea), 3 (Western Beaufort Sea), and 4 (Chukchi Sea).

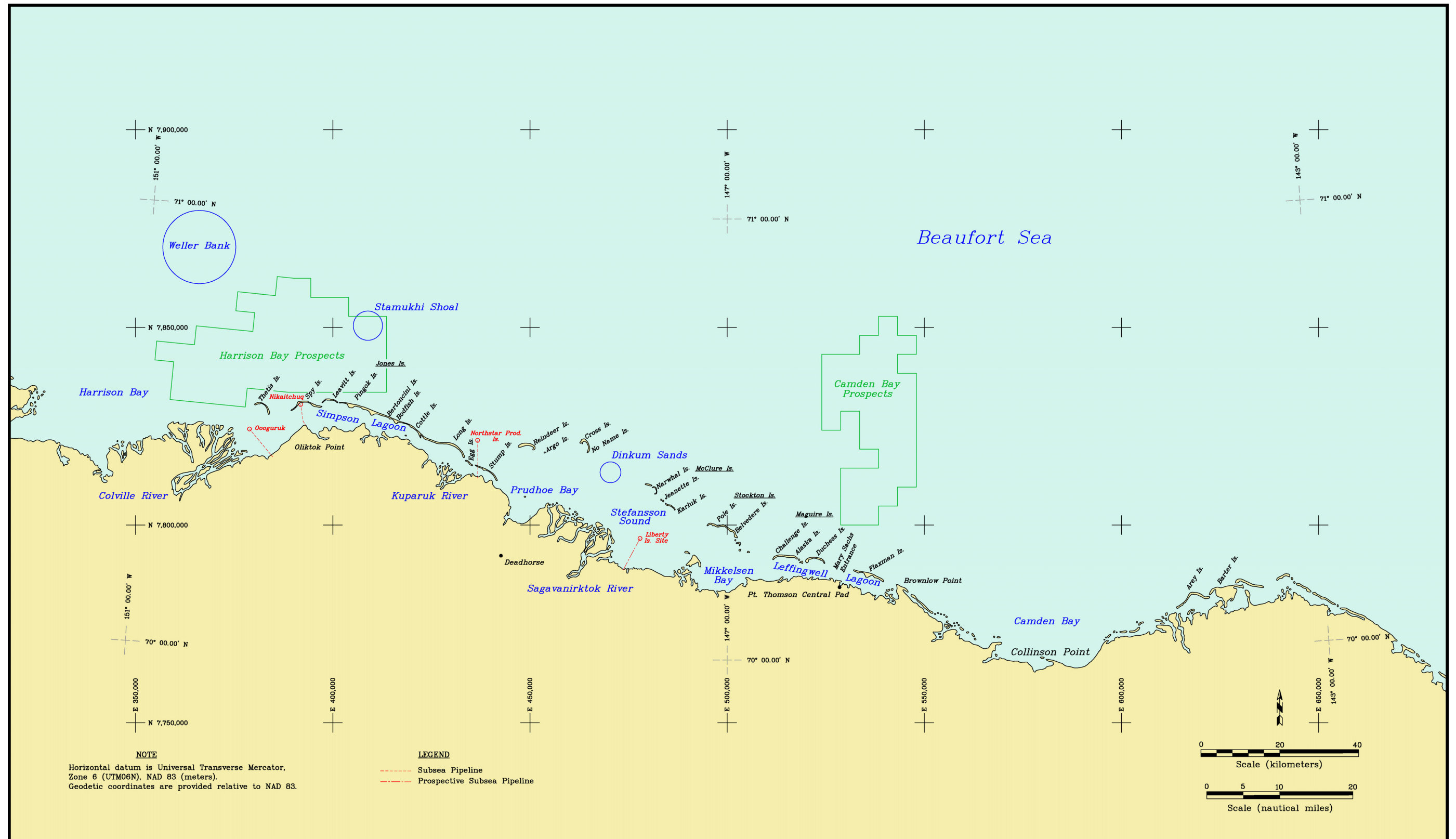


Figure 2. Geographic Points of Interest in Central Beaufort Sea

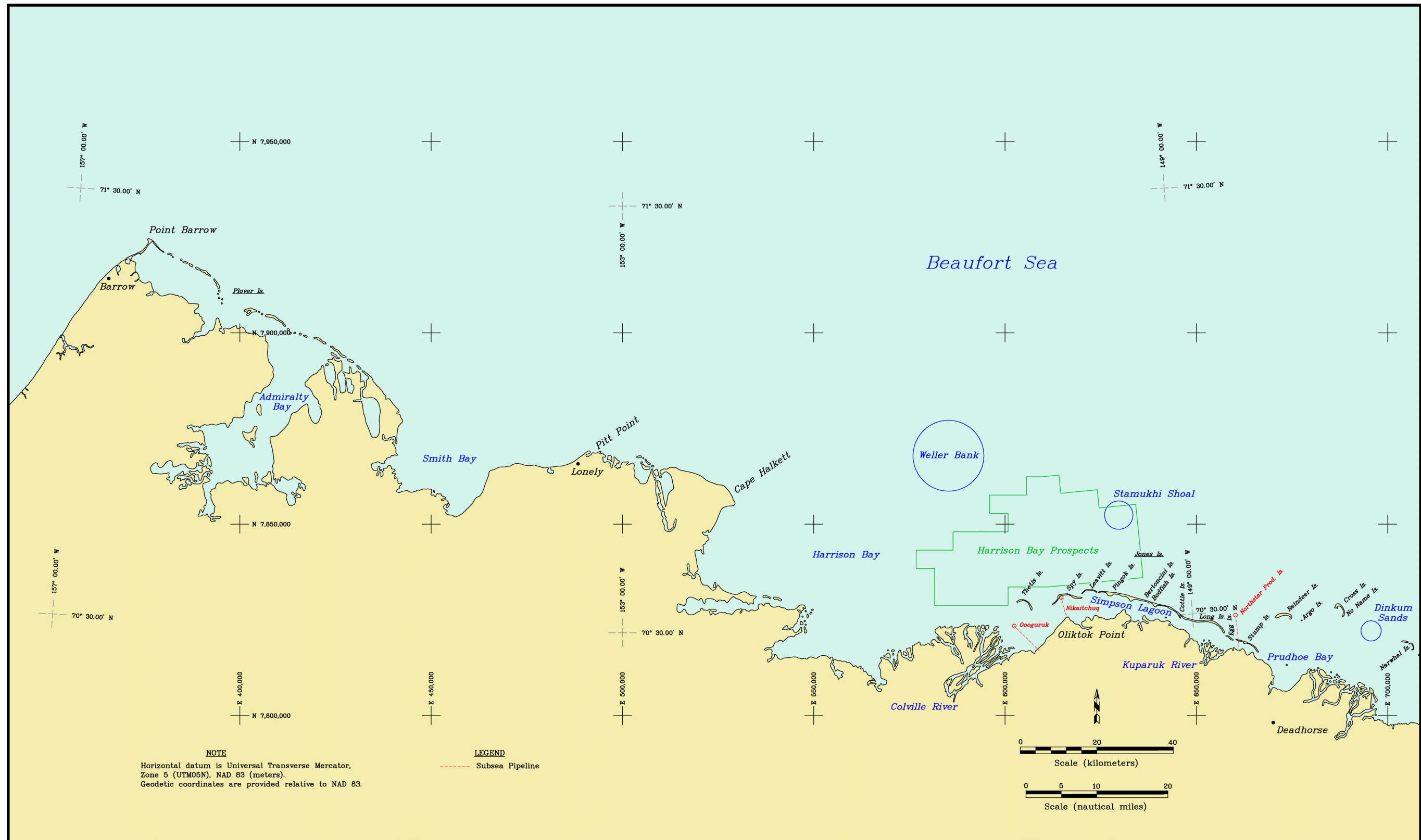


Figure 3. Geographic Points of Interest in Western Beaufort Sea

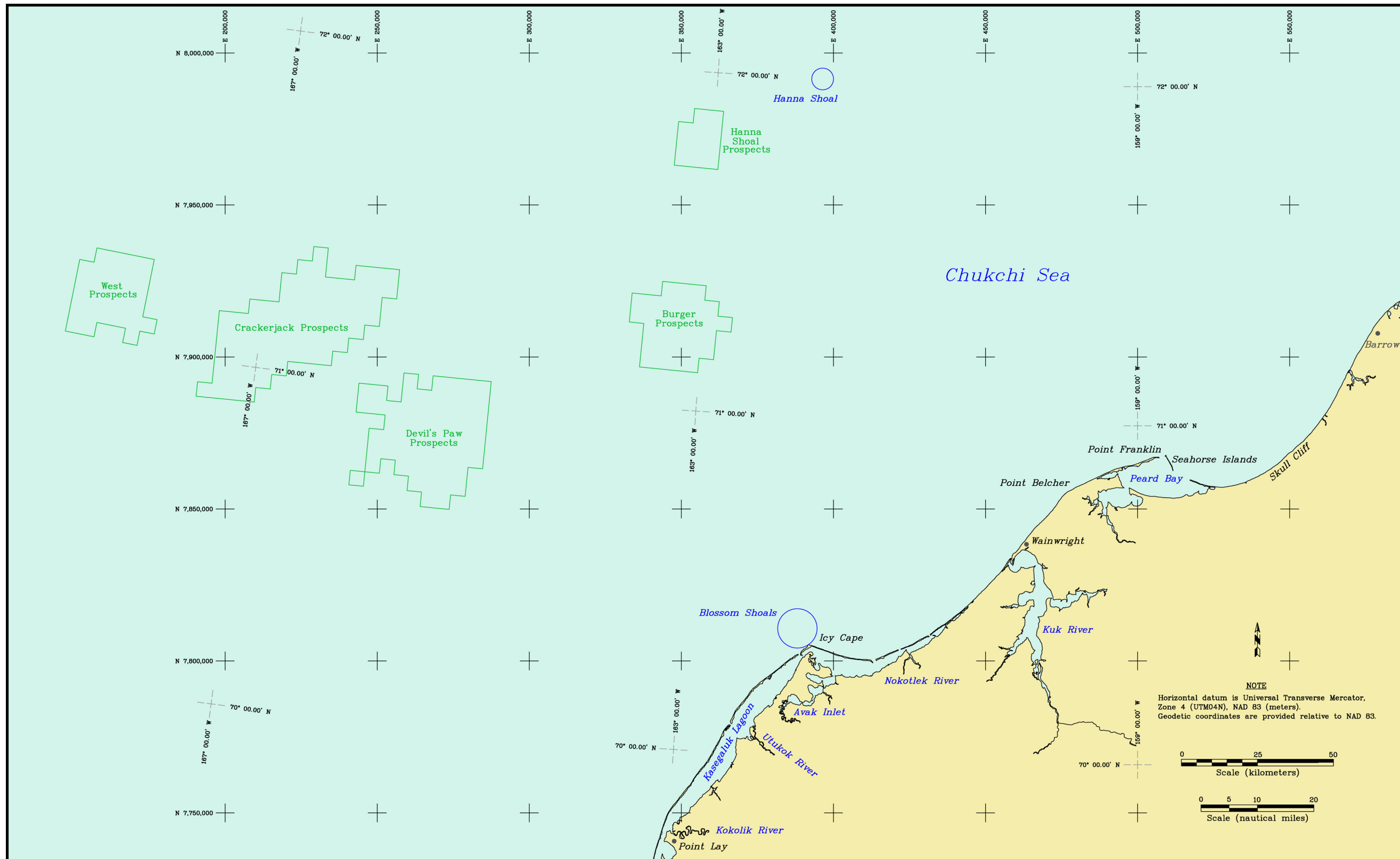


Figure 4. Geographic Points of Interest in Chukchi Sea

2. PRIOR STUDIES

As indicated in Section 1, six annual freeze-up studies were conducted from 1980-81 through 1985-86 (Vaudrey, 1981a; 1982a; 1983; 1984; 1985a; 1986). More recently, seven annual freeze-up studies were undertaken from 2009-10 through 2015-16 (Coastal Frontiers and Vaudrey, 2010; 2011; 2012a; 2013; 2014; 2015; 2016). The methods employed and results obtained in these prior studies are summarized below.

2.1 1980s Freeze-Up Studies

The freeze-up studies conducted in the 1980s were made available to the present project through the courtesy of Shell International Exploration and Production, Inc. (Reece, 2009). The primary objectives of each study were twofold: (1) observe and record major ice movement events and their effects on man-made structures, and (2) document the size and distribution of multi-year floes, the locations of major first-year ridges and rubble fields, and the zonation of the nearshore ice. Each study included a series of aerial surveys conducted at two- to three-week intervals from early October until early December to monitor the progression of freeze-up.

The first three studies (1980-81 through 1982-83) were limited to the central Beaufort Sea, from Cape Halkett on the west to Flaxman Island on the east. The last three studies (1983-84 through 1985-86) were expanded significantly to include the entire region between Icy Cape in the Chukchi Sea and Barter Island in the Beaufort Sea. Occasionally, the reconnaissance flights continued east of Barter Island to the Canadian border. Each of the studies commencing in 1983, 1984 and 1985 included an additional trip at the end of January to record late freeze-up ice movements caused by storms occurring after the early-December visit. The progress of the freeze-up season was documented by reporting the ice conditions observed during each successive trip. Meteorological data, including wind speed and direction as well as air temperature, were acquired from coastal or near-coastal reporting stations at Deadhorse, Barrow, and Barter Island.

Key findings from the six freeze-up studies in the 1980s are presented below:

Beaufort Sea: 1980s

- **Initiation of Freeze-Up:** Freeze-up occurred in the nearshore portion of the Beaufort Sea between late September and early October. Warming trends in

October retarded initial ice growth by seven to ten days in 1983 and 1985, and by almost three weeks in 1984.

- **Landfast Ice and Shear Zone Development:** Persistent easterly winds during freeze-up created a grounded shear zone that provided stability for the landfast ice. In contrast, westerly winds fostered offshore movement of the ice cover and retarded the development of landfast ice. In the absence of strong westerly winds, an extensive zone of landfast ice stabilized by a grounded shear zone tended to form by the end of November.
- **Ice Pile-Ups and Rubble Formation:** The primary cause of ice pile-ups on natural shorelines and man-made facilities was found to be a reversal in the wind direction, especially during the early months of the freeze-up season. Two such ice movement sequences were documented during the six-year study period. The first, in November 1981, was caused by a westerly that loosened the landfast ice followed by an easterly that drove the ice back onto the shoreline. The second, in mid-October 1982, resulted from an easterly that created a lead offshore of the temporary fast ice followed by a strong westerly that dislodged the fast ice and drove it up the slopes and onto the work surfaces of man-made exploration islands.

Wind reversals also tended to create significant rubble piles offshore, especially on Stamukhi Shoal and Weller Bank. Several large rubble piles were observed 10 to 15 nm (19 to 28 km) northwest of Seal Exploration Island (the current location of Northstar Production Island) in water depths of 10 to 12 m after a strong southwesterly in late December 1983.

- **Multi-Year Ice:** Significant concentrations of multi-year ice were noted in the nearshore portion of the central Beaufort Sea during three of the six freeze-up seasons studied. The most extensive invasion occurred in late September 1980, when concentrations of 3 to 5 tenths occurred 2 to 3 nm (4 to 6 km) offshore of the barrier islands from Cross to Flaxman. During the summer of 1983, mild winds and cold air temperatures produced a substantial concentration of second-year ice in the nearshore region in early October. Two years later, in October 1985, most of the multi-year ice remained north of a line that roughly paralleled the coast 15 to 20 nm (28 to 37 km) offshore. During the other three freeze-up seasons, (1981, 1982, and 1984), multi-year ice in the nearshore region was confined to localized belts and patches of small floes and isolated ridge fragments grounded on the barrier islands and in the shear zone.

Chukchi Sea: 1980s

- **Initiation of Freeze-Up:** In 1983, freeze-up near Barrow occurred around October 1st. This early date appears to have resulted, at least in part, from the cooling and stabilizing influence of old ice present in the region. In 1984 and 1985, the nearshore waters of the Chukchi remained ice free until late October and mid-October, respectively.
- **Landfast Ice:** Landfast ice development along the Chukchi coast was found to be very limited in extent due to the predominance of easterly winds. These winds repeatedly opened a flaw lead that, in turn, produced ice when it refroze.
- **Ice Pile-Ups:** As in the Beaufort Sea, abrupt wind reversals during the freeze-up season were found to cause shoreline pile-ups on the Chukchi coast, especially near Barrow and Point Belcher. However, an absence of strong winds in 1983 and a paucity of wind reversals in both 1984 and 1985 minimized the number of pile-ups observed during the three studies.
- **Multi-Year Ice:** Cold air temperatures and a lack of strong winds during the summer of 1983 produced a significant concentration of second-year ice north of the 71°N parallel in early October. In November 1984, a 2- to 3-tenths concentration of multi-year ice in the western Beaufort Sea moved into the Chukchi. It remained above the 71°N parallel through late January 1985, and was located well offshore of the prevailing 10- to 20-nm (19- to 37-km) wide coastal flaw lead. The multi-year floes typically ranged from 300 to 600 m in diameter, with a maximum extent of 4 km. In October 1985, multi-year ice attained higher concentrations and moved closer to the coast than in the Beaufort.

2.2 2009-10 Freeze-Up Study

The scope and methods of the 2009-2010 Freeze-Up Study, which were adopted with only minor modifications for the 2010-11 through 2015-16 studies, are described in detail by Coastal Frontiers and Vaudrey (2010). Significant findings are as follows:

Beaufort Sea: 2009-10

- **Initiation of Freeze-Up:** Freeze-up in the nearshore portion of Beaufort Sea occurred during the third week in October.
- **Landfast Ice and Shear Zone Development:** An intense easterly storm in late December 2009 created a grounded shear zone to the west of Prudhoe Bay that remained intact through midwinter. In contrast, westerly winds in January 2010

removed much of the landfast ice off the barrier islands to the east of Prudhoe Bay, and the ice in this region remained dynamic through mid-February.

- **Ice Pile-Ups:** Ice pile-ups were observed on or adjacent to six natural barrier islands and one man-made island during the reconnaissance flights conducted in early February. The estimated pile-up heights ranged from 1 to 16 m. The largest pile-up exceeded 2 km in length.
- **Multi-Year Ice:** For the first time since 2001-02, multi-year ice floes invaded the nearshore waters of the Alaskan Beaufort Sea. The floes remained 10 to 20 nm (19 to 37 km) offshore as they migrated toward the west and ultimately moved into the Chukchi Sea.

Chukchi Sea: 2009-10

- **Initiation of Freeze-Up:** Freeze-up proceeded more slowly than in the Beaufort, with the ice edge advancing to the south and west during the month of November. By the end of the month, ice covered the Chukchi Sea north of Cape Lisburne and east of 169°W.
- **Landfast Ice:** Alternating periods of easterly (offshore) and westerly (onshore) winds repeatedly dislodged the nearshore ice between Barrow and Point Lay, causing the freeze-up process to start anew. As a result, most of the coast lacked ridges and rubble fields that were sufficiently well-grounded to stabilize the landfast ice, and the ice remained susceptible to removal during easterly storms.
- **Flaw Lead:** The distinctive flaw lead that forms off the Chukchi Sea coast opened and closed repeatedly in response to the alternating easterly and westerly winds. The width of the lead varied substantially, depending on the duration and intensity of the easterlies. A maximum width of 40 to 50 nm (74 to 93 km) was noted during a 25-day period from mid-February to early March, and again during a 10-day period in late March.
- **Ice Pile-Ups:** Nineteen ice pile-ups were observed on the Chukchi Sea coast during the February reconnaissance flights, including three that encroached up to 6 m onto the subaerial beach. The most significant pile-up extended 150 m alongshore and attained a maximum height of 15 m. The maximum heights of the others ranged from 4 to 10 m.
- **Multi-Year Ice:** Multi-year ice entered the northern Chukchi Sea from the western Beaufort and split into two separate branches that persisted through mid-winter: (1) a northern branch that remained above the 71.5°N parallel in the eastern

and central Chukchi before dipping south, and (2) a southern branch that extended southwest from Barrow to the vicinity of the 70°N parallel.

2.3 2010-11 Freeze-Up Study

Key findings of the 2010-11 Freeze-Up Study (Coastal Frontiers and Vaudrey, 2011) are summarized below:

Beaufort Sea: 2010-11

- **Initiation of Freeze-Up:** Freeze-up in the nearshore portion of Beaufort Sea occurred during the second week of October.
- **Landfast Ice and Shear Zone Development:** The landfast ice zone remained narrow and unstable throughout the 2010-11 freeze-up season due to a lack of easterly storms and sustained easterly winds. In the western Beaufort, the landfast ice edge at the end of January passed through Weller Bank but fell short of its other typical anchor point, Stamukhi Shoal. In the central Beaufort, the landfast ice edge at the end of January was located in close proximity to the barrier islands east of Prudhoe Bay and within 10 nm (19 km) of the shoreline in Camden Bay.
- **Ice Pile-Ups:** Only one ice pile-up was observed in the Alaskan Beaufort Sea in 2010-11. It was located on the Ooguruk Offshore Drillsite in the shallow waters of the Colville River Delta, and consisted of 10- to 15-cm thick plates that were stacked against the south corner and southwest side in multiple waves with heights to 3 m. The pile-up did not encroach past the waterline of the island's gravel-bag armor.
- **Multi-Year Ice:** In contrast to 2009-2010, large multi-year ice floes did not invade the nearshore region of the Alaskan Beaufort Sea during the 2010-11 freeze-up season. Between November 2010 and mid-February 2011, such floes remained north of the 71°N parallel in the eastern Beaufort and 72°N parallel in the western Beaufort. However, fragments of old ice with diameters ranging from 1 to 6 m were observed on the shorelines of many of the barrier islands. The fragments originated from a band of grounded ice between Flaxman Island and Smith Bay that persisted throughout the 2010 open-water season.

Chukchi Sea: 2010-11

- **Initiation of Freeze-Up:** Freeze-up in the Chukchi Sea began during the first week in October but progressed slowly due to above-normal air temperatures and a prolonged easterly storm that dislodged the newly-formed landfast ice from the

coast in mid-month. Complete ice coverage in the region north of Cape Lisburne and east of the 169°W meridian occurred during the first week in December.

- **Landfast Ice:** Except in Peard Bay, Kasegaluk Lagoon, and the semi-protected embayment east of Point Franklin, landfast ice off the coast between Barrow and Point Lay was confined to a narrow strip that remained unstable through mid-February 2011. A paucity of westerly storms through mid-January limited the production of grounded rubble, thereby leaving the nearshore ice susceptible to break-out and removal during periods of easterly winds.
- **Flaw Lead:** The coastal flaw lead was detected on five occasions during the 2010-11 freeze-up season: late December, early January, late January, and twice in the first half of March. The dimensions of the lead varied substantially, from an estimated 50 nm (93 km) long and 5 nm (9 km) wide in late December to 140 nm (259 km) long and 60 nm (111 km) wide in late January. The feature's persistence also varied, from as little as several days during each appearance in March to about a week in early January.
- **Ice Pile-Ups:** Twenty-seven pile-ups were observed on the Chukchi Sea coast in February 2011, representing eight more than in 2010. The largest pile-ups were located between Point Belcher and Wainwright, where one ice pile attained both the maximum estimated height of 8 m and maximum estimated encroachment distance of 40 m onto the beach. The longest ice pile, stretching 2,300 m alongshore with a height of 3 m, also occurred in this region.
- **Multi-Year Ice:** Large multi-year ice floes remained well offshore throughout the 2010-11 freeze-up season, with the southern boundary located approximately 60 nm (111 km) north of Point Barrow at the end of December and 180 nm (333 km) north at the end of March. Nevertheless, fragments of old ice embedded in first-year floes were observed in Shell's Burger Prospects in February 2011. They comprised less than 5% of the ice cover, with maximum horizontal dimensions that ranged from one hundred to several hundred meters.

2.4 2011-12 Freeze-Up Study

The results of the 2011-12 Freeze-Up Study (Coastal Frontiers and Vaudrey, 2012a) are summarized below:

Beaufort Sea: 2011-12

- **Initiation of Freeze-Up:** Freeze-up began during the second week in October, when ice began to form along the coast. Complete ice coverage in the nearshore

region occurred on October 26th, followed soon thereafter by complete freeze-up in the entire Alaskan Beaufort Sea on November 1st.

- **Landfast Ice and Shear Zone Development:** After remaining narrow in November, the landfast ice zone grew dramatically in December in response to three easterly storms. The ice remained firmly grounded on Weller Bank and Stamukhi Shoal through mid-winter, but failed to achieve stability seaward of the 11-m isobath to the east of Prudhoe Bay.
- **Ice Pile-Ups:** Ten ice pile-ups occurred in the central portion of the Alaskan Beaufort Sea during the 2011-12 freeze-up season. Nine were located on natural barrier islands and one on Northstar Production Island. The heights ranged from 2 to 7.6 m, the encroachment distances from 0 to 20 m, and the alongshore lengths from 200 to 1,200 m.
- **Multi-Year Ice:** Except in the immediate vicinity of Point Barrow, multi-year ice remained well offshore in the Alaskan Beaufort Sea throughout the 2011-12 freeze-up season.

Chukchi Sea: 2011-12

- **Initiation of Freeze-Up:** As in 2010-11, freeze-up in the Chukchi Sea commenced during the first week in October but developed slowly in the weeks that followed. Complete coverage in the region north of Cape Lisburne occurred on November 30th.
- **Landfast Ice:** The landfast ice in the northeast Chukchi Sea remained unstable and discontinuous until January, when a predominance of westerly winds coupled with two westerly storms produced a narrow but continuous strip from Barrow to Point Lay. This configuration persisted through February despite the frequent occurrence of easterly winds, indicating that the ice had become well-grounded during the westerly winds in January.
- **Flaw Lead:** The coastal flaw lead was present during a significant portion of the 2011-12 freeze-up season, including more than half of the months of December and February. The width typically ranged from 10 to 30 nm (19 to 56 km) but expanded to as much as 60 nm (111 km) in December. The length, typically between 120 and 180 nm (222 and 334 km), equaled or exceeded 200 nm (371 km) on several occasions.
- **Ice Pile-Ups:** Thirty-one ice pile-ups were detected on the coast between Point Barrow and Point Lay. The highest concentrations were located on Point Franklin spit and on the barrier islands that bracket Icy Cape. The heights ranged from 3 to

18 m, the encroachment distances from 0 to 40 m, and the alongshore lengths from 100 to 5,400 m. All of the maximum dimensions were associated with a massive pile-up that overtopped the 15-m high bluff at Skull Cliff and spilled 3 m onto the surface of the tundra.

- **Multi-Year Ice:** Large multi-year ice floes began streaming into the region south and west of Point Barrow in mid-December when they encountered a northeasterly extension of the coastal flaw lead that caused them to turn to the southwest. This phenomenon, in which multi-year floes are diverted to the southwest by an extended flaw lead, produced another substantial multi-year ice invasion in late March. Between December and March, floes with diameters as large as 20 km moved as far south as the 68°N parallel and attained concentrations as high as 90%.
- **Grounded Ice Features:** Two grounded ice features believed to be icebergs from the Canadian Archipelago were discovered off the Chukchi Sea coast in February 2012. The larger of the two, located approximately 3 nm (6 km) off Point Belcher in a charted water depth of 32 m, was estimated to be 80 m long and 40 m wide, and to extend 20 m above sea level.

2.5 2012-13 Freeze-Up Study

Key findings from the 2012-13 Freeze-Up Study (Coastal Frontiers and Vaudrey, 2013) are as follows:

Beaufort Sea: 2012-13

- **Initiation of Freeze-Up:** Ice began to form in the brackish waters off river deltas and in semi-protected bays and lagoons during the second week in October. Freeze-up in the nearshore region took place on November 5th; basin-wide freeze-up occurred one week later on November 12th.
- **Ice Fracture Event:** From late January through late March, the ice canopy in the Beaufort Sea was disturbed by a massive fracture event that ultimately extended from Banks Island, Canada, on the east to well past Point Barrow on the west. Driven by sustained easterly winds and a series of easterly storms, the event caused large pieces of the pack ice to break free and rotate to the west.
- **Landfast Ice and Shear Zone Development:** The landfast ice zone remained narrow and poorly-developed through mid-December, but expanded dramatically from mid-December through late January in response to the same sustained easterly winds and storms that caused the fracture event. In mid-March, the

fracture event removed the outer portion of the landfast ice, and the seaward edge retreated to the vicinity of the 18-m isobath.

- **Ice Pile-Ups:** Thirty-eight ice pile-ups were noted in the central portion of the Alaskan Beaufort Sea, consisting of thirty-four on barrier islands, three on Northstar Production Island, and one on the mainland shore. The heights ranged from 2 to 10 m, the encroachment distances from 0 to 10 m, and the alongshore lengths from 100 to 2,200 m.
- **Multi-Year Ice:** As in 2010-11 and 2011-12, multi-year ice failed to invade the nearshore region of the Alaskan Beaufort Sea during the 2012-13 freeze-up season.

Chukchi Sea: 2012-13

- **Initiation of Freeze-Up:** Freeze-up began during the second week in October with the formation of ice in Kasegaluk Lagoon, the Kuk River Inlet, and Peard Bay. Complete ice coverage in the nearshore region occurred on November 15th, followed by complete coverage in the entire Chukchi Sea north of Cape Lisburne on November 28th.
- **Flash-Freeze Event:** On October 31st, a flash freeze occurred off Wainwright in a large area bounded by the 71°N and 72.5°N parallels, and the 160°W and 165°W meridians. The ice patch, which was surrounded by open water, covered all of the Hanna Shoal Prospects and portions of the Burger Prospects.
- **Landfast Ice:** At the end of November, a narrow strip of landfast ice extended from Barrow to the vicinity of Wainwright, and another narrow strip encircled Icy Cape. During the next four months, in the absence of westerly storms, the landfast ice zone alternated between a narrow, continuous strip and an even narrower, discontinuous strip.
- **Flaw Lead:** The coastal flaw lead remained open for about half of the month of December, three quarters of the month of January, the entire month of February, and half of the month of March. During the 46-day period from January 31st through March 17th, it never closed. Maintained by a combination of sustained easterly winds, energetic easterly storms, and the massive ice fracture event in the Beaufort, the lead reached a maximum width of 150 nm (278 km) while stretching from Cape Lisburne to well northeast of Point Barrow.
- **Ice Pile-Ups:** Thirty-two ice pile-ups were observed on the Chukchi Sea coast between Point Barrow and Point Lay, with the highest concentration located on the barrier islands that lie to the south of Icy Cape. The pile-ups were relatively small,

with heights ranging from 2 to 4 m, encroachment distances from 0 to 8 m, and alongshore lengths from 100 to 3,800 m.

- **Multi-Year Ice:** As in the case of the Beaufort, multi-year ice remained absent from the region south and west of Point Barrow during the 2012-13 freeze-up season.

2.6 2013-14 Freeze-Up Study

The 2013-14 Freeze-Up Study (Coastal Frontiers and Vaudrey, 2014) produced the following results:

Beaufort Sea: 2013-14

- **Initiation of Freeze-Up:** Ice began to form in the semi-protected waters adjacent to the coast in late September. Complete ice coverage in the nearshore region occurred on October 26th, followed by complete coverage in the Alaskan Beaufort Sea during the third week of November.
- **Landfast Ice and Shear Zone Development:** The landfast ice zone remained narrow and poorly-developed through the end of December. The situation changed in January, when persistent easterly winds caused the ice to expand past the 18-m isobath from Point Barrow to Barter Island. In February and March, the landfast ice edge advanced in response to easterly winds and retreated in response to westerly winds but tended to retreat no farther than the 18-m isobath due to the existence of a well-grounded shear zone.
- **Ice Pile-Ups:** Of the forty-six ice pile-ups that occurred in the central portion of the Alaskan Beaufort Sea, thirty-nine were located on natural barrier islands, four on man-made facilities, and three on the mainland shore. The heights ranged from 1 to 8 m, the encroachment distances from 0 to 20 m, and the alongshore lengths from 50 to 2,600 m.
- **Multi-Year Ice:** Multi-year ice was present in the offshore portion of the Alaskan Beaufort Sea throughout freeze-up and early winter, but remained absent from the nearshore region except in the immediate vicinity of Point Barrow.

Chukchi Sea: 2013-14

- **Initiation of Freeze-Up:** Freeze-up in the Chukchi Sea began during the first week in October but proceeded slowly in response to unseasonably warm air temperatures that persisted through mid-November. Complete ice coverage in the

nearshore region occurred on November 26th. Basin-wide freeze-up took place on December 14th.

- **Flash-Freeze Event:** On or about November 12th, a flash freeze created a patch of ice centered 130 nm (241 km) west of Icy Cape. Although much smaller than that which formed off Wainwright in October 2013, it nevertheless marked the second documented occurrence of flash freezing in the Chukchi Sea in five freeze-up seasons.
- **Landfast Ice:** At the end of November, the landfast ice zone between Barrow and Point Lay consisted of a narrow, discontinuous strip. It remained narrow in December except for an advance to Blossom Shoals (off Icy Cape) that occurred at the end of the month and persisted for the remainder of the study period. In mid-January, a prolonged easterly storm dislodged virtually all of the landfast ice north of the Nokotlek River Mouth. Subsequently, the width of the landfast ice zone ranged from negligible to 20 nm (37 km) in response to changing wind conditions. At the end of March, landfast ice was confined to a narrow strip located inside the 11-m isobath in most areas.
- **Flaw Lead:** The flaw lead was present on 57% of the days from December 2013 through March 2014. The maximum width of 100 nm (185 km) occurred in February, at which time the lead encompassed all of the Burger and Crackerjack Prospects and parts of the Hanna Shoal and West Prospects. The maximum length, 250 nm (463 km), occurred on repeated occasions in February and March. The maximum persistence of 15 days took place from mid-February to early March.
- **Ice Pile-Ups:** Twenty-two ice pile-ups were detected between Barrow and Point Lay, with the highest concentration located on the barrier islands to the east of Icy Cape. The pile-up heights, which varied from 1 to 3 m, were smaller than those recorded during the prior four freeze-up seasons. All 22 pile-ups encroached onto the subaerial beach, with encroachment distances ranging from 5 to 20 m, and alongshore lengths from 100 to 7,800 m.
- **Multi-Year Ice:** Multi-year ice remained north of Point Barrow until mid-December. During the month that followed, multi-year floes were channeled into the region south and west of the Point on four occasions by a northeasterly extension of the coastal flaw lead. The last invasion, which occurred in mid-January, produced a significant southerly displacement of the multi-year ice edge. The ice continued to advance slowly to the south in February and March, crossing the 71°N parallel in late February and reaching the vicinity of Icy Cape in mid-March.

2.7 2014-15 Freeze-Up Study

Salient findings from the 2014-15 Freeze-Up Study (Coastal Frontiers and Vaudrey, 2015) are summarized below:

Beaufort Sea: 2014-15

- **Initiation of Freeze-Up:** Freeze-up commenced in early October, when ice began to form in the semi-protected bays and lagoons adjacent to the coast. Complete ice coverage in the nearshore region occurred on October 30th, followed soon thereafter by complete coverage in the entire Alaskan Beaufort Sea on November 5th.
- **Landfast Ice and Shear Zone Development:** Landfast ice, which began to form during the second week in October, advanced to the 11-m isobath in late November, the 18-m isobath in late December, and well beyond the 18-m isobath in mid-January, with each advance precipitated by one or more easterly storms. Westerly storms in late January produced significant losses, with the ice remaining grounded on Weller Bank and Stamukhi Shoal but retreating to the vicinity of the 11-m isobath on either side. Subsequently, in February and March, the landfast ice edge advanced in response to easterly winds and retreated in response to westerly winds but remained between the 11- and 18-m isobaths.
- **Ice Pile-Ups:** Thirty-five ice pile-ups occurred in central portion of the Alaskan Beaufort Sea during the 2014-15 freeze-up season. Thirty-one were located on natural barrier islands, three on man-made islands, and one on a spit adjacent to the mainland shore. The heights ranged from 1 to 15 m, the encroachment distances from 0 to 25 m, the alongshore lengths from 50 to 1,500 m, and the ice block thicknesses from 30 to 90 cm.
- **Multi-Year Ice:** For the fifth consecutive year, multi-year ice failed to invade the nearshore region of the Alaskan Beaufort Sea. It remained well offshore, never less than 90 nm (167 km) from the coast at the U.S.-Canadian border, 75 nm (139 km) from Cross Island, and 25 nm (46 km) from Point Barrow.

Chukchi Sea: 2014-15

- **Initiation of Freeze-Up:** Freeze-up began in early October, but was delayed by a severe easterly storm in mid-month. Complete ice coverage in the nearshore region occurred on November 28th; complete coverage in the entire Chukchi Sea north of Cape Lisburne occurred nearly three weeks later on December 17th. These dates were later than in any of the five prior freeze-up seasons.

- **Landfast Ice:** Landfast ice began to form in late October. During the next three months, the landfast ice zone expanded and contracted in response to changing wind conditions, but remained narrow and discontinuous. Westerly winds and a westerly storm produced a significant expansion during the first half of February, but easterly winds and two easterly storms erased this gain by month-end. Another major expansion followed in mid-March, again in response to westerly winds. This time, however, the ice became sufficiently well-grounded to resist displacement during the easterly winds that followed at the end of the month.
- **Flaw Lead:** The flaw lead was present 64% of the time from December through March. The frequency of occurrence varied with the wind direction, peaking at 90% in December when easterlies prevailed 90% of the time, and falling to 46% in February when easterlies prevailed only 54% of the time. The maximum width, 110 nm (204 km), occurred in February, when the lead encompassed all of the Burger Prospects and the southern portion of the Crackerjack Prospects. The maximum length, 250 nm (463 km), occurred in both December and March. The maximum persistence of 27 days took place in December.
- **Ice Pile-Ups:** Fifty-five ice pile-ups were observed on the coast during the 2014-15 freeze-up season. The highest concentrations were located between Barrow and Peard Bay, and on the barrier islands east of Icy Cape. The pile-up heights ranged from 1 to 8 m, the encroachment distances from 0 to 30 m, and the alongshore lengths from 50 to 9,500 m. The block thicknesses were estimated to vary from 20 to 60 cm.
- **Multi-Year Ice:** Multi-year ice briefly entered the region south and west of Point Barrow in mid-November, when a small tongue of such floes advanced to within 25 nm (46 km) of Point Belcher. By the end of November, however, the southern boundary had retreated to the 73°N parallel. It remained well north of Point Barrow, between the 72°N and 73°N parallels, from December through March.

2.8 2015-16 Freeze-Up Study

Key findings from the 2015-16 Freeze-Up Study (Coastal Frontiers and Vaudrey, 2016) are as follows:

Beaufort Sea: 2015-16

- **Initiation of Freeze-Up:** Freeze-up began in late September with the formation of ice adjacent to the coast. Complete ice coverage in the nearshore region occurred

on October 26th, followed soon thereafter by complete coverage in the entire basin on October 31st.

- **Landfast Ice and Shear Zone Development:** Landfast ice began to form in mid-October, and grew to cover all of Stefansson Sound, the central portion of Harrison Bay, and the southern portion of Camden Bay in early November. The next major expansion, which was triggered by a four-day easterly storm in late November and early December, caused the ice to become grounded on its customary anchor points, Weller Bank and Stamukhi Shoal. In January, the landfast ice edge advanced seaward of the 18-m isobath over the entire length of the study area. This configuration persisted virtually unchanged through mid-March in response to a predominance of easterly winds coupled with a complete absence of westerly storms.
- **Ice Pile-Ups:** Only four ice pile-ups occurred in central portion of the Alaskan Beaufort Sea during the 2015-16 freeze-up season. Two were located on natural barrier islands to the west of Prudhoe Bay, one on the Nikaitchuq Spy Island Drillsite (SID), and one on Northstar Production Island. The pile-ups were small by historical standards, with heights of 2 to 5 m, alongshore lengths of 100 to 900 m, encroachment distances of 0 to 5 m, and ice block thicknesses of 20 to 40 cm.
- **Multi-Year Ice:** Except in the immediate vicinity of Point Barrow, multi-year pack ice remained absent from the nearshore portion of the Alaskan Beaufort Sea throughout freeze-up and early winter. However, numerous small fragments of first-year ice survived the 2015 open-water season to become second-year ice that became grounded on and around the barrier islands at the outset of freeze-up. At Point Barrow, low concentrations of multi-year ice entered the nearshore region during the first week in November and remained within 15 nm (28 km) of the coast until mid-January.

Chukchi Sea: 2015-16

- **Initiation of Freeze-Up:** Ice began to form in Kasegaluk Lagoon, the Kuk River Inlet, and Peard Bay during the second week in October. Complete coverage of these semi-enclosed basins took place during the third week, along with initial ice growth in the exposed waters adjacent to the coast. Freeze-up in the nearshore region was delayed by a combination of relatively warm air temperatures and easterly storms. It finally occurred on December 5th, after several days of low temperatures and moderate winds. Freeze-up in the entire Chukchi Sea north of Cape Lisburne followed a week later, on December 12th.

- **Landfast Ice:** Landfast ice remained narrow and ephemeral throughout the study period, reflecting the disruptive influence of easterly storms and a complete absence of westerly storms. The first landfast ice appeared in late October, when small strips formed off Peard Bay, the Kuk River Inlet, and the northern portion of Kasegaluk Lagoon. Modest growth followed in November and December, producing a narrow, near-continuous strip from Point Barrow to Icy Cape and a narrow, intermittent strip from Icy Cape to Point Lay. This configuration persisted through January, but strong easterly storms in February completely removed the ice at the base of Skull Cliff. In the remainder of the study area, the thin strip remained in place through February and the first half of March, indicating that the ice had become sufficiently well-grounded to resist displacement.
- **Flaw Lead:** From December 2015 through March 2016, the flaw lead opened on seven different occasions. The frequency of occurrence, which averaged 83% over the four-month period, varied from a low of 61% in March to a high of 100% in February. The maximum width, 80 nm (148 km), occurred in March while the maximum length, 250 nm (463 km), occurred in both December and January. The lead persisted for periods that ranged from one day to an extraordinary 64 consecutive days (from January 10th through March 13th).
- **Ice Pile-Ups:** Fifty-two ice pile-ups were observed on the shoreline between Barrow and Point Lay during the 2015-16 freeze-up season, with more than half located between Barrow and Peard Bay. The dimensions were unexceptional: the heights ranged from 1 to 8 m, the encroachment distances from 0 to 10 m, the alongshore lengths from 100 to 4,400 m, and the ice block thicknesses from 20 to 60 cm.
- **Multi-Year Ice:** Multi-year pack ice moved south to the vicinity of Point Barrow in late October, and began streaming into the region south and west of the Point in mid-November. This early-season invasion consisted of low concentrations of small floes entering an area of predominantly open water. Multi-year floes continued to move south and west of Point Barrow for the next two and a half months. From mid-November until mid-December, the concentrations remained at or below one tenth as the ice advanced to the 70°N parallel off Point Lay. From mid-December until the end of January, the concentrations increased to as much as five tenths. The invasion ceased in early February, when the southern boundary of the multi-year ice retreated rapidly to the north. The ice that already had entered the region south and west of Point Barrow continued to drift to the west, moving past the 168°W meridian in late February.

3. DATA ACQUISITION AND ANALYSIS

As outlined in Section 1, the 2016-17 Freeze-Up Study was conducted using a combination of remotely-sensed data and on-site observations. This section describes the sources of data and methods of analysis. The discussion is divided into the following five categories: meteorological data (Section 3.1), ice charts (Section 3.2), satellite imagery (Section 3.3), drift buoy data (Section 3.4), and aerial reconnaissance missions (Section 3.5). Digital data files are provided in Appendix B.

3.1 Meteorological Data

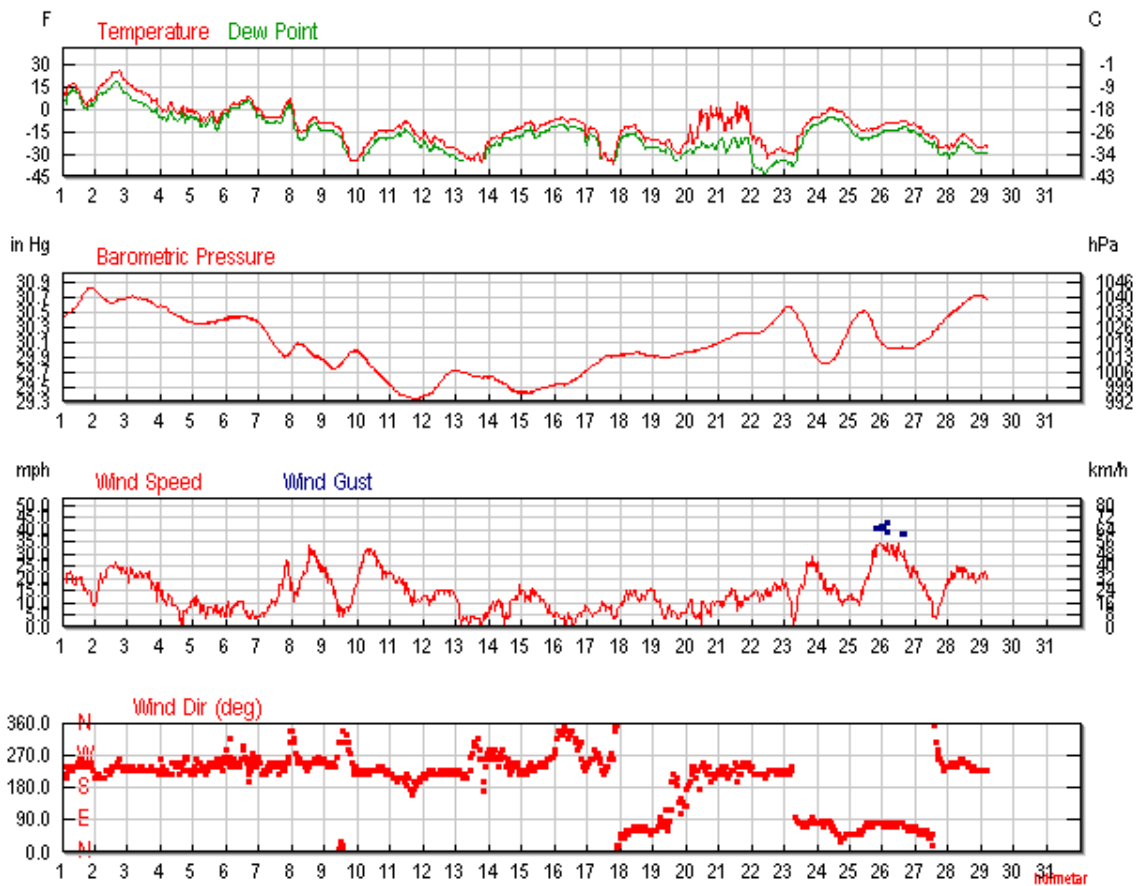
Meteorological data were obtained from two primary, publicly-available sources: the Weather Underground (2017) and the National Ocean Service (2017). The following data were downloaded from the Weather Underground website for the Deadhorse and Barrow Airports for the nine-month period from September 2016 through May 2017:

- Monthly tabulations of daily air temperature, wind speed and direction, dew point, humidity, barometric pressure, visibility, and precipitation (compiled in Excel spreadsheets in Appendix B);
- Monthly plots of air temperature, barometric pressure, wind speed, and wind direction (included as GIF files in Appendix B, with a representative example shown in Figure 5).

In March 2017, the Weather Underground ceased tabulating the average daily wind directions. The missing data were replaced by averaging the hourly observations acquired by the Automated Surface Observing System (ASOS) at Deadhorse and Barrow airports (Iowa Environmental Mesonet, Iowa State University, 2017).

The wind data were used to identify storm events and changes in wind direction that impacted the ice canopy. Such impacts included the accumulation and loss of landfast ice, the opening and closing of the Chukchi Sea flaw lead, and the generation of ice pile-ups. Although the monthly plots developed by the Weather Underground provide a useful overview of the wind conditions (*e.g.*, Figure 5), the tabulated values were replotted to obtain better resolution while displaying the wind speeds in knots rather than miles per hour. These plots appear in Sections 4 and 5.

The air temperature data were used to derive freezing degree days (FDD), which were computed for each day as the difference between the freezing point of seawater (29°F; -2°C)



Source: Weather Underground, 2017

Figure 5. Meteorological Data Recorded at Deadhorse Airport in February 2017

and the average air temperature. Days in which the temperature exceeded 29°F produced negative FDD. The daily values were summed over the period that produced the maximum number of accumulated FDD: October 16th through May 24th at Barrow Airport, and October 14th through May 21st at Deadhorse Airport. The results are shown in Table 1.

Table 1. Accumulated Freezing-Degree Days (<29°F) at Barrow and Deadhorse Airports in 2016-17

Site	Sep	Oct	Nov	Dec	Jan	Feb	Mar	Apr	May
Barrow	0	32	495	1,383	2,283	3,263	4,385	5,047	5,194
Deadhorse	0	176	799	1,897	2,983	4,109	5,320	6,036	6,144

To provide historical perspective, the normal range of daily air temperatures at each weather station was obtained from the National Oceanic and Atmospheric Administration (Arguez, *et al.*, 2010) for the 30-year period from 1980-81 through 2009-10. The appropriate range is included in each plot of daily average temperature that appears in Sections 4 and 5. It should be noted that the “normal ranges” used for the five freeze-up studies from 2009-10 through 2013-14 were derived from the period from 1970-71 through 1999-2000 rather than 1980-81 through 2009-10.

As in each of the prior seven freeze-up studies, Barrow Airport was adopted as the primary source of weather data for the Chukchi Sea. Although the data from Wainwright Airport have become sufficiently reliable to warrant consideration, a comparison with the Barrow data for the 2014-15 freeze-up season indicated that the differences were relatively minor (Coastal Frontiers and Vaudrey, 2015). As a result, to maintain continuity with the prior studies, all of the wind and temperature data presented in Section 5 were obtained from Barrow.

To supplement the data from Deadhorse Airport, monthly plots of wind speed, wind direction, air temperature and barometric pressure measured at the Prudhoe Bay West Dock Seawater Treatment Plant (STP) were downloaded from the National Ocean Service website (2017) for the period from October 2016 through February 2017. These plots are included as PNG files in Appendix B.

3.2 Ice Charts

Ice charts pertaining to the study area were downloaded from two government sources: the Canadian Ice Service (CIS; 2017) and the National Ice Center (NIC; 2017). Although the charts from both organizations provide similar information, the CIS products tend to incorporate greater detail while offering separate displays for ice concentration and stage of development. However, coverage is limited to the Beaufort Sea and extreme northeast portion of the Chukchi. The NIC produces separate charts for the Beaufort and the entire Chukchi.

Twenty-two pairs of ice charts showing concentration and stage of development were obtained from the CIS for the period from October 3, 2016, through February 27, 2017. The charts, which were issued on a weekly basis, are provided as GIF files in Appendix B. Figure 6 presents the CIS stage of development chart for November 28, 2016, shortly after basin-wide freeze-up had occurred in the Alaskan Beaufort Sea.

2016-17 Freeze-Up Study of the Alaskan Beaufort and Chukchi Seas

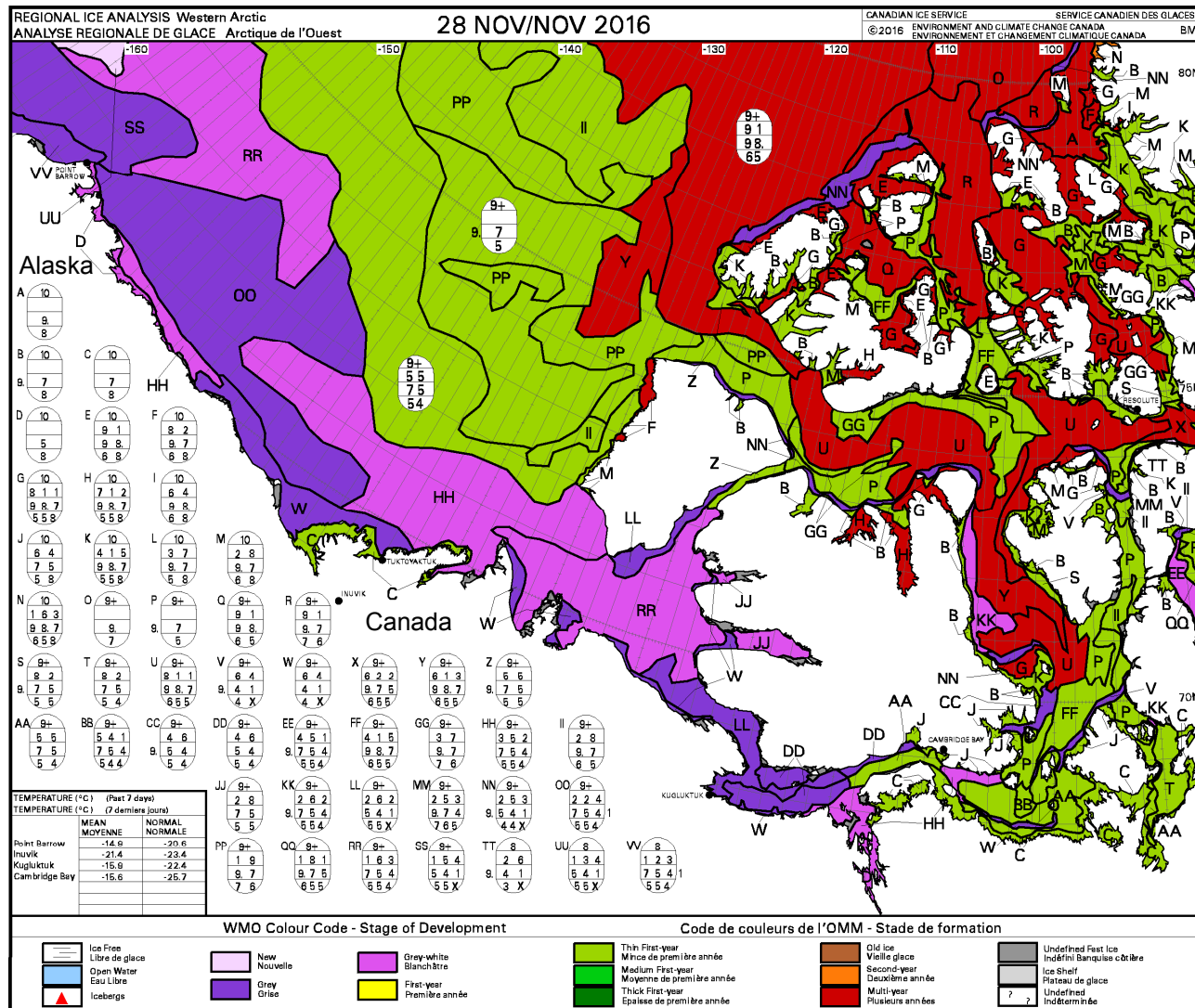
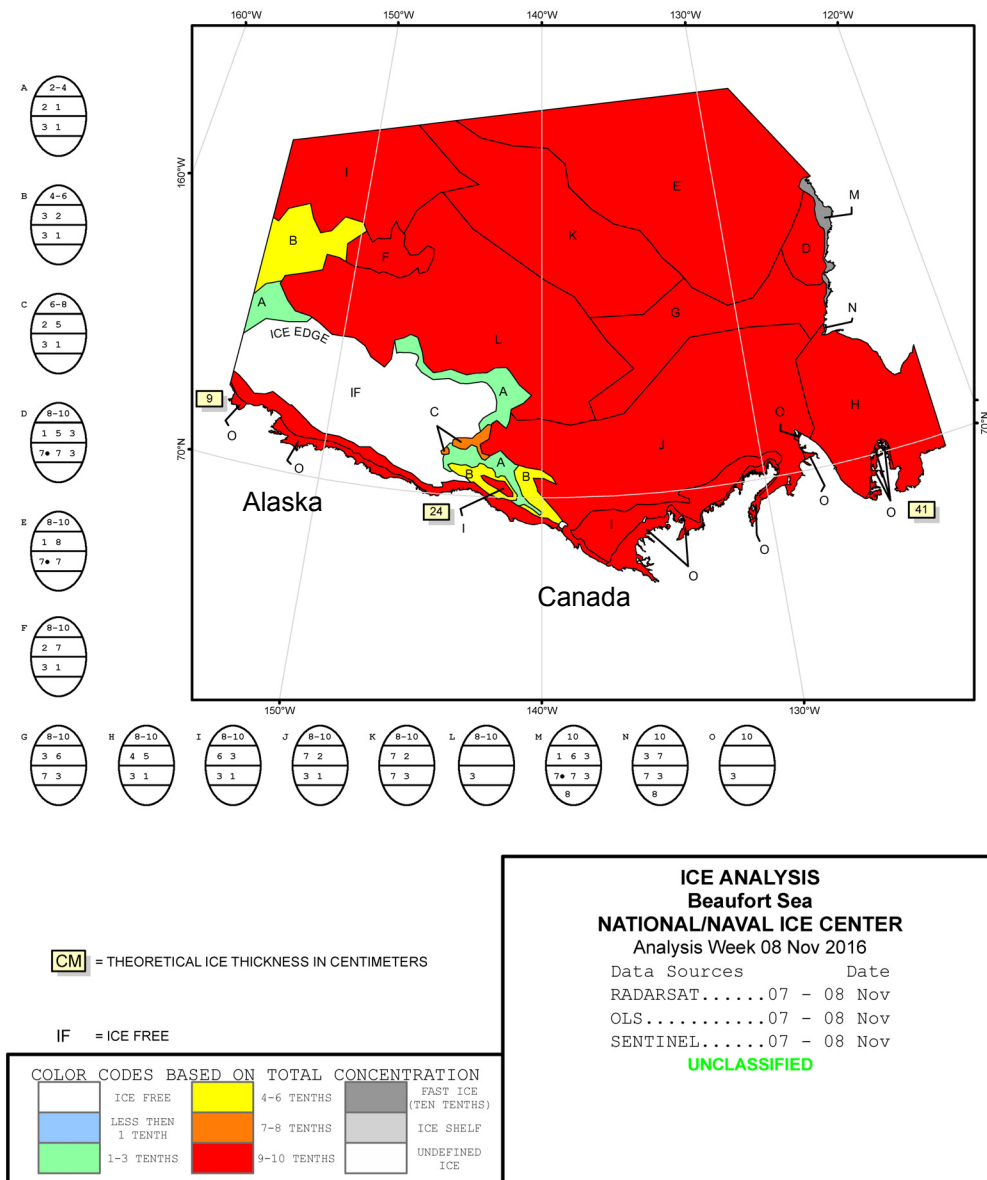


Figure 6. CIS Ice Stage of Development Chart of Beaufort Sea for November 28, 2016

2016-17 Freeze-Up Study of the Alaskan Beaufort and Chukchi Seas

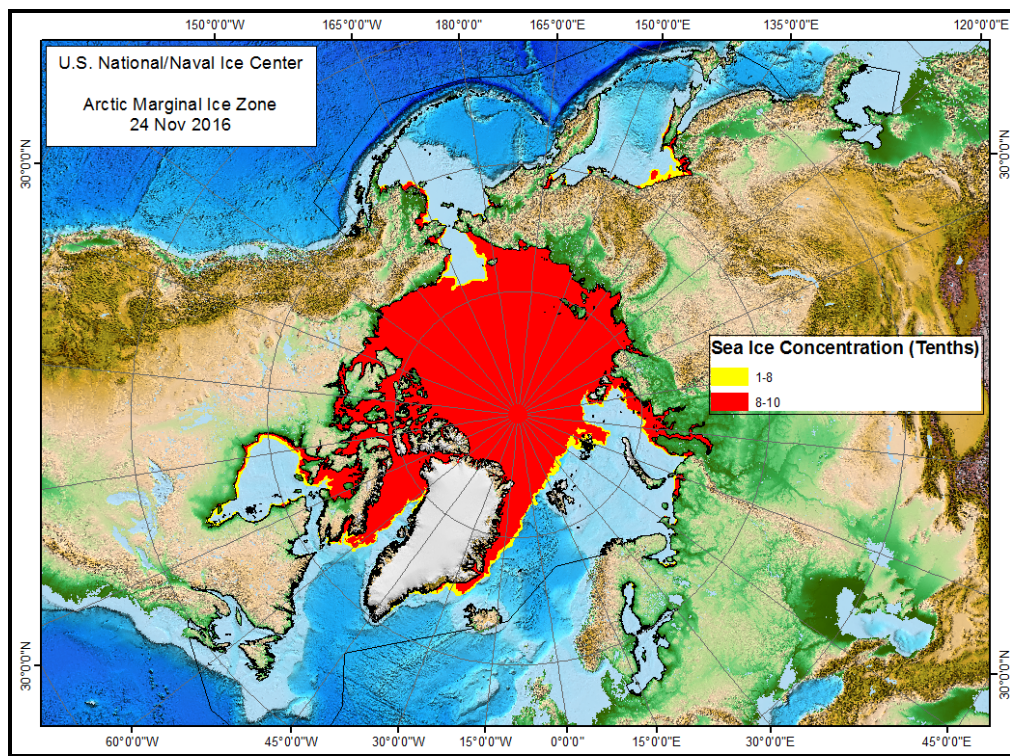
Forty-seven ice charts covering the period from October 4, 2016, through February 23, 2017 were obtained from the NIC, consisting of 20 for the Beaufort Sea and 27 for the Chukchi. The charts typically were issued twice per week prior to the occurrence of complete freeze-up in each basin, and once per week thereafter. A sample NIC chart that shows the Beaufort Sea on November 8, 2016, one day after the occurrence of nearshore freeze-up, is provided as Figure 7. The charts were available in both PDF and shapefile format through December 8, 2016, but only as shapefiles thereafter. All of the available chart files (both PDF and shapefiles) are included in Appendix B.



After: National Ice Center, 2016

Figure 7. NIC Ice Chart of Beaufort Sea for November 8, 2016

Background information on the progression of freeze-up in the entire Arctic region was obtained from the NIC Arctic Marginal Ice Zone charts, which depict the extent of the pack ice and marginal ice zone on a daily basis. For the purpose of preparing these charts, pack ice is assumed to occupy the region with eight tenths or more coverage, while the marginal ice zone is assumed occupy the region with one to eight tenths coverage (NIC, 2017). A representative example corresponding to November 24, 2016, after basin-wide freeze-up had occurred in the Beaufort but prior to nearshore freeze-up in the Chukchi, is provided as Figure 8. PNG files of the NIC Arctic Marginal Ice Zone charts beginning on October 1, 2016 and ending on February 28, 2017, are included in Appendix B.



After: National Ice Center, 2016

Figure 8. NIC Arctic Marginal Ice Zone Chart for November 24, 2016

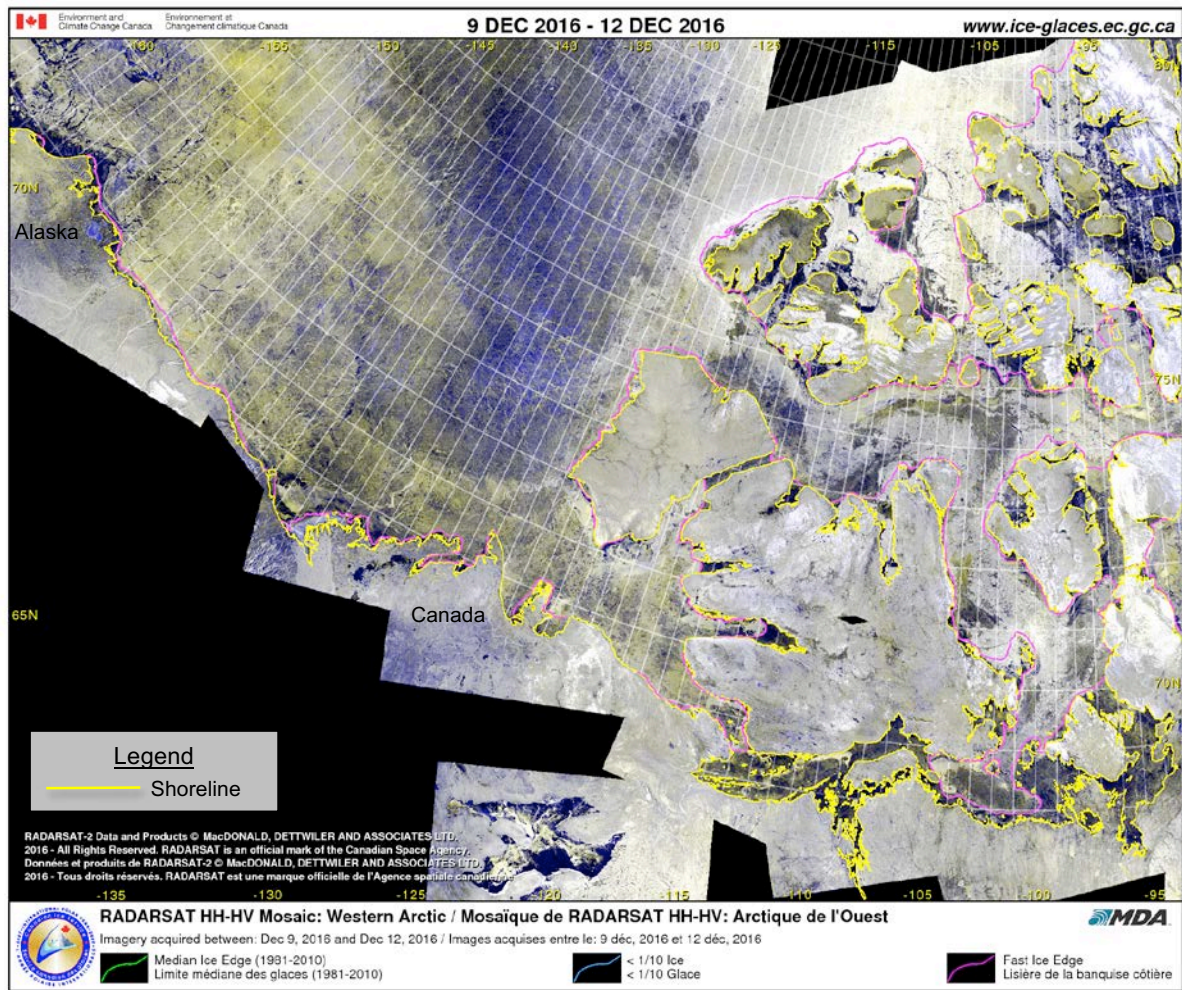
The ice charts from the CIS and NIC were used to track the evolution of freeze-up on a coarse scale, particularly during the early stages of the process. They were not sufficiently detailed to support the investigation of fine-scale features such as individual ice floes, rubble fields, and ice movement lines.

3.3 Satellite Imagery

Three different types of satellite imagery were used to study the ice conditions that prevailed during the 2016-17 freeze-up season: RADARSAT-2, AVHRR (Advanced Very

High Resolution Radiometer), and MODIS (Moderate Resolution Imaging Spectroradiometer). The RADARSAT-2 imagery served as the primary source of ice data, while the AVHRR imagery played a supplemental role. The MODIS imagery was used only sparingly.

General information about the progress of freeze-up was obtained from 22 publicly-available RADARSAT-2 mosaics compiled by the CIS (2017) for the period from October 3, 2016, through February 27, 2017. The mosaics, which were produced on a weekly basis, are provided as GIF files in Appendix B. Although the resolution was inadequate to support detailed analysis, the composite images provided useful data on synoptic-scale ice conditions. A representative example from mid-December, 2016, is provided as Figure 9 (CIS, 2016).



After: Canadian Ice Service, 2016

Figure 9. CIS RADARSAT-2 Mosaic for December 9-12, 2016

The most useful RADARSAT-2 images were the 20 high-resolution, geo-referenced scenes captured using the ScanSAR Wide beam mode, which provides a nominal resolution of 100 m over a nominal area of 270 x 270 nm (500 x 500 km; MacDonald, Dettwiler and Associates, 2017). The data set consisted of 10 images of the Beaufort Sea obtained between October 15, 2016, and February 26, 2017, and 10 images of the Chukchi Sea obtained between October 17, 2016, and February 28, 2017. The image characteristics were sufficient not only to track the general evolution of the ice cover during freeze-up and early winter, but also to support detailed investigations of features and phenomena that included the development of the landfast ice zone, individual multi-year ice floes, leads, and ice movement.

As the licensing agreement for the RADARSAT-2 images prohibits the distribution of the original geo-referenced TIFF files, each scene is provided in Appendix B in PDF format. A sample image of the Chukchi Sea that was acquired on January 31st, and that illustrates a prominent coastal flaw lead, is provided as Figure 10.

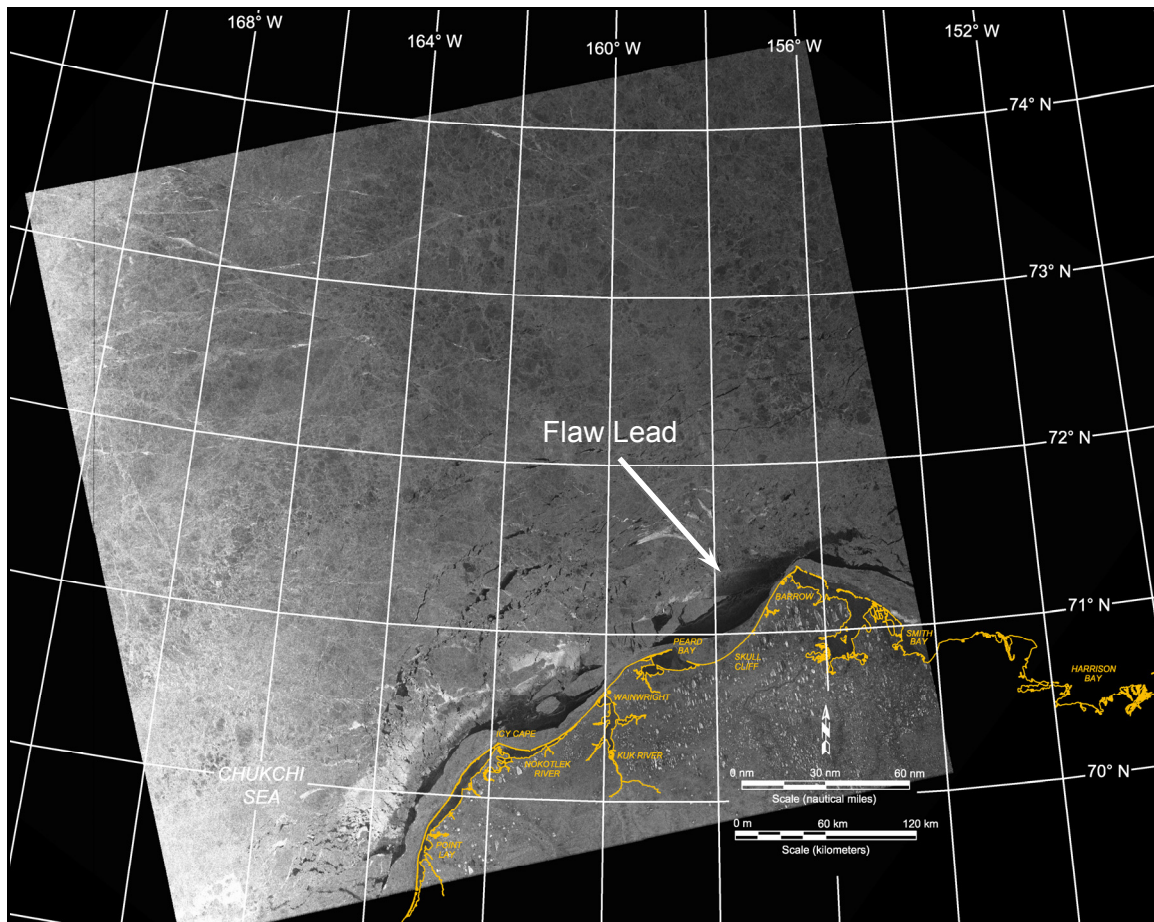
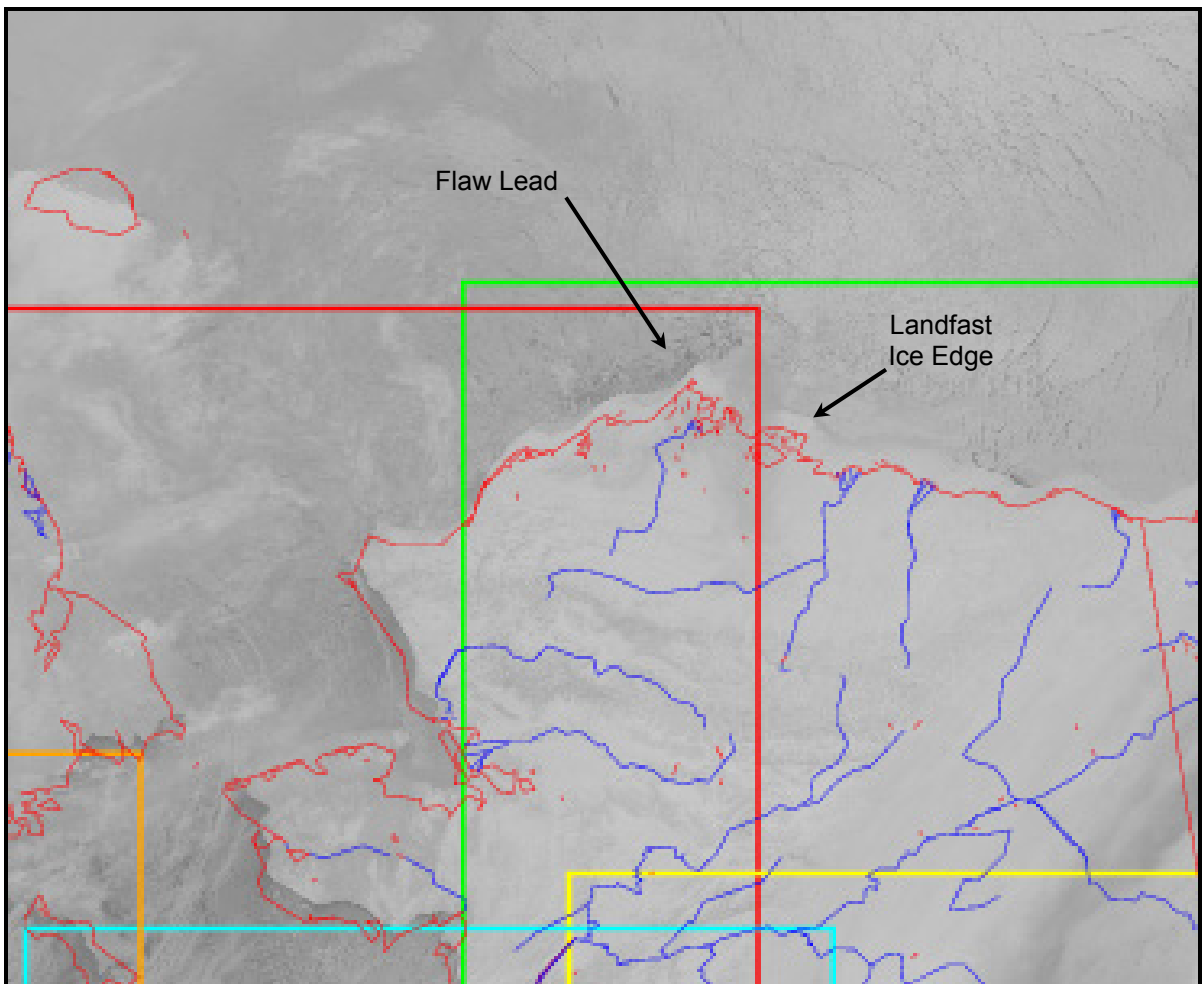


Image Source: RADARSAT-2 Data and Products © MacDonald Dettwiler and Associates Ltd., 2017 – All Rights Reserved

Figure 10. RADARSAT-2 Image of Chukchi Sea Acquired on January 31, 2017

One hundred and fifty-one AVHRR images obtained on a daily basis from October 1, 2016, through February 28, 2017, were downloaded from the National Weather Service Alaska Region Headquarters (2016 and 2017) to bridge the chronological gaps between RADARSAT-2 scenes. The utility of this imagery was limited by the sensor's 1-km resolution and inability to penetrate cloud cover. Notwithstanding these drawbacks, the high frequency of image capture (multiple scenes per day subject to suitable weather conditions) allowed large-scale changes in the ice canopy to be tracked on a short-term basis. The imagery was particularly useful in ascertaining the status of the coastal flaw lead in the Chukchi.

The AVHRR images are provided as JPG files in Appendix B. A representative example in Figure 11 shows the coastal flaw lead in the Chukchi Sea and the landfast ice edge in the Beaufort Sea on January 16, 2017.

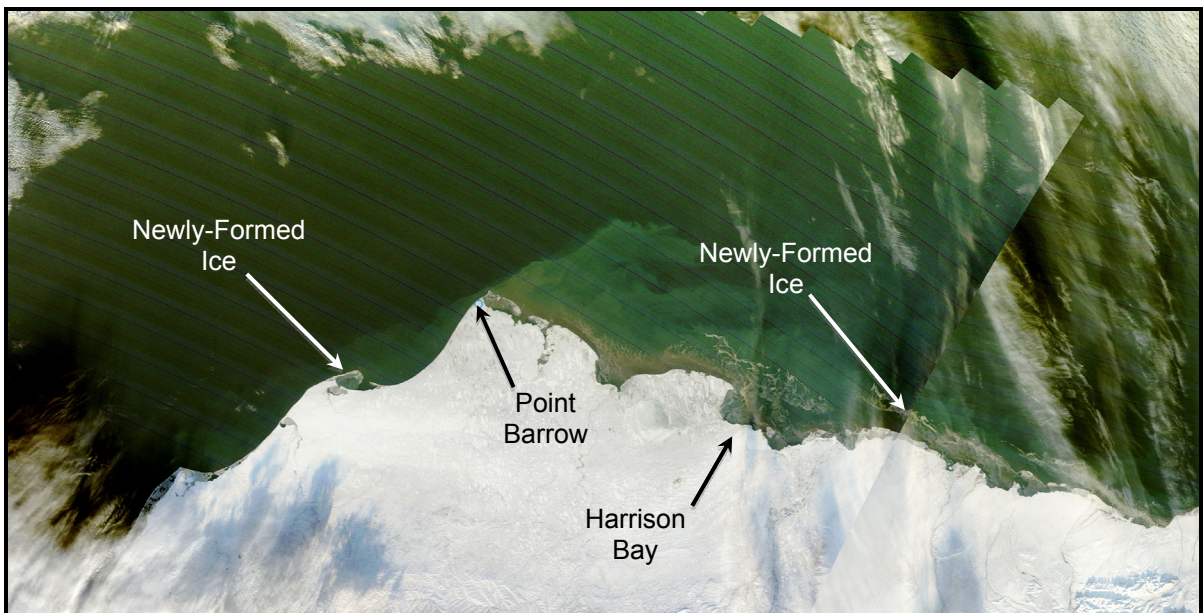


After: National Weather Service, 2017

Figure 11. AVHRR Image of Beaufort and Chukchi Seas Acquired on January 16, 2017

MODIS imagery, like AVHRR imagery, was acquired to supplement the RADARSAT-2 scenes. Unfortunately, the sensor's maximum resolution of 250 m was outweighed by its inability to penetrate cloud cover, its dependence on light in the visible spectrum, and its inability to image the region above 72°N. As a result, useful scenes were confined to two periods: (1) prior to the onset of darkness (October 1 through November 9, 2016) and (2) following the return of daylight (February 2 through 28, 2017). The sixty-seven images that were obtained from the MODIS Rapid Response website (NASA, 2016 and 2017a) are provided as JPG files in Appendix B.

Figure 12 presents a MODIS image acquired on October 26th, when ice had begun to form in the protected, nearshore waters of both basins.



After: NASA, 2016a

Figure 12. MODIS Image Acquired on October 26, 2016

3.4 Drift Buoys

As in each of the three most recent freeze-up studies (Coastal Frontiers and Vaudrey, 2014; 2015; 2016), information on ice drift was obtained from telemetry buoys monitored through the International Arctic Buoy Programme (“IABP”; Rigor, 2017). Four such buoys, all deployed during the 2016 open-water season, were present in the study area when freeze-up data acquisition began on October 1st. Their characteristics are summarized in Table 2. Note that the lengthy buoy identification numbers used by the IABP have been replaced by one-letter designations in this study in the interest of simplicity.

Table 2. IABP Drift Buoy Characteristics

Buoy Identifier		Sponsor	Period of Ice Drift ¹	Basin
This Report	IABP			
A	300234063991680	UpTempO ²	Nov. 15, 2016 – Feb. 28, 2017	Beaufort
B	300234063323700	AOML ³ -USIABP ⁴	Nov. 15 – Dec. 31, 2016	Beaufort
C	300234063320260	AOML ³ -USIABP ⁴	Nov. 30 – Dec. 31, 2016	Beaufort
D	300234063990600	UpTempO ²	Dec. 14, 2016 – Feb. 17, 2017	Chukchi

Notes:

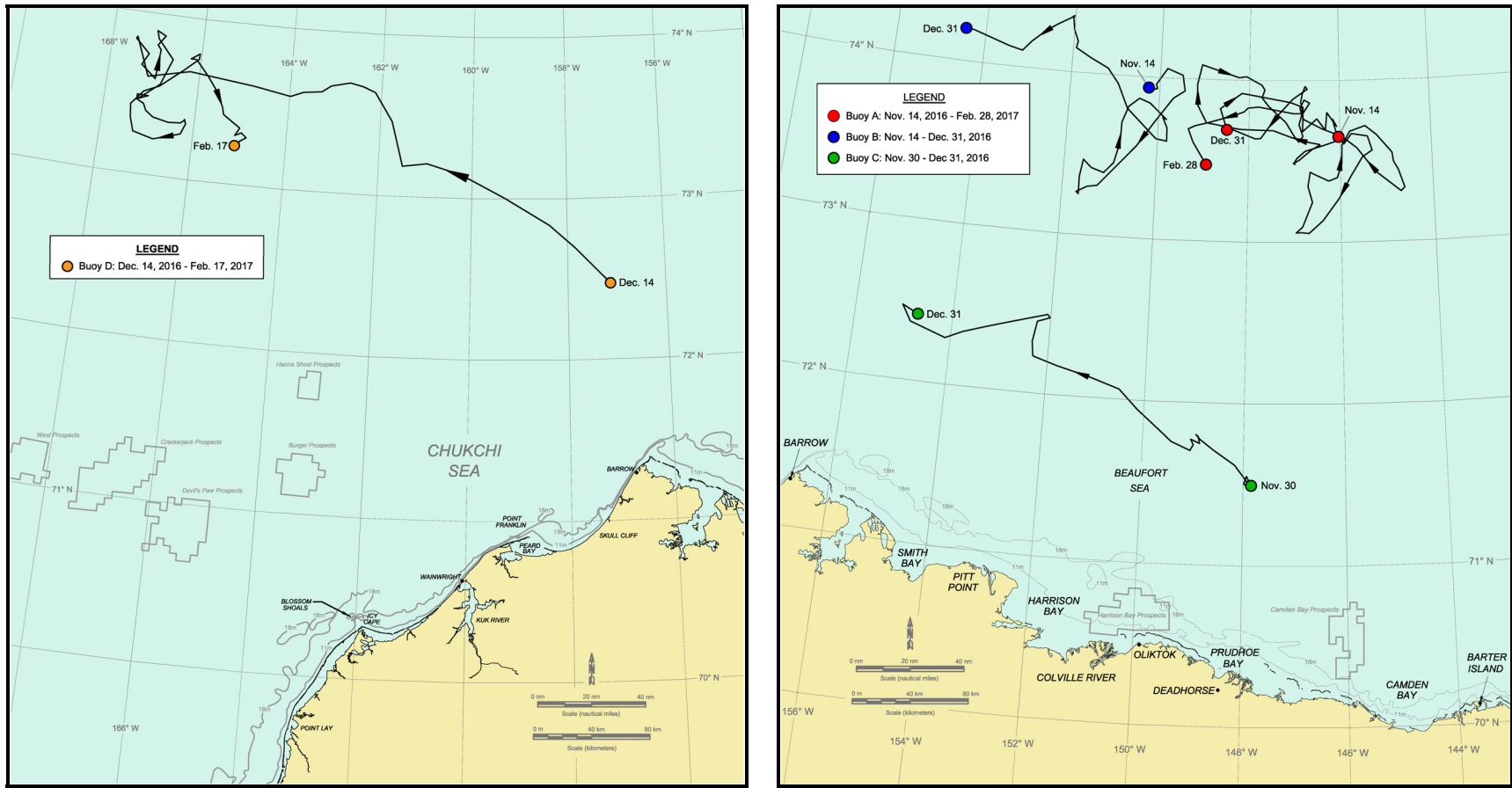
- ¹ The period in which the movement of each buoy could be used to quantify ice drift was determined by superimposing its trajectory on available satellite imagery.
- ² UpTempO Buoy Project (Polar Ice Center, 2017a).
- ³ Atlantic Oceanographic & Meteorological Laboratory (NOAA, 2017).
- ⁴ U.S. Interagency Buoy Program (Polar Ice Center, 2017b).

To determine the period in which the motion of a particular buoy could be used to quantify ice drift, its track was superimposed on the available RADARSAT-2 and AVHRR satellite images (Section 3.3). Those portions that corresponded to open water or partial ice cover were discarded, while those portions that corresponded to complete ice cover were retained. The resulting on-ice drift tracks are shown in Figure 13, which was constructed from the daily position of each buoy at midnight.

3.5 Aerial Reconnaissance Missions

Four aerial reconnaissance missions were undertaken in the Beaufort and Chukchi Seas in late February and early March to observe the conditions that prevailed at the end of freeze-up. The specific objectives of the missions were as follows:

- Obtain ground truth information to confirm and expand upon the conclusions drawn from satellite imagery;
- Investigate major features identified in the satellite imagery, such as leads, landfast ice and well-developed shear lines;
- Detect, investigate, and document small-scale features that were beneath the resolution of the satellite imagery, including ridges, rubble fields, and shoreline pile-ups.



Data Source: Rigor, 2017

Figure 13. On-Ice Drift Buoy Tracks during 2016-17 Freeze-Up Season

All of the flights were conducted using an Aero Commander 690 (Plate 1). This fixed-wing aircraft offered the benefits of an extended range, an ability to fly at relatively low speeds, a high wing that permitted unobstructed views of the ice below, and a moderate cost per flight hour.



Plate 1. Aero Commander 690 at Barrow Airport (February 27, 2017)

Each flight path was mapped using a Garmin GPSMap 78sc. To improve the accuracy of the position data, differential corrections broadcast in real time via satellite by the U.S. Government’s Wide Area Augmentation System (WAAS) were received by the GPS unit when available. Static position checks conducted at North Slope survey monuments in the past have indicated that the accuracy attainable with WAAS is about 1 m. When operated in the stand-alone mode, the GPS accuracy typically is on the order of 10 m.

The GPS position data were displayed on a base map of the study area in real time using a laptop computer and Hypack survey software. This arrangement allowed the field crew both to direct the aircraft to locations of interest identified in advance in the satellite imagery, and to record the positions of small-scale features noted during the flight.

The flight paths are shown in Drawings CFC-994-01-001, -002 and -003 (Appendix A). The drawings display the locations of ice features observed during the flights as well as those of photographs and videos taken during the flights. Each photo is identified by a unique number such as “B1-17”, and each video by unique number such as “C2-V5”. The first letter, “B” or “C”, indicates whether the flight was conducted in the Beaufort or Chukchi; the number that follows indicates which flight was involved. The second number indicates the order in which the photo or video was obtained during that flight. Hence,

C2-V5 designates the 5th video acquired during the second Chukchi Sea reconnaissance flight.

The photographs and videos are provided in digital form in Appendix B, with the file names corresponding to the identification numbers shown on the drawings. The ice features observed during the flights are denoted on the drawings using the abbreviations listed in Table 3, while the objective and path of each flight are summarized below.

Table 3. Abbreviations for Ice Features

Ice Feature	Abbreviation
Active Shear Line	ASL
Broken Ice	BRK
Crack	CRK
Finger Rafting	FR
First-Year Ice (> 30 cm)	FY
Inactive Shear Line	ISL
Lead	LD
Landfast Ice Edge	LFI
Nilas (< 10 cm)	NLS
Open Water (concentration in %)	OW (_%)
Pancake Ice	PNK
Pile-Up (height, encroachment in m)	P/U (_,_m)
Polynya	PLN
Refrozen Lead	RFL
Ridge (height in m)	RDG (_m)
Rubble (height in m)	RBL (_m)
Thermal Crack (height in m)	TCK (_m)
Undeformed Ice	UDI
Young Ice (10-30 cm)	YNG

Note: The prefixes “i” and “m” are used to indicate intermittent features and multiple features, respectively (*i.e.*, “iRBL” indicates intermittent rubble).

February 2017 Beaufort Sea Flight No. 1 (“B1” on Drawing CFC-994-01-001)

The first reconnaissance flight was undertaken with the Aero Commander 690 on February 23rd to observe the ice conditions in the Central Beaufort Sea. The route is outlined below:

- Deadhorse Airport
- Transit north
- Barrier islands from Cross to North Star (heading east)
- Sivulliq Development prospective pipeline route
- Flaxman Island, Brownlow Point, and adjacent spit
- Transit east across southern Camden Bay
- Transit northwest across northern Camden Bay
- Camden Bay Prospects
- Transit southwest to vicinity of McClure Islands
- Transit northwest until 12 nm (22 km) off Cross Island, and then west to Stamukhi Shoal.
- Harrison Bay Prospects
- Thetis Island
- Spy Island Drillsite (SID)
- Barrier islands from Spy to Stump (heading east)
- Northstar Production Island
- Reindeer Island
- West Dock Causeway
- Prudhoe Bay
- Deadhorse Airport
- Flight time = 3.9 hr.

February 2017 Beaufort Sea Flight No. 2 (“B2” on Drawing CFC-994-01-002)

A reconnaissance flight was undertaken on February 27th to observe the ice conditions in the Western Beaufort Sea. The flight path is summarized below:

- Deadhorse Airport
- Transit northwest over land
- Oooguruk Offshore Drillsite (ODS)
- Harrison Bay Prospects
- Weller Bank
- Transit northwest until 20 nm (37 km), and then southwest
- Smith Bay

- Transit northwest at distances of 1 to 12 nm (2 to 22 km) offshore
- Transit south
- Barrow Airport
- Flight time = 1.7 hr.

February 2017 Chukchi Sea Flight No. 1 (“C1” on Drawing CFC-994-01-003)

Favorable weather conditions allowed for a second reconnaissance mission to be undertaken on February 27th. The flight, which covered the offshore portion of the northeast Chukchi Sea, proceeded in the following manner:

- Barrow Airport
- Transit northwest
- Hanna Shoal
- Transit southwest
- Hanna Shoal Prospects
- Transit south-southeast
- Burger Prospects
- Transit west and then south to within 10 nm (19 km) of Devil’s Paw Prospects (Note: closer approach to Devil’s Paw was precluded by the need to remain within range of the North Slope Borough Search and Rescue helicopter.)
- Transit east-northeast
- Barrow Airport
- Flight time = 2.5 hr.

March 2017 Chukchi Sea Flight No. 2 (“C2” on Drawing CFC-994-01-003)

The fourth reconnaissance flight was undertaken on March 1st to observe nearshore ice conditions and shoreline pile-ups between Barrow and Point Lay, a region where pipelines from the offshore prospects could make landfall. The flight described the following path:

- Barrow Airport
- Transit southwest to Point Lay at distances of 1 to 19 nm (2 to 35 km) offshore
- Barrier islands fronting Kasegaluk Lagoon
- Shoreline from Kasegaluk Lagoon to Point Franklin
- Seahorse Islands and Peard Bay
- Shoreline from Peard Bay to Barrow
- Barrow Airport
- Flight time = 2.8 hr.

As in each of the seven prior freeze-up studies (Coastal Frontiers and Vaudrey, 2010; 2011; 2012a; 2013; 2014; 2015; 2016), the reconnaissance flights undertaken in 2016-17 provided invaluable opportunities to confirm and refine the findings derived from satellite imagery, and to expand upon those findings with respect to small-scale features and processes.

4. BEAUFORT SEA FREEZE-UP

Section 4.1 provides an overview of the 2016-17 freeze-up season in the Alaskan Beaufort Sea, while Sections 4.2 through 4.5 present a more in-depth analysis of the conditions that prevailed from late summer 2016 through February 2017.

4.1 Overview

Air Temperatures: When compared with the long-term average values for the 30-year period from 1981 through 2010, the air temperatures at Deadhorse Airport were exceptionally warm from the beginning of October until the last week in November. During these first two months of freeze-up, the daily average values exceeded the normal range on 45 occasions and fell below on only two. Normal to subnormal temperatures prevailed in early December, but unseasonably warm temperatures returned at mid-month and again at the end. January was a month of extremes, with the daily average temperatures ranging from 31° to -38°F (-1 to -39°C). Warm temperatures in late January continued through the first eight days of February, followed by normal or near-normal temperatures thereafter. Over the entire five-month study period (October through February), the daily average air temperature exceeded the normal range on 87 days (58% frequency) and dropped below on only 18 days (12% frequency).

Winds: Table 4 presents the daily average wind speeds and directions recorded at Deadhorse Airport during the 2016-17 freeze-up season. Easterlies predominated in October, with a frequency of 65%. Westerlies prevailed in each of the four months that followed, with frequencies ranging from 65% to 77%. Over the entire five-month study period, westerlies outnumbered easterlies by a margin of 64% to 36%. The average monthly speeds were clustered in a relatively narrow range, from a low of 9 kt (5 m/s) in November and December to a high of 12 kt (6 m/s) in January and February.

Table 4. Beaufort Sea Wind Characteristics, October 2016 – February 2017

Month	Days		Average Speed (kt)
	Easterly	Westerly	
October	20	11	10
November	10	20	9
December	11	20	9
January	7	24	12
February	7	21	12
Total Days	55	96	n/a
Frequency (%)	36	64	n/a

Note: Table 4 is based on the daily average values recorded at Deadhorse Airport.

Storms: The characteristics of all storms with a daily average sustained wind speed exceeding 15 kt (8 m/s) at Deadhorse Airport are presented in Table 5. Thirteen such events occurred from October 2016 through February 2017, consisting of seven easterlies and six westerlies. The most severe storm, a westerly with a maximum wind speed of 28 kt (14 m/s) and duration of seven days, occurred in early January, while the highest numbers of storms (four) and storm-days (11) occurred in February.

Table 5. Beaufort Sea Storm Characteristics, October 2016 – February 2017¹

Month	Day	Duration (days)	Maximum Wind Speed (kt) ²	
			Easterly	Westerly
October	8	1	17	
	11-14	4	23	
November	3-4	2	27	
	11	1	17	
December	15	1	17	
	30-31	2		17
January	5-11 ^{3,4}	7		28
	14	1	18	
	21	1		17
February	Jan 31-Feb 3	4		17
	8-11 ⁵	4		23
	25-26	2	26	
	28 ⁶	1		18
Total Duration (days)		31		
Total Number of Events			7	6

Notes:

- ¹ Table 5 includes all storm events with a daily average sustained wind speed exceeding 15 kt (8 m/s) at Deadhorse Airport.
- ² “Maximum Wind Speed” refers to highest daily average sustained wind speed that occurred during each storm event.
- ³ Daily average wind speed decreased to 14 kt on January 6th but freshened to 22 kt on January 7th.
- ⁴ Daily average wind speed decreased to 11 kt on January 8th but freshened to 16 kt on January 9th.
- ⁵ Daily average wind speed decreased to 14 kt on February 9th but freshened to 23 kt on February 10th.
- ⁶ Storm continued through March 4th and attained a maximum daily average wind speed of 29 kt, but four days in March are not included because they fall outside study period.

Ice Cover: Freeze-up began in mid-October with the formation of ice in the semi-protected waters adjacent to the coast. Complete ice coverage in the nearshore region occurred on November 7th, followed by complete coverage in the entire Alaskan Beaufort Sea on November 23rd.

Ice Thickness: The thickness of undeformed first-year ice at the end of each month was estimated using the relationship of Lebedev (Bilello, 1960) in concert with the freezing degree days (FDD) accumulated at Deadhorse Airport (Table 1). The relationship is as follows:

$$t = 0.94(\Sigma\text{FDD})^{0.58} \quad (1)$$

where:

- t = ice thickness in cm
- ΣFDD = accumulated freezing-degree days relative to 29°F

Although Lebedev originally calculated FDD relative to 32°F, ice thickness measurements in the Beaufort Sea obtained by Vaudrey and Associates, Inc., have indicated that Equation (1) provides more accurate results if FDD are referenced to 29°F, the approximate freezing point of sea water.

The computed values of ice thickness for the 2016-17 winter season are provided in Table 6, which indicates that undisturbed first-year ice attained a maximum thickness of 148 cm on May 21st. Subsequent to that date, the daily average air temperatures equaled or exceeded 29°F.

Landfast Ice: Landfast ice began to develop during the last week in October. Substantial expansion followed in November, resulting in coverage of all of the coastal lagoons and a significant portion of Harrison Bay by month-end. The expansion stalled in December, however, with gains during the first half of the month erased by losses during the second in response to westerly winds and a two-day westerly storm.

The landfast ice edge remained nearly stationary during the first half of January despite the occurrence of a prolonged westerly storm, indicating that it had become well-grounded. It then moved seaward to the vicinity of the 11-m isobath in late January, reflecting moderate easterly winds. After another period of minimal change, the ice edge advanced to the 18-m isobath in late February in response to a strong easterly storm. This advance was noteworthy in that it marked the first occasion during the 2016-17 freeze-up season on which the ice reached its customary anchor points on Weller Bank and Stamukhi Shoal.

Table 6. Beaufort Sea Computed Ice Thickness, September 2016 – May 2017¹

Date	FDD	Accumulated FDD	Ice Thickness ² (cm)
30 September 2016	0	0	0
31 October 2016	176	176	19
30 November 2016	623	799	45
31 December 2016	1,098	1,897	75
31 January 2017	1,086	2,983	97
29 February 2017	1,126	4,109	117
31 March 2017	1,211	5,320	136
30 April 2017	716	6,036	147
21 May 2017	108	6,144	148

Notes:

¹ Table 6 is based on the daily average air temperature data recorded at Deadhorse Airport.

² Ice thickness is computed from accumulated FDD using method of Lebedev (Bilello, 1960).

Ice Pile-Ups: Thirty-eight ice pile-ups formed in the central portion of the Alaskan Beaufort Sea during the 2016-17 freeze-up season (Table 7). One was located on the Ooguruk Offshore Drillsite (ODS), one on the Spy Island Drillsite (SID), one on Northstar Production Island, two on Thetis Island (a natural barrier island in Harrison Bay), and 33 on natural barrier islands and shoals to the east of Prudhoe Bay.

The pile-up heights, which ranged from 1 to 8 m above sea level, and encroachment distances, which ranged from negligible to 12 m onto the subaerial beach, were unexceptional by historical standards. Several of the features extended alongshore for substantial distances, however, including a maximum length of 5.9 km on a spit that emanates from Point Brownlow. Twenty-five of the pile-ups arrived from the north, northeast, or east, while the remaining 13 arrived in limited numbers from the southeast (1), south (3), southwest (3) and northwest (6). The thicknesses of the ice blocks comprising the piles were estimated to range from 20 to 40 cm.

Table 7. Ice Pile-Ups on Beaufort Sea Coast during 2016-17 Freeze-Up Season

No.	Location	Formation Date	Arrived From	Length¹ (m)	Height² (m)	Encroachment³ (m)
1	Oooguruk ODS	Nov 10-12	NW	100	3	5
2	Thetis Island	Nov 10-12	NE	350	1	2
3	Thetis Island	Nov 10-12	NE	100	1	0
4	Nikaitchuq SID	Nov 10-12	S	100	2	3
5	Northstar Production Is.	Nov 10-12	N	150	3	7
6	Cross Island	Nov 10-12	SW	150	2	3
7	Cross Island	Nov 10-12	NW	450	3	5
8	Cross Island	Nov 10-12	NE	950	2	8
9	Cross Island	Nov 10-12	NE	400	2	5
10	Dinkum Sands (Shoal)	Nov 10-12	E	500	8	n/a
11	Narwhal Island	Nov 10-12	NW	150	4	5
12	Narwhal Island	Nov 10-12	NE	650	4	5
13	Narwhal Island	Nov 10-12	NE	150	2	5
14	Narwhal Island	Nov 10-12	S	1,000	2	3
15	Jeanette Island	Nov 10-12	NE	100	5	6
16	Jeanette Island	Nov 10-12	NE	300	3	5
17	Jeanette Island	Nov 10-12	NE	100	4	5
18	Karluk Island	Nov 10-12	NE	450	2	3
19	Pole Island	Nov 10-12	SE	700	2	5
20	Pole Island	Nov 10-12	NE	1,800	1	3
21	Pole Island	Nov 10-12	NE	1,500	1	6
22	Pole Island	Nov 10-12	NE	400	1	2

(continued)

Table 7. Ice Pile-Ups on Beaufort Sea Coast during 2016-17 Freeze-Up Season (continued)

No.	Location	Formation Date	Arrived From	Length ¹ (m)	Height ² (m)	Encroachment ³ (m)
23	Belvedere Island	Nov 10-12	E	100	2	3
24	Belvedere Island	Nov 10-12	NE	400	1	3
25	Belvedere Island	Nov 10-12	NE	200	1	2
26	Challenge Island	Nov 10-12	NW	800	2	3
27	Alaska Island	Nov 10-12	NE	5,300	2	8
28	Alaska Island	Nov 10-12	S	200	2	0
27	Duchess Island	Nov 10-12	NW	400	2	5
28	Duchess Island	Nov 10-12	NE	2,500	6	12
29	Duchess Island	Nov 10-12	SW	100	2	0
30	Duchess Island	Nov 10-12	SW	100	2	0
33	Flaxman Island	Nov 10-12	NW	1,200	2	3
34	Flaxman Island	Nov 10-12	NE	350	3	3
35	Flaxman Island	Nov 10-12	NE	450	3	2
36	Pt. Brownlow West Spit	Nov 10-12	NE	2,600	2	0
37	Pt. Brownlow East Spit	Nov 10-12	NE	3,300	2	3
38	Pt. Brownlow East Spit	Nov 10-12	NE	5,900	2	2

Notes:

- ¹ “Length” indicates alongshore extent of pile-up.
- ² “Height” indicates maximum height of pile-up relative to MSL.
- ³ “Encroachment” indicates distance ice advanced onto subaerial beach.

As discussed by Coastal Frontiers and Vaudrey (2012b), pile-ups tend to form when the ice loses confinement, typically in response to abrupt changes in wind direction accompanied by speeds greater than or equal to 15 kt (8 m/s). The pile-ups listed in Table 7 are believed to have resulted from such an event that occurred from November 10th through 12th. During this period, westerly winds with one-hour sustained speeds to 10 kt (5 m/s) veered through north to east, freshened to 27 kt (14 m/s), and then continued veering through south and returning to the west while diminishing to between 5 and 15 kt (3 and

8 m/s). Although some of the pile-ups could have resulted from other, similar wind shifts, the available RADARSAT-2 images suggest that insufficient ice was present to produce pile-ups prior to early November, and the ice in the immediate vicinity of the pile-up sites tended to remain landfast after the November 10th-12th event.

Multi-Year Ice: Other than two patches of second-year ice that were located in the vicinity of Point Barrow at the beginning of October but moved to the northwest and dissipated by mid-month, multi-year ice remained absent from the nearshore region of the Alaskan Beaufort Sea throughout the five-month study period. The minimum separation between multi-year pack ice and the coast, 170 nm (315 km), occurred off Barter Island at the end of February.

Ice Drift: Figure 14 shows the trajectories of three drift buoys that were embedded in the Beaufort Sea pack ice during a portion of the five-month study period. A monthly average drift rate was computed for each buoy based on its first and last position in each month for which data were available, with the results presented in Table 8. The buoys had been deployed in open water prior to the start of the study period, and were monitored through the International Arctic Buoy Program (“IABP”; Section 3.4).

In keeping with the set of the Beaufort Gyre, all three buoys experienced net displacements to the west. The displacements were small and the associated drift rates were low, however, reflecting the countervailing influence of the westerly winds that predominated in each of the four months in which data were obtained (November through February). The monthly average drift rates ranged from 0.8 to 4.5 nm/day (1.5 to 8.3 km/day).

Table 8. Beaufort Sea Ice Drift, November 2016 - February 2017

Month	No. of Buoys	Monthly Average Speed (nm/day)		
		Maximum	Minimum	Average
November	2	2.6	1.4	2.0
December	3	4.5	1.2	2.6
January	1	0.8	0.8	0.8
February	1	1.3	1.3	1.3
Average				1.7

Note: Monthly average speeds were derived for periods that ranged from 16 to 31 days (based on the availability of IABP drift buoys).



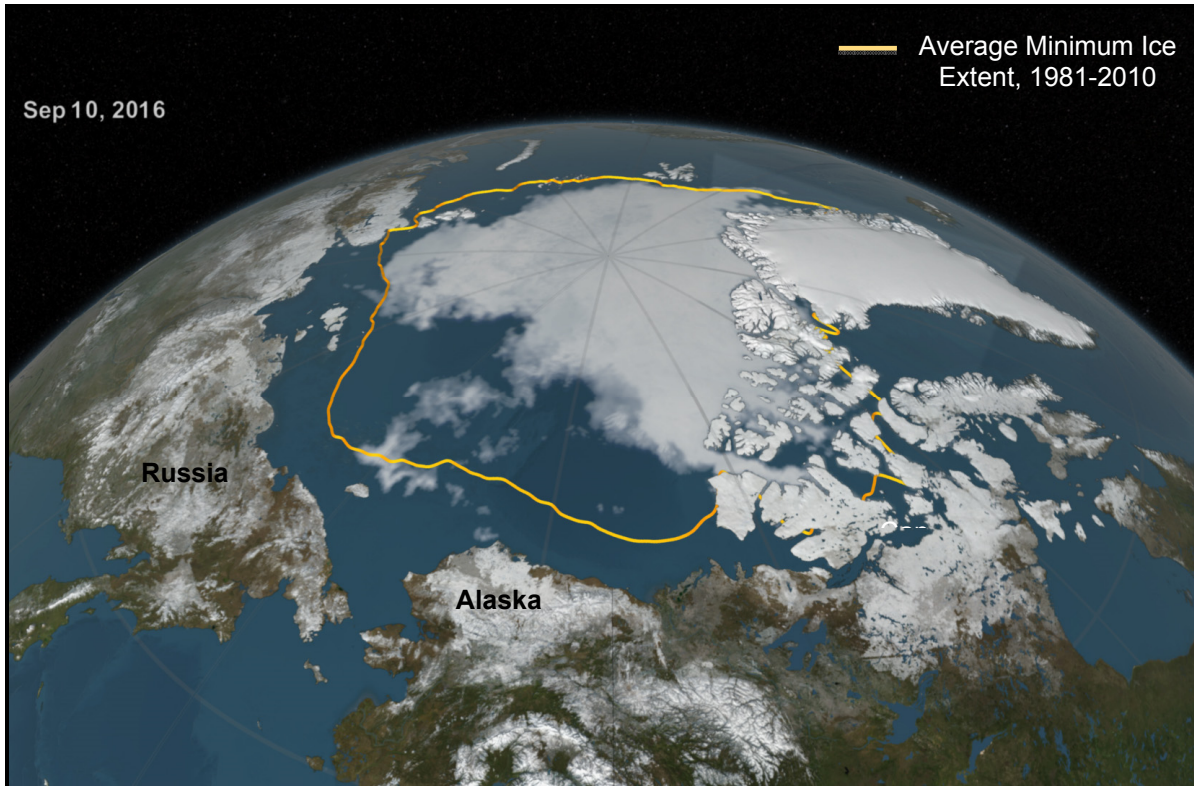
Data Source: Rigor, 2017

Figure 14. Beaufort Sea Drift Buoy Tracks, November 2016 – February 2017

4.2 Late Summer 2016

The ice cover in the Alaskan Beaufort Sea diminished slowly in June, July, and early August, reflecting the prevalence of cloudy skies and reduced solar insolation (NASA, 2017b). The pace quickened appreciably in late August and early September, however, creating a large expanse of open water off the coast. This rapid reduction in the extent of the sea ice may have resulted from two strong cyclones that consolidated the remaining ice

canopy and initiated upward mixing of warm ocean water as they traversed the region (National Snow & Ice Data Center, 2016). As shown in Figure 15, the open water was interspersed with patches of ice located primarily to the northwest of Point Barrow.



After: NASA, 2017b

Figure 15. Large Expanse of Open Water off Alaskan Beaufort Sea Coast on September 10, 2016

The minimum extent of the pack ice, 4.14 million km² (Figure 16), occurred on September 10, 2016 (National Snow & Ice Data Center, 2016; “extent” refers to the area in which ice covers at least 15% of the ocean surface). This value ties that in 2007 as the second lowest since the acquisition of satellite-based data began in 1979. The smallest extent, 3.39 km², occurred in 2012 (Table 9). It is noteworthy that the ice extents recorded in each of the last ten years represent the ten lowest values on record.

Based on satellite data compiled by NASA (2017b), the average extent of the Arctic sea ice in September is declining at a rate of 13.3% per decade relative to the 1981-2010 average. As illustrated in Figure 17, substantial interannual variations have occurred around this long-term trend.



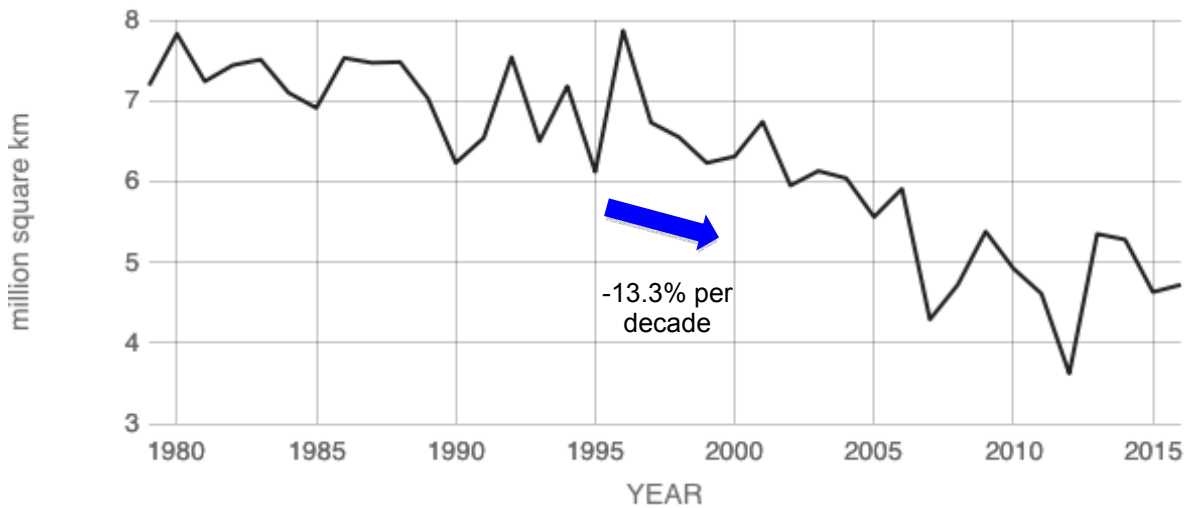
After: National Snow & Ice Data Center, 2016

Figure 16. Sea Ice Minimum Extent on September 10, 2016

Table 9. Minimum Arctic Sea Ice Extent, 2007-2016

Rank	Year	Minimum Ice Extent (km ²)	Date
1	2012	3.39	Sep 17
2	2016	4.14	Sep 10
	2007	4.15	Sep 18
4	2011	4.34	Sep 11
5	2015	4.43	Sep 09
6	2008	4.59	Sep 20
7	2010	4.62	Sep 21
8	2014	5.03	Sep 17
9	2013	5.06	Sep 13
10	2009	5.12	Sep 13
Decadal Average		4.49	Sep 15

After: National Snow & Ice Data Center, 2016



Source: NASA, 2017b

Figure 17. Average Sea Ice Extent in September, 1979-2016

4.3 Early Freeze-Up

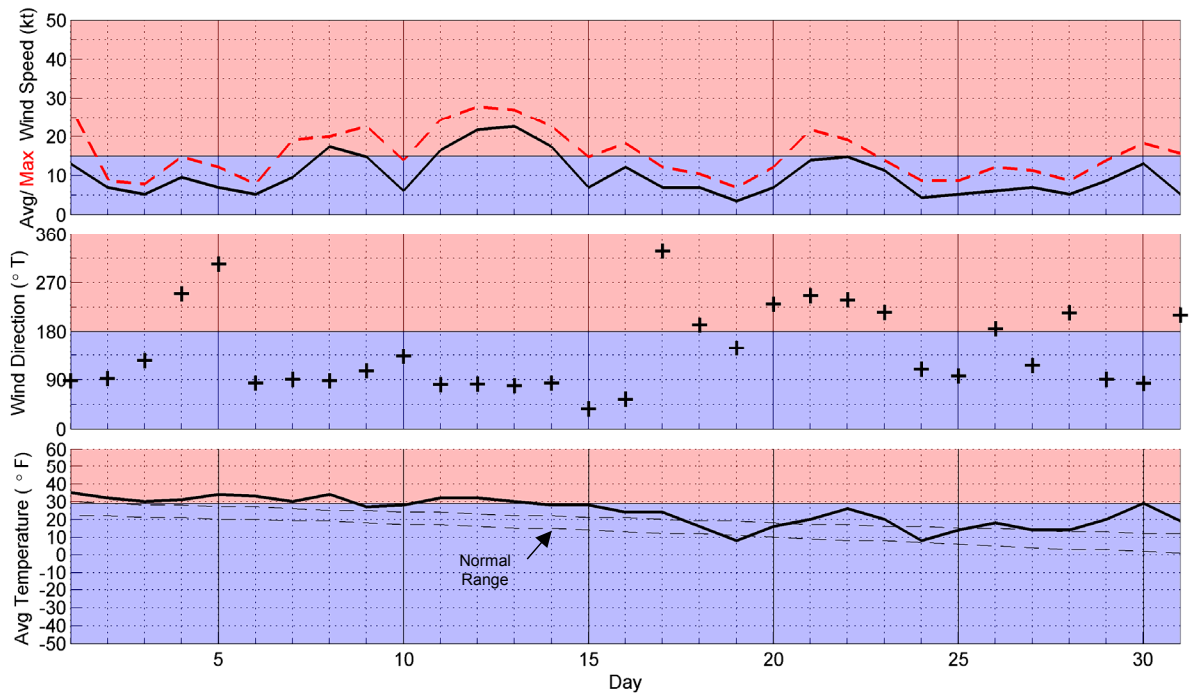
4.3.1 October 2016

Meteorological Conditions: The daily values of average sustained wind speed, maximum sustained wind speed, average wind direction, and average air temperature at Deadhorse Airport are shown in Figure 18 along with the normal range of air temperatures defined by the average values of the daily highs and lows from 1981 through 2010. The significance of the red and blue color bands in this and all subsequent meteorological plots is illustrated in Table 10. Unless stated otherwise, the wind speeds discussed in the text refer to the daily average values rather than the daily maximum values or hourly values.

The air temperatures in October were exceptionally warm by historical standards, with the daily average values exceeding the normal range on 25 occasions and falling below on only one (October 19th). The warm weather peaked on the 30th, when the daily average temperature of 29°F (-2°C) exceeded the long-term average by 17°F (9°C). The average temperature for the entire month was 24°F (-4°C).

Easterly winds predominated in October, occurring on 20 days versus 11 days for westerlies. The speeds were relatively low, with a monthly average value of 10 kt (5 m/s) and only two storm events (Table 5):

- October 8th: one-day easterly with maximum speed of 17 kt (9 m/s);
- October 11th-14th: four-day easterly with maximum speed of 23 kt (12 m/s).



Source: Weather Underground, 2016

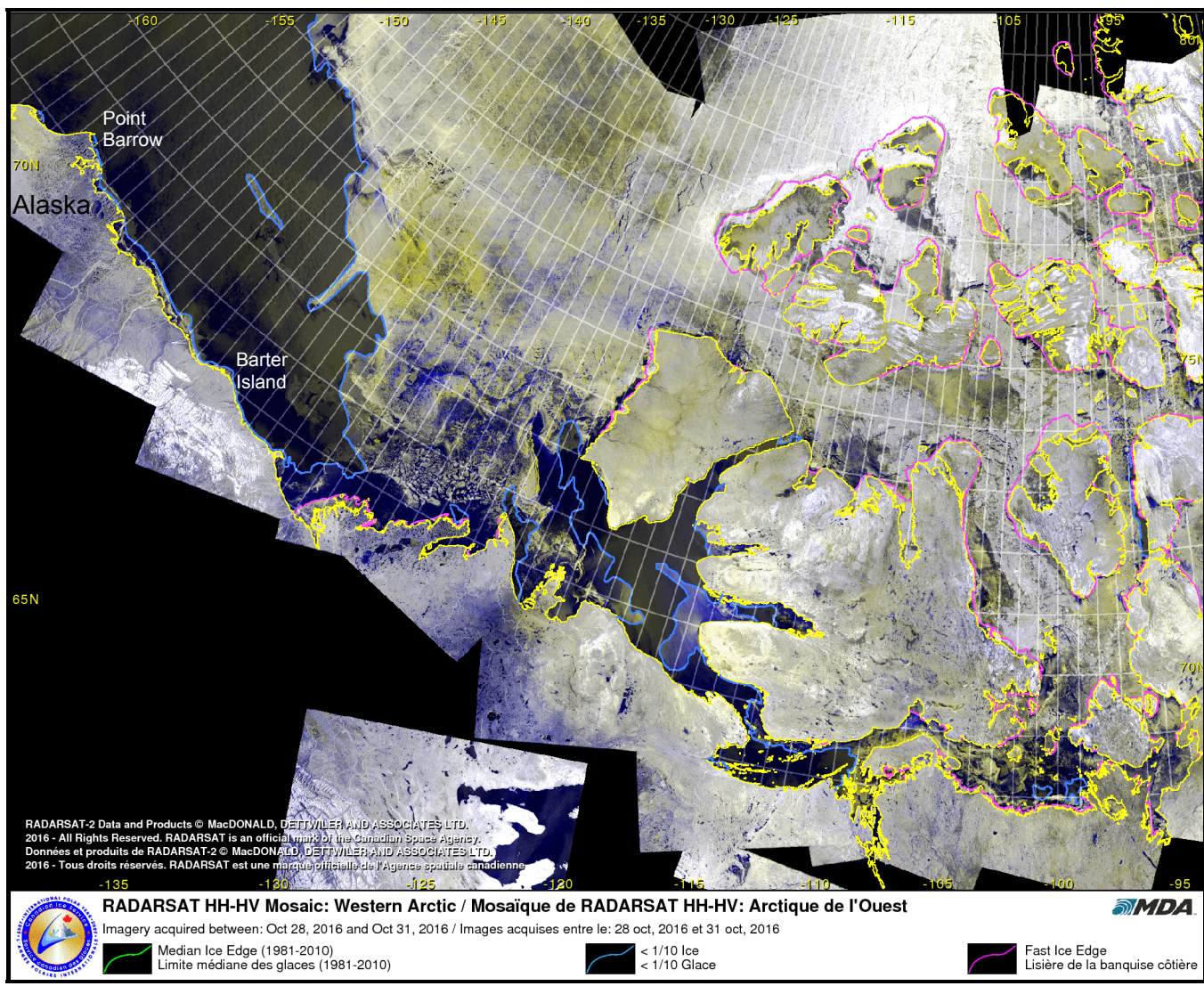
Figure 18. Meteorological Conditions at Deadhorse Airport in October 2016

Table 10. Significance of Color Bands in Plots of Meteorological Conditions

Parameter	Band Color	
	Blue	Red
Wind Speed	≤ 15 kt	> 15 kt (Storm)
Wind Direction	Easterly	Westerly
Air Temperature	$\leq 29^{\circ}\text{F}$ (Freezing Point of Seawater)	$>29^{\circ}\text{F}$

Ice Cover: Reflecting the warm air temperatures, ice did not begin to appear in the semi-protected waters adjacent to the coast until mid-October, and remained sparse for the rest of the month. Offshore, the pack ice advanced slowly to the south, with the majority located north of the 73°N parallel at month-end. The two masses of ice were separated by a large wedge of open water approximately 180 nm (334 km) wide off Barter Island and more than 250 nm (463 km) wide off Point Barrow (Figure 19).

Ice Thickness: As indicated in Table 6, the computed thickness of undisturbed first-year ice at the end of October was 19 cm.



Source: CIS, 2016

Figure 19. CIS RADARSAT-2 Mosaic of Beaufort Sea for October 31, 2016

Landfast Ice : Based on an analysis of MODIS and RADARSAT-2 imagery, landfast ice began to develop off the Alaskan Beaufort Sea coast during the last week in October. As shown in Figure 20, the landfast ice zone at the end of the month was limited to small patches in Smith and Harrison Bays, and off Pitt Point and the East Channel of the Sagavanirktok River.

Multi-Year Ice: The southern boundary of the multi-year pack ice remained well offshore in October, typically ranging from 75°N to 77°N. The minimum distance from the coast, 240 nm (445 km), occurred off Barter island during the third week of the month.

Although two relatively small patches of second-year ice were located in close proximity to Point Barrow at the beginning of October (Figure 21), they drifted to the northwest and dissipated over the next two weeks. The patches were composed of first-year ice that had survived the summer melt season.

4.3.2 November 2016

Meteorological Conditions: The meteorological conditions at Deadhorse Airport are summarized in Figure 22. The warm air temperatures that prevailed in October continued until the last week in November, producing 20 days on which the average value exceeded the normal range. The sole occasion on which the daily average fell below normal was the last day of the month. The average temperature for the month was 8°F (-13°C).

The predominance of easterly winds in October was reversed in November, with westerlies occurring on 20 of the 30 days. The speeds were relatively low, averaging 9 kt (5 m/s). The storm population was limited to two brief easterlies, both of which occurred during the first half of the month (Table 5):

- November 3rd-4th: two-day easterly with maximum speed of 27 kt (14 m/s);
- November 11th: one-day easterly with maximum speed of 17 kt (9 m/s).

Ice Cover: During the first week in November, the pack ice advanced rapidly to the south while the band of ice along the coast expanded to the north. Based on the information presented in the CIS ice charts (Figure 23), complete freeze-up in the nearshore region occurred on or about November 7th, when 280 FDD had accumulated at Deadhorse Airport. (Note: for the purpose of establishing a date for freeze-up, the “nearshore region” is defined as that portion of the Alaskan Beaufort Sea that typically becomes covered with landfast ice.)

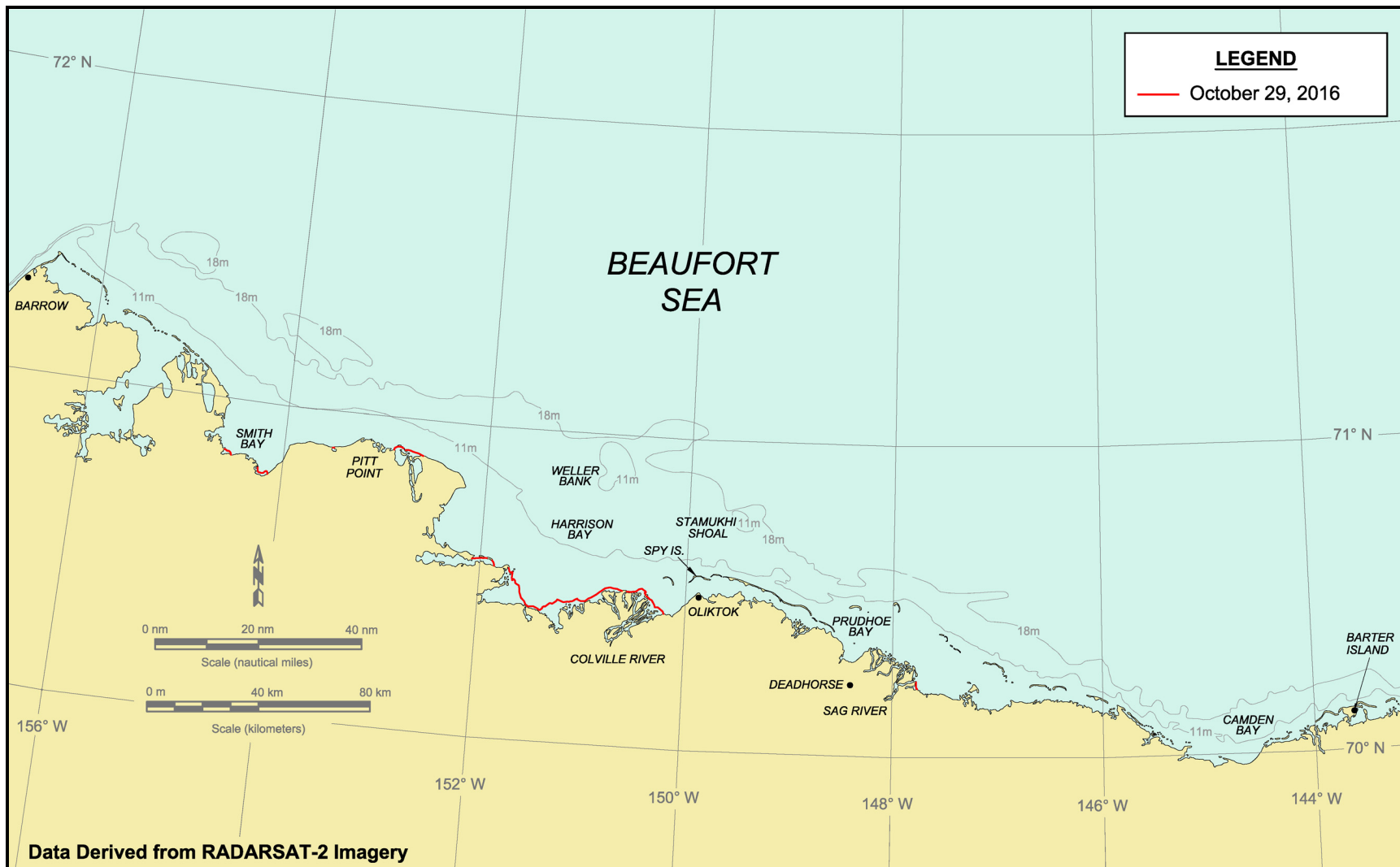
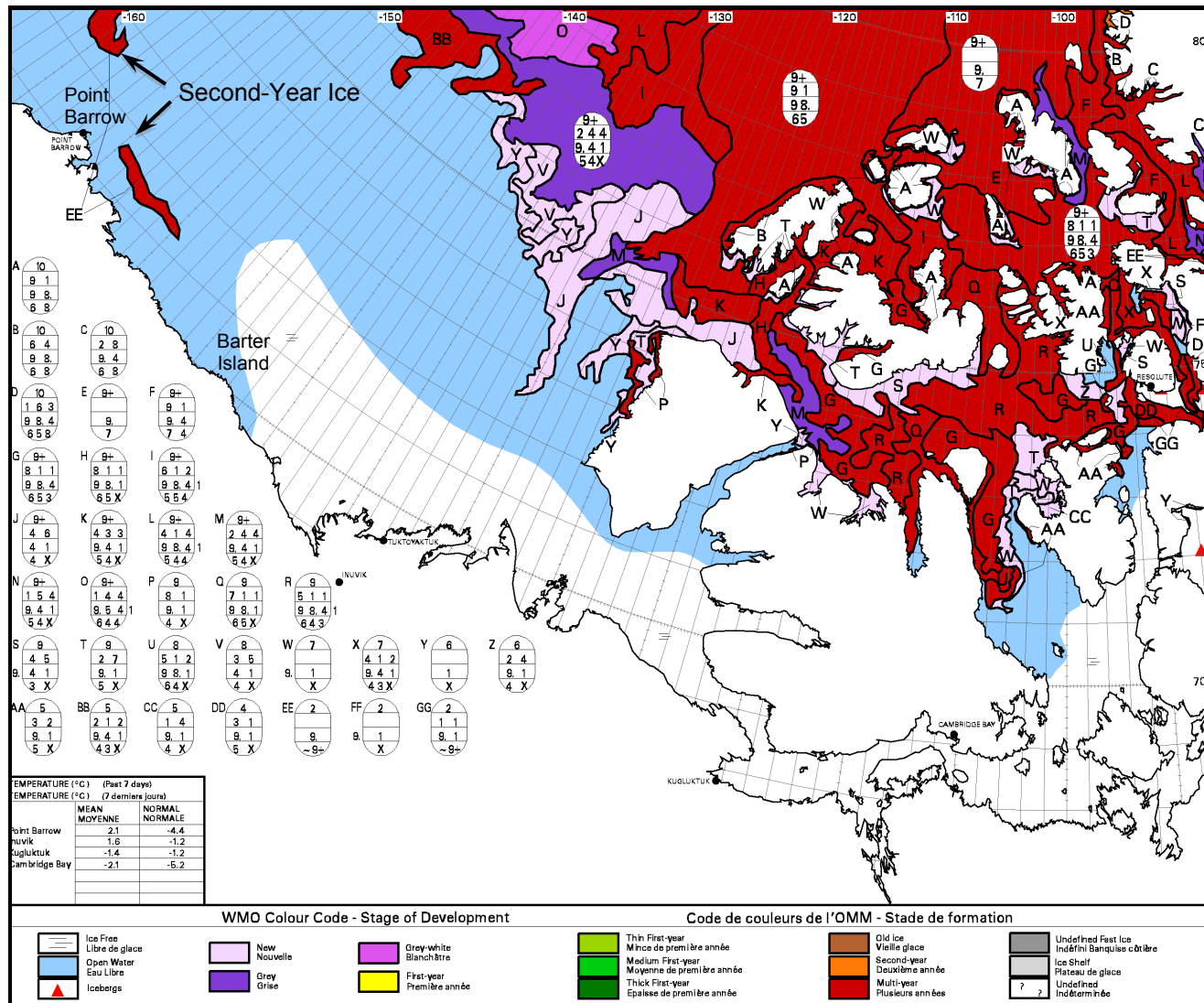
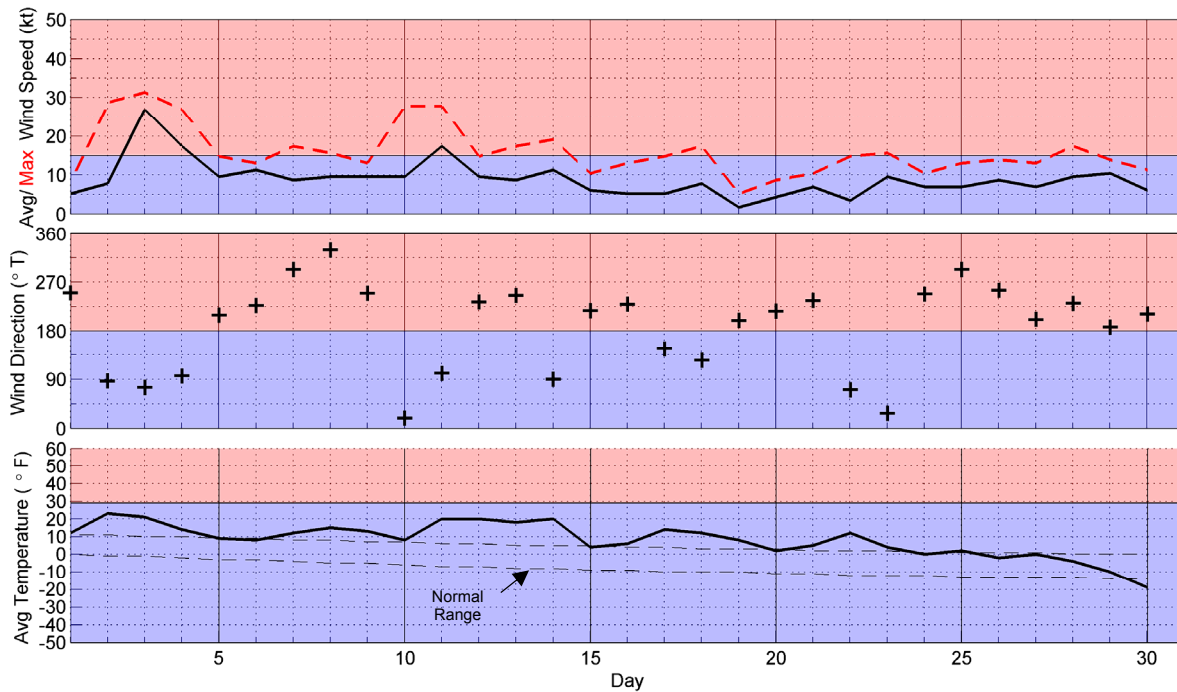


Figure 20. Beaufort Sea Landfast Ice Edge in October 2016



Source: CIS, 2016

Figure 21. CIS Stage-of-Development Ice Chart of Beaufort Sea for October 3, 2016



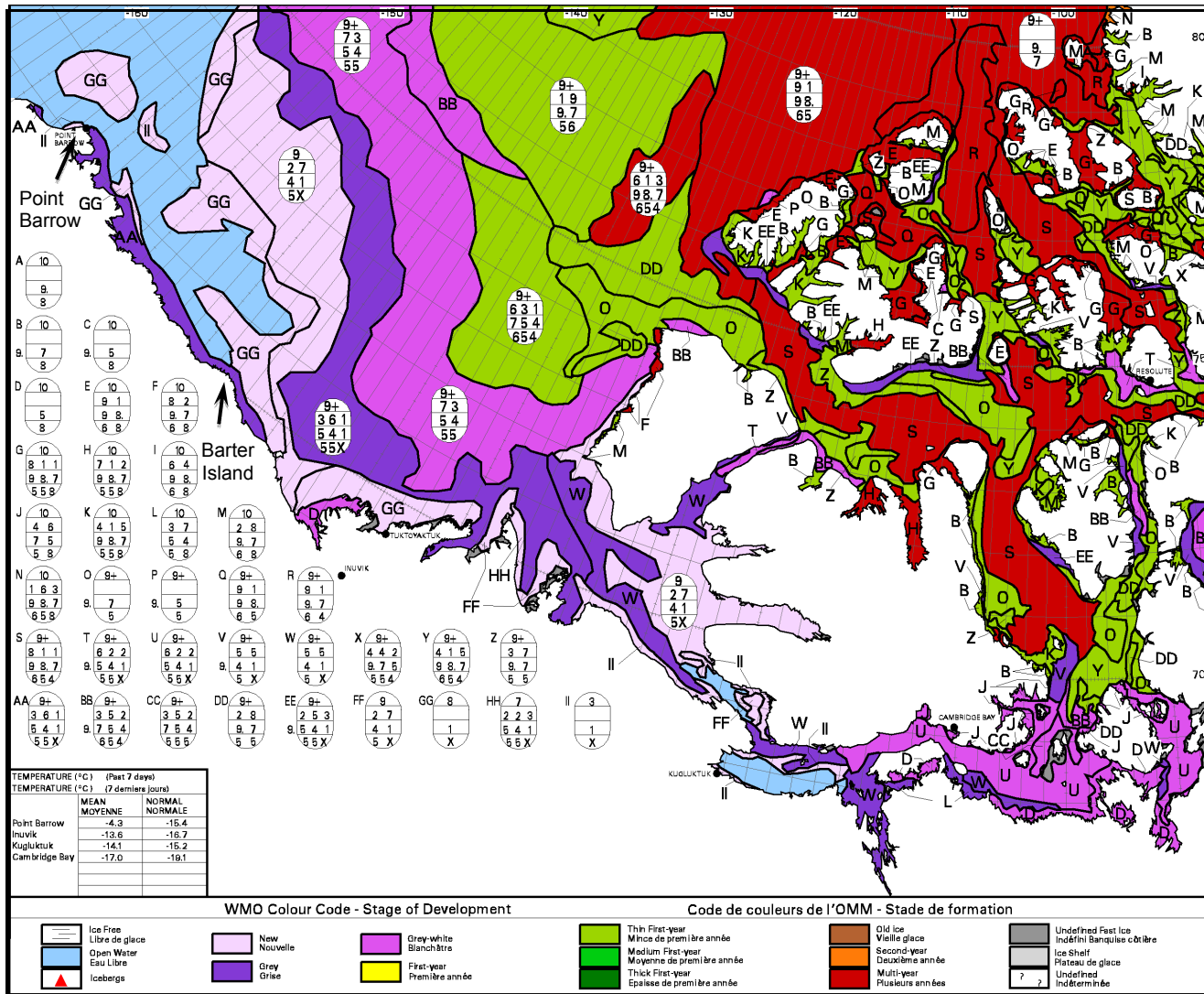
Source: Weather Underground, 2016

Figure 22. Meteorological Conditions at Deadhorse Airport in November 2016

The pack ice continued to expand to the south as the month progressed (Figure 24), producing basin-wide freeze-up on or about November 23rd. A total of 563 FDD had accumulated at Deadhorse Airport on this date. The nascent ice canopy remained intact thereafter, with concentrations exceeding 9/10s throughout the Alaskan Beaufort Sea.

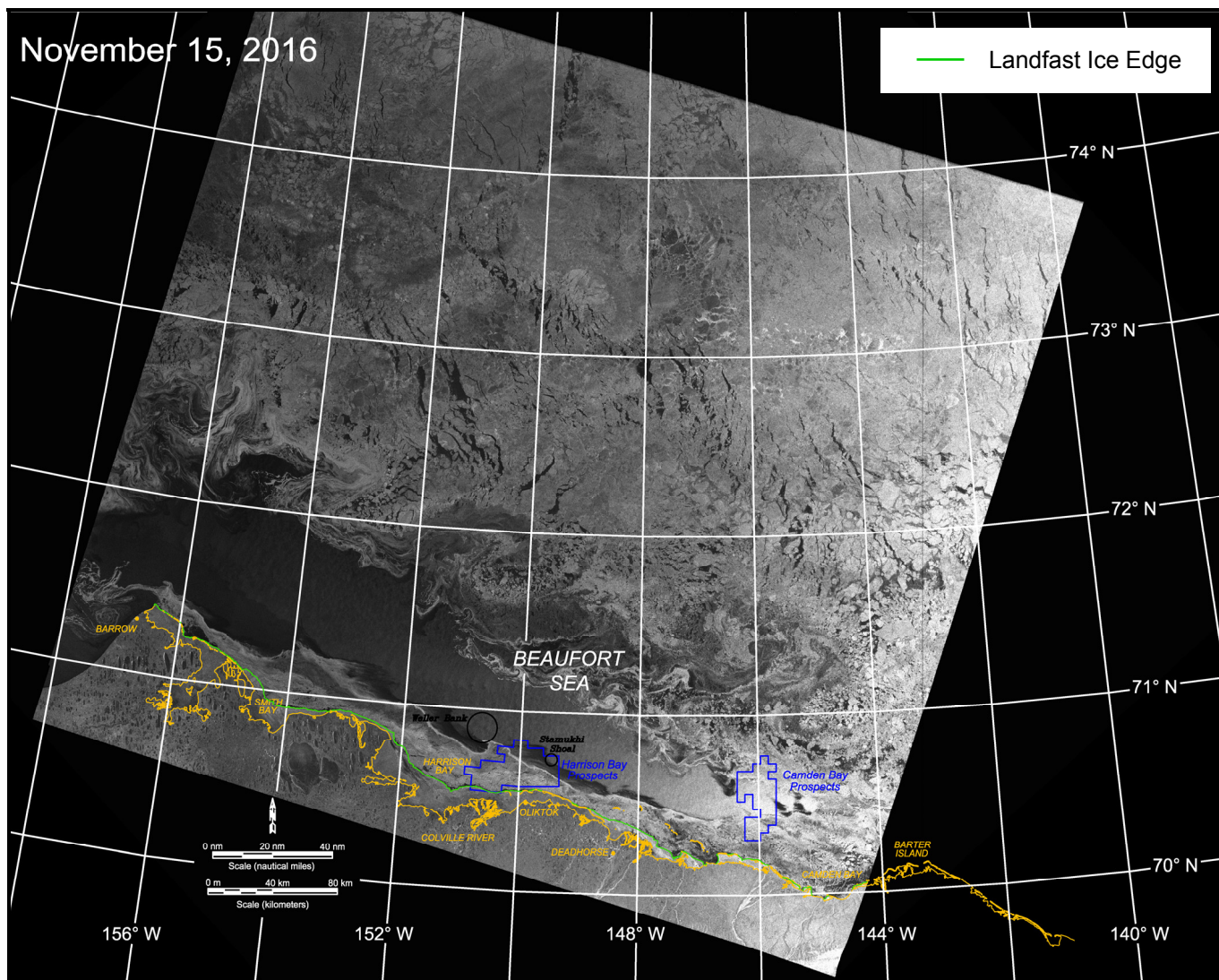
Ice Thickness: The calculated thickness of undisturbed first-year ice increased from 19 cm at the beginning of the month to 45 cm at the end (Table 6).

Landfast Ice: The successive locations of the landfast ice edge as interpreted from RADARSAT-2 images obtained on October 29th, November 15th, and December 2nd are shown in Figure 25. Between October 29th and November 15th, the landfast ice zone grew substantially in response to the two easterly storms. At the end of this period, it encompassed a significant portion of Harrison Bay and all of the coastal lagoons except the outer portion of Stefansson Sound. Subsequently, between November 15th and December 2nd, the landfast ice zone expanded into the outer portion of Stefansson Sound but otherwise remained nearly static – an outcome consistent with the falling air temperatures and absence of strong winds that occurred at this time (Figure 22).



Source: CIS, 2016

Figure 23. CIS Stage-of-Development Ice Chart of Beaufort Sea for November 7, 2016



Source: RADARSAT-2 Data and Products © MacDonald Dettwiler and Associates Ltd., 2016 – All Rights Reserved

Figure 24. RADARSAT-2 Image of Beaufort Sea Acquired on November 15, 2016

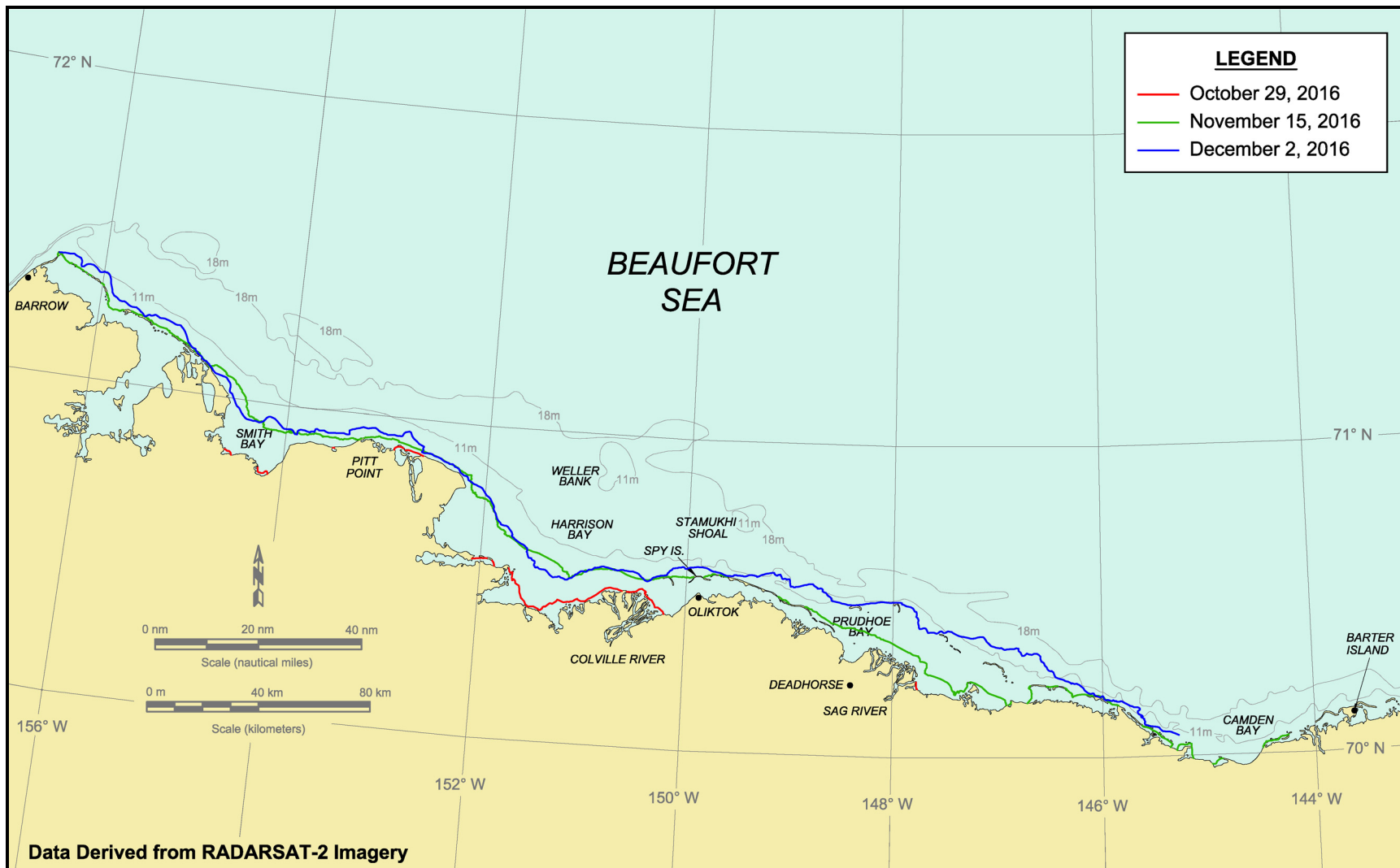


Figure 25. Beaufort Sea Landfast Ice Edge in November 2016

Ice Pile-Ups: As discussed in Section 4.1, the thirty-eight ice pile-ups observed in the central portion of the Beaufort Sea during the February 2017 reconnaissance flights are believed to have formed between November 10th and 12th. During this period, westerly winds with one-hour sustained speeds to 10 kt (5 m/s; Weather Underground, 2016) veered through north to east, freshened to 27 kt (14 m/s), and then continued veering through south to west while diminishing to between 5 and 15 kt (3 and 8 m/s). The locations and characteristics of the pile-ups are summarized in Table 7.

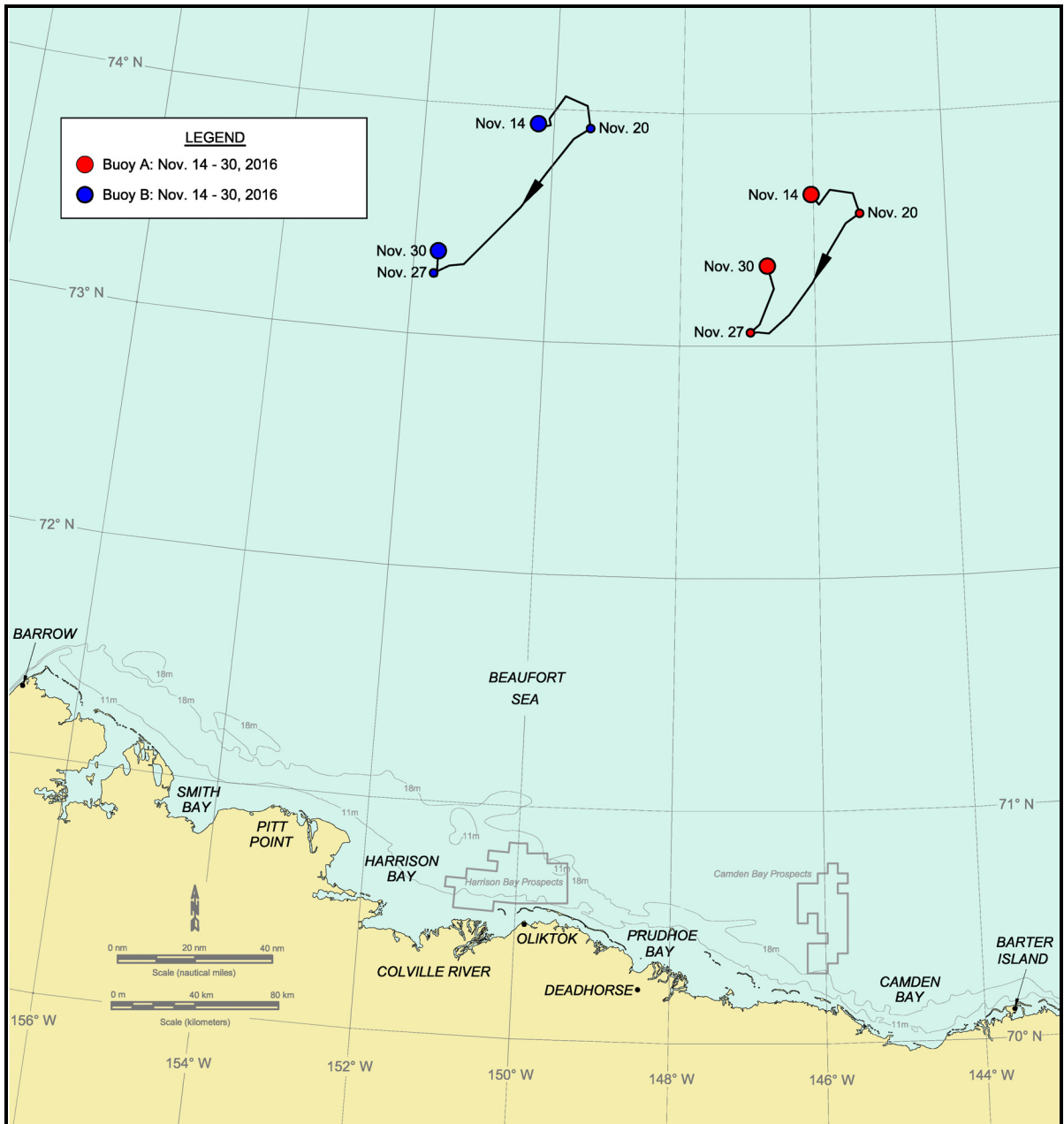
Multi-Year Ice: The southern boundary of the multi-year pack ice remained quasi-stationary and far north of the nearshore region in November. The minimum separation from the coast occurred at the end of the month, when the ice edge was located 210 nm (389 km) from Barter Island.

Ice Drift: Based on a comparison of the available RADARSAT-2 and AVHRR imagery with the tracks of drift buoys deployed during the 2016 open-water season (Section 3.4), it was concluded that Buoys A and B had been incorporated into the the pack ice by November 15th, and that their movements thereafter would be indicative of the ice drift rate. Both buoys described similar trajectories during the second half of November, as illustrated in Figure 26 and summarized below:

- November 15th – 20th: Net displacement to the east during a period in which southwesterly winds outnumbered southeasterlies;
- November 20th – 27th: Net displacement to the southwest during a period in which northeasterlies occurred less frequently than southwesterlies, but tended to be stronger;
- November 27th – 30th: Net displacement to the north under the influence of uninterrupted southwesterly winds.

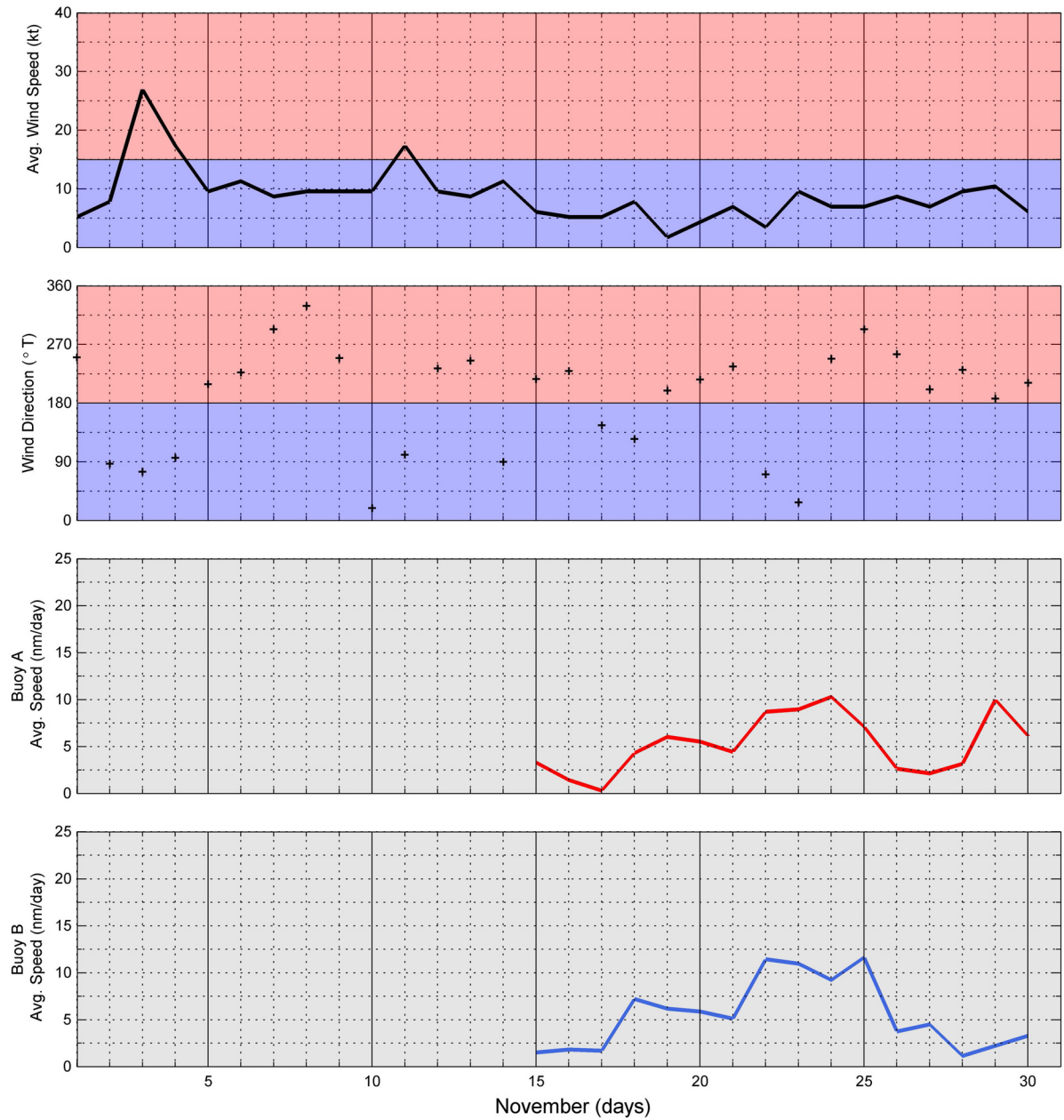
The net displacements during the 16-day period were extremely small, amounting to only 22 nm (40 km) to the southwest for Buoy A and 42 nm (78 km) to the southwest for Buoy B. The corresponding average speeds, computed on the basis of the net displacements over the entire 16-day period, were 1.4 and 2.6 nm/day (2.6 and 4.8 km/day).

The daily average speeds of the two buoys are plotted in Figure 27 along with the corresponding wind data from Deadhorse Airport. Buoy A averaged 5.3 nm/day (9.8 km/day), with a peak speed of 10.3 nm/day (19.1 km/day) on November 24th. The corresponding values for Buoy B were an average speed of 5.7 nm/day (10.5 km/day) and a peak of 11.6 nm/day (21.5 km/day) on the 22nd and 25th. The peak speeds for both buoys occurred during or soon after a two-day period of moderate easterly winds.



Data Source: Rigor, 2017

Figure 26. Beaufort Sea Drift Buoy Tracks in November 2016



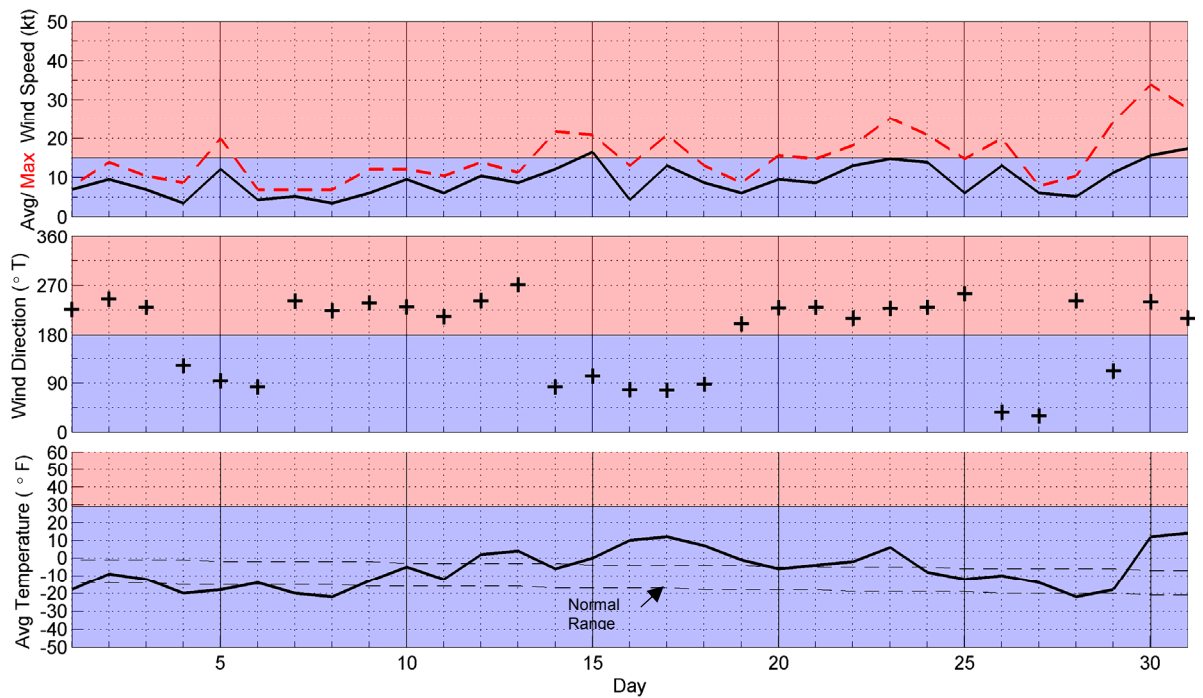
Data Sources: Weather Underground, 2017; Rigor, 2017

Figure 27. Beaufort Sea Drift Buoy Daily Average Speeds in November 2016

4.4 Late Freeze-Up

4.4.1 December 2016

Meteorological Conditions: The wind and temperature data recorded at Deadhorse Airport in December 2016 are provided in Figure 28. Normal to subnormal air temperatures prevailed during the first 11 days, followed by unseasonably warm weather at mid-month and again at month-end. The net result was 12 days in which the daily average air temperature exceeded the normal range and six days in which it fell below. The average value for the month was -6°F (-21°C).



Source: Weather Underground, 2017

Figure 28. Meteorological Conditions at Deadhorse Airport in December 2016

The wind regime in December resembled that in November, with a predominance of westerly winds (20 of 31 days), a low average speed (9 kt; 5 m/s), and two brief storms. Whereas both of the storms in November were easterly, however, the second storm in December was westerly:

- December 15th: one-day easterly with maximum speed of 17 kt (9 m/s);
- December 30th-31st: two-day westerly with maximum speed of 17 kt (9 m/s).

Ice Thickness: The calculated thickness of undisturbed first-year ice increased by 30 cm over the course of the month, from 45 to 75 cm.

Landfast Ice: The locations of the landfast ice edge were estimated from RADARSAT-2 images obtained on December 2nd, December 16th, and January 2nd. The results are presented in Figure 29.

During the first half of December, when light winds preceded the brief easterly storm on the 15th, the landfast ice edge advanced past the 11-m isobath in Harrison Bay but otherwise experienced only minor changes. The second half of the month, a period dominated by westerly winds that culminated in the two-day westerly storm on the 30th and 31st, produced a complete reversal of the prior gain in Harrison Bay and modest losses elsewhere. The westerly storm also created an unusually large flaw lead that extended from Point Barrow to the Colville River Delta and attained widths to 15 nm (28 km; Figure 30). At month-end, the landfast ice zone consisted of a relatively narrow strip that encompassed the lagoon areas but did not extend very far north of the barrier islands or the mainland coast in those areas lacking islands.

Multi-Year Ice: The large separation between the multi-year ice edge and the Alaskan Beaufort Sea coast that existed in October and November persisted throughout December. The closest approach occurred at the beginning of the month, when the ice edge was located approximately 200 nm (482 km) off Barter Island.

Ice Drift: The daily positions of three IABP drift buoys were used to provide an indication of ice drift in December. Buoys A and B were embedded deeply within the polar pack, while Buoy C was located farther south, about 80 nm (148 km) off the coast. Their tracks and daily average speeds are provided in Figures 31 and 32, respectively.

Buoys A and B described serpentine trajectories in response to winds that were predominantly westerly but shifted between easterly and westerly on eight occasions. Both buoys experienced net displacements to the northwest, with Buoy A moving 37 nm (69 km) and Buoy B 69 nm (128 km) over the course of the month. These small changes produced monthly average speeds of only 1.2 and 2.2 nm/day (2.2 and 4.1 km/day). The daily average speeds were substantially higher, averaging 5.5 nm/day (10.2 km/day) for Buoy A and 5.8 nm/day (10.8 m/day) for Buoy B. The peak daily average speeds, 12.1 nm/day (22.4 km/day) for Floe A and 15.5 nm/day (28.7 km/day) for Buoy B, occurred on December 15th during the month's only easterly storm. If the buoy speeds on this day are expressed in knots (0.51 and 0.65 kt, respectively) and compared with the daily average wind speed measured at Deadhorse Airport (17 kt), a wind factor of 3.0% is obtained for Buoy A, and 3.8% for BuoyB.

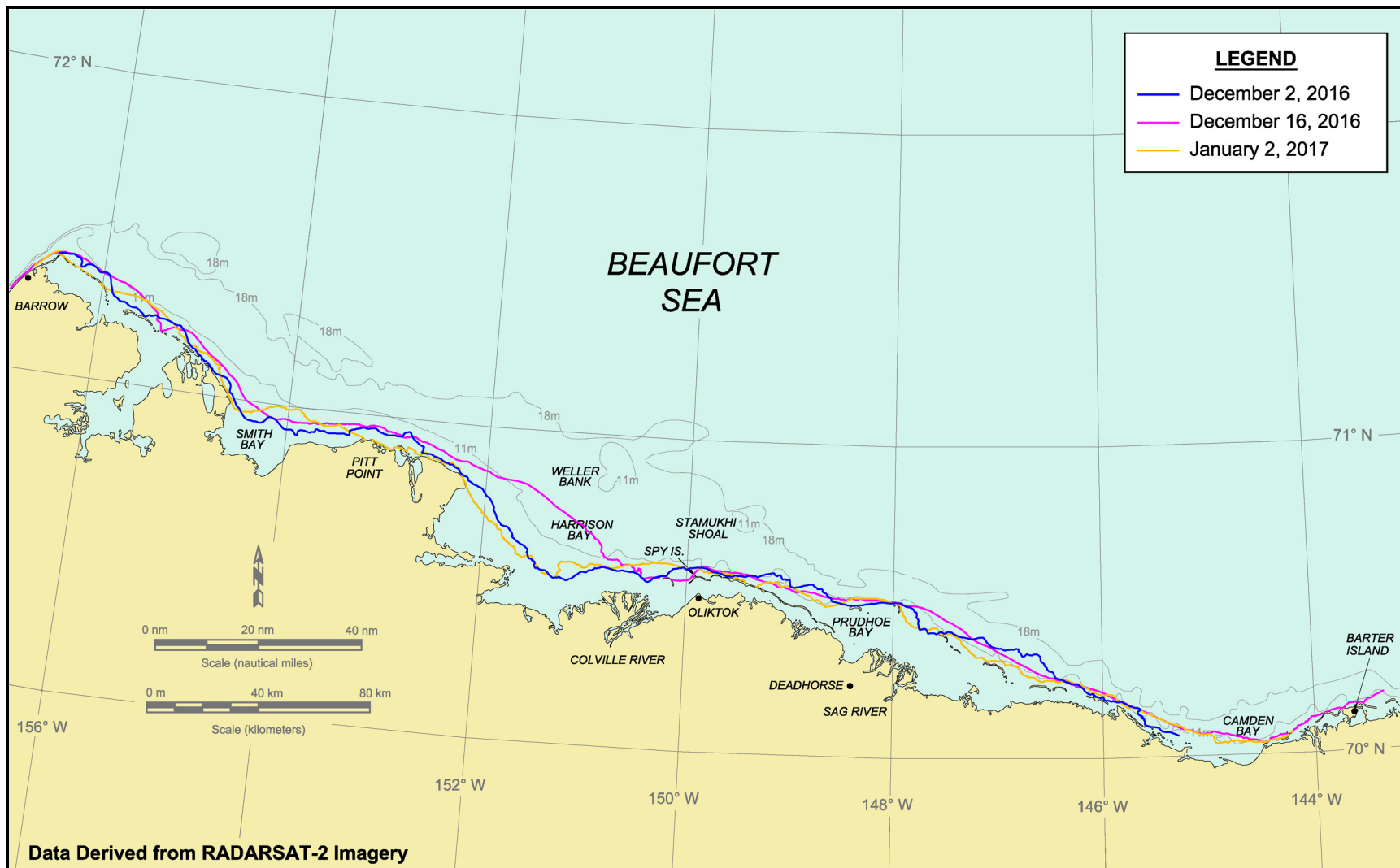
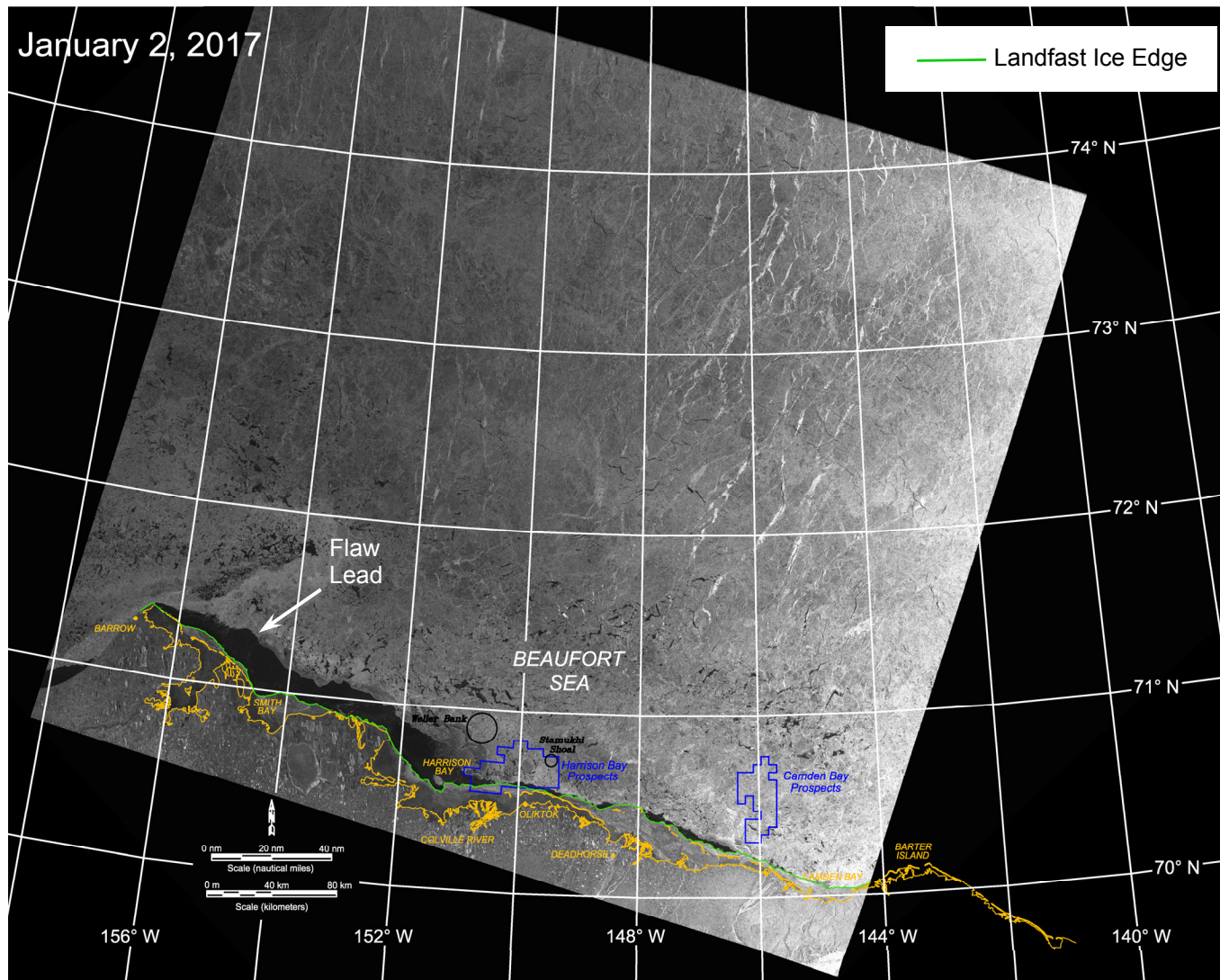
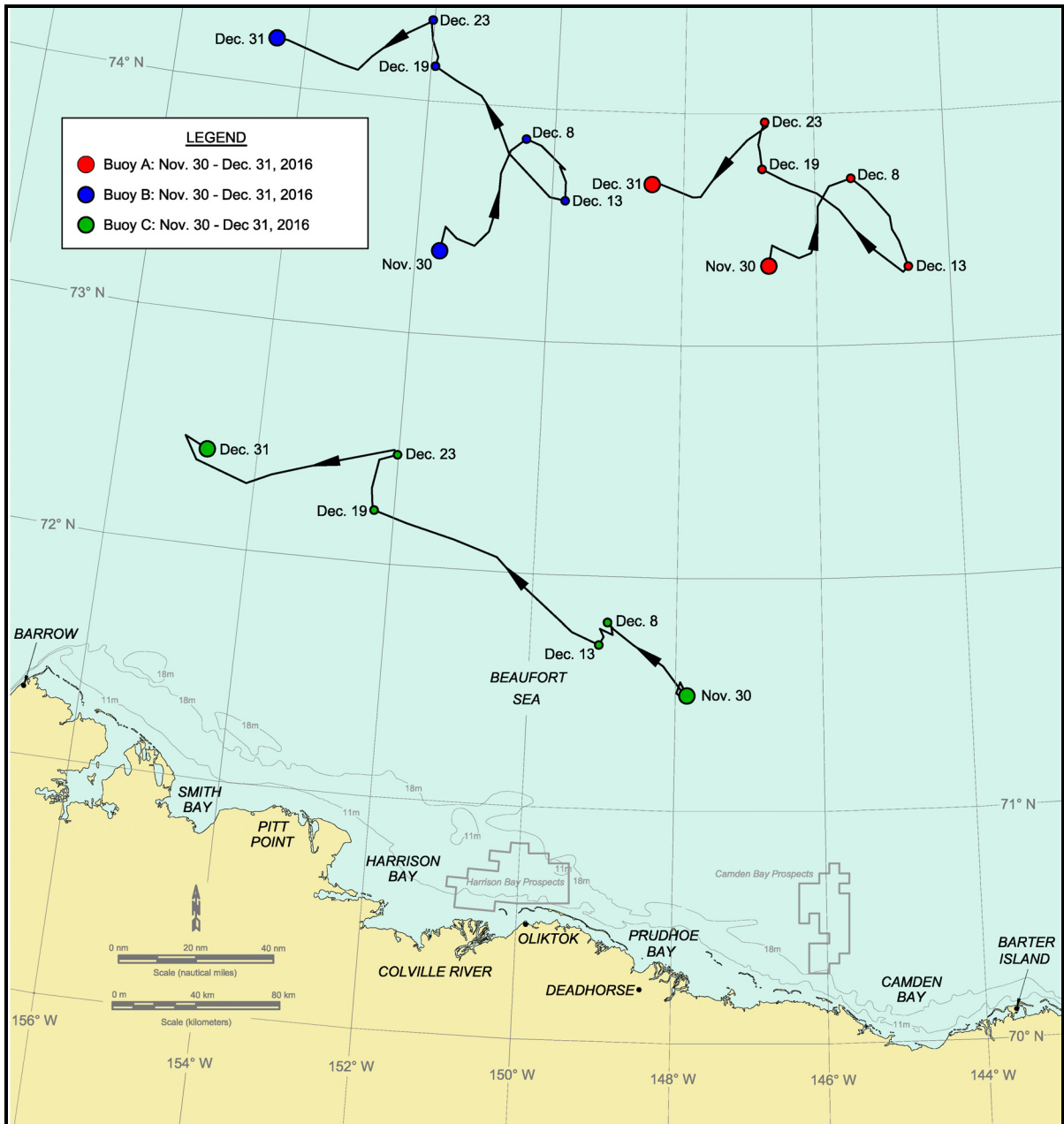


Figure 29. Beaufort Sea Landfast Ice Edge in December 2016



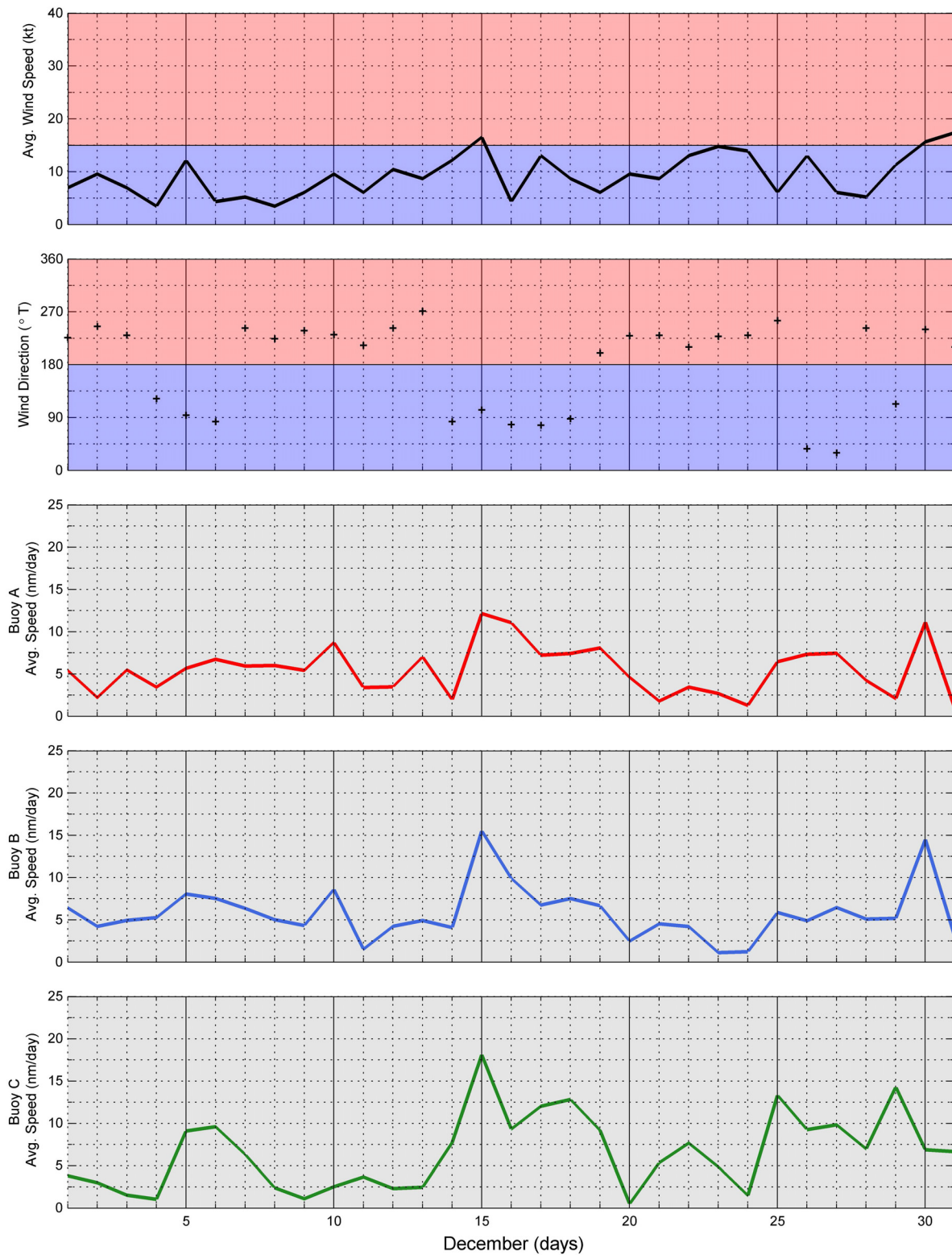
Source: RADARSAT-2 Data and Products © MacDonald Dettwiler and Associates Ltd., 2017 – All Rights Reserved

Figure 30. RADARSAT-2 Image of Beaufort Sea Acquired on January 2, 2017



Data Source: Rigor, 2017

Figure 31. Beaufort Sea Drift Buoy Tracks in December 2016



Data Sources: Weather Underground, 2017; Rigor, 2017

Figure 32. Beaufort Sea Drift Buoy Daily Average Speeds in December 2016

Buoy C followed a trajectory that differed markedly from those of Buoys A and B during the first half of the month. Whereas the latter moved to the northeast between November 30th and December 8th, and then to the southeast between the 8th and 13th, Buoy C moved to the northwest during the first of these two periods and then remained nearly stationary during the second. Possible explanations include different wind conditions, as Buoy C was located more than 100 nm (185 km) south of the other two buoys at the beginning of the month, different current conditions, as Buoy C tended to move parallel the coast, and different degrees of confinement.

Subsequent to December 13th, Buoy C moved to the northwest in a direction similar to that of Buoys A and B, but at higher speeds. The net displacement for the month, 139 m (258 km) to the northwest, produced a monthly average speed of 4.5 nm/day (8.3 km/day). The mean daily average speed was 6.6 nm/day (12.2 km/day), with the peak daily average value of 18.1 nm/day (33.5 km/day; 0.75 kt) occurring on the 15th. The wind factor corresponding to this peak speed, representing the ratio between the 0.75-kt floe speed and 17-kt wind speed, was 4.4%.

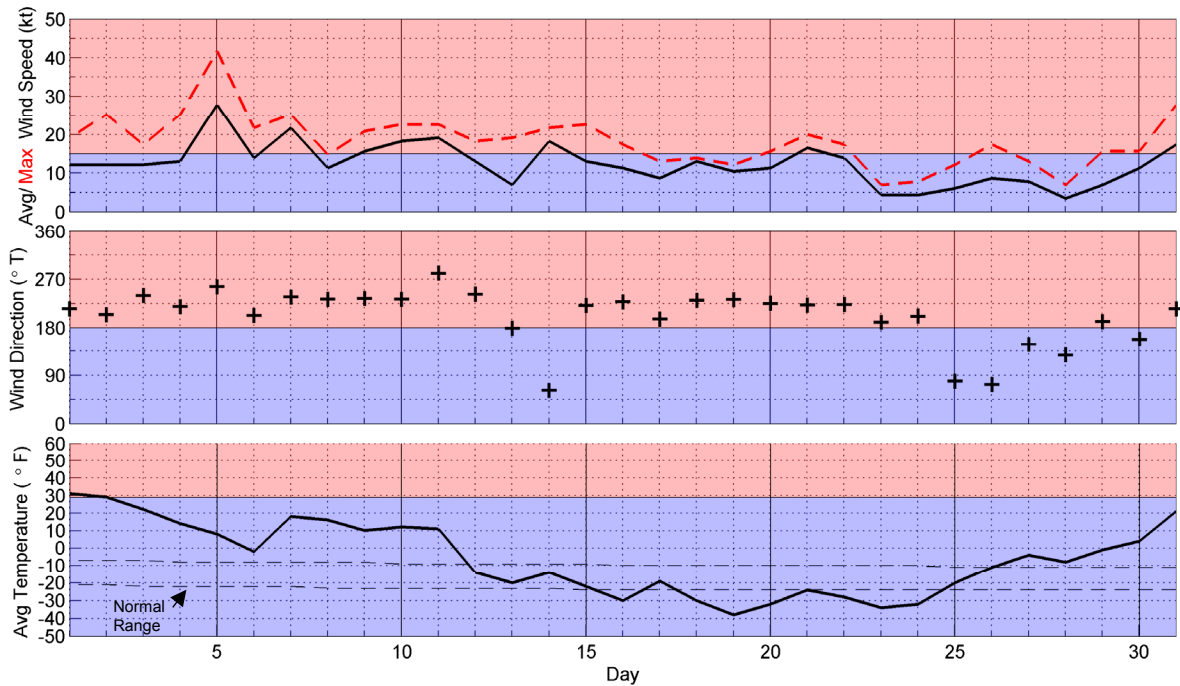
4.4.2 January 2017

Meteorological Conditions: Figure 33 presents the wind and temperature data recorded at Deadhorse Airport in January 2017. The daily average air temperatures varied over a wide range, starting at 31°F (-1°C) on the first day of the month, falling to -38°F (-39°C) on the 19th, and rebounding to 21°F (-6°C) on the 31st. The first of these exceeded the normal range by 38°F (21°C), the second fell below by 14°F (8°C), and the third exceeded by 32°F (18°C). Over the course of the month, the daily average temperatures exceeded the normal range on 16 days and fell below on seven. The average temperature for the month, -6°F (-21°C), was identical to that in December.

The daily average wind speed, 12 kt (6 m/s), tied that in February as the highest recorded during the five-month study period. The predominance of westerly winds noted in November and December continued in January, with westerlies occurring on 24 of the 31 days. Three storms took place over the course of the month, including a seven-day westerly that began on the 5th:

- January 5th-11th: seven-day westerly with maximum speed of 28 kt (14 m/s);
- January 14th: one-day easterly with maximum speed of 18 kt (9 m/s);
- January 21st: one-day westerly with maximum speed of 17 kt.

A fourth storm, a westerly that began on January 31st and continued through February 3rd, is attributed to February and will be discussed in Section 4.4.3



Source: Weather Underground, 2017

Figure 33. Meteorological Conditions at Deadhorse Airport in January 2017

Ice Thickness: The calculated thickness of undisturbed first-year ice increased from 75 cm at the beginning of January to 97 cm at the end, a gain of 22 cm.

Landfast Ice: Figure 34 illustrates the locations of the landfast ice edge derived from RADARSAT-2 images obtained on January 2nd (Figure 30), January 16th, and February 2nd (Figure 35). During the first interval, which contained the prolonged westerly storm followed by a brief easterly storm, the ice edge remained virtually unchanged except for a retreat of up to 4 nm (7 km) in Camden Bay. The fact that the narrow strip of landfast ice remained intact throughout the westerly storm indicates that it was well-grounded.

During the second interval, from January 16th through February 2nd, the landfast ice edge advanced seaward along much of the Beaufort Sea coast, including gains of up to 14 nm (26 km) in Harrison Bay and 12 nm (22 km) in Camden Bay. Since no easterly storms took place during this period, the gains appear to have resulted from the moderate easterly winds that occurred at the end of the month.

Multi-Year Ice: The southern boundary of the multi-year ice remained well offshore and quasi-stationary in January. Its minimum distance from the coast, 210 nm (389 km), occurred off Barter Island at the end of the month.

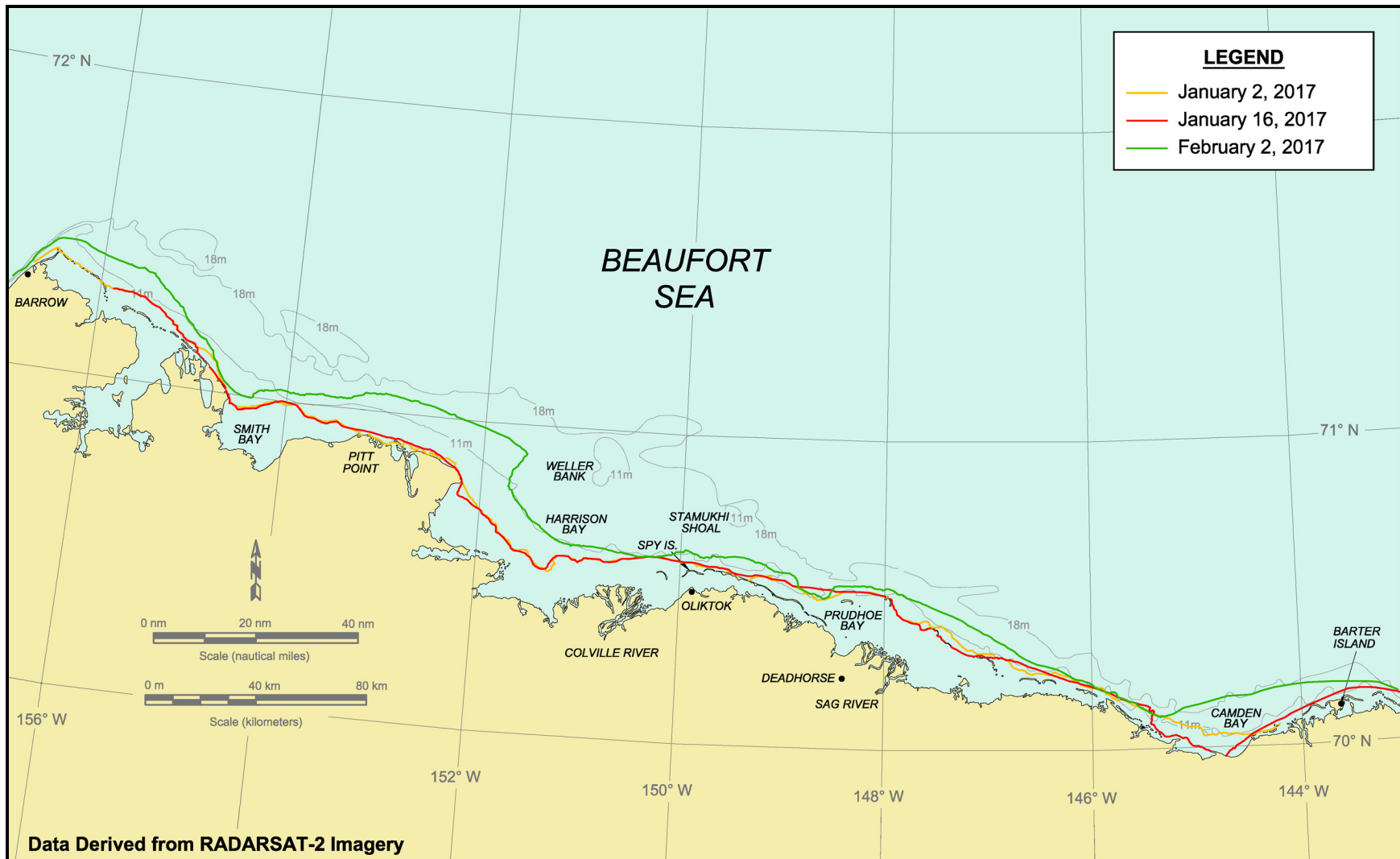
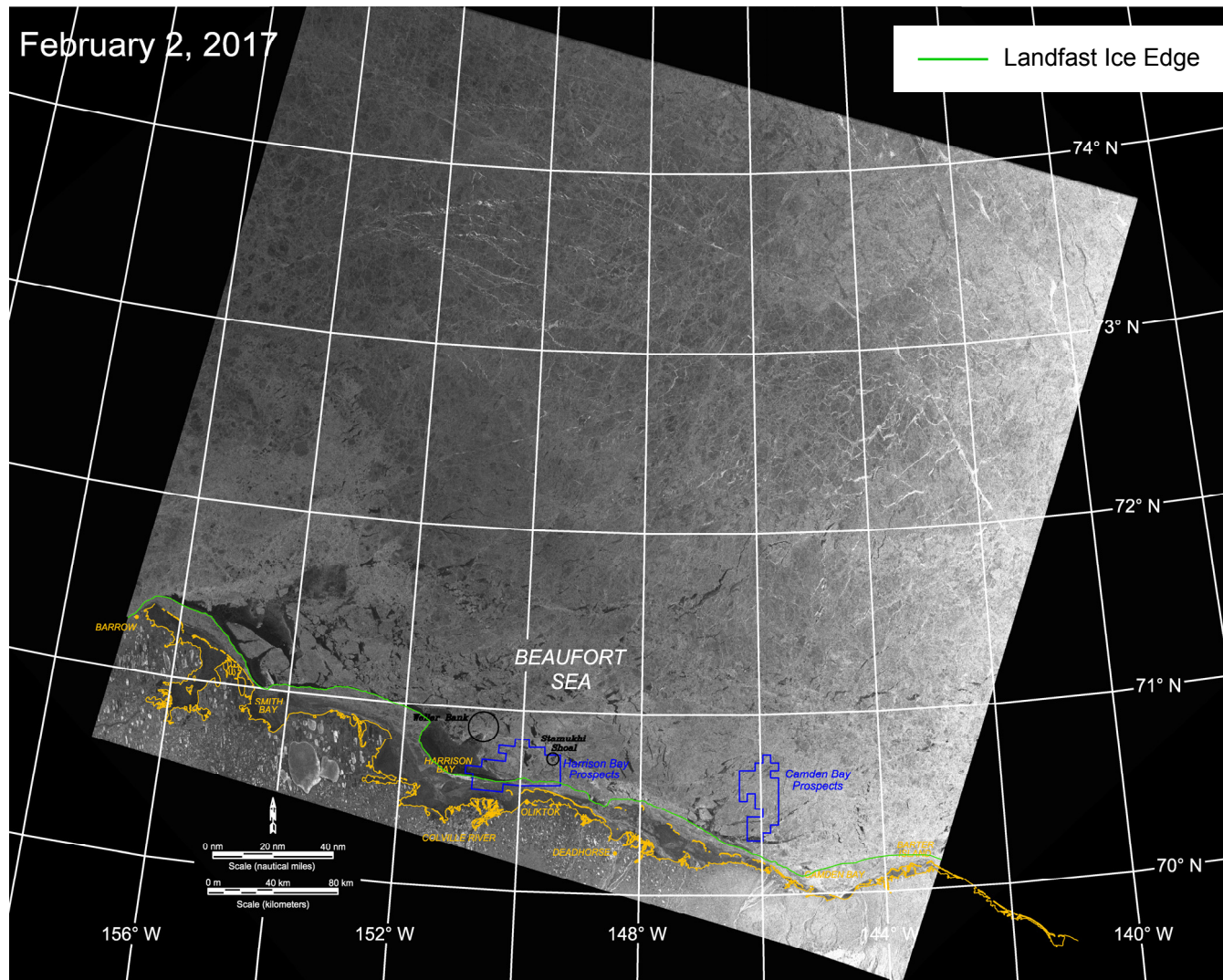


Figure 34. Beaufort Sea Landfast Ice Edge in January 2017



Source: RADARSAT-2 Data and Products © MacDonald Dettwiler and Associates Ltd., 2017 – All Rights Reserved

Figure 35. RADARSAT-2 Image of Beaufort Sea Acquired on February 2, 2017

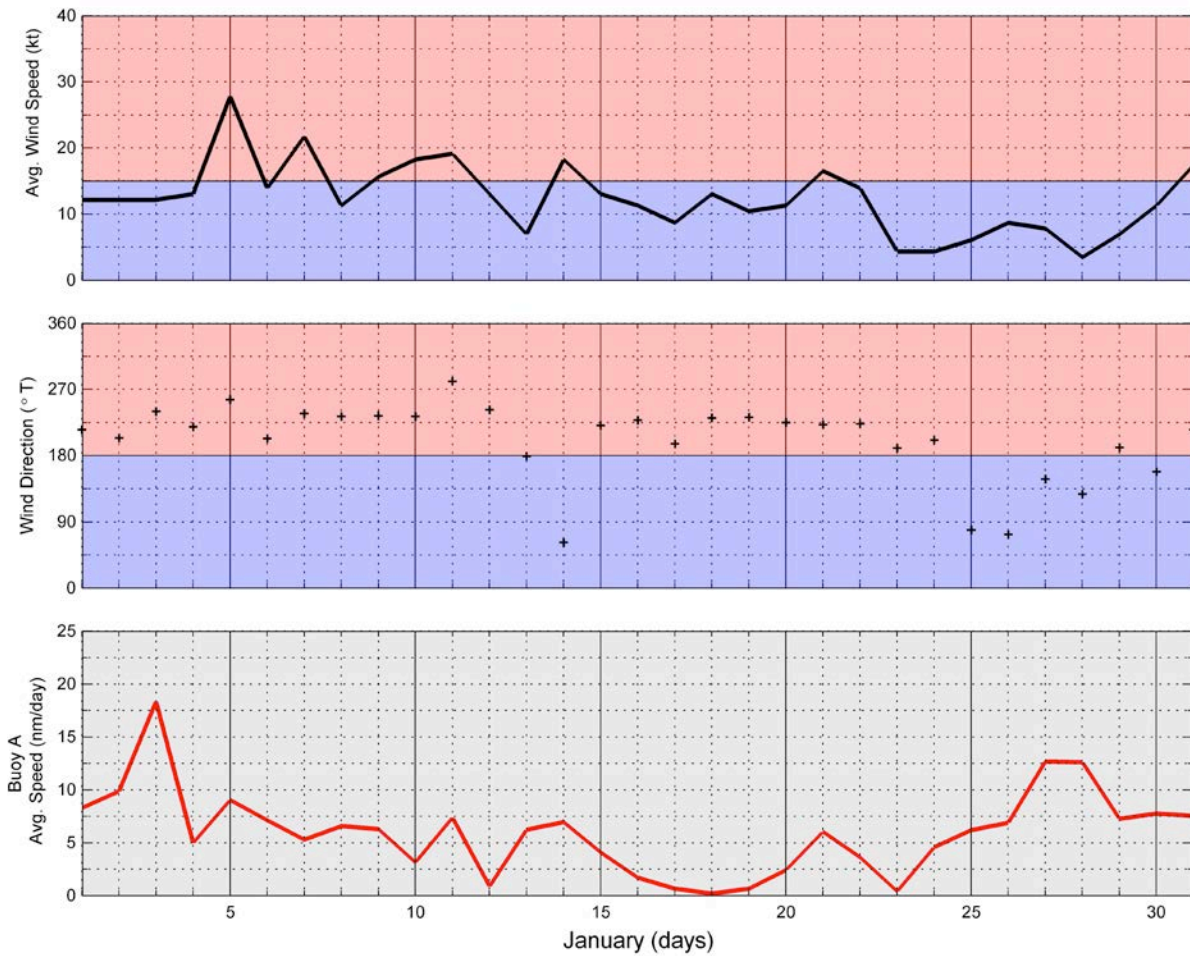
Ice Drift: The only IAPB buoy that remained in the Beaufort Sea study area in January was Buoy A. As shown in Figure 36, it described a clockwise loop consisting of a northerly leg followed by an easterly leg during an extended period of southwesterly winds, a westerly leg during the period that contained the one-day easterly storm, and finally a northerly leg driven by southerly winds. The net displacement for the month, 26 nm (48 km) to the north northwest, produced a monthly average speed of only 0.8 nm/day (1.5 km/day).



Data Source: Rigor, 2017

Figure 36. Beaufort Sea Drift Buoy Track in January 2017

The mean daily average speed for Buoy A was 6.0 nm/day (11.1 km/day). The peak daily average value, 18.3 nm/day (33.9 km/day; 0.76 kt), occurred on January 3rd during a period of uninterrupted southwesterly winds when the daily average speed at Deadhorse Airport was a modest 12 kt (6 m/s; Figure 37). The simultaneous occurrence of a 0.76-kt floe speed and 12-kt wind speed represents a wind factor of 6.3%. Although the cause of this high value is unknown, it may reflect an abrupt loss of confinement initiated by a release of stress in the pack ice, or a difference in wind conditions between the buoy and Deadhorse Airport, which were separated by 200 nm (371 km).

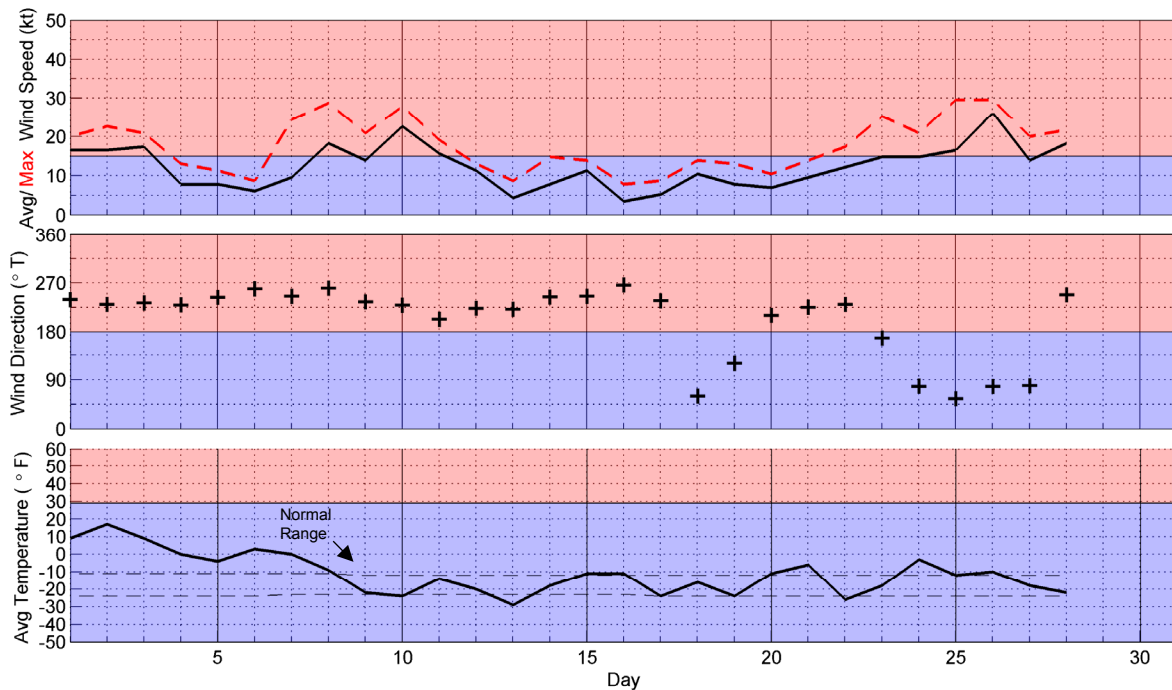


Data Sources: Weather Underground, 2017; Rigor, 2017

Figure 37. Beaufort Sea Drift Buoy Daily Average Speed in January 2017

4.4.3 February 2017

Meteorological Conditions: The meteorological conditions at Deadhorse Airport in February 2017 are displayed in Figure 38. Unseasonably warm air temperatures prevailed during the first eight days, followed by normal or near-normal temperatures thereafter. Over



Source: Weather Underground, 2017

Figure 38. Meteorological Conditions at Deadhorse Airport in February 2017

the course of the month, the daily average values exceeded the normal range on 14 days and dropped below on three. The average was -11°F (-24°C).

As in each of the prior three months, westerly winds predominated in February, occurring on 21 of the 28 days. The average speed was 12 kt (6 m/s). Of the four storms that took place, three were westerlies (including the event that began on January 31st; Figure 33) and one was easterly:

- Jan 31st-Feb 3rd: four-day westerly with maximum speed of 17 kt (9 m/s);
- February 8th-11th: four-day westerly with maximum speed of 23 kt (12 m/s);
- February 25th-26th: two-day easterly with maximum speed of 26 kt (13 m/s);
- February 28th: one-day westerly with maximum speed of 18 kt (9 m/s).

The storm that began on February 28th continued through March 4th and ultimately attained a maximum daily average wind speed of 29 kt (15 m/s), but the four days in March are excluded from consideration because they fall outside the five-month study period (October through February).

Ice Thickness: The calculated thickness of undisturbed first-year ice increased by 20 cm, from 97 to 117 cm.

Landfast Ice: Figure 39 presents the locations of the landfast ice edge derived from RADARSAT-2 images obtained on February 2nd (Figure 35), 19th, and 26th (Figure 40). The ice edge remained nearly unchanged between the 2nd and 19th despite a strong predominance of westerly winds, indicating that it was securely grounded in the vicinity of the 11-m isobath. Subsequently, it advanced to the 18-m isobath in response to the easterly storm that began on the 25th. This advance was noteworthy in that it marked the first occasion during the 2016-17 freeze-up season on which the ice reached its customary anchor points on Weller Bank and Stamukhi Shoal. The timing contrasts sharply with that in 2015-16, when the same milestone was attained more than two months earlier, in early December (Coastal Frontiers and Vaudrey, 2016).

Multi-Year Ice: The multi-year ice edge drifted slowly to the south over the course of February, reducing the minimum distance offshore from 210 nm (389 km) at the beginning of the month to 170 nm (315 km) at the end. In both instances, the minimum distance occurred off Barter Island.

Ice Drift: As in January, Floe A was the only IAPB drift buoy located in the Beaufort Sea study area in February. It moved in a zigzag pattern consisting of a leg to the southeast under westerly winds (January 31st – February 9th), a leg to the north under southwesterly winds (February 9th - 13th), a period of minimal displacement under westerly winds (February 13th – 17th), a leg to the west during a period dominated by easterly winds that culminated in a two-day easterly storm (February 17th – 26th), and finally a leg to the southeast at the beginning of a westerly storm (Figure 41). As in each of the prior three months, the net displacement and monthly average speed were modest: 37 nm (69 km) to the south and 1.3 nm/day (2.4 km/day).

The mean daily average speed over the course of the month was 4.8 nm/day (8.9 km/day), while the maximum was 14.5 nm/day (26.9 km/day; 0.6 kt; Figure 42). The maximum value occurred on the first day of the month, when westerly winds averaging of 17 kt (9 m/s) prevailed at Deadhorse Airport. The resulting wind factor was 3.5%.

4.5 Reconnaissance Flights

As discussed in Section 3.5, aerial reconnaissance missions were undertaken on February 23rd and 27th to document the ice conditions that prevailed in the Alaskan Beaufort Sea at the end of the freeze-up study period. Beaufort Sea Flight No. 1 (Flight “B1” on Drawing CFC-994-01-001) was conducted in the central Beaufort on a day when the wind shifted from southwesterly to easterly and freshened to 15 kt (8 m/s) at the outset of the

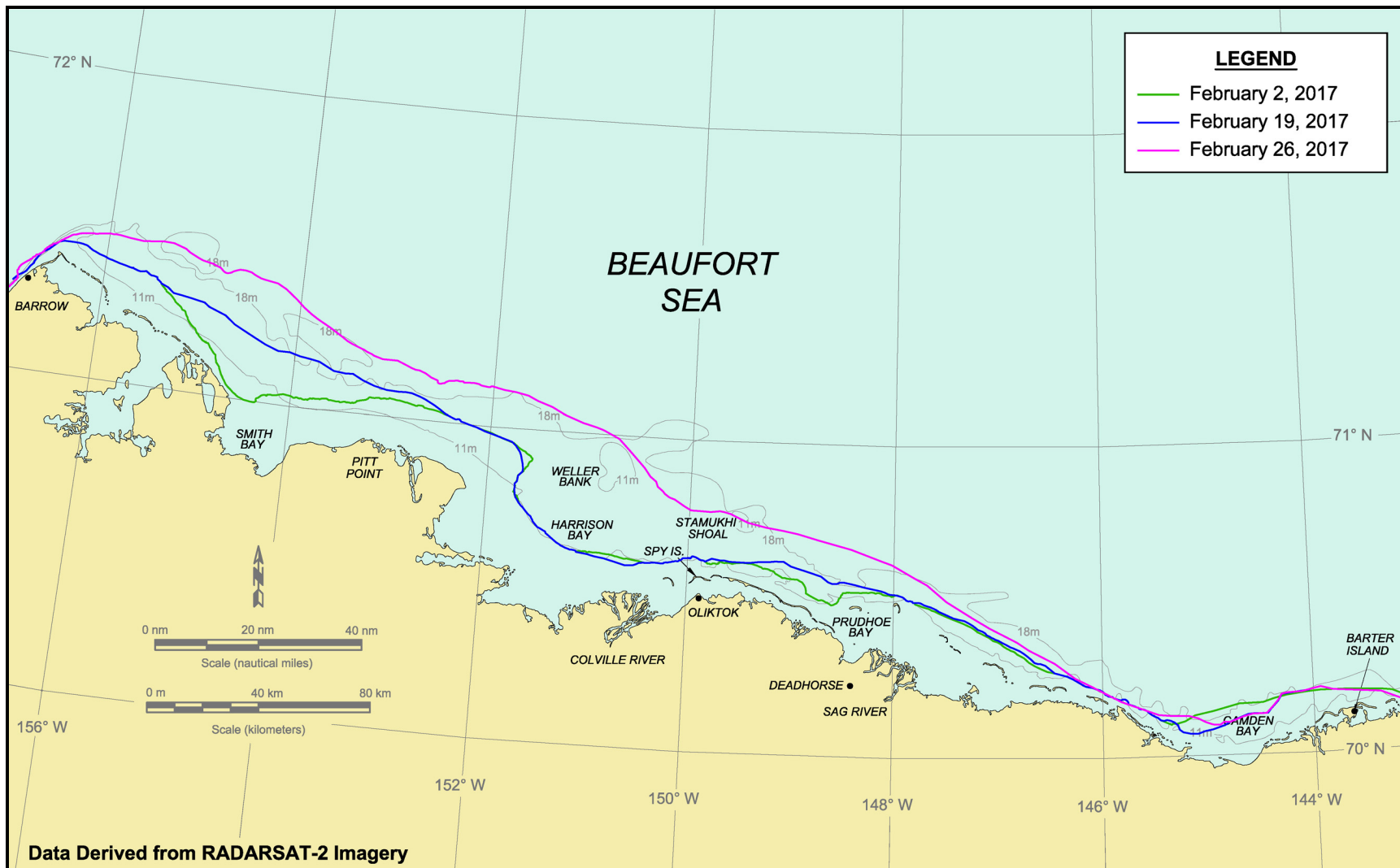
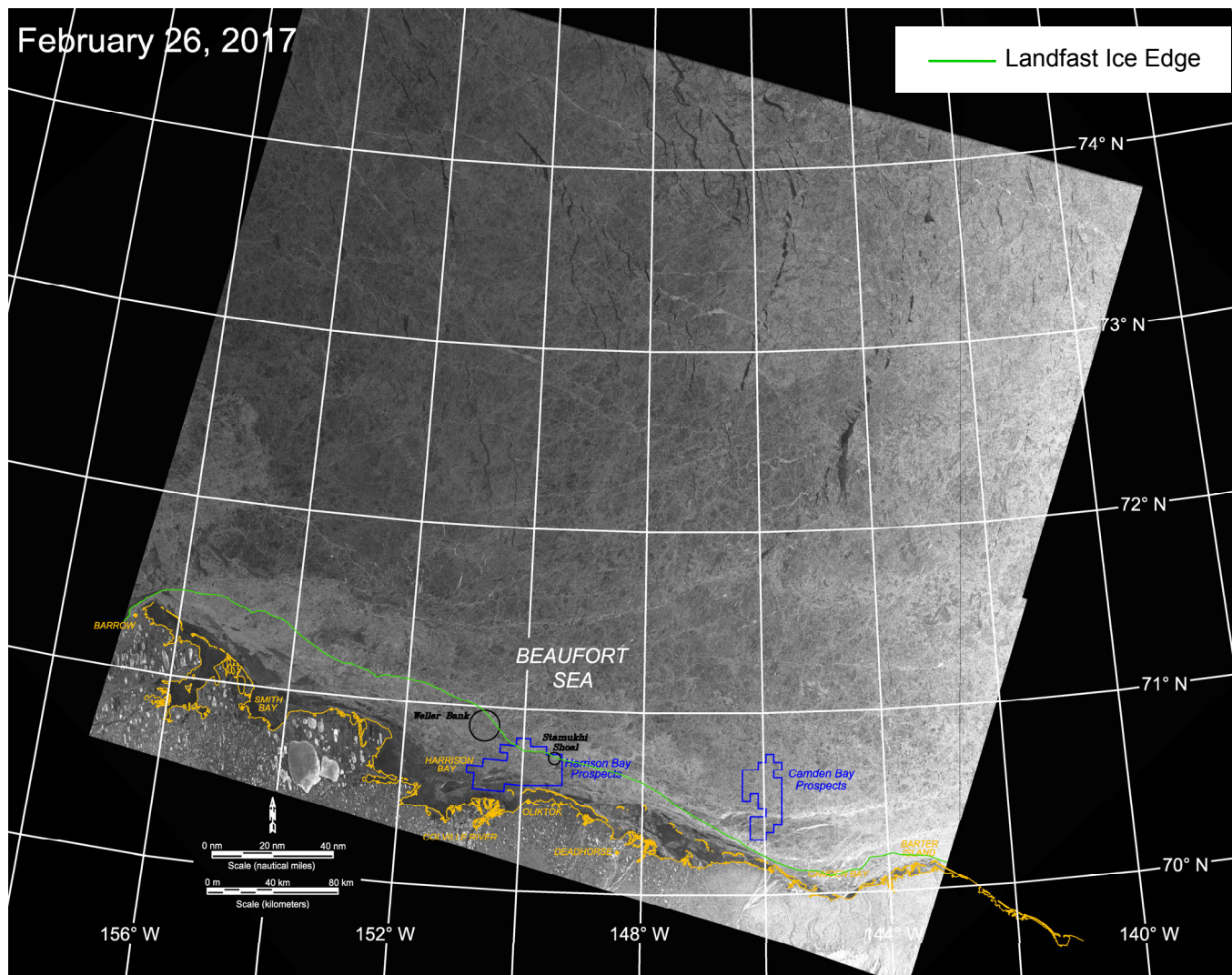


Figure 39. Beaufort Sea Landfast Ice Edge in February 2017



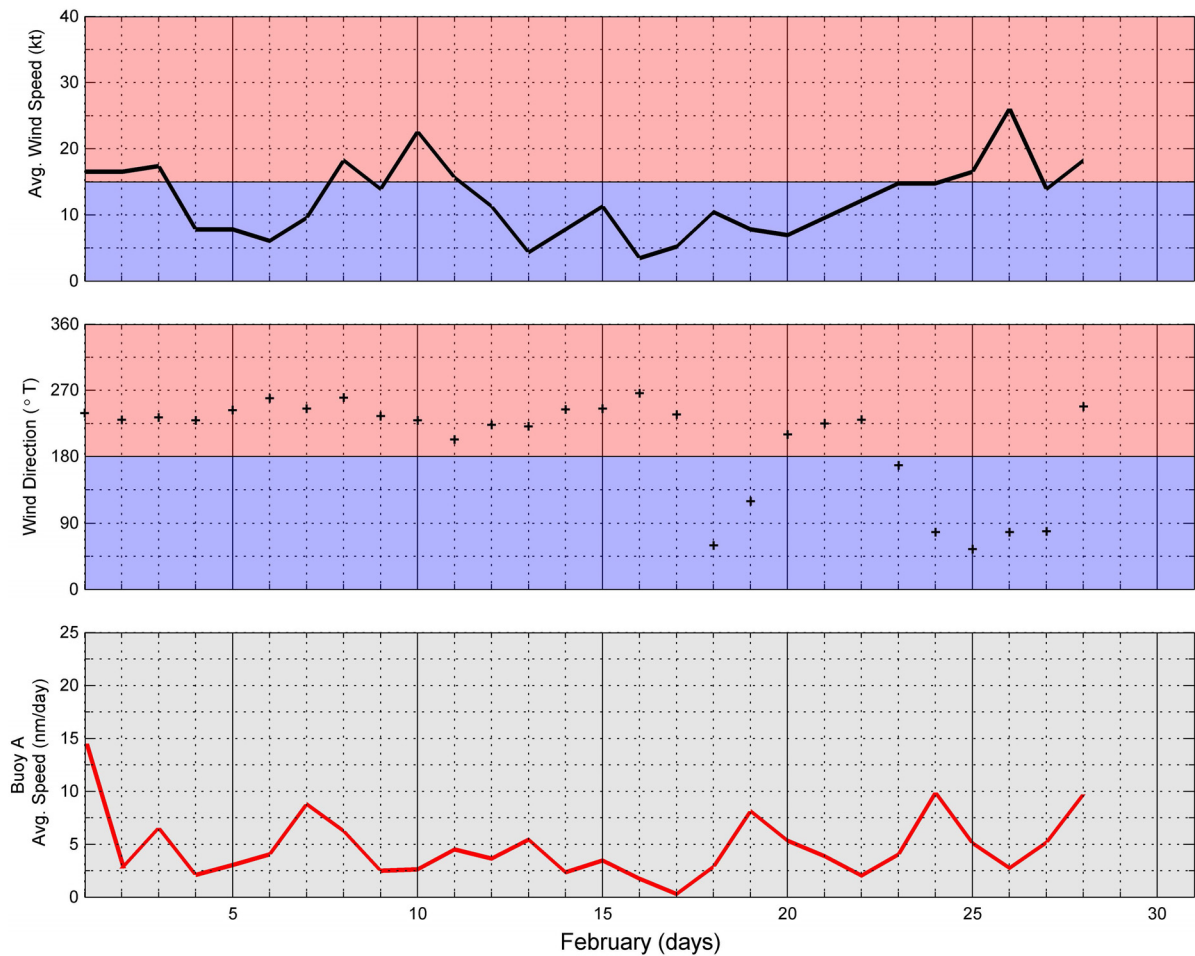
Source: RADARSAT-2 Data and Products © MacDonald Dettwiler and Associates Ltd., 2017 – All Rights Reserved

Figure 40. RADARSAT-2 Image of Beaufort Sea Acquired on February 26, 2017



Data Source: Rigor, 2017

Figure 41. Beaufort Sea Drift Buoy Track in February 2017



Data Sources: Weather Underground, 2017; Rigor, 2017

Figure 42. Beaufort Sea Drift Buoy Daily Average Speed in February 2017

easterly storm that peaked on the 26th. Beaufort Sea Flight No. 2 (Flight “B2” on Drawing CFC-994-01-002) took place in the western Beaufort after a three-day delay caused by the high winds and blowing snow that prevailed during the storm. The flight occurred at the end of the storm, during a period in which the winds diminished rapidly.

4.5.1 Lagoon Ice

As in past years, the ice in the semi-protected lagoons behind the barrier islands was primarily flat and featureless (Plate 2). The only exception occurred in Stefansson Sound, where widely-scattered rubble with a typical height of 0.5 m was noted off Prudhoe Bay.

In contrast to many of the prior freeze-up studies, when numerous thermal cracks were observed in the lagoon ice (Coastal Frontiers and Vaudrey, 2011; 2012a; 2013; 2014; 2015; 2016), only four such features were discovered in February 2017. As discussed in the

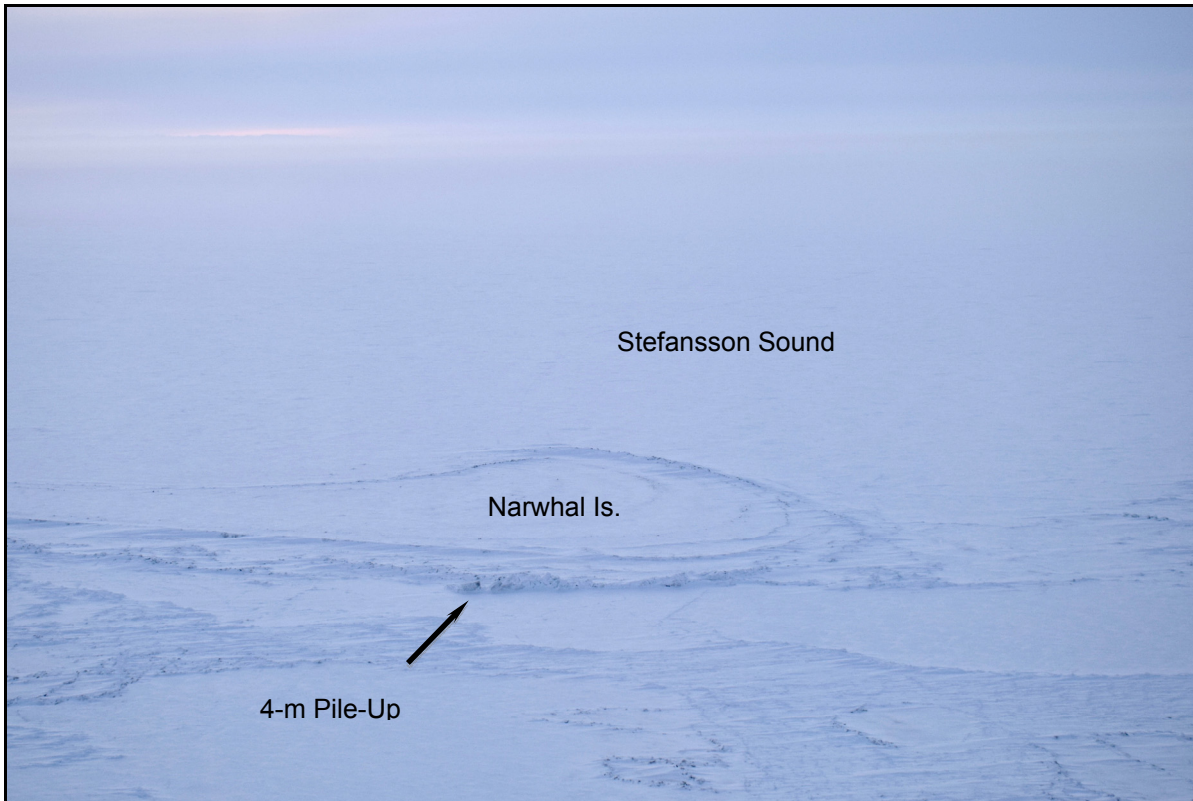


Plate 2. Undeformed Ice in Stefansson Sound and 4-m Pile-Up on West End of Narwhal Island (looking south on February 23, 2017)

2010-11 Freeze-Up Study report (Coastal Frontiers and Vaudrey, 2011), thermal cracks tend to form when a rapid drop in air temperature is followed by a rapid rise. The drop causes contraction and cracking of the ice sheet, while the ensuing rise causes compression and extrusion of the refreezing slush in the crack, creating a ridge.

Three of the cracks noted during the February flights were located in Stefansson Sound, while one was located in Smith Bay. The heights of the associated ridges ranged from 0.5 to 1 m. Based on a review of the temperature data at Deadhorse Airport, the cracks probably formed during the first week in January, when the daily average air temperature dropped from 31° to -2°F (-1° to -19°C) before rebounding to 18°F (-8°C). The most prominent crack, which extended south from Dinkum Sands shoal (between Cross and Narwhal Islands) with a ridge height of 1 m, is shown in Plate 3.

The primary importance of thermal cracks from the standpoint of offshore development is their potential to disrupt on-ice activities such as transportation and construction. This circumstance arose in 1982, when thermal cracks in Stefansson Sound disrupted ice road operations during the construction of Tern Island (Vaudrey, 1982b).

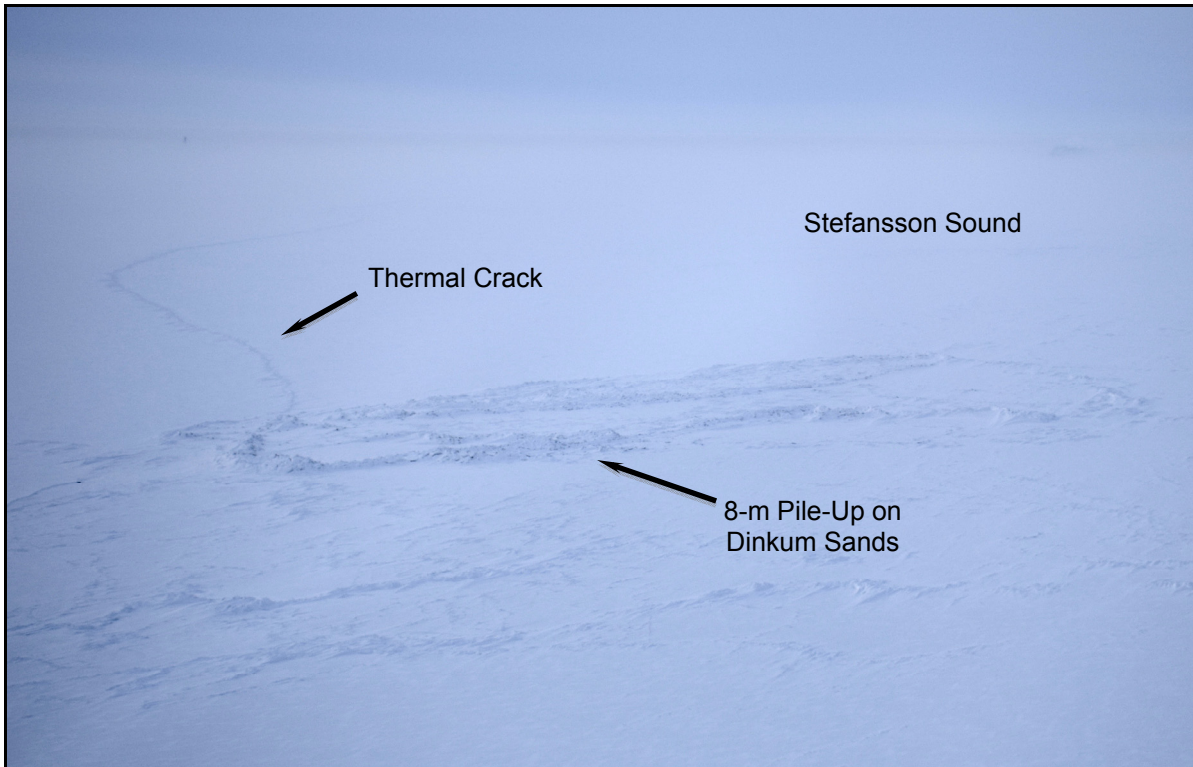


Plate 3. Thermal Crack Extending South from Dinkum Sands into Stefansson Sound along with 8-m Pile-Up (looking south on February 23, 2017)

4.5.2 Landfast Ice and Shear Zone

The extent of the landfast ice zone changed dramatically during the three-day period between the two Beaufort Sea flights, reflecting the influence of the aforementioned easterly storm. When the first flight was undertaken in the central Beaufort on February 23rd, the landfast ice zone was found to be narrow and poorly-developed. The location of the seaward edge matched that derived from the RADARSAT-2 image obtained four days earlier, on February 19th (Figure 39). The edge was marked by a shear line with a low shear wall typically 2 to 3 m high (Plate 4), while the strip between the edge and the barrier islands contained extensive rubble with typical heights of 4 to 6 m (Plate 5).

Of particular note was Stamukhi Shoal, which was located outside the landfast ice zone at the time of the flight. As shown in Plate 6, ice had begun to ground on the shoal in the recent past, creating a compact rubble field up to 8 m high that had not yet stabilized the surrounding canopy. The grounding and rubble formation were precipitated by the wind shift and ensuing 15-kt (8-m/s) winds that occurred at the beginning of the easterly storm.



**Plate 4. Shear Line with Low Shear Wall at Landfast Ice Edge
3.5 nm off Narwhal Island (looking east on February 23, 2017)**



**Plate 5. 6-m Rubble in Shear Zone 2 nm off Narwhal Island
(looking south on February 23, 2017)**



**Plate 6. Newly-Grounded Rubble with Heights to 8 m on Stamukhi Shoal
(looking west on February 23, 2017)**

When the flight over the western Beaufort Sea was conducted on February 27th, the landfast ice zone had expanded substantially. Numerous grounded ridges and rubble fields with heights to 6 m were observed on Weller Bank (Plate 7), while the landfast ice edge consisted of an intermittent shear line with typical wall heights of 3 to 4 m (Plate 8). The location of the ice edge matched that derived from the RADARSAT-2 image obtained a day earlier, on February 26th (Figure 39).

4.5.3 Offshore Ice

Outside the landfast ice zone, flat first-year floes with diameters of 500 m to 1 km predominated (Plate 9). Larger floes with diameters to 5 km were observed in some areas, but were relatively rare. Deformation was modest, with ridge and rubble heights typically ranging from 1 to 2 m.

4.5.4 Leads

Numerous leads, both open and refreezing, were observed in the ice canopy north of the landfast ice zone. Their sizes ranged from small, with widths less than 10 m, to



**Plate 7. 6-m Grounded Ridge Backed by Extensive Rubble Field on Weller Bank
(looking west on February 27, 2017)**



**Plate 8. Shear Line at Landfast Ice Edge 20 nm off Admiralty Bay
(looking east on February 27, 2017)**

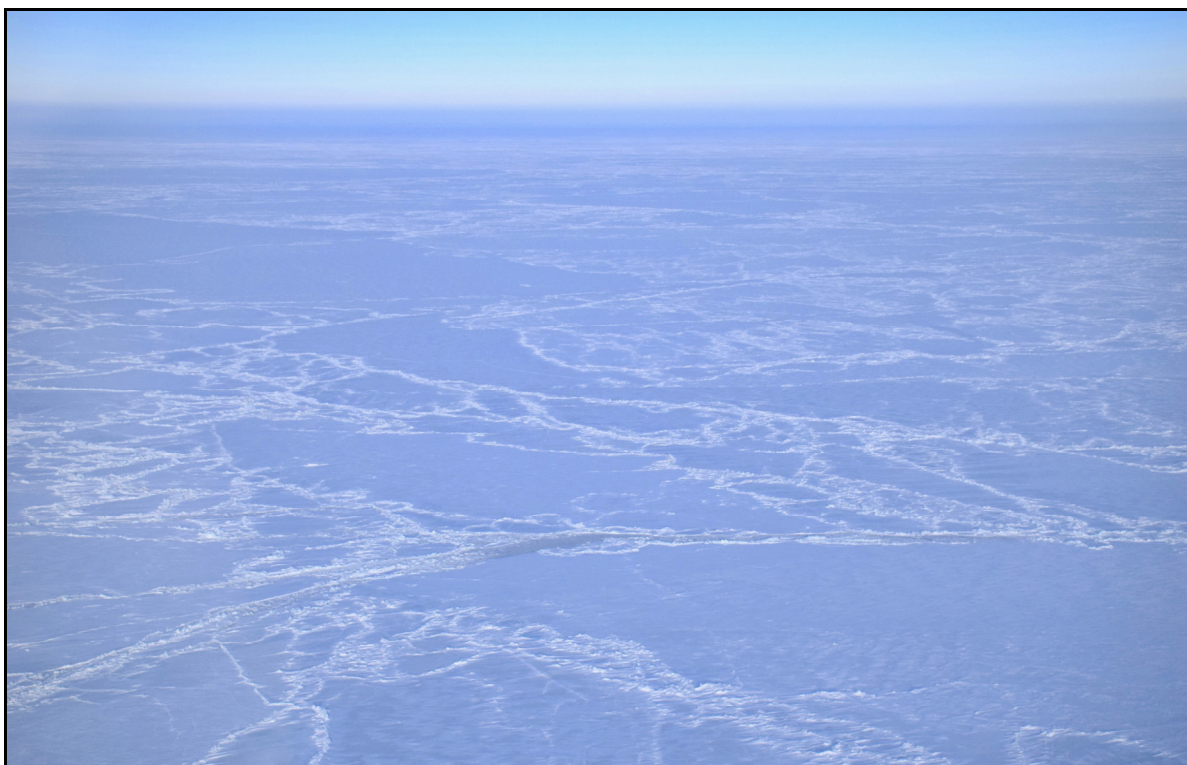


Plate 9. Flat First-Year Floes and Intermittent Ridges and Rubble with Heights to 2 m off Camden Bay (looking north on February 27, 2017)

substantial, with widths exceeding 500 m. Representative examples are provided in Plates 10 and 11. The leads in the central Beaufort on February 23rd appeared to reflect the disruptive influence of the wind shift that occurred at the outset of the easterly storm, while those in the western Beaufort on the 27th appeared to reflect the disturbance caused by the storm itself.

4.5.5 Ice Pile-Ups

Thirty-eight ice pile-ups were discovered in the central portion of the Alaskan Beaufort Sea during the two reconnaissance flights conducted in February. As discussed in Section 4.1, the pile-ups are believed to have formed between November 10th and 12th in response to shifting winds with one-hour sustained speeds to 27 kt (14 m/s). The characteristics of these features are summarized in Table 7, with representative examples shown in Plates 2, 3, and 12.

4.5.6 Multi-Year Ice

No multi-year ice floes were observed during the flights, which were conducted far to the south of the multi-year ice edge.



Plate 10. Multiple Small Leads off Harrison Bay (looking north on February 27, 2017)



Plate 11. Large Refreezing Lead off Camden Bay (looking north on February 23, 2017)



Plate 12. 5-m High Pile-Up that Encroached 12 m onto North Shore of Duchess Island (looking southeast on February 23, 2017)

4.5.7 Ice Conditions in Camden Bay Prospects

The ice conditions in the Camden Bay Prospects were found to be relatively uniform, consisting of flat first-year floes interspersed with small ridges, intermittent rubble fields, and occasional leads. The floe diameters typically varied between 500 m and 1 km, while the ridge and rubble heights ranged from 1 to 2 m in the central portion of the Prospects (Plate 13) and 1 to 3 m in the southern portion (Plate 14).

The landfast ice edge was located well south of the Camden Bay Prospects, and only 2 nm (3 km) north of Mary Sachs Entrance (which separates North Star and Flaxman Islands). As illustrated in Plate 15, it was marked by an intermittent shear line surrounded by 2-m rubble.

4.5.8 Ice Conditions in Harrison Bay Prospects

The ice canopy in the Harrison Bay Prospects consisted primarily of flat, first-year floes with diameters ranging from tens of meters to several kilometers. Ridges and rubble



Plate 13. Flat First-Year Floes, Scattered 1-m Rubble, and Refreezing Lead in Central Portion of Camden Bay Prospects (looking north on February 23, 2017)



Plate 14. Flat First-Year Floes with Scattered Rubble to 3 m in Southern Portion of Camden Bay Prospects (looking east on February 23, 2017)



**Plate 15. Intermittent Shear Line with 2-m Rubble at Landfast Ice Edge
2 nm off Mary Sachs Entrance (looking east on February 23, 2017)**

with heights of 1 to 2 m were present throughout the Prospects, but the density of these features increased with distance from south to north (Plates 16 and 17).

The most significant deviation from the foregoing characteristics occurred on Stamukhi Shoal, in the northeast corner of the Prospects, where the 8-m rubble field discussed in Section 4.5.2 was located (Plate 6). Also noteworthy was a well-defined shear line with a 4-m shear wall that trended east-west in the southern portion of the Prospects (Plate 18). This feature marked the northern edge of the landfast ice zone when first discovered on February 23rd, but was completely contained within the expanded landfast ice zone that prevailed on the 27th (Figure 39).



Plate 16. First-Year Floes with Widely-Scattered 1-m Rubble near Southern Boundary of Harrison Bay Prospects (looking east on February 27, 2017)

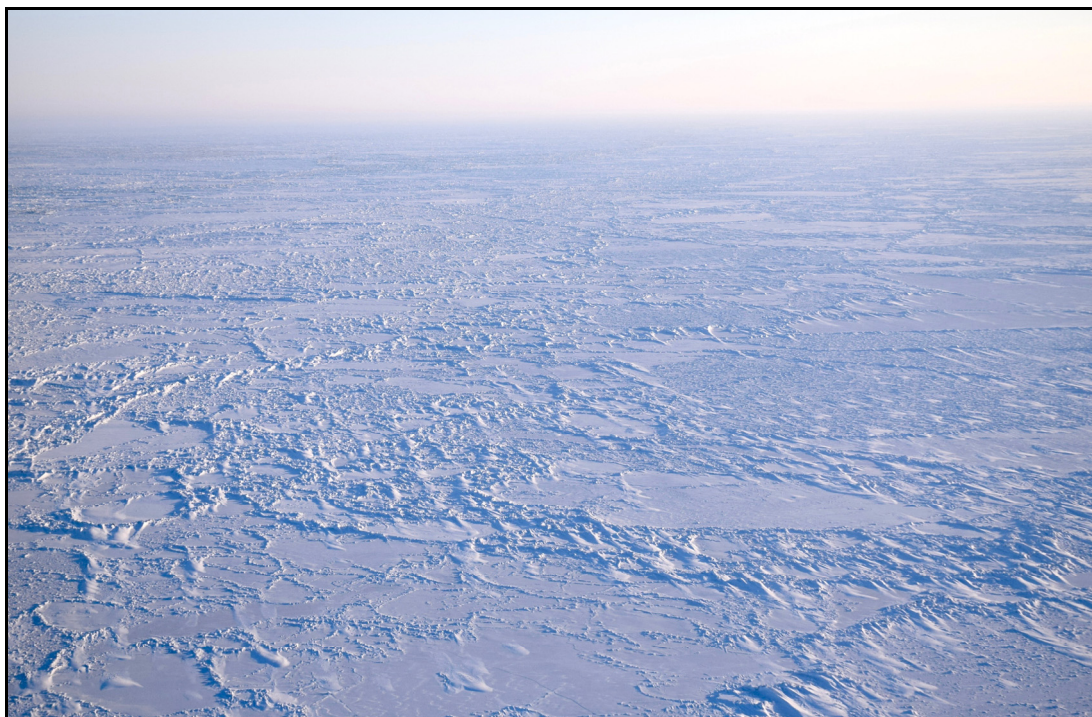


Plate 17. First-Year Floes with 2-m Rubble in Northern Portion of Harrison Bay Prospects (looking east on February 27, 2017)

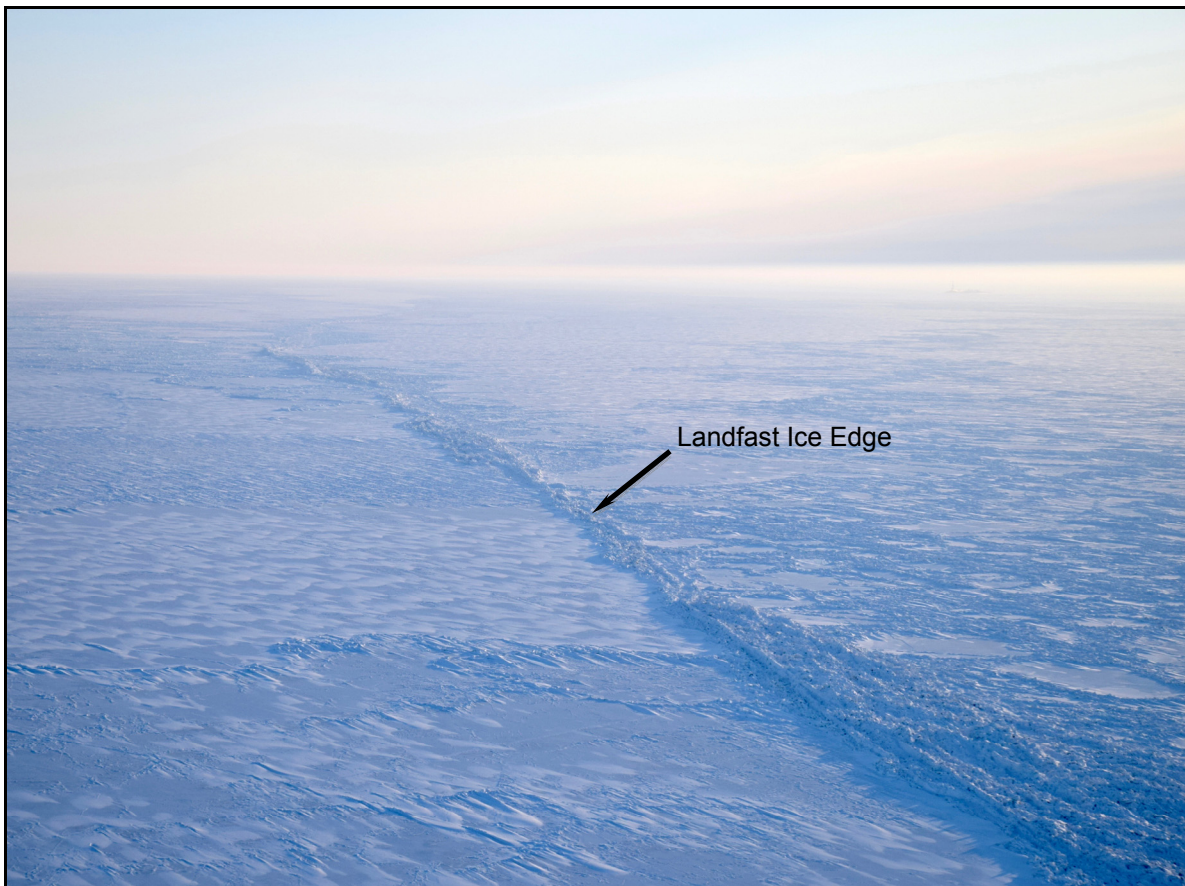


Plate 18. Well-Defined Shear Line with 4-m Shear Wall at Landfast Ice Edge in Southern Portion of Harrison Bay Prospects (looking east on February 23, 2017)

5. CHUKCHI SEA FREEZE-UP

Section 5.1 presents a concise overview of the 2016-17 freeze-up season in the northeast Chukchi Sea. As in the case of Section 4.1, emphasis is placed on summary tables. A detailed analysis of the conditions that prevailed from late summer 2016 through February 2017 follows in Sections 5.2 through 5.4.

5.1 Overview

Air Temperatures: Unseasonably warm air temperatures prevailed at Barrow Airport throughout the five-month study period (October through March). This trend was particularly strong in October and November, when the daily average temperatures exceeded the normal range on 56 occasions while never falling below. With the exception of brief cold spells in early December and mid-January, the elevated temperatures persisted into early February before dropping back to the normal range. As in the case of the Beaufort, the deviation from historical norms peaked in early January, when temperatures as high as 28°F (-2°C) were recorded. Over the entire study period (October through February), the daily average air temperatures exceeded the normal range on 101 days (67% frequency) and dropped below the normal range on only seven days (5% frequency).

Winds: Wind conditions during the 2016-17 freeze-up season are summarized in Table 11, which is based on the daily average speeds and directions recorded at Barrow Airport. Easterlies outnumbered westerlies by substantial margins in October, November, and December, while westerlies prevailed over easterlies by narrow margins in January and February. Over the entire five-month study period, easterlies occurred 61% of the time versus 39% for westerlies. The monthly average speeds ranged from a low of 9 kt (5 m/s) in November to a high of 12 kt (6 m/s) in October and January.

Storms: The characteristics of all storm events with daily average sustained wind speeds that exceeded 15 kt (8 m/s) at Barrow Airport are presented in Table 12. Of the 14 storms that occurred during the study period, eight were easterlies and six were westerlies. The most severe event, in terms of both peak wind speed (27 kt; 14 m/s) and duration (9 days), began on December 30th and continued through January 7th.

Ice Cover: Ice began to form in Kasegaluk Lagoon, the Kuk River Inlet, and Peard Bay during the third week in October, but freeze-up proceeded slowly in the weeks that followed due to air temperatures that hovered near the freezing point of sea water (29°F;

Table 11. Chukchi Sea Wind Characteristics, October 2016 – February 2017

Month	Days		Average Speed (kt)
	Easterly	Westerly	
October	23	8	12
November	23	7	9
December	18	13	11
January	15	16	12
February	13	15	10
Total Days	92	59	n/a
Frequency (%)	61	39	n/a

Note: Table 11 is based on the daily average wind speeds and directions recorded at Barrow Airport.

-2°C). Complete coverage of these semi-enclosed basins and initial ice formation in the open ocean adjacent to the coast occurred in early November. The pack ice, after advancing rapidly to the south during the first week in November, reached the vicinity of Point Barrow during the second week and began to coalesce with the nascent strip of coastal ice.

On or about December 7th, a flash-freeze created an isolated patch of ice centered approximately 150 nm (278 km) west of Icy Cape. Similar events occurred in 2012 and 2013 (Coastal Frontiers and Vaudrey, 2014). Freeze-up in the nearshore region took place three days later, on December 10th, after a cold spell that brought five days of air temperatures below -10°F (-23°C) and moderate winds. Basin-wide freeze-up north of Cape Lisburne followed on December 27th.

Ice Thickness: The thickness of undeformed first-year ice at the end of each month was estimated using the relationship of Lebedev (Bilello, 1960) in concert with the accumulated freezing degree days (FDD) at Barrow Airport shown in Table 1. The method of calculation is identical to that presented for the Beaufort Sea in Section 4.1. The results are provided in Table 13, which indicates that undisturbed first-year ice attained a maximum thickness of 134 cm on May 23rd.

Landfast Ice: The first traces of landfast ice appeared in Peard Bay at the end of October. An extremely narrow, discontinuous strip developed along the coast between Point Barrow and Point Lay in November, its growth retarded by a strong predominance of

Table 12. Chukchi Sea Storm Characteristics, October 2016 – February 2017¹

Month	Day	Duration (days)	Maximum Wind Speed (kt) ²	
			Easterly	Westerly
October	2	1	17	
	8-13 ³	6	18	
	19	1		17
	29	1	16	
November	2-4	3	23	
	11	1	16	
December	14-15	2	18	
	22-23	2		21
January	Dec 30-Jan 7	9		27
	11	1		17
	30	1	16	
February	Jan 31-Feb 2	3		19
	8-10	3		17
	24-26	3	26	
Total Duration		37		
Total Number of Events			8	6

Notes:

- ¹ Table 12 includes all storm events with a daily average sustained wind speed exceeding 15 kt at Barrow Airport.
- ² “Maximum Wind Speed” refers to highest daily average sustained wind speed that occurred during each storm event.
- ³ Daily average wind speed decreased to 8 kt on October 10th but freshened to 18 kt on October 11th.

easterly winds, two easterly storms, and a complete absence of westerly storms. Modest expansion ensued in December, but the strip remained narrow and discontinuous in response to a continuing predominance of easterly winds. At the end of December, it attained a maximum width of only 2 nm (4 km) to the southwest of Icy Cape.

The situation changed in January, when an increased frequency of westerly winds, two westerly storms at the beginning of the month, and the start of a third storm at the end produced a continuous band of landfast ice up to 10 nm (19 km) wide off Skull Cliff

Table 13. Chukchi Sea Computed Ice Thickness, October 2016 – May 2017¹

Date	FDD	Accumulated FDD	Ice Thickness ² (cm)
31 October 2016	32	32	7
30 November 2016	463	495	34
31 December 2016	888	1,383	62
31 January 2017	900	2,283	83
29 February 2017	980	3,263	103
31 March 2017	1,122	4,385	122
30 April 2017	662	5,047	132
23 May 2017	147	5,194	134

Notes:

¹ Table 13 is based on the average daily air temperature data recorded at Barrow Airport.

² Ice thickness is computed from accumulated FDD using method of Lebedev (Bilello, 1960).

and 8 nm (15 km) wide between Icy Cape and Point Lay. During the second half of the month, the ice grounded on Blossom Shoals, its customary anchor point off Icy Cape. Additional expansion followed in early February, driven by the aforementioned westerly storm that began in late January along with another that occurred soon thereafter. At mid-month, the landfast ice attained the maximum width observed during the study period, 20 nm (37 km) between Wainwright and the Nokotlek River mouth. Subsequently, at the end of February, a strong easterly storm dislodged the new ice and caused the landfast ice edge to retreat to the location it occupied at the beginning of the month. The fact that a continuous strip of ice survived the storm, with ample widths in some areas, indicates that substantial grounding had occurred in January and early February.

Ice Pile-Ups: Sixty-three ice pile-ups occurred on the shoreline between Barrow and Point Lay during the 2016-17 freeze-up season. Fifty-two were located to the south of Point Belcher, while 11 were located to the north. As shown in Table 14, their dimensions were relatively small compared to those observed in the past. The heights ranged from 1 to 5 m, the encroachment distances from 0 to 10 m onto the subaerial beach, and the alongshore lengths from 50 m to 4 km. The block thicknesses were estimated to vary from 30 to 40 cm.

Table 14. Ice Pile-Ups on Chukchi Sea Coast during 2016-17 Freeze-Up Season

No.	Location	Formation Date	Arrived From	Length¹ (m)	Height² (m)	Encroachment³ (m)
1	Barrow - Peard Bay	Dec 19-20	NW	400	2	3
2	Barrow - Peard Bay	Dec 19-20	NW	500	3	5
3	Barrow - Peard Bay	Dec 19-20	NW	500	3	5
4	Barrow - Peard Bay	Dec 19-20	NW	350	3	10
5	Barrow - Peard Bay	Dec 19-20	NW	250	2	3
6	Barrow - Peard Bay	Dec 19-20	NW	2,900	3	10
7	Barrow - Peard Bay	Dec 19-20	NW	200	3	5
8	Barrow - Peard Bay	Dec 19-20	NW	1,000	2	5
9	Barrow - Peard Bay	Dec 19-20	NW	150	1	5
10	Barrow - Peard Bay	Dec 19-20	N	300	1	5
11	Barrow - Peard Bay	Dec 19-20	N	400	1	5
12	Pt. Belcher - Kuk River	Dec 19-20	NW	1,000	2	5
13	Pt. Belcher - Kuk River	Dec 19-20	NW	350	3	5
14	Pt. Belcher - Kuk River	Dec 19-20	NW	600	2	3
15	Pt. Belcher - Kuk River	Dec 19-20	NW	500	3	6
16	Pt. Belcher - Kuk River	Dec 19-20	NW	250	2	3
17	Pt. Belcher - Kuk River	Dec 19-20	NW	350	2	4
18	Pt. Belcher - Kuk River	Dec 19-20	NW	350	2	3
19	Pt. Belcher - Kuk River	Dec 19-20	NW	350	3	3
20	Pt. Belcher - Kuk River	Dec 19-20	NW	350	3	0
21	Pt. Belcher - Kuk River	Dec 19-20	NW	100	2	2
22	Kuk R. – Kasegaluk Lag.	Dec 19-20	NW	200	2	3
23	Kuk R. – Kasegaluk Lag.	Dec 19-20	NW	350	2	5
24	Kuk R. – Kasegaluk Lag.	Dec 19-20	NW	1,100	2	5
25	Kuk R. – Kasegaluk Lag.	Dec 19-20	NW	300	3	5
26	Kuk R. – Kasegaluk Lag.	Dec 19-20	NW	300	3	3

(continued)

**Table 14. Ice Pile-Ups on Chukchi Sea Coast during 2016-17 Freeze-Up Season
(continued)**

No.	Location	Formation Date	Arrived From	Length ¹ (m)	Height ² (m)	Encroachment ³ (m)
27	Kuk R. – Kasegaluk Lag.	Dec 19-20	NW	200	2	3
28	Kuk R. – Kasegaluk Lag.	Dec 19-20	NW	350	1	0
29	East of Icy Cape ⁴	Dec 19-20	NW	100	1	3
30	East of Icy Cape ⁴	Dec 19-20	NW	1,000	3	5
31	East of Icy Cape ⁴	Dec 19-20	NW	500	1	3
32	East of Icy Cape ⁴	Dec 19-20	NW	50	1	3
33	East of Icy Cape ⁴	Dec 19-20	NW	1,800	3	5
34	East of Icy Cape ⁴	Dec 19-20	NW	4,000	3	10
35	East of Icy Cape ⁴	Dec 19-20	N	100	3	5
36	East of Icy Cape ⁴	Dec 19-20	N	200	2	5
37	East of Icy Cape ⁴	Dec 19-20	N	100	1	3
38	East of Icy Cape ⁴	Dec 19-20	N	750	2	0
39	East of Icy Cape ⁴	Dec 19-20	N	500	2	8
40	East of Icy Cape ⁴	Dec 19-20	N	600	5	5
41	South of Icy Cape ⁵	Dec 19-20	NW	800	2	8
42	South of Icy Cape ⁵	Dec 19-20	NW	800	2	8
43	South of Icy Cape ⁵	Dec 19-20	NW	750	2	0
44	South of Icy Cape ⁵	Dec 19-20	NW	350	1	3
45	South of Icy Cape ⁵	Dec 19-20	NW	600	1	4
46	South of Icy Cape ⁵	Dec 19-20	NW	450	3	5
47	South of Icy Cape ⁵	Dec 19-20	NW	100	2	0
48	South of Icy Cape ⁵	Dec 19-20	NW	350	3	0
49	South of Icy Cape ⁵	Dec 19-20	NW	2,800	4	8
50	South of Icy Cape ⁵	Dec 19-20	NW	450	1	3

(continued)

**Table 14. Ice Pile-Ups on Chukchi Sea Coast during 2016-17 Freeze-Up Season
(continued)**

No.	Location	Formation Date	Arrived From	Length ¹ (m)	Height ² (m)	Encroachment ³ (m)
51	South of Icy Cape ⁵	Dec 19-20	NW	1700	3	7
52	South of Icy Cape ⁵	Dec 19-20	NW	500	2	4
53	South of Icy Cape ⁵	Dec 19-20	NW	1,100	1	2
54	South of Icy Cape ⁵	Dec 19-20	NW	800	1	2
55	South of Icy Cape ⁵	Dec 19-20	NW	650	1	3
56	South of Icy Cape ⁵	Dec 19-20	NW	550	3	6
57	South of Icy Cape ⁵	Dec 19-20	NW	2,300	3	5
58	South of Icy Cape ⁵	Dec 19-20	NW	700	1	3
59	South of Icy Cape ⁵	Dec 19-20	NW	2,900	1	3
60	South of Icy Cape ⁵	Dec 19-20	NW	100	2	2
61	South of Icy Cape ⁵	Dec 19-20	NW	1,900	3	3
62	South of Icy Cape ⁵	Dec 19-20	NW	100	2	3
63	South of Icy Cape ⁵	Dec 19-20	NW	1,500	2	4

Notes:

- ¹ “Length” indicates alongshore extent of pile-up.
- ² “Height” indicates maximum height of pile-up relative to MSL.
- ³ “Encroachment” indicates distance ice advanced onto subaerial beach.
- ⁴ Pile-up occurred on barrier islands east of Icy Cape.
- ⁵ Pile-up occurred on barrier islands south of Icy Cape.

The pile-ups probably resulted from a wind shift that occurred on December 19th and 20th. During this period, strong easterly winds that had begun six days earlier veered through south to northwest and attained a one-hour sustained speed of 20 kt (10 m/s). Although some of the pile-ups could have resulted from other wind events, the available RADARSAT-2 images and wind data suggest that December 19th-20th marked the first simultaneous occurrence of the ice cover and wind conditions necessary to initiate the formation of these features.

Coastal Flaw Lead: From December 2016 through February 2017, the flaw lead that forms off the Chukchi Sea coast in response to easterly winds opened on nine separate occasions. The frequency of occurrence, which averaged 51% for the entire three-month

period, increased from 42% in December to 52% in January and 61% in February (Figure 43). The maximum width, 50 nm (93 km), and maximum length, 250 nm (463 km), both occurred during a single event that began in late January and continued into early February. The lead persisted for periods that ranged from one to 15 days.

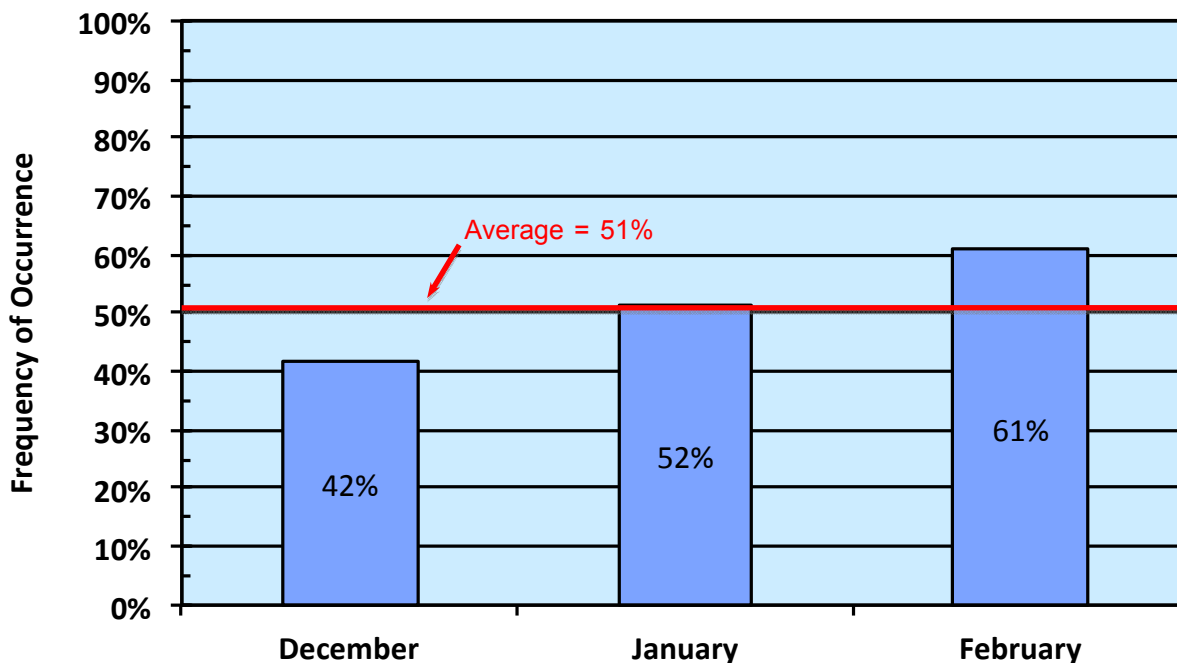
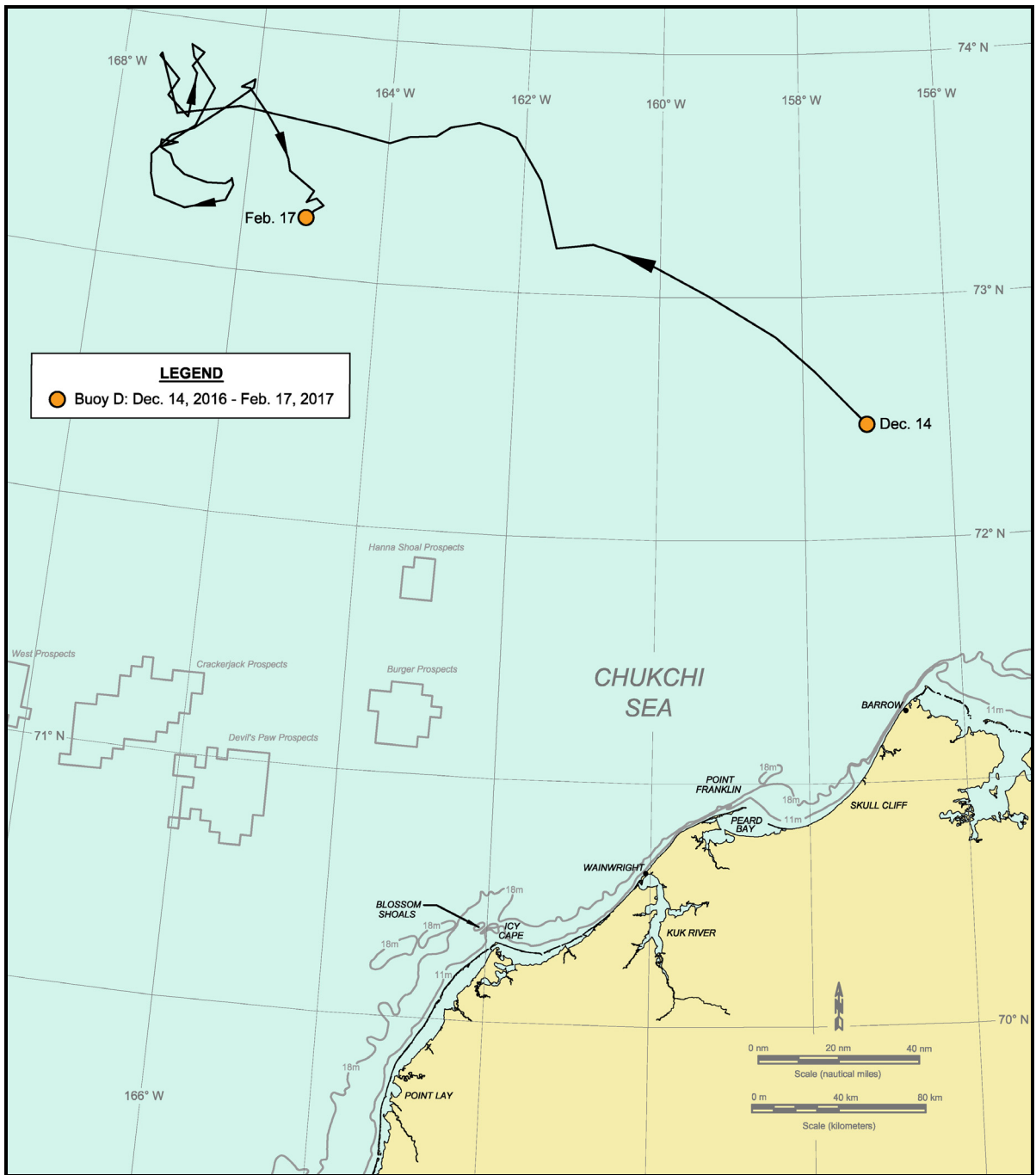


Figure 43. Frequency of Occurrence of Chukchi Sea Flaw Lead, December 2016 - February 2017

Multi-Year Ice: With the exception of two patches of second-year ice that were located in the vicinity of Point Barrow at the beginning of October but moved to the northwest and dissipated over the next two weeks (Figure 21), multi-year ice remained completely absent from the Chukchi Sea study area throughout the five-month study period.

Ice Drift: Ice drift was investigated using a single drift buoy (Buoy D) that had been deployed in open water and was monitored through the International Arctic Buoy Program (IABP; Section 3.4). As shown in Figure 44, the buoy was embedded in the pack ice inside the study area from mid-December until mid-February.

Monthly average drift rates, computed from the first and last position of the buoy in each of the three months for which data are available, are provided in Table 15. During the second half of December, when easterly winds predominated and the buoy was located near the southern edge of the pack ice, it moved rapidly to the northwest at an average rate



Data Source: Rigor, 2017

Figure 44. Chukchi Sea Drift Buoy Track, December 2016 – February 2017

of 11.2 nm/day (20.8 km/day). This pattern changed dramatically in January and the first half of February, when a predominance of westerly winds produced small net displacements and associated drift rates of only 0.2 and 2.3 nm/day (0.4 and 4.3 km/day), respectively.

Table 15. Chukchi Sea Ice Drift, December 2016 - February 2017

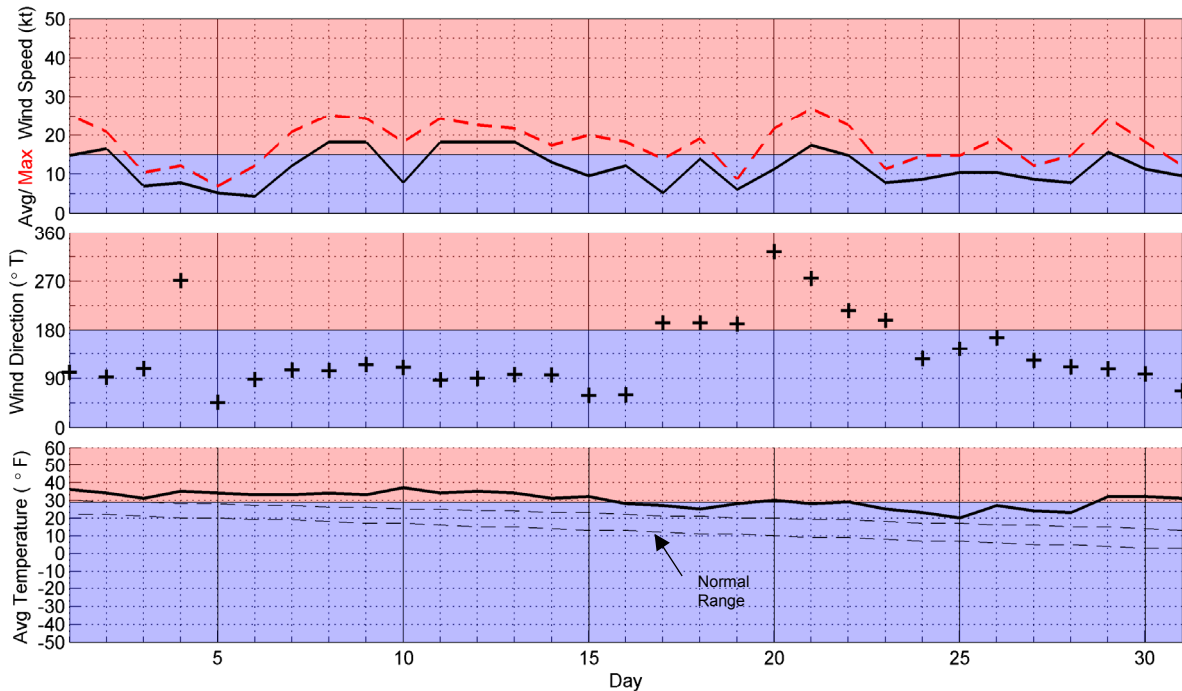
Month	No. of Buoys	Monthly Average Speed (nm/day)
December	1	11.2
January	1	0.2
February	1	2.3
Average		4.6

Note: Monthly average speeds were derived for periods that ranged from 17 to 31 days (based on the presence of an IABP drift buoy in the study area).

5.2. Early Freeze-Up

5.2.1. October 2016

Meteorological Conditions: The daily values of average and maximum sustained wind speed, average wind direction, and average air temperature at Barrow Airport are shown in Figure 45. As in Section 4, the red and blue color bands in this and all subsequent meteorological plots denote the ranges of parameters defined in Table 10. Unless indicated otherwise, the wind speeds discussed in the text refer to the daily average values of the sustained speed rather than the daily maximum values or hourly values.



Source: Weather Underground, 2016

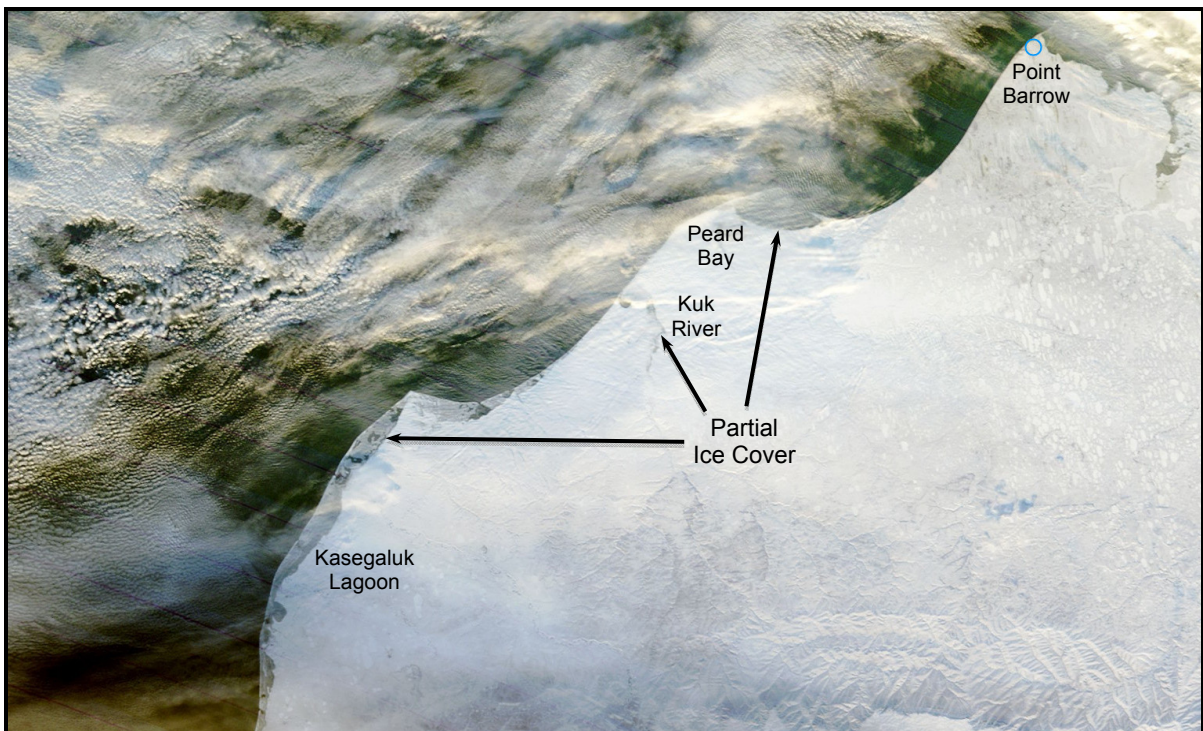
Figure 45. Meteorological Conditions at Barrow Airport in October 2016

The average daily air temperatures in October 2017 were exceptionally warm, exceeding the normal range on each day of the month. They averaged 30°F (-1°C), and dropped below the freezing point of sea water (29°F; -2°C) on only 11 occasions.

Easterly winds outnumbered westerlies by a margin of nearly three to one, occurring on 23 of the 31 days (Table 11). The average wind speed, 12 kt (6 m/s), matched that in January as the highest recorded during the study period. The storm population consisted of three easterly events and one westerly:

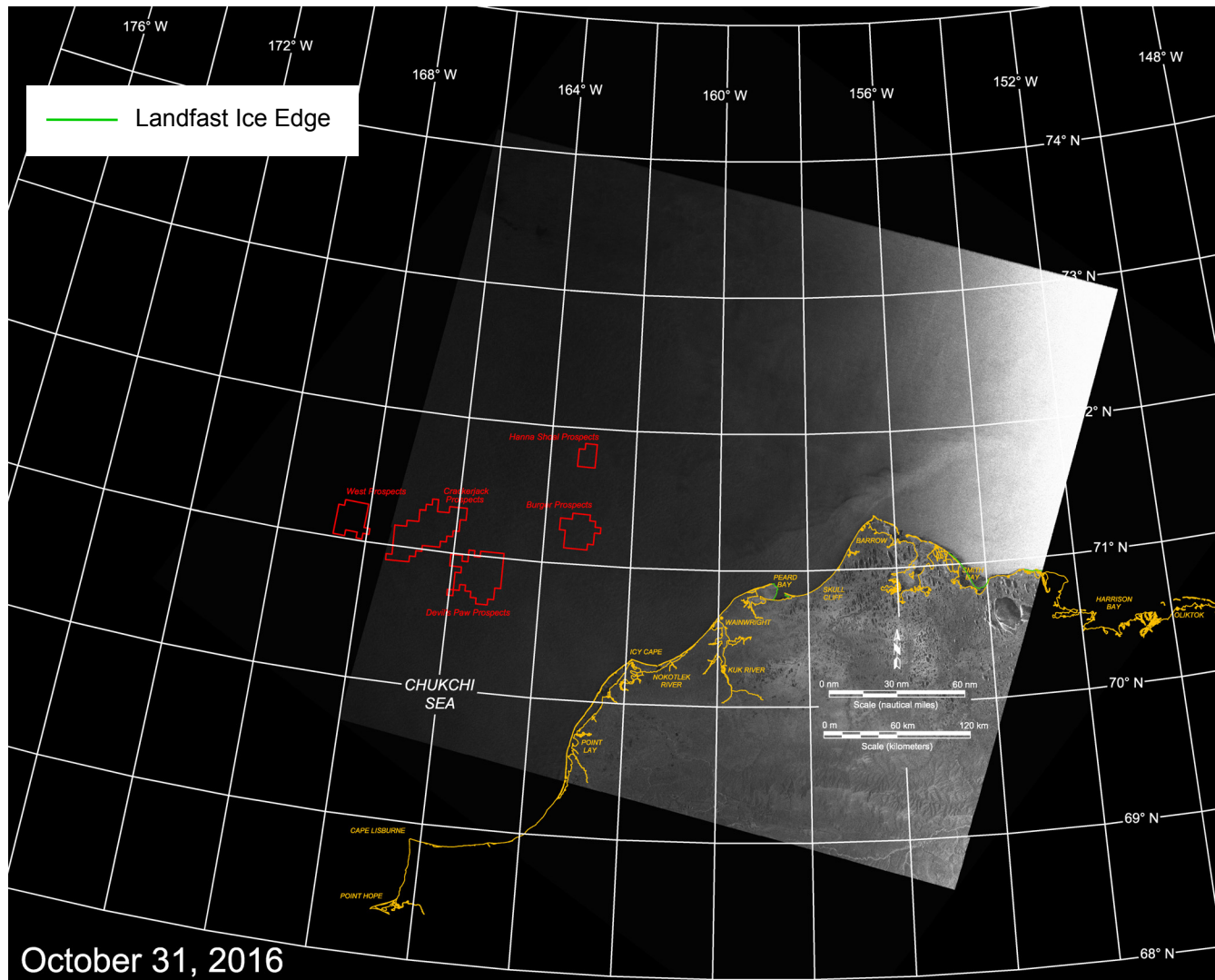
- October 2nd: one-day easterly with maximum speed of 17 kt (9 m/s);
- October 8th-13th: six-day easterly with maximum speed of 18 kt (9 m/s);
- October 19th: one-day westerly with maximum speed of 17 kt (9 m/s);
- October 29th: one-day easterly with maximum speed of 16 kt (8 m/s).

Ice Cover: Ice began to form in Kasegaluk Lagoon, the Kuk River Inlet, and Peard Bay during the third week in October, when the air temperatures fell below 29°F (-2°C). As illustrated in Figures 46 and 47, freeze-up proceeded slowly during the remainder of the month, with incomplete ice coverage in the lagoon areas and a complete absence of ice in the exposed waters adjacent to the coast at month-end.



After: NASA, 2016a

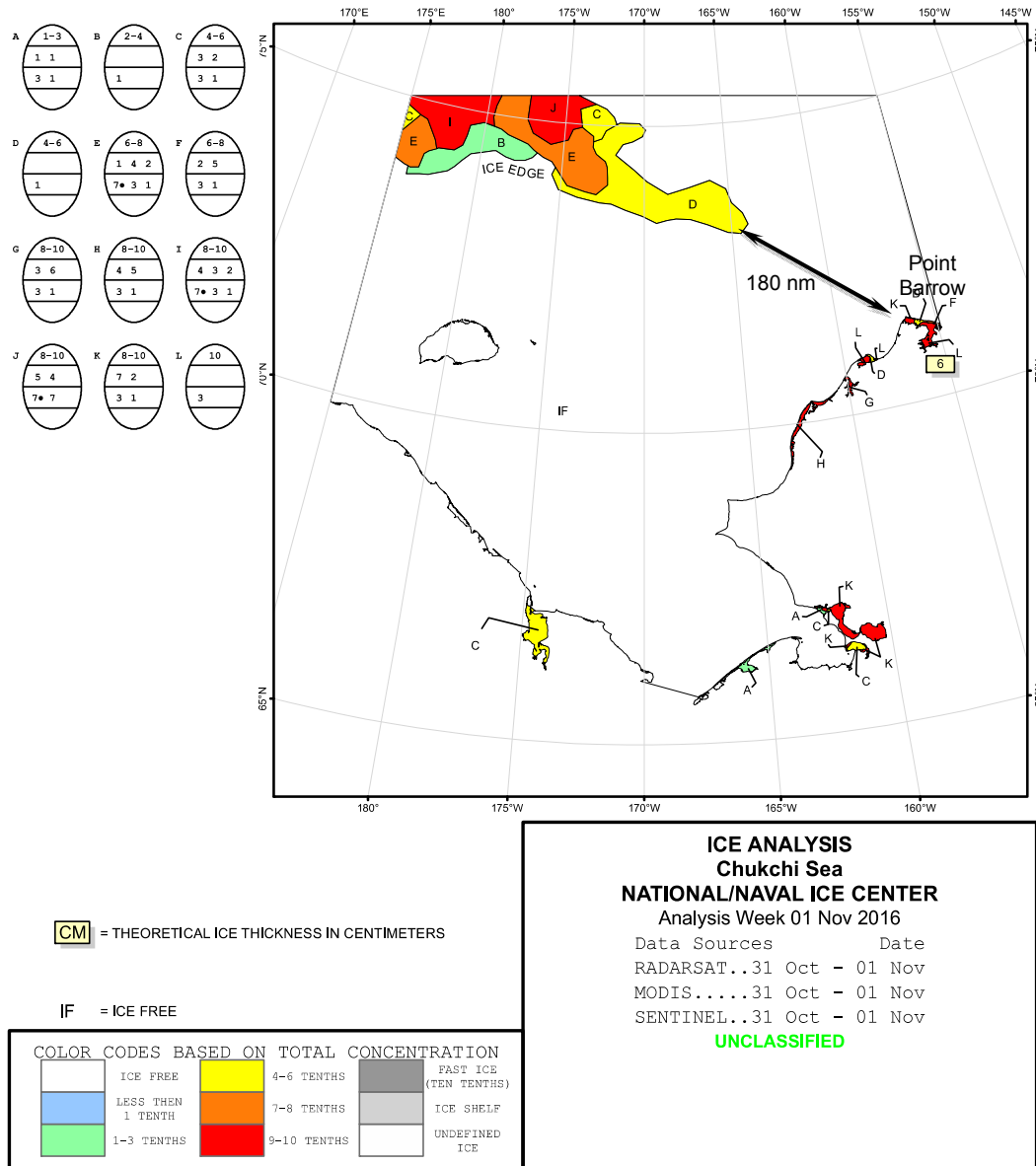
Figure 46. MODIS Image Acquired on October 28, 2016



Source: RADARSAT-2 Data and Products © MacDonald Dettwiler and Associates Ltd., 2016 – All Rights Reserved

Figure 47. RADARSAT-2 Image of Chukchi Sea Acquired on October 31, 2016

The pack ice remained well offshore throughout October. At the end of the month, the southern boundary was located north of the 73°N parallel, with the point of closest approach located 180 nm (334 km) to the northwest of Point Barrow (Figure 48).



After: National Ice Center, 2017

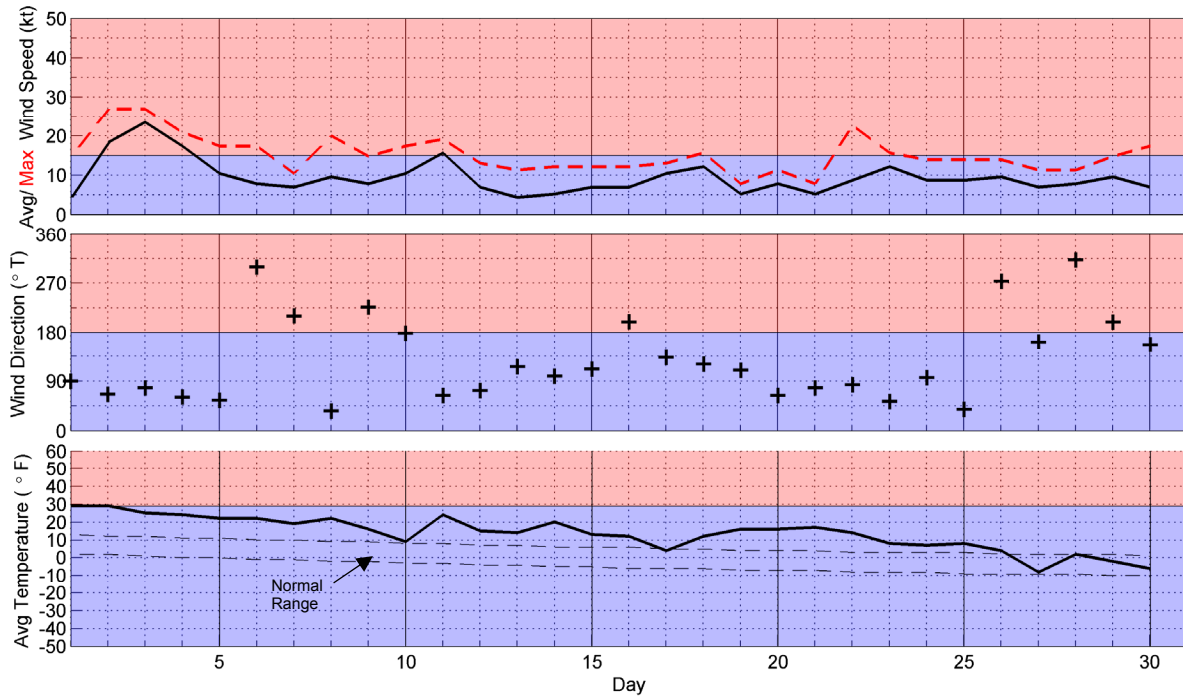
Figure 48. NIC Ice Chart for November 1, 2016

Ice Thickness: The thickness of undisturbed first-year ice at the end of October was computed to be 7 cm (Table 13).

Landfast Ice: As shown in Figures 47 and 49, landfast ice appeared in and adjacent to Peard Bay at the end of October.

5.2.2. November 2016

Meteorological Conditions: The wind and temperature data acquired at Barrow Airport in November are shown in Figure 50. The unseasonably warm air temperatures that prevailed in October continued until the final week of November. Over the course of the month, the daily average readings topped the normal range on 25 days and never dropped below. The average for the month was 14°F (-10°C).



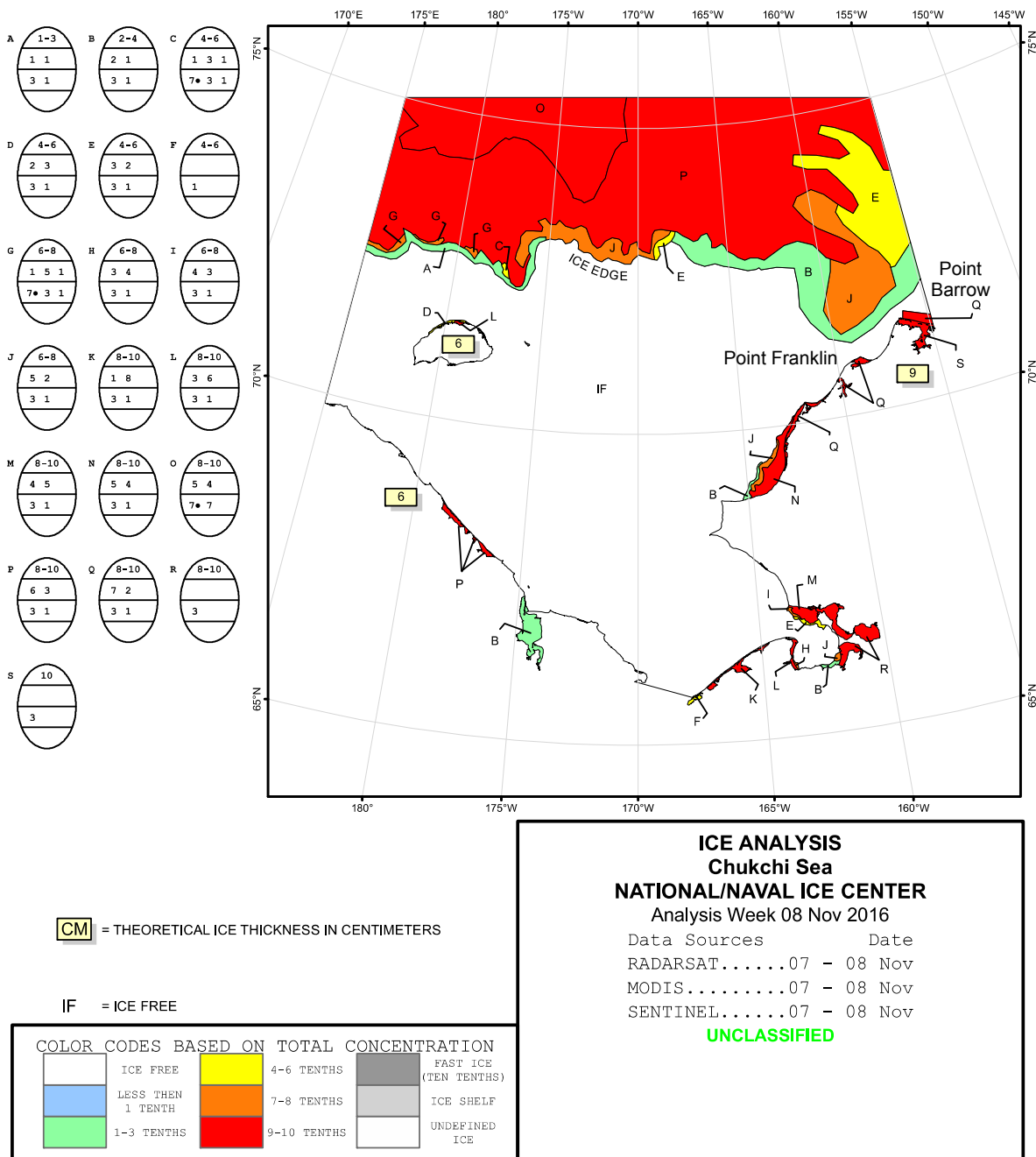
Source: Weather Underground, 2016

Figure 50. Meteorological Conditions at Barrow Airport in November 2016

As in October, easterlies outnumbered westerlies by a wide margin (23 of 30 days). The wind regime differed, however, in that the average speed (9 kt; 5 m/s) was the lowest recorded during the entire study period. The storm population consisted of only two events, both of which occurred during the first half of the month:

- November 2nd-4th: three-day easterly with maximum speed of 23 kt (12 m/s);
- November 11th: one-day easterly with maximum speed of 16 kt (8 m/s).

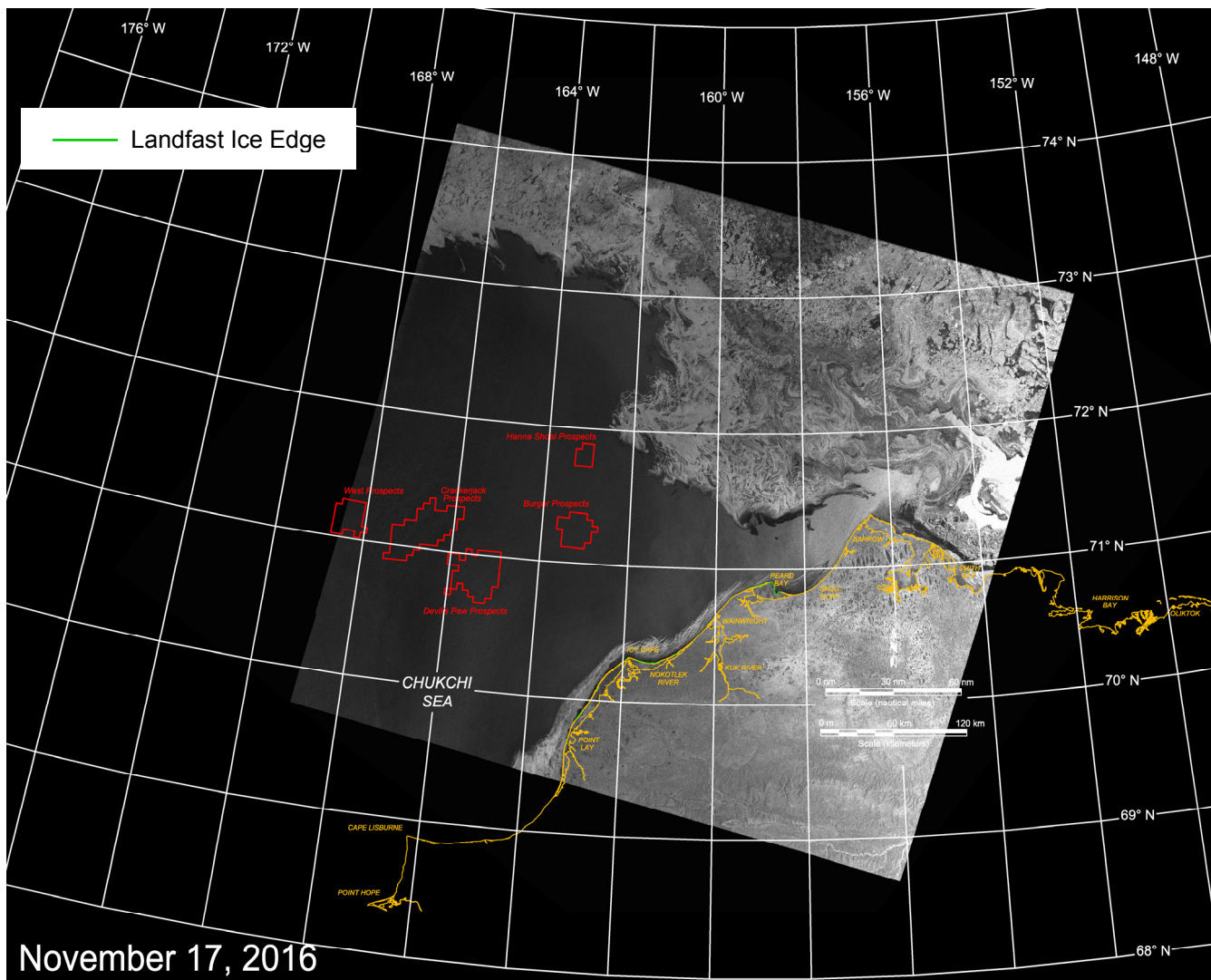
Ice Cover: During the first week in November, when the air temperatures dropped below freezing, complete ice coverage occurred in Kasegaluk Lagoon, the Kuk River Inlet, and Peard Bay, ice began to form in the open ocean adjacent to the coast, and the pack ice advanced rapidly to the south. As shown in Figure 51, the southern boundary of the pack ice was located approximately 20 nm (37 km) north of Point Franklin on November 8th.



After: National Ice Center, 2016

Figure 51. NIC Ice Chart for November 8, 2016

Changes were muted during the remainder of the month, with the pack ice moving slowly to the south and coalescing with the expanding band of nearshore ice. The extent of the ice canopy on November 17th is shown in Figure 52. At month-end, the southern boundary of the pack ice had advanced to the vicinity of Wainwright.



Source: RADARSAT-2 Data and Products © MacDonald Dettwiler and Associates Ltd., 2016 – All Rights Reserved

Figure 52. RADARSAT-2 Image of Chukchi Sea Acquired on November 17, 2016

Ice Thickness: The calculated thickness of undisturbed first-year ice increased from 7 cm at the beginning of the month to 34 cm at the end (Table 13).

Landfast Ice: Landfast ice growth in November was retarded not only by the warm air temperatures, but also by a predominance of easterly winds, two easterly storms, and a complete absence of westerly storms (which tend to initiate grounding when they push the ice against the coast). During the first half of the month, the landfast ice at Peard Bay experienced modest expansion, while extremely narrow strips appeared off the Kuk River Inlet and portions of the barrier islands that define Kasegaluk Lagoon (Figures 52 and 53).

Between mid-November and early December, the existing areas of landfast ice expanded laterally and a new strip appeared between Point Barrow and Skull Cliff. The gains were small, however. As illustrated in Figure 53, the landfast ice zone in early December consisted of an extremely narrow, discontinuous strip.

5.3 Late Freeze-Up

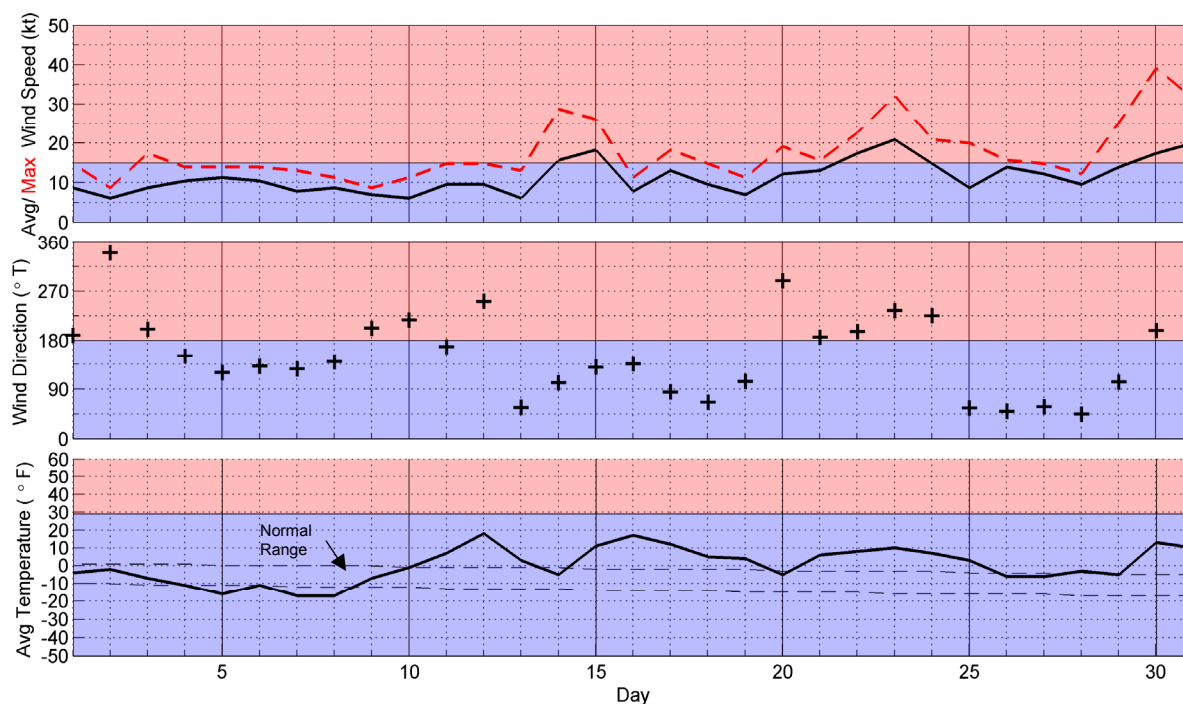
5.3.1 December 2016

Meteorological Conditions: The wind and temperature data recorded at Barrow Airport in December 2016 are provided in Figure 54. Relatively cold temperatures prevailed during the first eight days, with the daily average values lying within the normal range on five occasions and dropping below on three. The warm temperatures that characterized October and November then returned, producing above-normal values on 16 of the remaining 23 days. The average temperature for the month was 0°F (-18°C).

For the third consecutive month, easterly winds outnumbered westerlies, but the margin was narrower than in October and November: 18 days with easterlies versus 13 with westerlies. The average speed was 11 kt (6 m/s). Two relatively brief storms occurred over the course of the month, one easterly and one westerly:

- December 14th-15th: two-day easterly with maximum speed of 18 kt (9 m/s);
- December 22nd-23rd: two-day westerly with maximum speed of 21 kt (11 m/s).

The westerly storm that took place on the 22nd and 23rd was the first to occur in over two months, and only the second of the freeze-up season. Another westerly began on December 30th, but is included in the January storm population because it continued through the 7th of that month (Section 5.3.2).



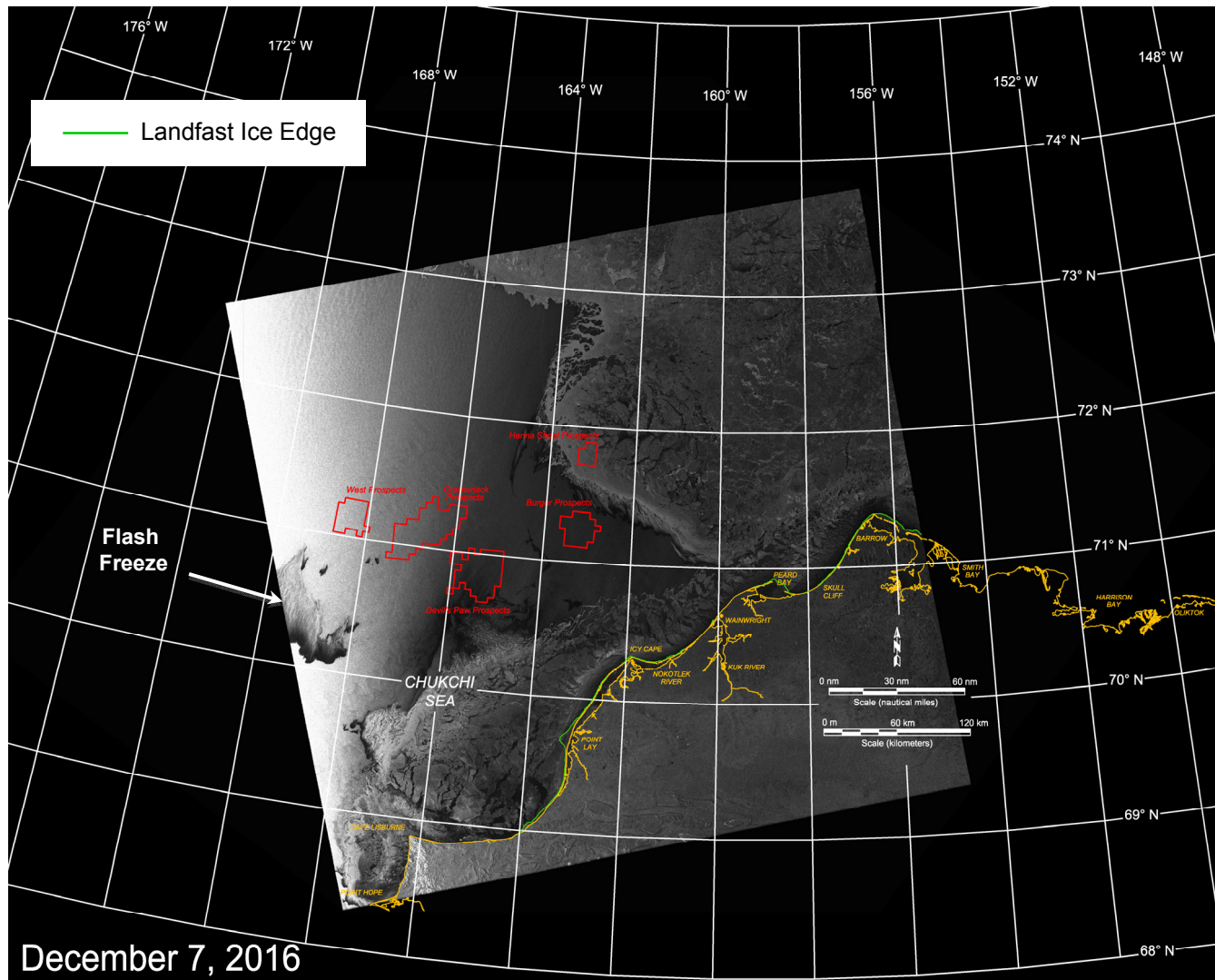
Source: Weather Underground, 2017

Figure 54. Meteorological Conditions at Barrow Airport in December 2016

Ice Cover: On or about December 7th, when the air temperatures at Barrow dropped to -17°F (-27°C) a flash-freeze created an isolated patch of ice centered approximately 150 nm (278 km) west of Icy Cape (Figure 55). Similar events were noted in 2012 and 2013, but on much earlier dates: October 31st in the case of the former, and November 12th in the case of the latter (Coastal Frontiers and Vaudrey, 2013; 2014).

Freeze-up in the nearshore region took place on December 10th, precipitated by the cold spell that began at the start of the month. (For the present purpose, the “nearshore region” of the Chukchi is defined as the area south of the 71°24’ N parallel, which passes through Point Barrow, and east of the 163° W meridian, which passes through Point Lay.) Eight hundred and seventy-eight FDD had accumulated at Barrow Airport on this date. It should be noted that the coastal flaw lead, which produces open water near the coast, was excluded from the determination of the freeze-up date.

Complete freeze-up in the region north of Cape Lisburne occurred on or about December 27th, when 1,282 FDD had accumulated at Barrow Airport. Subsequently, the ice canopy was subject to lead formation but otherwise remained intact.



Source: RADARSAT-2 Data and Products © MacDonald Dettwiler and Associates Ltd., 2016 – All Rights Reserved

Figure 55. RADARSAT-2 Image of Chukchi Sea Acquired on December 7, 2016

To provide a quantitative understanding of the progress of freeze-up in the Chukchi Sea lease areas, the percentage of ice coverage was assessed in five representative prospects (Hanna Shoal, Burger, Crackerjack, West, and Devil’s Paw) using RADARSAT-2 images and NIC ice charts (National Ice Center, 2016). As shown in Table 16, pack ice entered the Hanna Shoal Prospects in mid-November and achieved complete coverage on or about the 24th. The ice first entered the Burger and Crackerjack Prospects at the end of November, but failed to achieve complete and lasting coverage until mid-December in the case of Burger, and late December in the case of Crackerjack. Ice began to invade the final two prospects, West and Devil’s Paw, in mid-December, with complete coverage occurring prior to month-end.

Table 16. Ice Cover in Chukchi Sea Prospects during Freeze-Up

Date	Ice Cover (%)				
	Hanna Shoal	Burger	Crackerjack	West	Devil’s Paw
November 17 ¹	0	0	0	0	0
November 22 ²	85	0	0	0	0
November 24 ²	100	0	0	0	0
November 29 ²	100	100	15	0	0
December 1 ²	100	100	0	0	0
December 6 ²	100	50	0	0	0
December 7 ¹	100	0	0	0	0
December 8 ²	100	20	0	0	0
December 14 ¹	100	100	35	0	35
December 20 ²	100	100	70	90	100
December 31 ¹	100	100	100	100	100

Notes:

- ¹ Ice cover estimated using RADARSAT-2 images.
- ² Ice cover estimated using NIC ice charts.

Ice Thickness: The calculated thickness of undisturbed first-year ice increased by 28 cm in December, from 34 to 62 cm.

Landfast Ice: The successive locations of the landfast ice edge were estimated from RADARSAT-2 images obtained on December 7th, 14th, and 31st (Figure 56). During the first interval, when easterly winds predominated, the narrow, discontinuous strip of landfast ice experienced little change. During the second, losses occurred off the north-facing coastlines to the east of Point Franklin and Icy Cape, while a gain occurred off the barrier islands to the southwest of Icy Cape. These changes probably resulted from the southwesterly storm that occurred on December 22nd and 23rd. At the end of the month, the strip of landfast ice remained narrow and discontinuous, with prominent gaps to the east of Peard Bay, in the vicinity of Wainwright, and to the east of Icy Cape.

Ice Pile-Ups: During the aerial reconnaissance flight conducted on March 1st, 63 ice pile-ups were observed on the coast between Barrow and Point Lay. As discussed in Section 5.1, the pile-ups are believed to have formed in response to winds that shifted from easterly to northwesterly on December 19th and 20th.

Although the number of pile-ups was large, their dimensions were relatively small by historical standards. The heights ranged from 1 to 5 m, the encroachment distances from 0 to 10 m, and the alongshore lengths from 50 m to 4 km (Table 14). The pile-ups were composed of ice blocks estimated to be 30 to 40 cm thick.

Coastal Flaw Lead: Based on analysis of daily AVHRR imagery (National Weather Service, 2016) and three RADARSAT-2 images, the coastal flaw lead opened on three occasions in December. The aggregate duration, 13 days, represented a 42% frequency of occurrence. Easterly winds, which create the lead by pushing the pack ice offshore, prevailed on each of these days. The lead's maximum length, 150 nm (279 km), occurred on December 18th, while the maximum width, 35 nm (65 km), occurred on the 27th.

Ice Movement: Ice drift was investigated using an IABP buoy that, based on a review of the available RADARSAT-2 and AVHRR images, was embedded in the pack ice by December 14th (Buoy D; Section 3.4). The trajectory is shown in Figure 57, while the daily average speeds are plotted in concert with the corresponding wind data from Barrow Airport in Figure 58.

The buoy raced to the northwest during the 18-day tracking period, averaging 12.3 nm/day (22.8 km/day). Its rapid progress appears to have been aided not only by a predominance of easterly winds, but also by the minimal confinement afforded by the nascent ice canopy. The highest daily average speed, 24.5 nm/day (45.4 km/day; 1.0 kt) occurred on December 30th, when the wind shifted from easterly to southerly and freshened to 17 kt (9 m/s). The resulting wind factor was 5.9%.

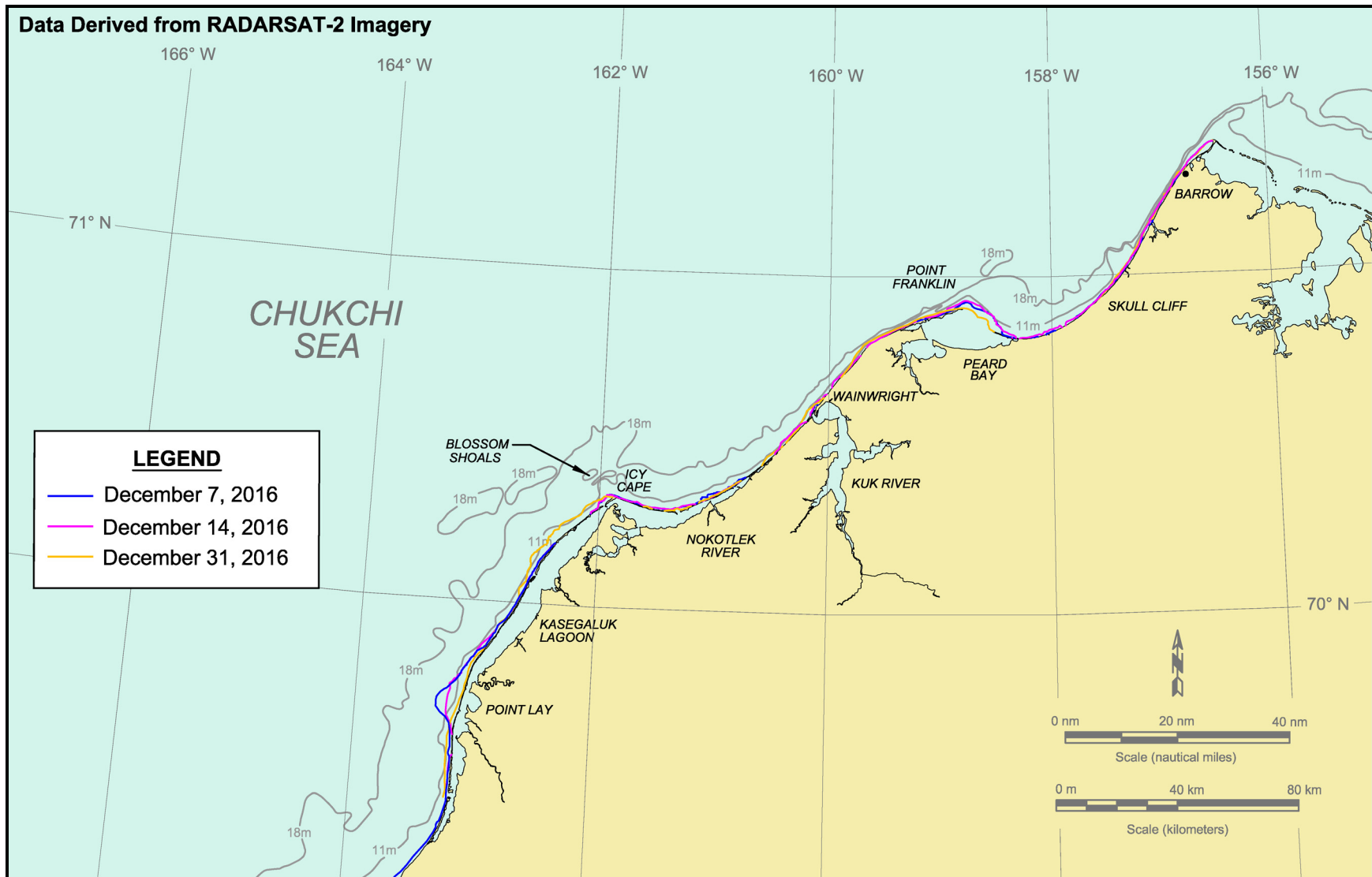
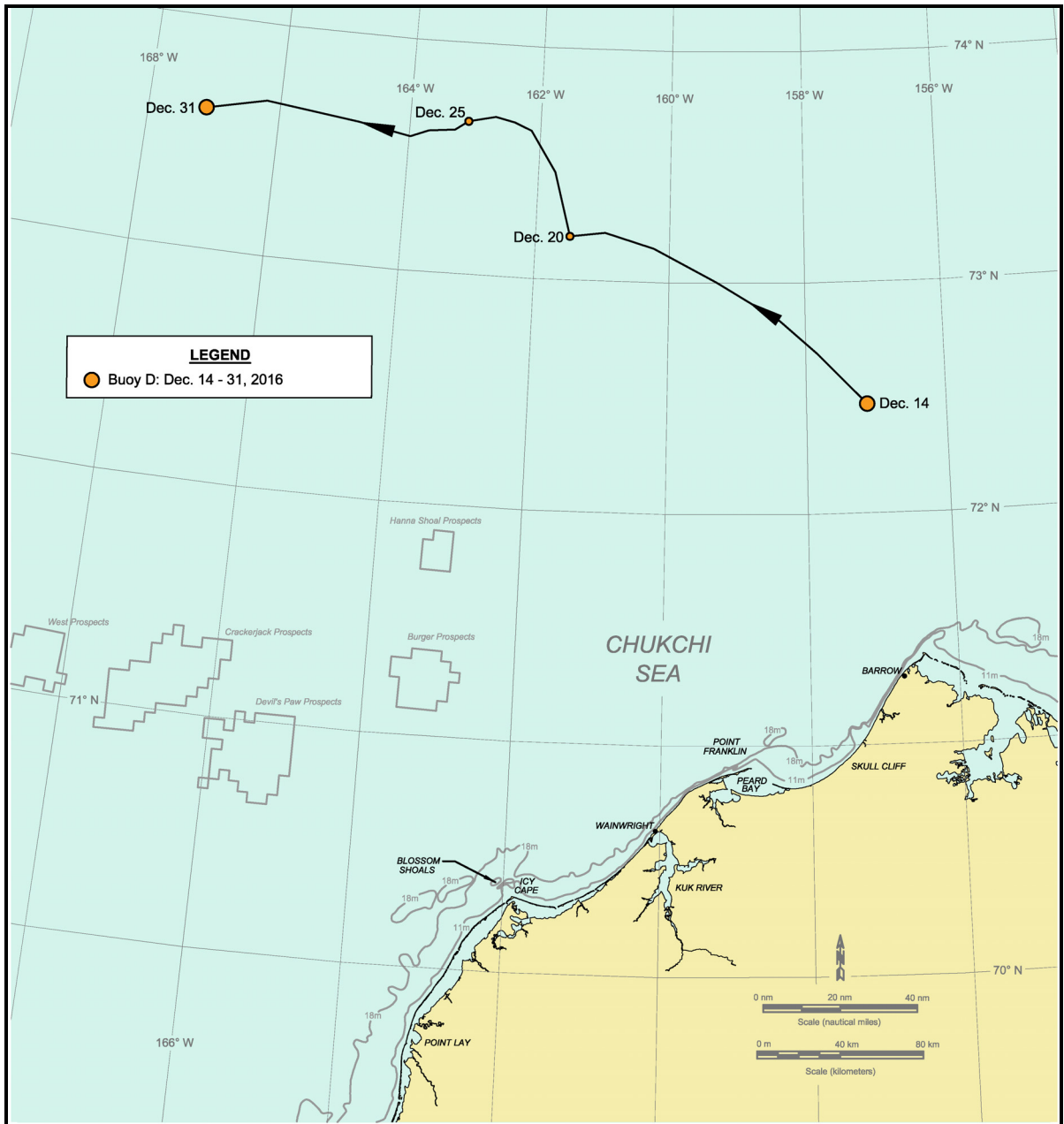
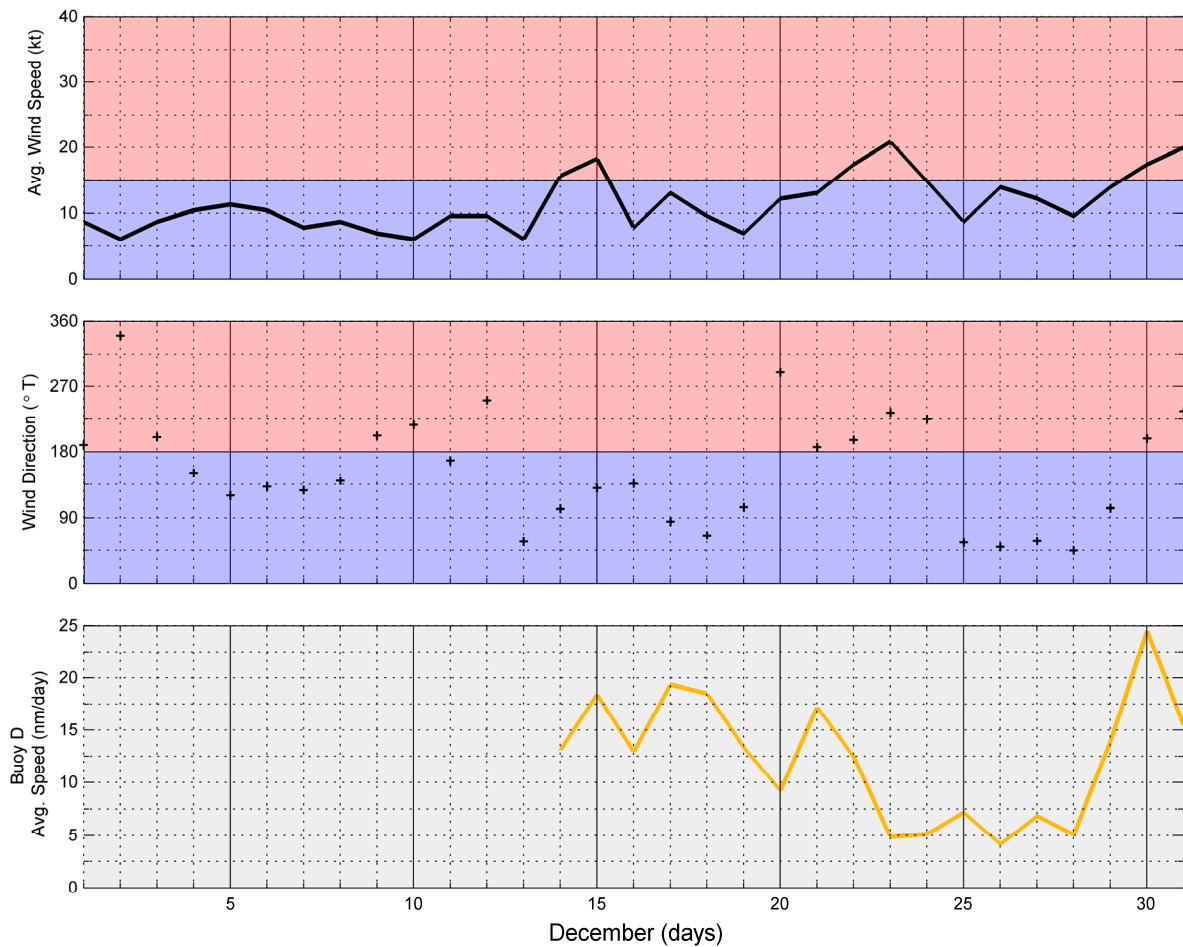


Figure 56. Chukchi Sea Landfast Ice Edge in December 2016



Data Source: Rigor, 2017

Figure 57. Chukchi Sea Drift Buoy Track in December 2016



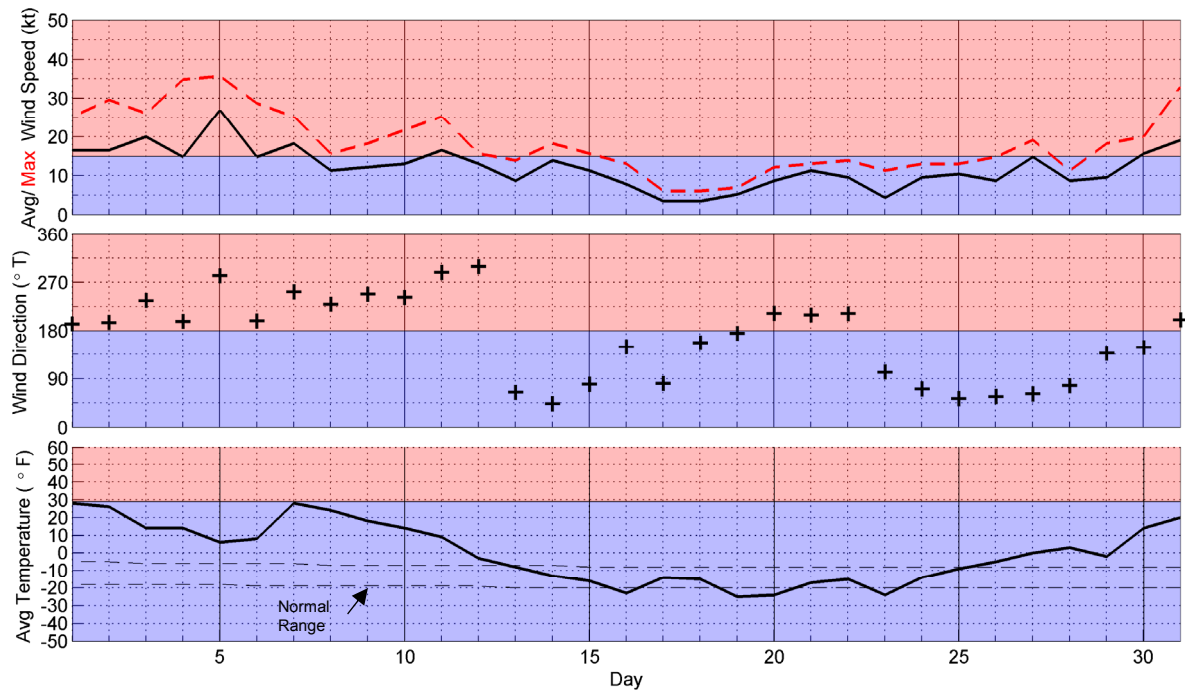
Data Sources: Weather Underground, 2017; Rigor, 2017

Figure 58. Chukchi Sea Drift Buoy Daily Average Speed in December 2016

5.3.2. January 2017

Meteorological Conditions: Figure 59 presents the wind and temperature data recorded at Barrow Airport in January 2017. Unseasonably warm air temperatures prevailed at the beginning and end of the month, separated by a 13-day period in which the values ranged from normal to slightly below. The deviation from historical norms was exceptionally large during the first warm spell, when daily average temperatures of 28°F (-2°C) on the 1st and 7th exceeded the normal range by 33°F and 34°F (18°C and 19°C), respectively. For the entire month, the temperatures exceeded the normal range on 18 days and dropped below on four. The mean value was 0°F (-18°C).

In contrast to October, November and December, when easterly winds predominated, westerlies outnumbered easterlies by the narrowest of margins in January (16 days with westerlies versus 15 with easterlies). The average speed for the month, 12 kt (6 m/s),



Source: Weather Underground, 2017

Figure 59. Meteorological Conditions at Barrow Airport in January 2017

matched that in October as the highest recorded during the five-month study period. Storm activity consisted of two westerlies and one easterly:

- Dec 30th-Jan 7th: nine-day westerly with maximum speed of 27 kt (14 m/s);
- January 11th: one-day westerly with maximum speed of 17 kt (9 m/s);
- January 30th: one-day easterly with maximum speed of 16 kt (8 m/s).

The westerly storm that began on December 30th proved to be the most severe event of the freeze-up period in terms of both peak wind speed (27 kt; 14 m/s) and duration (9 days). Another westerly storm that began on January 31st and continued through February 2nd is included in the February storm population (Section 5.3.3).

Ice Thickness: The calculated ice thickness increased from 62 cm at the beginning of the month to 83 cm at the end (Table 13).

Landfast Ice: Figure 60 illustrates the locations of the landfast ice edge derived from RADARSAT-2 images obtained on December 31st, January 14th and January 31st. The narrow, discontinuous strip of ice that existed on the 31st experienced substantial growth during the first half of January, becoming continuous from Point Barrow to Point Lay and achieving a maximum width of 8 nm (15 km) to the east of Peard Bay. These changes occurred in response to a strong predominance of westerly winds and two westerly storms.

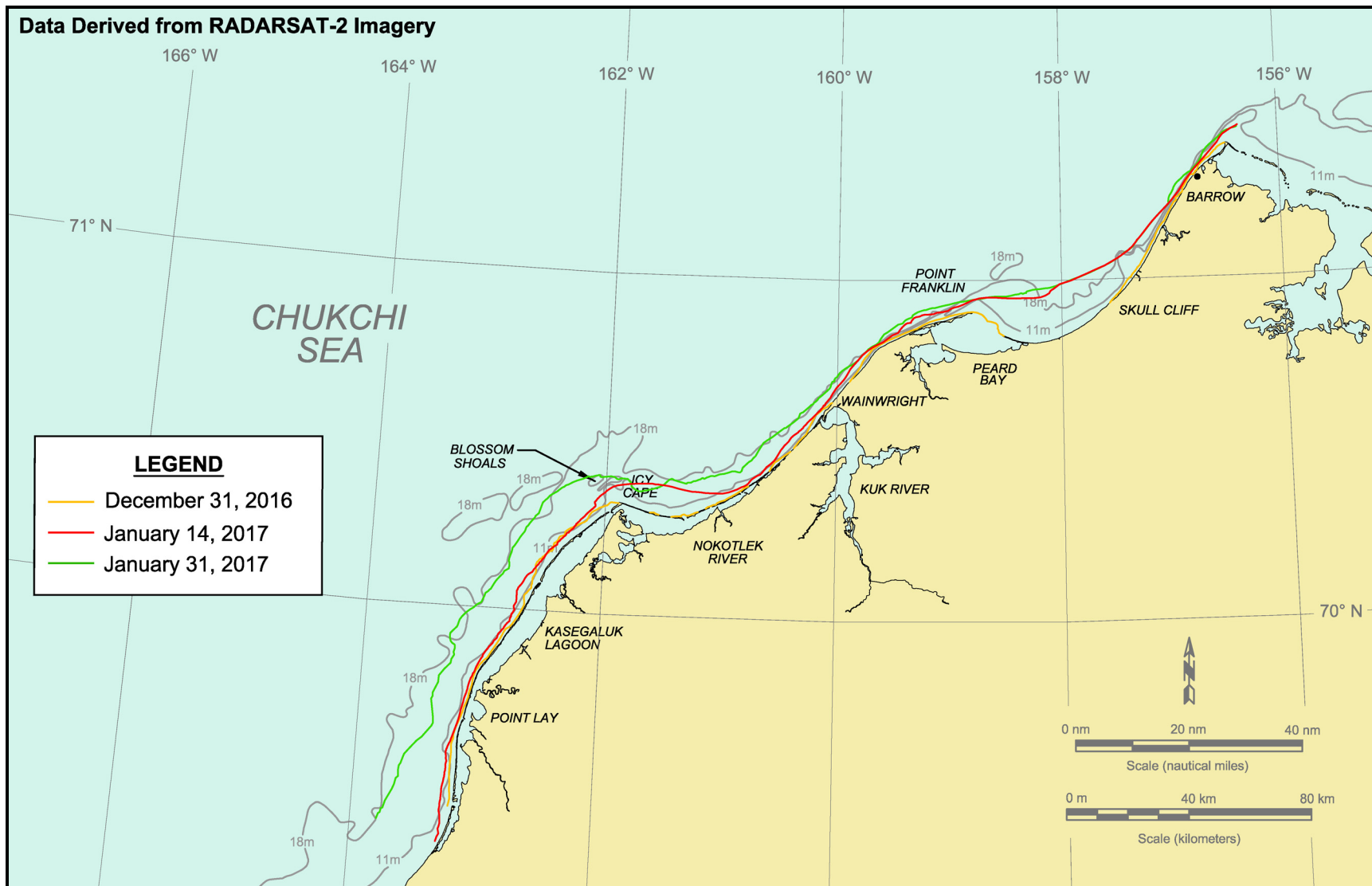
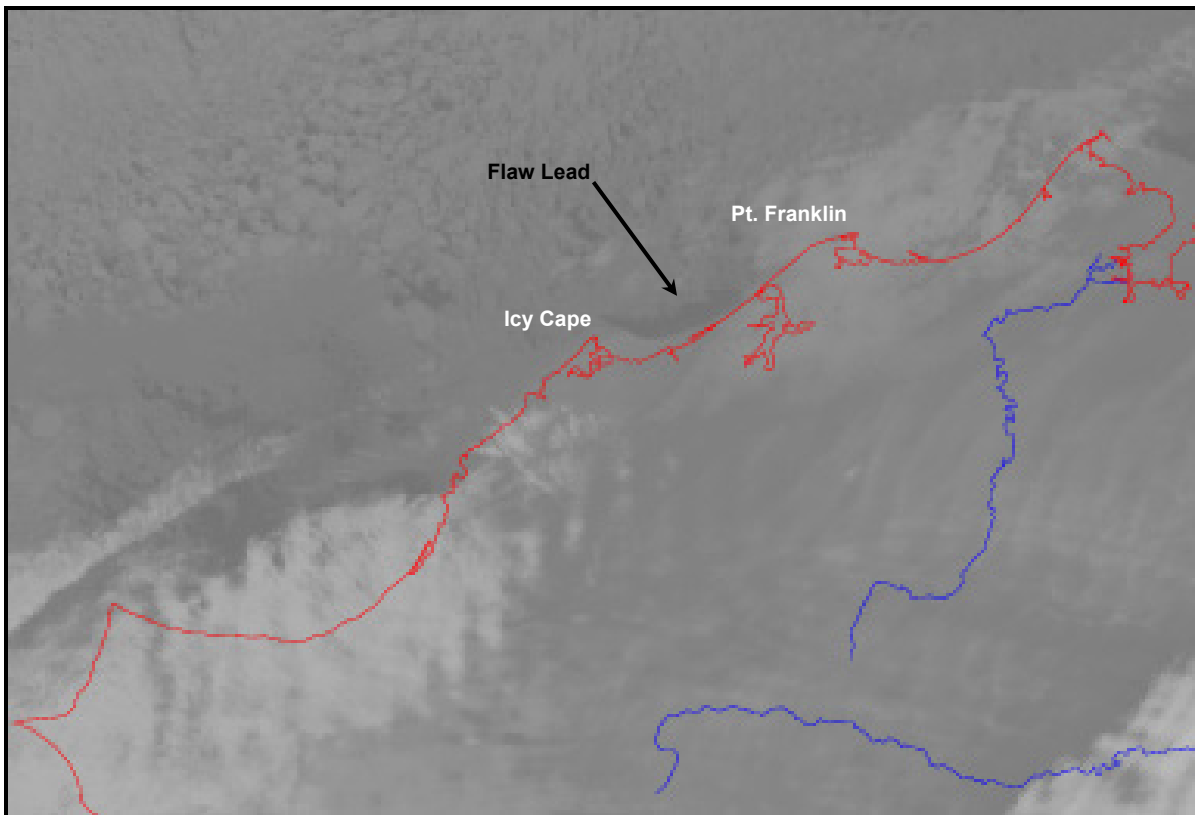


Figure 60. Chukchi Sea Landfast Ice Edge in January 2017

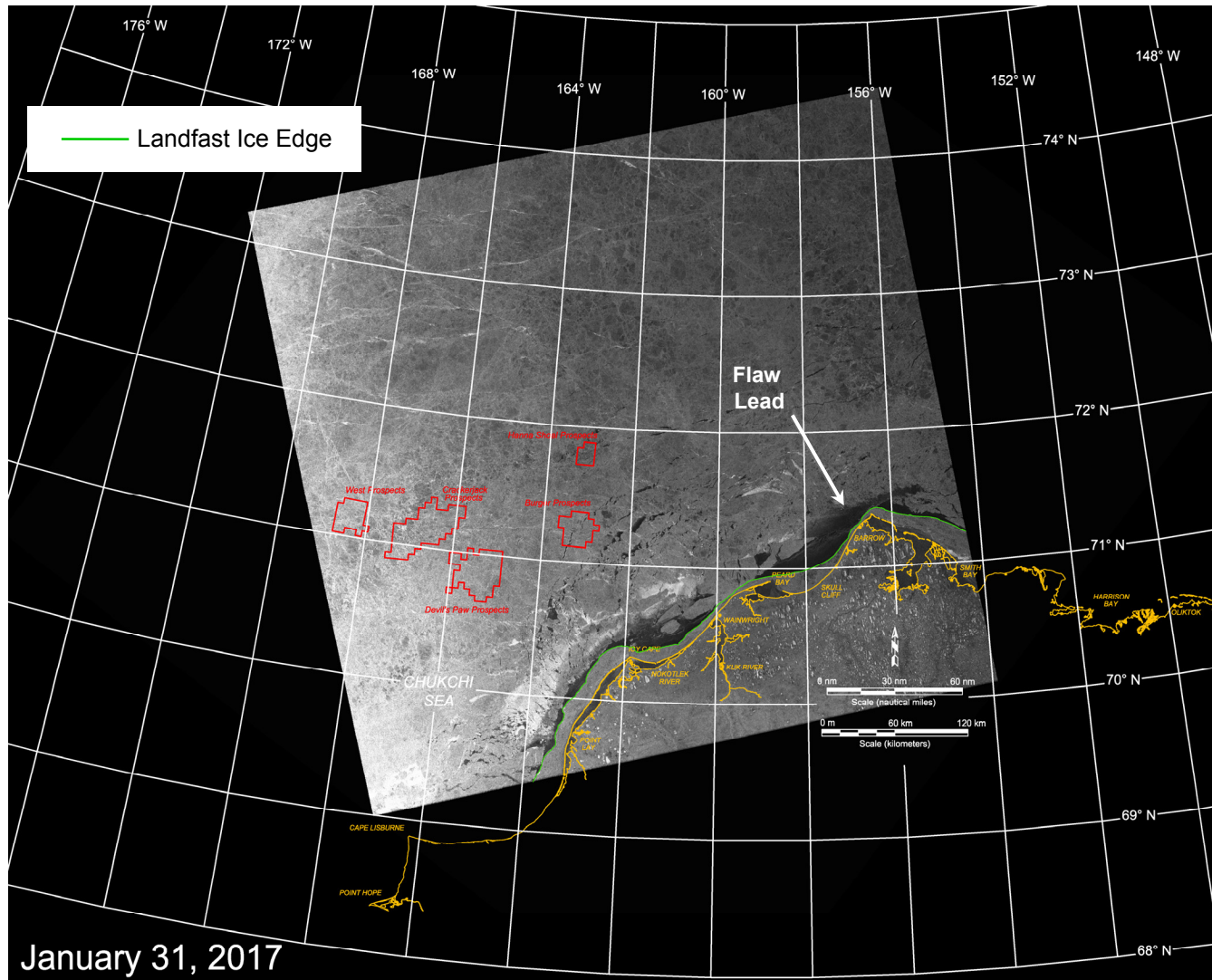
During the second half of January, the landfast ice edge remained nearly stationary to the north of Point Franklin but continued to expand in the region to the south. Easterly winds outnumbered westerlies by a wide margin during this period, suggesting that the gains did not take place until the westerly storm that began at month-end. Substantial growth occurred in the vicinity of Icy Cape, where the ice reached its customary anchor point on Blossom Shoals and achieved its maximum width of 12 nm (22 km).

Coastal Flaw Lead: The coastal flaw lead opened on three occasions, persisting from January 3rd through 5th, 14th through 18th, and 24th through February 7th. The aggregate duration in January was 16 days, representing a 52% frequency of occurrence. Whereas the second and third openings were caused by easterly winds, the first resulted from southwesterlies that pushed the ice offshore between Icy Cape and the Kuk River Inlet. As shown in Figure 61, the resulting lead was small, with a maximum length of 35 nm (65 km) and width of 7 nm (13 km). The maximum dimensions for the month, a length of 250 nm (463 nm) and width of 50 nm (93 km), occurred on January 29th, when the lead extended from Point Barrow to Cape Lisburne. Its configuration on the 31st is shown in Figure 62.



After: National Weather Service, 2017

Figure 61. AVHRR Image of Chukchi Sea Acquired on January 3, 2017



Source: RADARSAT-2 Data and Products © MacDonald Dettwiler and Associates Ltd., 2017 – All Rights Reserved

Figure 62. RADARSAT-2 Image of Chukchi Sea Acquired on January 31, 2017

Ice Drift: As illustrated in Figure 63, Buoy D followed a complex trajectory in January that produced a net displacement of only 7 nm (13 km). This outcome indicates that the westerly set of the Beaufort Gyre was completely neutralized by the westerly winds that predominated over the course of the month. The highest daily average drift speed, 15.6 m/day (28.9 km/day; 0.7 kt; Figure 64), occurred during the westerly storm on January 1st, when the wind speed at Barrow was 17 kt (9 m/s). The associated wind factor was a modest 4.1%, reflecting the countervailing influences of the winds and the Gyre. The mean daily average drift speed for the month was 5.2 nm/day (9.6 km/day).

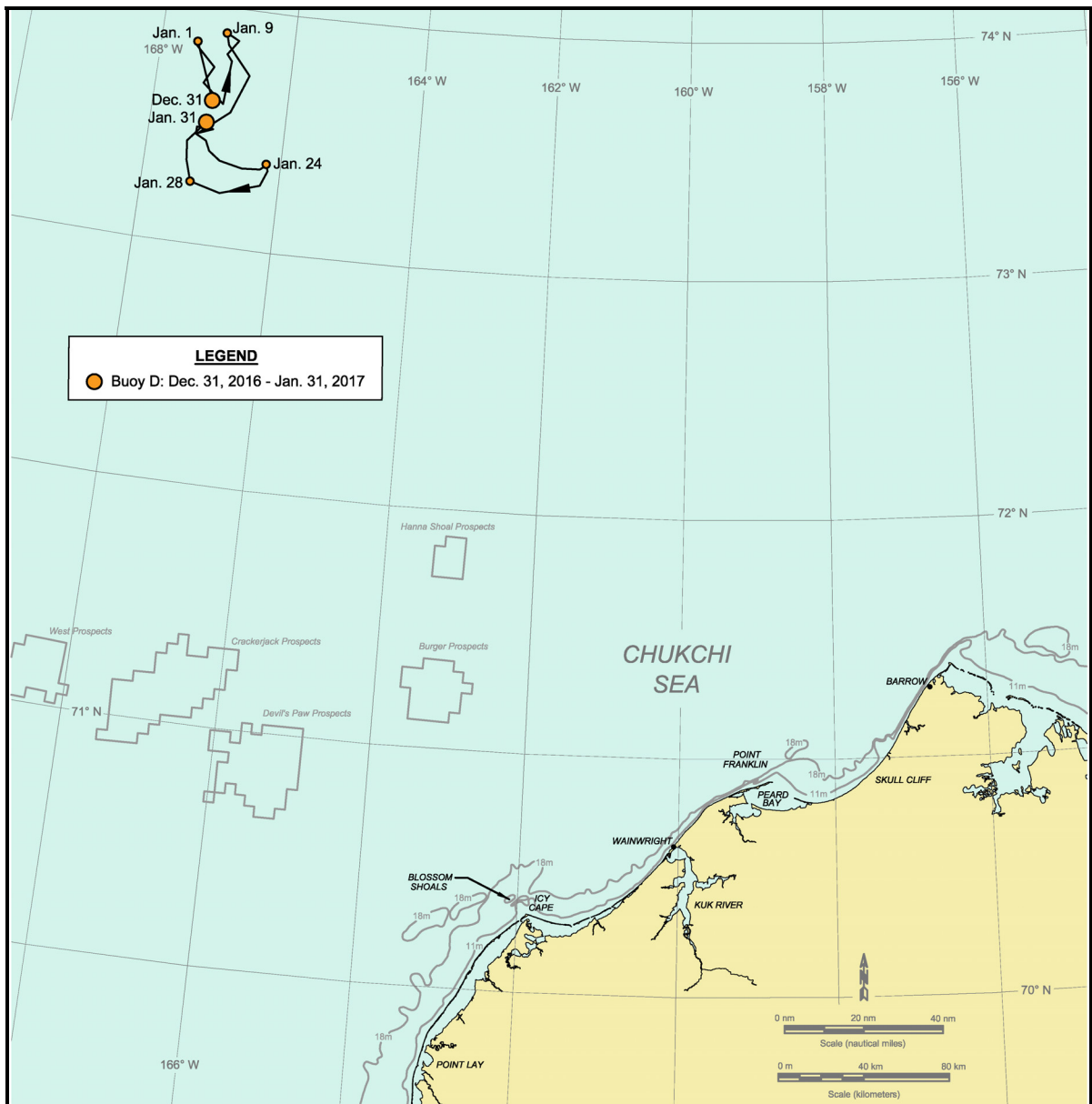
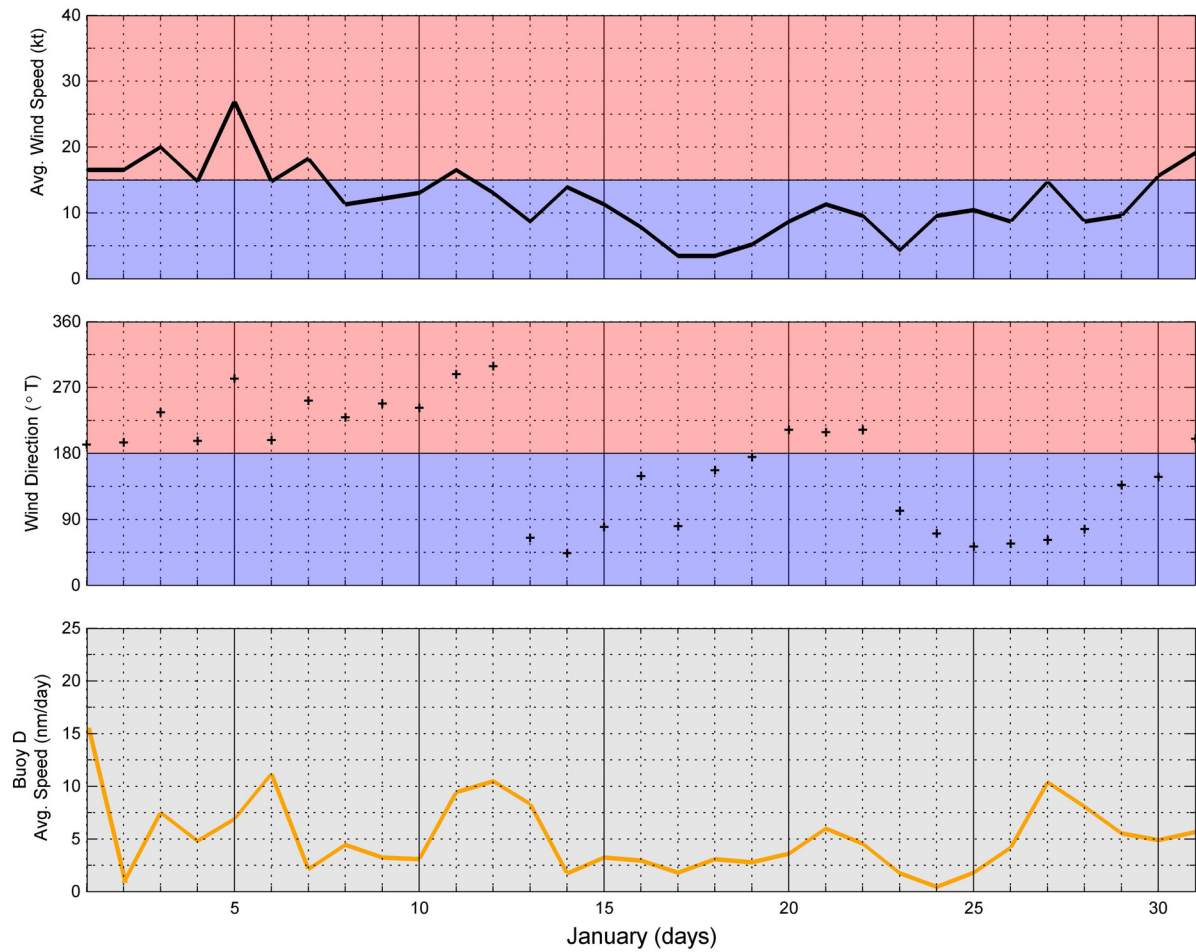


Figure 63. Chukchi Sea Drift Buoy Track in January 2017



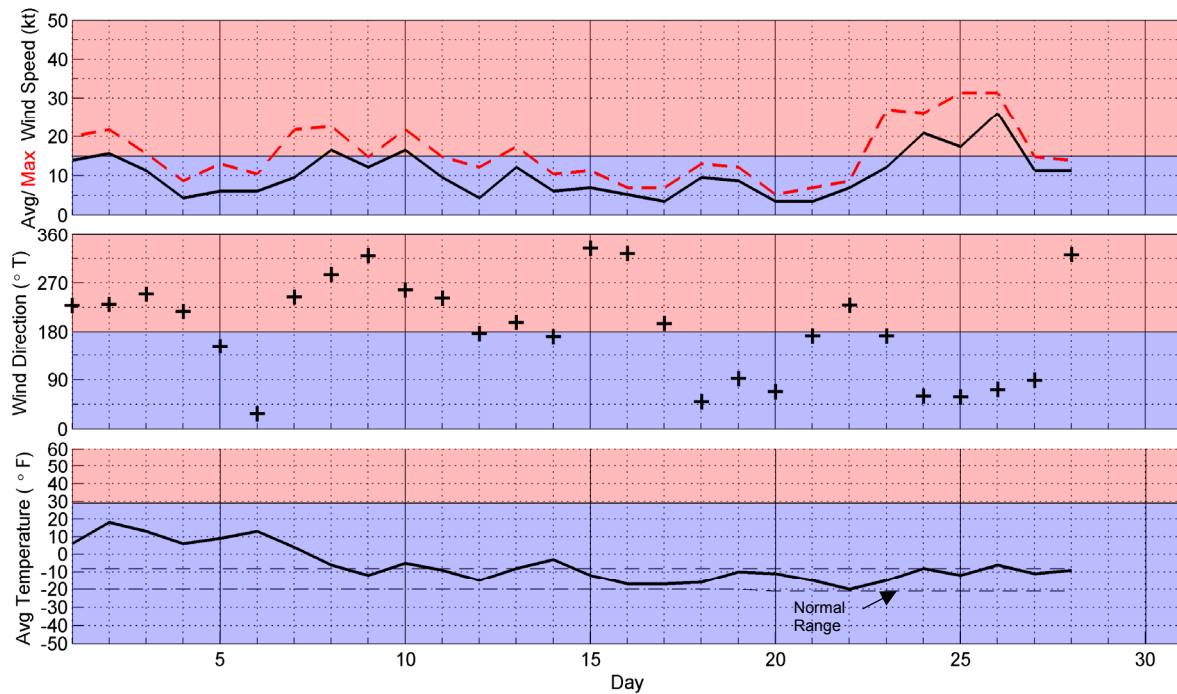
Data Sources: Weather Underground, 2017; Rigor, 2017

Figure 64. Chukchi Sea Drift Buoy Daily Average Speed in January 2017

5.3.3. February 2017

Meteorological Conditions: The wind and temperature data acquired at Barrow Airport in February 2017 are presented in Figure 65. The elevated air temperatures at the end of January (Figure 59) continued during the first eight days in February, followed by temperatures in or slightly above the normal range for the remainder of the month. Taken together, these two periods produced average daily values that exceeded the normal range on 11 occasions and never fell below.

As in January, westerly winds occurred with a slightly higher frequency than easterlies (15 days versus 13 days). The average speed for the month was 10 kt (5 m/s). The storm population was comprised of two westerlies and one easterly, with the first westerly commencing on January 31st:



Source: Weather Underground, 2017

Figure 65. Meteorological Conditions at Barrow Airport in February 2017

- Jan 31st-Feb 2nd: three-day westerly with maximum speed of 19 kt (10 m/s);
- February 8th-10th: three-day westerly with maximum speed of 17 kt (9 m/s);
- February 24th-26th: three-day easterly with maximum speed of 26 kt (13 m/s).

Ice Thickness: The calculated ice thickness at the end of the month was 103 cm, representing 20 cm more than at the beginning.

Landfast Ice: Figure 66 presents the locations of the landfast ice edge derived from RADARSAT-2 images obtained on January 31st, February 17th, and February 28th, while Figure 67 provides the last of these three images. The ice edge experienced substantial changes over the course of the month, reflecting changes in the wind conditions.

During the first interval, between January 31st and February 17th, the landfast ice zone expanded dramatically in response to a predominance of westerly winds and two westerly storms. Its width increased to as much as 16 nm (30 km) off Skull Cliff, 20 nm (37 km) off the Nokotlek River Mouth, and 13 nm (4 km) to the south of Icy Cape, representing the maximum values recorded in the five-month study period.

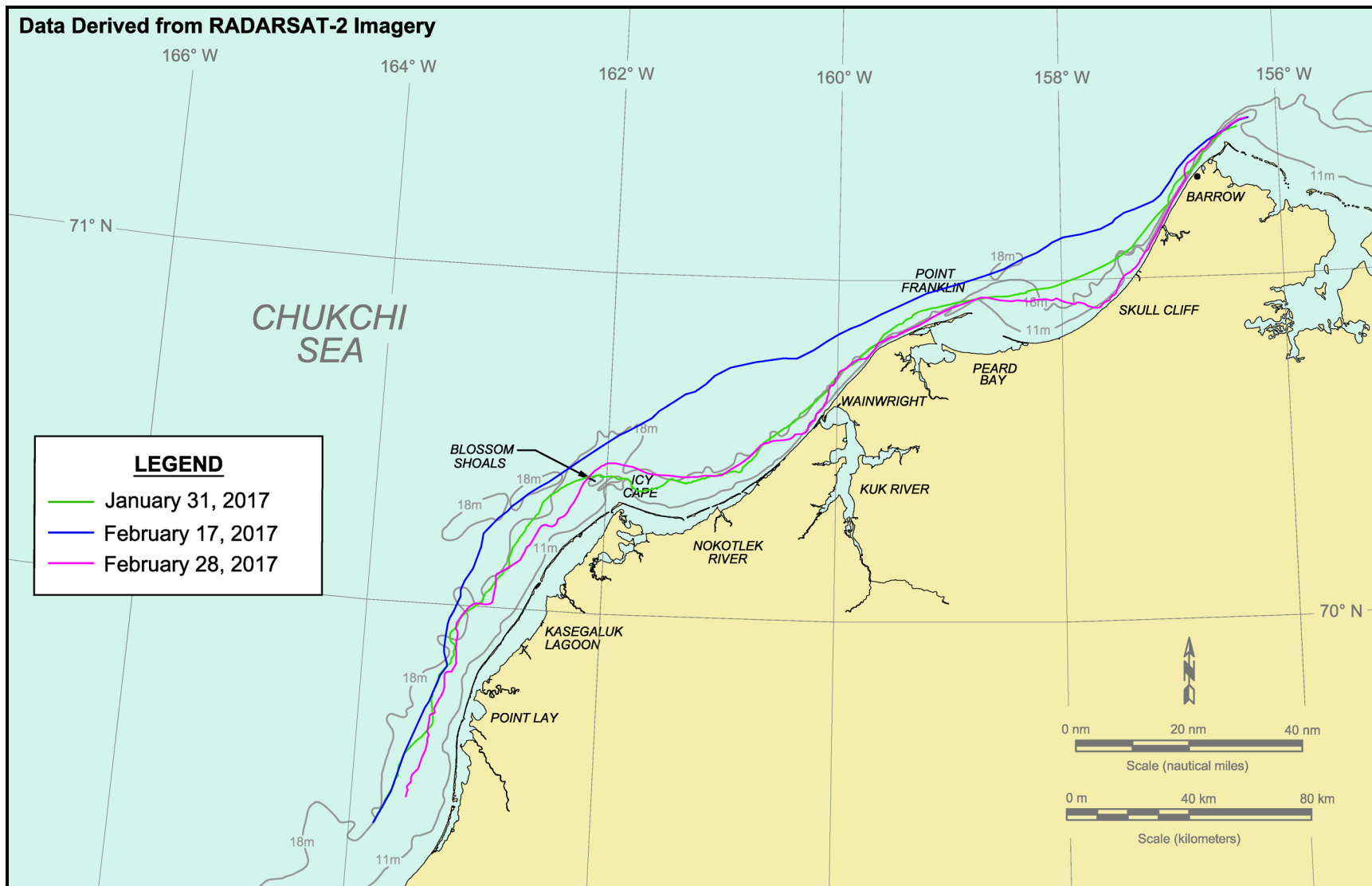
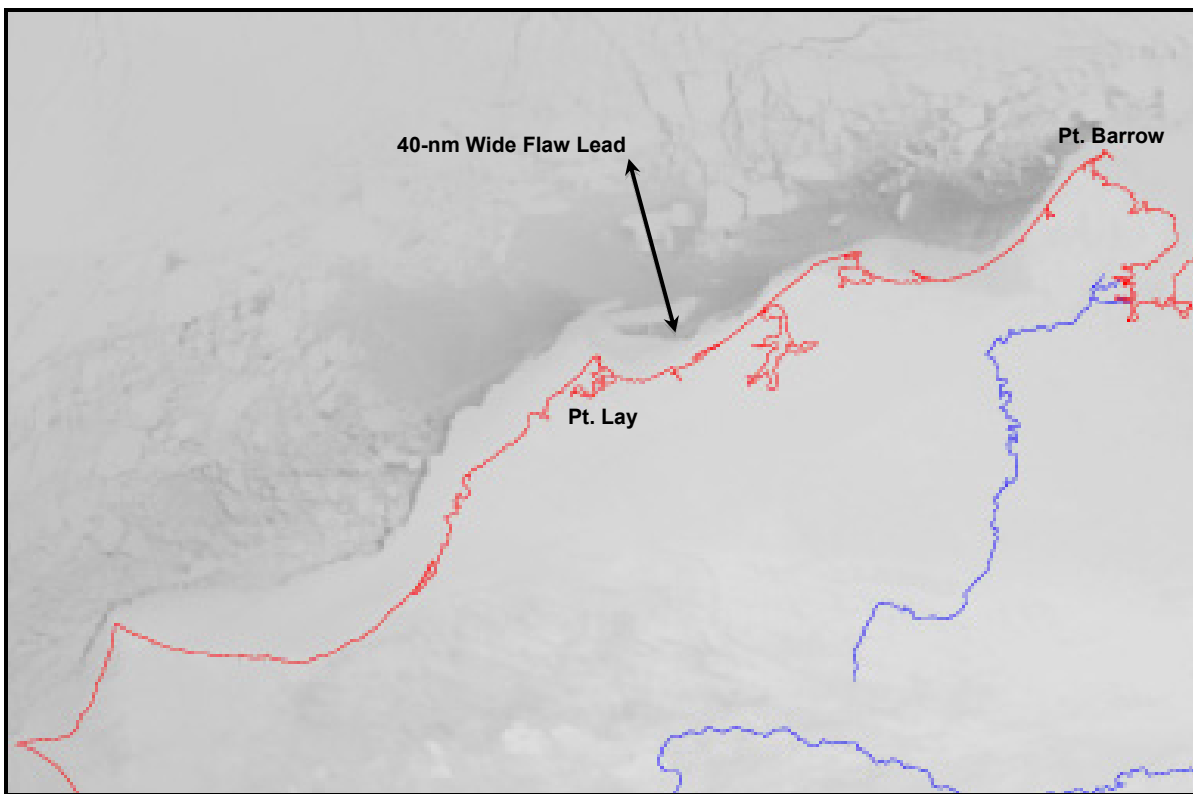


Figure 66. Chukchi Sea Landfast Ice Edge in February 2017

During the second interval, between February 17th and 28th, the recent gains were erased by a predominance of easterly winds that culminated in a severe easterly storm. As illustrated in Figures 66 and 67, the landfast ice zone was reduced to a narrow strip from Barrow to Skull Cliff and in the vicinity of Point Belcher and Wainwright. Its maximum width was 8 nm (15 km) to the east of Point Franklin, 10 nm (19 km) to the east of Icy Cape, and 8 nm (15 km) to the north of Point Lay. The fact that a continuous strip of ice survived the storm, with ample widths in some areas, indicates that substantial grounding had occurred in January and early February.

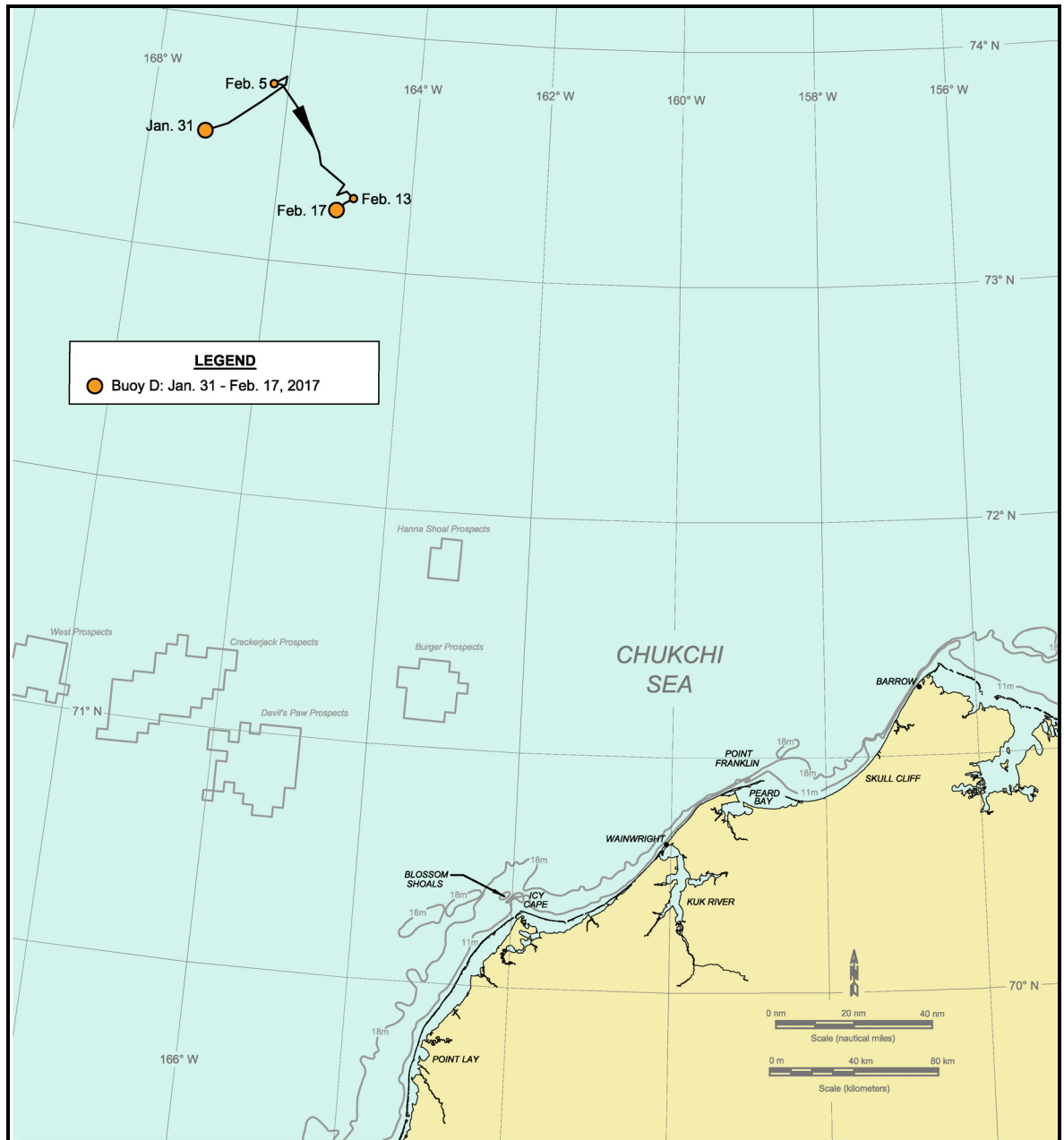
Coastal Flaw Lead: As discussed in Section 5.3.2, the flaw lead that formed on January 24th persisted through February 7th, a duration of 15 days. Although the lead was created by easterly winds in January, it remained open during the southwesterlies that followed in early February. It reopened on three subsequent occasions in response to easterlies: February 5th, 18th through 21st, and 24th through 28th (Figure 68). The aggregate duration, 17 days, represented a 61% frequency of occurrence. The maximum length and width, 250 and 50 nm (463 and 93 km), respectively, occurred at the beginning of the month in conjunction with the lead that developed in late January.



After: National Weather Service, 2017

Figure 68. AVHRR Image of Chukchi Sea Acquired on February 28, 2017

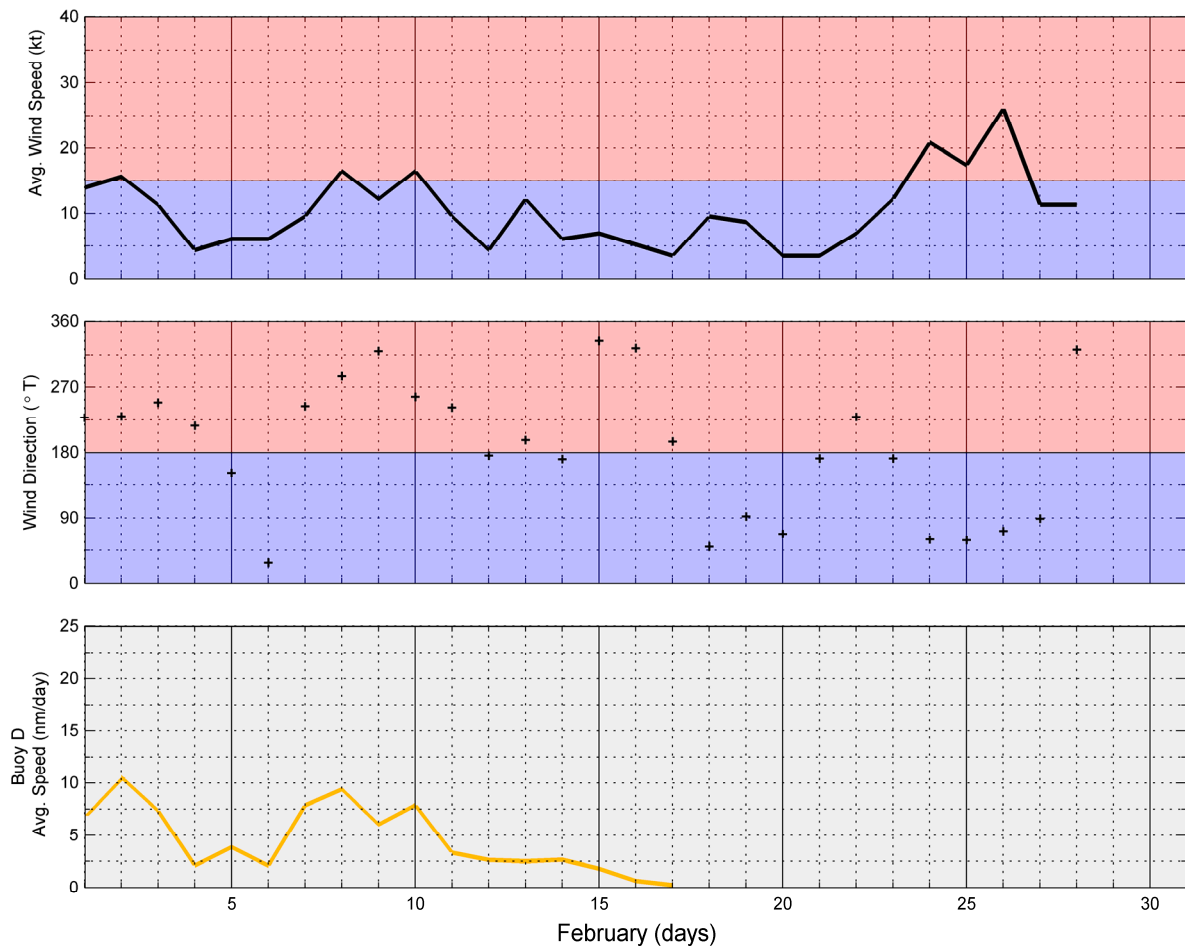
Ice Drift: Buoy D remained in the study area through mid-February before departing to the northwest. As shown in Figure 69, it experienced a net displacement of 39 nm (72 km) to the southeast during the 17-day tracking period, with a leg to the northeast in response to southwesterly winds followed by a longer leg to the southeast in response to westerly and northwesterly winds. The buoy's movement to the east indicates that the westerly set of the Beaufort Gyre had been completely reversed by the opposing winds.



Data Source: Rigor, 2017

Figure 69. Chukchi Sea Drift Buoy Track in February 2017

The mean daily average drift speed for the tracking period was 4.6 nm/day (8.5 km/day), which was comparable to that in January. The maximum drift speed, 10.5 nm/day (19.5 km/day; 0.44 kt; Figure 69), occurred on February 2nd at the end of a three-day westerly storm (Figure 70). The corresponding wind speed at Barrow was 16 kt (8 m/s), producing a wind factor of 2.8%. As in the case of the 4.1% wind factor obtained for the peak drift speed in January (Section 5.3.2), this relatively low value reflects the countervailing influences exerted by westerly winds and the Beaufort Gyre.



Data Sources: Weather Underground, 2017; Rigor, 2017

Figure 70. Chukchi Sea Drift Buoy Daily Average Speed in February 2017

5.4. Reconnaissance Flights

Aerial reconnaissance missions were undertaken in the Chukchi Sea on February 27th and March 1st. Chukchi Sea Flight No. 1 (Flight “C1” on Drawing CFC-994-01-003) focused on the offshore region to the northwest and west of Barrow, including Hanna Shoal

and the Hanna Shoal and Burger Prospects. It should be noted that the Hanna Shoal Prospects are centered approximately 25 nm (46 km) to the southwest of Hanna Shoal itself (Figure 4). Chukchi Sea Flight No. 2 (Flight “C2” on the same drawing) was used to observe the coastal and nearshore region between Barrow and Point Lay. The RADARSAT-2 and AVHRR images that illustrate the ice conditions on February 28th, the day between the two flights, are provided in Figures 67 and 68.

5.4.1. Lagoon Ice

The ice in the protected waters of Kasegaluk Lagoon, the Kuk River Inlet, and Peard Bay was flat and nearly featureless. The conditions in Kasegaluk Lagoon approximately 14 nm (26 km) to the east of Icy Cape are illustrated in Plate 19.

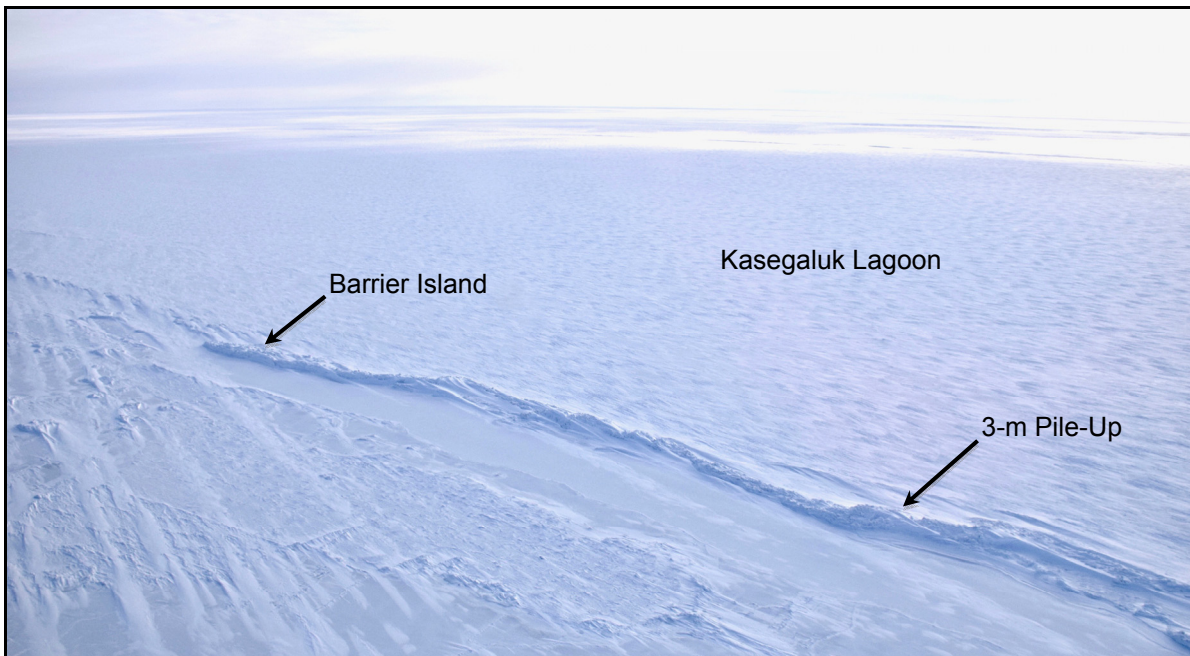


Plate 19. Flat Ice in Kasegaluk Lagoon and 3-m Pile-Up that Encroached 10 m onto Barrier Island 14 nm East of Icy Cape (looking southeast on March 1, 2017)

5.4.2. Landfast Ice

The landfast ice edge observed during the flights was consistent with that derived from the RADARSAT-2 image acquired on February 28th (Figure 66). Although the ice formed a continuous strip from Point Barrow to Point Lay, its width decreased to as little as 600 m off Point Belcher. The strip was anchored by grounded ridges and rubble with typical heights of 2 to 4 m, and maximum heights of 5 to 7 m (Plate 20). A large expanse of landfast ice with ridge and rubble heights ranging from 2 to 5 m was present on Blossom Shoals (Plate 21).



**Plate 20. Narrow Strip of Landfast Ice and Flaw Lead off Barrow
(looking northeast on February 27, 2017)**

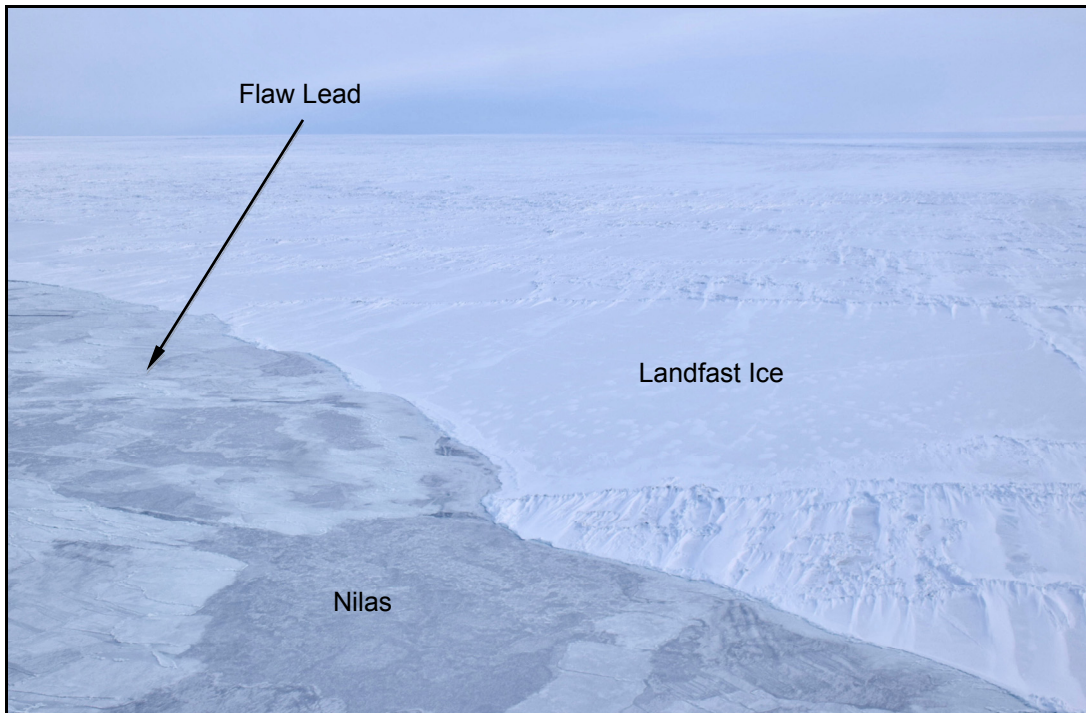


**Plate 21. Large Expanse of Landfast Ice Grounded on Blossom Shoals
(looking northeast on March 1, 2017)**

5.4.3. Leads

Reflecting the strong easterly storm that prevailed from February 24th through 26th, a wide flaw lead was evident during the flights conducted on February 27th and March 1st. The maximum width was estimated to be 40 nm (74 km) during the flight on the 27th, a finding corroborated by the AVHRR image obtained on the 28th (Figure 68). Open water and nilas predominated on the eastern (upwind) side of the lead (Plates 20 and 21), while young and first-year ice predominated on the western (downwind) side (Plate 22).



Plate 22. Mixture of Young and First-Year Ice on Western Side of Flaw Lead 20 nm off Point Franklin (looking southeast on February 27, 2017)

Farther offshore, the ice canopy was interrupted by numerous leads in the early stages of refreezing – a circumstance that reflected the disruptive influence of the easterly storm preceding the flights. As illustrated in Plates 23 and 24, the widths ranged from less than 10 m to more than 1 km.

5.4.4. Offshore Ice

The ice on the west side of the flaw lead was found to be relatively uniform, consisting of first-year floes typically ranging from less than 500 m to 1 km in diameter (Plate 23). Deformation was modest, with ridge and rubble heights typically varying from 1 to 2 m and occasionally reaching 3 m.

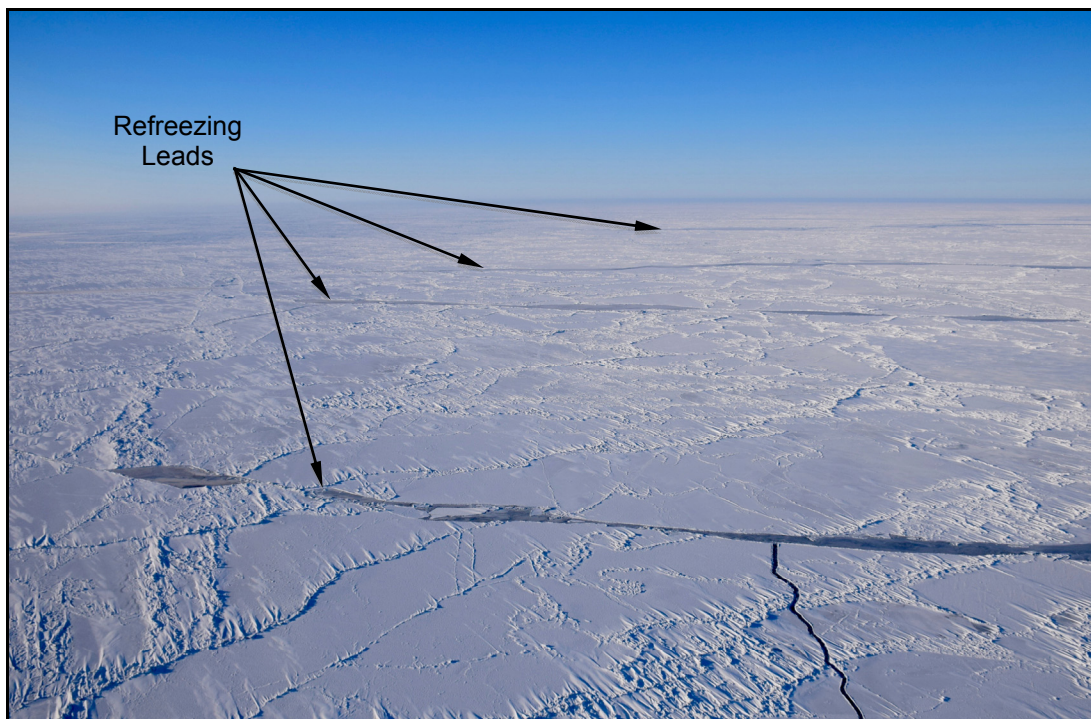


Plate 23. First-Year Ice with Ridges and Rubble to 2 m and Refreezing Leads in Central Portion of Burger Prospects (looking northwest on February 27, 2017)



Plate 24. Large Refreezing Lead 60 nm Northwest of Point Barrow (looking northeast on February 27, 2017)

5.4.5. Ice Pile-Ups

Sixty-three ice pile-ups were observed during the flight conducted on March 1st. As discussed in Section 5.1, the pile-ups probably formed in response to winds that shifted from easterly to northwesterly on December 19th and 20th. The characteristics of the pile-ups are summarized in Table 14, with representative examples shown in Plates 19 and 25.



Plate 25. 3-m Pile-Up that Encroached 5 m onto Barrier Island 15 nm Southwest of Kuk River Inlet (looking southeast on March 1, 2017)

5.4.6. Multi-Year Ice

No multi-year ice was observed during either of the two reconnaissance flights.

5.4.7. Ice Conditions in Chukchi Sea Prospects

The ice canopy was relatively uniform in the Hanna Shoal Prospects, consisting of flat first-year floes with diameters to 1 km, intermittent ridges and rubble with heights to 2 m, and multiple refreezing leads (Plate 26). Similar conditions prevailed in the Burger Prospects, but the ice was more consolidated with smaller leads and denser accumulations of ridges and rubble, the heights of which occasionally reached 3 m (Plate 23).

The Devil's Paw Prospects, while not on the flight path, were visible to the west. The ice canopy resembled that in the Burger Prospects, with first-year floes to 1 km and intermittent ridges and rubble to 2 m (Plate 27). The primary difference arose in connection with the leads, which were found to be sparse and relatively small.



Plate 26. First-Year Ice with Ridges and Rubble to 2 m and Refreezing Lead in Central Portion of Hanna Shoal Prospects (looking northwest on February 27, 2017)



Plate 27. Compact Ice Canopy with Ridges and Rubble to 2 m Located 10 nm East of Devil's Paw Prospects (looking west on February 27, 2017)

5.4.8. *Katie's Floeberg*

Katie's Floeberg forms each winter when ice rubble accumulates on Hanna Shoal, which lies 110 nm (204 km) northwest of Barrow at 72°N, 162°W (Drawing CFC-994-01-003). The shallowest water depth on the shoal is about 12 m, while the surrounding depths exceed 30 m.

The floeberg was identified as early as 1966 using Nimbus satellite imagery (Kovacs, *et al.*, 1976). Its formation and growth have been described by a number of prior investigators, including Stringer and Barrett (1975), Kovacs, *et al.* (1976), Toimil and Grantz (1976), Barrett and Stringer (1978), and Vaudrey and Thomas (1981). In April 1980, the feature existed as a large oval of grounded first-year and multi-year rubble measuring 9 km long, 4.6 km wide, and up to 18 m above sea level (Vaudrey and Thomas, 1981). The long axis was oriented northeast-southwest, and the shallowest water depth was located at the southwest tip.

During the seven freeze-up studies conducted from 2009-10 through 2015-16, the floeberg was observed on five occasions: February 2011, February 2012, March 2014, February 2015, and February 2016 (Coastal Frontiers and Vaudrey, 2011; 2012a; 2014; 2015; 2016). The dimensions varied substantially, with lengths ranging from 2.8 to 10.0 km, widths from 1.2 to 5.0 km and maximum rubble heights from 8 to 12 m above sea level. The configuration documented in 2016, which included a length of 9.0 km, width of 5.0 km, and maximum height of 10 m, is shown in Plate 28.

In February 2017, as in 2010 and 2013 (Coastal Frontiers and Vaudrey, 2010; 2013), Katie's Floeberg had not formed yet at the time of the offshore reconnaissance flight. As shown in Plate 29, the ice over Hanna Shoal consisted of relatively flat first-year floes separated by ridges and rubble with heights to 3 m, and occasional refreezing leads. The absence of the floeberg is consistent with the absence of deep-keeled first-year and multi-year ice floes, which tend to initiate the formation of the feature when they run aground.

In mid-March, several weeks after the end of the study period, evidence of the floeberg appeared in MODIS satellite imagery. A representative example is provided in Figure 71, which shows an open-water wake on the east side of the feature during a period of westerly winds.

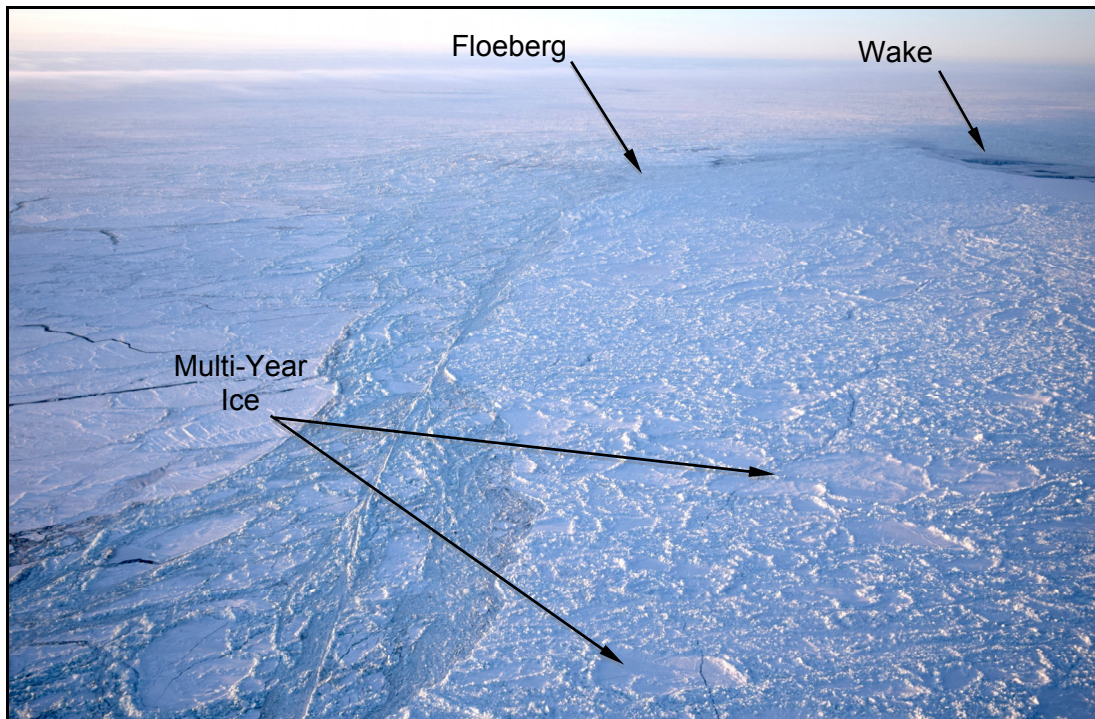


Plate 28. Katie's Floeberg in 2016 (looking southwest on February 21, 2016)

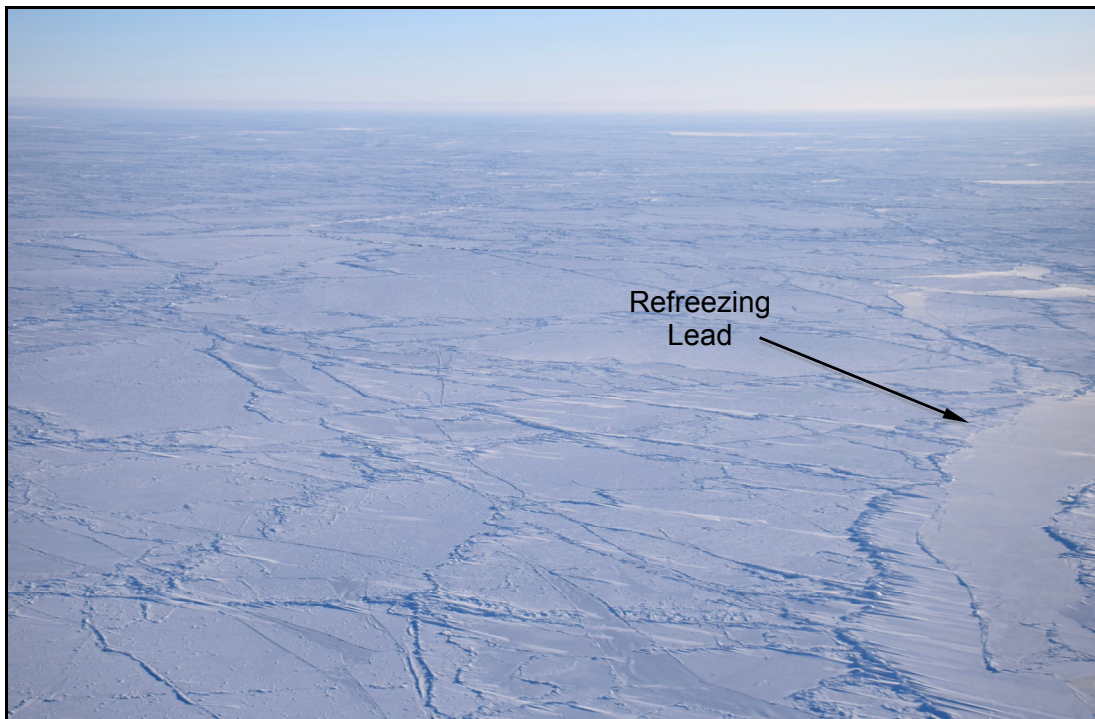
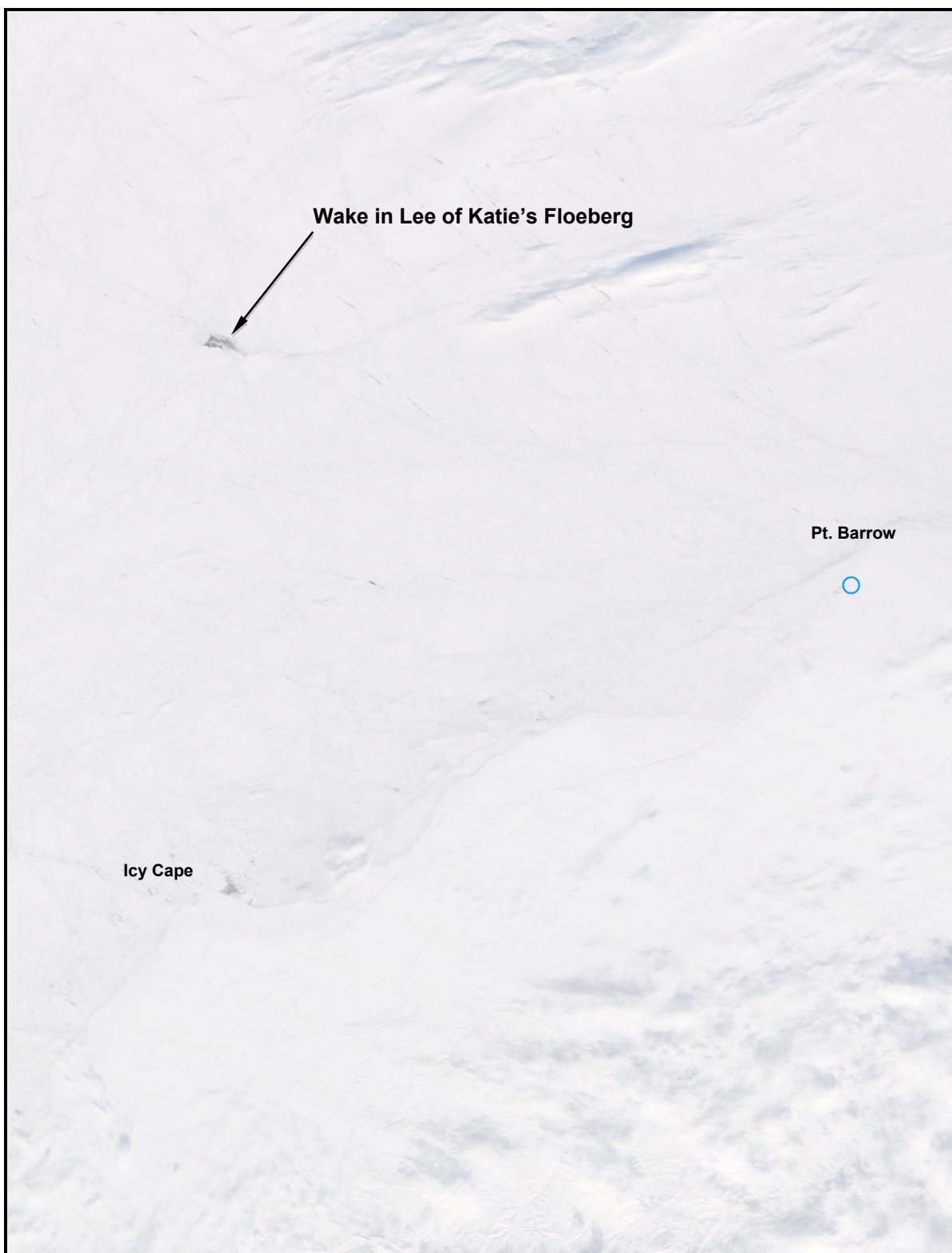


Plate 29. First-Year Ice with Ridges and Rubble to 3 m and Refreezing Lead over Hanna Shoal (looking southeast on February 27, 2017)



After: NASA, 2017a

Figure 71. MODIS Image of Chukchi Sea Acquired on March 14, 2017

6. TRENDS

The primary objectives of this section are to characterize present-day freeze-up processes and recent trends using the data acquired during the past eight years (2009-10 through 2016-17), and to identify long-term trends by comparing the present-day processes with those in the 1980s (1980-81 through 1985-86).

Two of the most important influences on freeze-up are the air temperatures and wind conditions. Accordingly, the temperature and wind data from Barrow Airport are analyzed to investigate perceived trends toward warmer conditions and higher storm frequencies. Both of these trends may make the sea ice more dynamic during freeze-up (Walsh and Eicken, 2007). Barrow was selected over Deadhorse due to its longer period of record for meteorological data.

Following the analysis of air temperatures and winds, six key aspects of the freeze-up season are evaluated: the timing of freeze-up, duration of freeze-up, first-year ice growth, landfast ice development and stability, the Chukchi Sea coastal flaw lead, and multi-year ice invasions. Based on analyses of the recently-acquired data and comparisons with the 1980s, both short- and long-term trends in the environmental driving forces and resulting ice behavior are assessed.

6.1. Air Temperatures

As discussed in Section 3.1, freezing-degree days (FDD) were computed as the difference between the freezing point of seawater (29°F; -2°C) and the daily average air temperature, and then accumulated by month. Negative FDD (>29°F) that occurred after freeze-up had begun were subtracted from the total.

Table 17 presents the accumulated FDD at Barrow Airport for each winter season from 1970-71 through 2016-17. The table is divided into two parts, with the top portion showing the 23-year period from 1970-71 through 1992-93 and the bottom portion the subsequent 24-year period from 1993-94 through 2016-17. The column on the right side displays the rank of each winter over the 47-year period of record, with the highest ranking (No. 1) assigned to the warmest winter (fewest FDD at the end of the winter season) and the lowest ranking (No. 47) to the coldest (most FDD at the end of the winter season). The ten warmest winter seasons (Ranking Nos. 1 through 10) are shown in red type.

Table 17: Accumulated Freezing-Degree Days (<29°F) at Barrow, 1970-71 through 2016-17

Year	Sep	Oct	Nov	Dec	Jan	Feb	Mar	Apr	May	47-yr Rank
1970-71	129	1,013	2,009	3,224	4,727	6,270	7,734	8,738	9,098	46
1971-72	7	466	1,351	2,603	4,004	5,402	6,912	7,914	8,252	42
1972-73	30	275	1,103	2,092	3,410	4,591	6,135	7,086	7,393	26
1973-74	9	307	958	2,024	3,255	4,859	6,381	7,488	7,826	37
1974-75	18	725	1,823	3,546	5,263	6,453	7,579	8,584	8,891	45
1975-76	155	893	2,102	3,677	5,162	6,667	8,043	8,976	9,342	47
1976-77	12	486	1,281	2,689	3,836	5,107	6,694	7,756	8,066	40
1977-78	0	272	1,309	2,444	3,529	4,738	5,963	6,785	7,176	19
1978-79	17	696	1,404	2,734	3,710	5,082	6,496	7,393	7,684	31
1979-80	0	310	895	2,166	3,496	4,636	5,891	6,875	7,247	20
1980-81	117	566	1,586	2,969	3,896	5,148	6,384	7,221	7,389	25
1981-82	105	564	1,452	2,602	3,845	4,839	6,122	7,022	7,407	27
1982-83	32	723	1,896	3,084	4,578	5,821	7,136	7,925	8,300	43
1983-84	153	835	1,666	2,546	3,919	5,717	7,128	8,316	8,700	44
1984-85	0	366	1,479	2,799	3,925	5,218	6,517	7,585	7,780	34
1985-86	60	635	1,424	2,537	3,901	4,959	6,407	7,508	7,784	35
1986-87	13	404	1,262	2,359	3,661	5,033	6,295	7,306	7,579	30
1987-88	51	240	1,272	2,447	3,672	4,931	6,224	7,052	7,337	23
1988-89	49	886	2,164	3,351	4,994	5,546	6,637	7,327	7,687	32
1989-90	0	363	1,611	2,805	4,417	5,878	7,131	7,776	7,903	39
1990-91	25	400	1,477	2,863	4,177	5,499	6,947	7,718	7,748	33
1991-92	27	384	1,494	2,883	4,358	5,788	6,972	7,818	8,076	41
1992-93	154	666	1,569	2,737	4,027	5,150	6,439	7,114	7,300	22
Average	51	542	1,504	2,747	4,077	5,362	6,703	7,621	7,912	
Std. Dev.	55	228	332	429	555	576	567	591	607	
Year	Sep	Oct	Nov	Dec	Jan	Feb	Mar	Apr	May	47-yr Rank
1993-94	27	210	924	2,074	3,252	4,313	5,776	6,649	6,972	15
1994-95	60	699	1,827	3,222	4,493	5,758	7,175	7,817	7,898	38
1995-96	0	326	1,076	2,343	3,463	4,776	5,849	6,719	6,830	14
1996-97	87	816	1,431	2,469	3,911	5,120	6,425	7,184	7,473	28
1997-98	5	293	830	2,089	3,441	4,661	5,644	6,178	6,339	6
1998-99	0	132	1,023	2,275	3,681	4,860	6,243	7,179	7,375	24
1999-00	18	371	1,251	2,657	3,979	5,263	6,493	7,337	7,792	36
2000-01	31	392	1,251	2,300	3,510	4,388	5,764	6,584	7,137	18
2001-02	39	638	1,507	2,654	4,070	5,371	6,315	7,127	7,273	21
2002-03	0	175	849	1,811	3,028	4,269	5,483	6,104	6,329	5
2003-04	0	167	945	2,061	3,210	4,703	6,063	6,897	7,065	17
2004-05	9	243	1,045	2,205	3,341	4,501	5,636	6,436	6,648	11
2005-06	8	237	1,143	2,156	3,421	4,475	5,930	6,908	7,059	16
2006-07	0	102	790	1,769	3,160	4,258	5,615	6,232	6,599	9
2007-08	0	170	616	1,525	2,922	4,387	5,792	6,428	6,648	11
2008-09	3	195	933	1,809	3,109	4,103	5,492	6,297	6,438	8
2009-10	6	125	981	1,988	3,391	4,479	5,687	6,312	6,608	10
2010-11	7	199	739	1,925	3,121	4,113	5,216	6,117	6,388	7
2011-12	3	183	1,059	2,264	3,814	5,013	6,588	7,319	7,556	29
2012-13	0	76	765	1,959	3,131	4,463	5,598	6,451	6,676	13
2013-14	34	161	799	1,786	2,889	3,897	4,945	5,696	5,775	2
2014-15	0	235	809	1,926	3,150	4,149	5,398	6,066	6,174	4
2015-16	9	260	1,058	2,292	3,198	4,159	5,290	5,847	5,911	3
2016-17	0	32	495	1,383	2,283	3,263	4,385	5,047	5,194	1
Average	14	268	1,006	2,123	3,374	4,531	5,783	6,539	6,757	
Std. Dev.	22	195	295	391	458	529	581	616	649	

Note: FDD were calculated using average daily air temperatures from Weather Underground (2017).

The most recent winter, 2016-17, was the warmest in the 47-year period of record by a wide margin. The total accumulation of 5,194 FDD was more than 10% lower than the prior minimum of 5,775, which occurred in 2013-14. It is noteworthy that the past four winters were the warmest on record, while seven of the past ten winters rank among the top ten. The coldest winter, with 9,342 FDD, occurred in 1975-76.

The accumulated freezing-degree days at the end of each winter season are plotted as a time series in Figure 72. The long-term warming trend implied by the recent air temperatures is readily apparent, with the number of FDD decreasing at an average rate of 49 per year since 1970-71. In addition, the rate of warming appears to be increasing: whereas the accumulated FDD trended lower at an average rate of 34 per year from 1970-71 through 1992-93, the rate nearly doubled to 62 per year from 1993-94 through 2016-17.

Acceleration in the rate of warming also is evident on a decadal time scale. Based on the data presented in Table 17, the average annual accumulated FDD declined by 3.8% from the 1970s to the 1980s, 5.2% from the 1980s to the 1990s, 8.1% from the 1990s to the 2000s, and 8.0% during the past seven winters (which extrapolates to an 11.4% decrease over ten winters). The total decline from the 1970s to the most recent seven-year period is 22.9%. Melling and Riedel (2005) reported a more gradual warming trend in the air temperatures at Tuktoyaktuk, Canada. For the 30-year period from 1975 through 2004, they found that the average annual accumulated FDD decreased at a rate of 3.3% per decade.

Substantial deviations from the long-term warming trend, with durations of one to five years, are clearly evident in Figure 72. The relative magnitude of these deviations has increased; as shown in Table 17, the standard deviation in FDD at the end of the winter season amounted to 7.7% of the mean value from 1970-71 through 1992-93, versus 9.6% from 1993-94 through 2016-17.

Additional information on the increase in air temperatures that has occurred since the 1970s is provided in Figure 73, which compares the monthly average values at Barrow over the past eight winters (2009-10 through 2016-17) with those from 1971-72 through 1999-2000. The differences between the monthly values in 2016-17 alone and the long-term monthly averages also are shown. During the past eight years, the monthly average value has exceeded the long-term value by at least 3.2°F (1.8°C) in each month from September through May. The largest increases occurred in October (9.7°F; 5.4°C), November (7.4°F; 4.1°C) and February (7.2°F; 4.0°C). Seasonally, the greatest rise took place during early freeze-up, averaging: 6.7°F (3.7°C) from September through November. Subsequently,

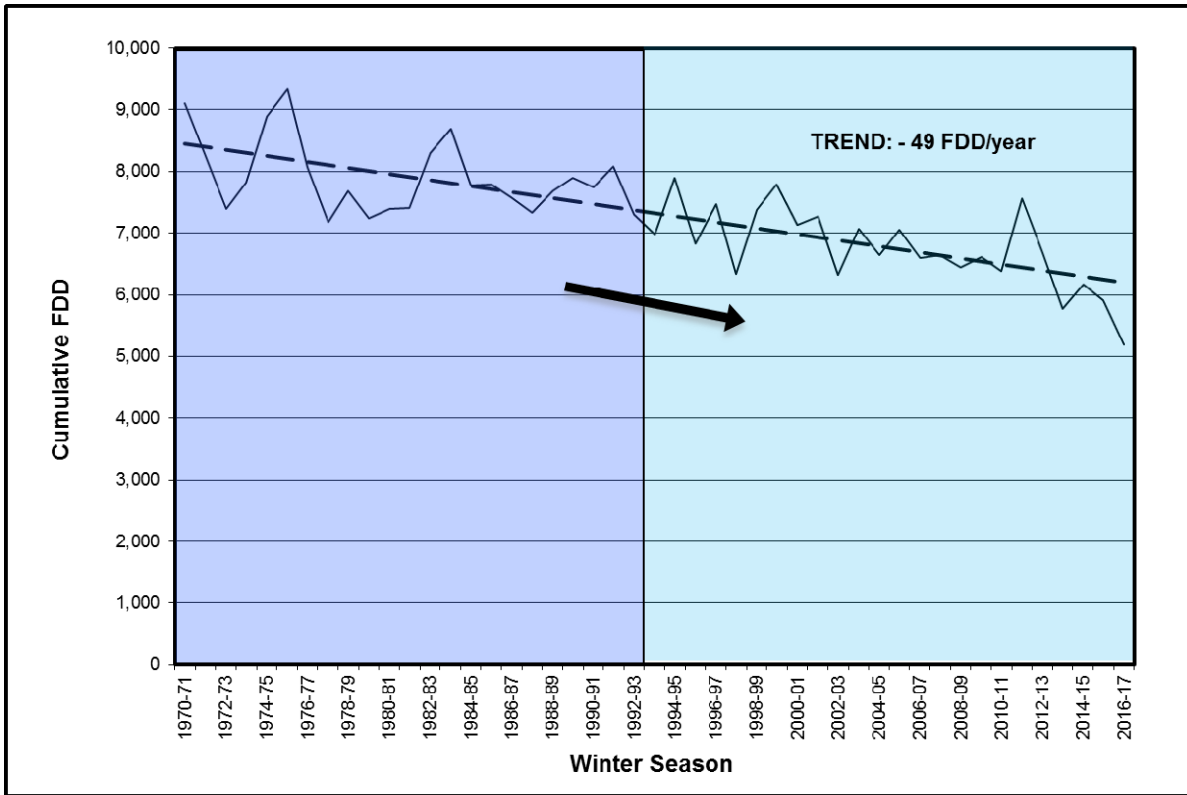


Figure 72. Accumulated Freezing-Degree Days (<29°F) at Barrow, 1970-71 through 2016-17

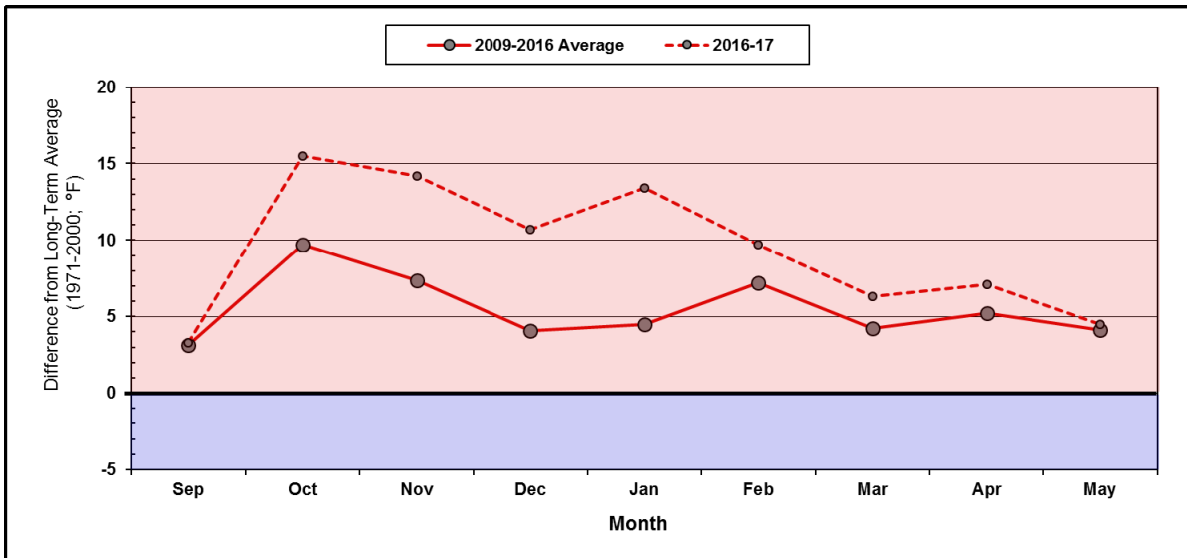


Figure 73. Differences between Recent Monthly Air Temperatures and Long-Term Average Values at Barrow

from December through February, the increase was a more modest 5.3°F (2.9°C). Over the nine-month period from September through May, the average temperature exceeded the long-term average value by 5.5°F (3.1°C). Lindsay and Zhang (2005) reported a similar pattern of pronounced increases in surface air temperatures over the Arctic Ocean during the fall and winter months.

As shown in Figure 73, the differences between the monthly and long-term average temperatures were exceptionally large in 2016-17. The magnitudes ranged from a minimum of 3.3°F (1.8°C) in September to an eye-popping 15.5°F (8.6°C) in October. The average superelevation over the nine-month period from September through May was 9.4°F (5.2°C), nearly 40% higher than the prior maximum value of 6.8°F (3.8°C) recorded since 2009-10.

Trends: Since the 1970s, progressively warmer winter seasons have caused the number of accumulated freezing-degree days at Barrow to decline at an average rate of 49 per year. The rate of warming has accelerated, with the greatest increase in temperature taking place during the early portion of freeze-up.

6.2. Winds

The wind directions that prevailed at Deadhorse and Barrow Airports during each of the past eight freeze-up seasons from October through February are provided in Tables 18 and 19. The data are displayed graphically in Figure 74, which shows the frequency of occurrence of easterly winds at each site.

Unlike 2014-15 and 2015-16, when easterly winds occurred with unusually high frequencies, westerlies staged a resurgence in 2016-17. In the Beaufort, westerlies prevailed 64% of the time, representing the maximum frequency in the eight-year period encompassed by the recent freeze-up studies (2009-10 through 2016-17). When the data from all eight freeze-up seasons are aggregated, westerlies outnumbered easterlies by the narrowest of margins: 51% to 49%.

In the Chukchi, easterlies prevailed during each of the past eight freeze-up seasons. The frequencies ranged from 61% to 88% while averaging 69%. The minimum value, 61%, was recorded in both 2013-14 and 2016-17.

The storms that occurred at Deadhorse and Barrow Airports during each of the past eight freeze-up seasons are summarized in Tables 20 and 21. Both the number of discrete storm events and the total number of days with storm conditions (“storm-days”) are shown.

Table 18. Beaufort Sea Wind Directions, 2009-10 through 2016-17

Month	2009-10		2010-11		2011-12		2012-13		2013-14		2014-15		2015-16		2016-17	
	Days		Days		Days		Days		Days		Days		Days		Days	
	East	West														
October	20	11	25	6	23	8	6	25	15	16	18	13	22	9	20	11
November	19	11	15	15	7	23	4	26	10	20	23	7	19	11	10	20
December	15	16	13	18	15	16	14	17	13	18	20	11	16	15	11	20
January	7	24	16	15	3	28	18	13	18	13	14	17	21	10	7	24
February	16	12	8	20	19	10	21	7	11	17	12	16	28	1	7	21
Total Days	77	74	77	74	67	85	63	88	67	84	87	64	106	46	55	96
Frequency	51%	49%	51%	49%	44%	56%	42%	58%	44%	56%	58%	42%	70%	30%	36%	64%

Note: Table 18 is based on the average daily wind directions recorded at Deadhorse Airport.

Table 19. Chukchi Sea Wind Directions, 2009-10 through 2016-17

Month	2009-10		2010-11		2011-12		2012-13		2013-14		2014-15		2015-16		2016-17	
	Days		Days		Days		Days		Days		Days		Days		Days	
	East	West														
October	23	8	29	2	28	3	10	21	22	9	20	11	27	4	23	8
November	21	9	18	12	16	14	13	17	16	14	26	4	26	4	23	7
December	22	9	22	9	27	4	21	10	17	14	28	3	22	9	18	13
January	13	18	21	10	14	17	29	2	22	9	21	10	29	2	15	16
February	22	6	10	18	23	6	25	3	15	13	15	13	29	0	13	15
Total Days	101	50	100	51	108	44	98	53	92	59	110	41	133	19	92	59
Frequency	67%	33%	66%	34%	71%	29%	65%	35%	61%	39%	73%	27%	88%	13%	61%	39%

Note: Table 19 is based on the average daily wind directions recorded at Barrow Airport.

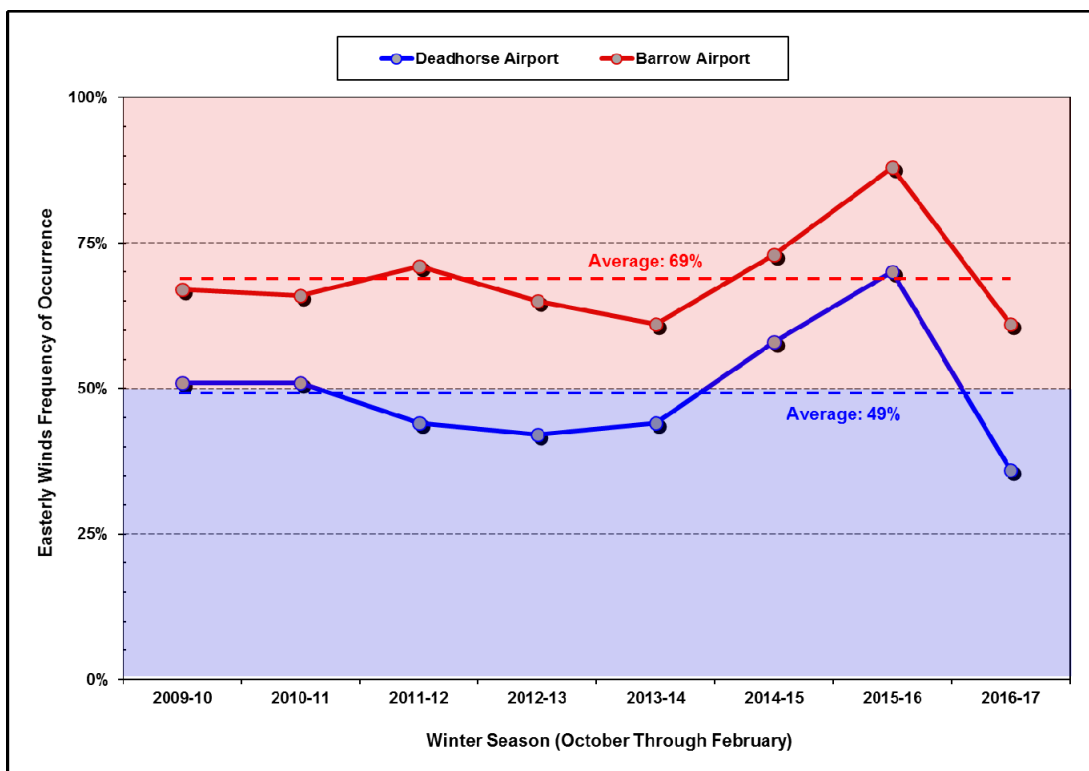


Figure 74. Frequency of Occurrence of Easterly Winds at Deadhorse and Barrow Airports

As in the case of Sections 4 and 5, a storm is defined as an event during which the average daily sustained wind speed exceeds 15 kt (8 m/s).

In the Beaufort, nine easterly and seven westerly storms occurred on average during each freeze-up season (Table 20). In addition to being more numerous, the easterlies tended to be of longer duration, persisting for an average of 2.6 days/event versus 2.1 days for the westerlies. The numbers of easterly storms (7), westerly storms (6), and easterly storm days (12) all were below average in 2016-17, but the number of westerly storm-days (19) was above average. The total number of storm-days, 31, tied that in 2009-10 as the lowest on record.

In the Chukchi, easterly storms outnumbered westerlies not only in 2016-17 but also in each of the prior seven years (Table 21). The annual averages consisted of 11 easterly events producing 30 storm-days (2.7 storm-days/event) and only four westerly events producing eight storm-days (2.0 storm-days/event). In 2016-17, the numbers of easterly storms and easterly storm-days were well below average, while the numbers of westerly storms and westerly storm-days were well above average. These countervailing trends produced total numbers of storms (14) and storm-days (37) that were nearly identical to the long-term averages.

Table 20. Beaufort Sea Storms, 2009-10 through 2016-17¹

Freeze-Up ²	Storm Events			Storm-Days		
	Easterly	Westerly	Total	Easterly	Westerly	Total
2009-10	8	4	12	20	11	31
2010-11	8	10	18	19	21	40
2011-12	7	5	12	15	17	32
2012-13	8	8	16	25	14	39
2013-14	9	11	20	23	20	43
2014-15	10	6	16	26	16	42
2015-16	12	4	16	41	4	45
2016-17	7	6	13	12	19	31
Average	9	7	15³	23	15	38

Notes:

- ¹ Table 20 includes all storm events with a daily average sustained wind speed exceeding 15 kt (8 m/s) at Deadhorse Airport.
- ² The period of record extends from October 1st through February 28th/29th.
- ³ The total no. of storms differs from the sum of easterly and westerly storms due to rounding.

Table 21. Chukchi Sea Storms, 2009-10 through 2016-17¹

Freeze-Up ²	Storm Events			Storm-Days		
	Easterly	Westerly	Total	Easterly	Westerly	Total
2009-10	11	2	13	32	3	35
2010-11	10	8	18	27	13	40
2011-12	8	3	11	21	6	27
2012-13	10	4	14	31	7	38
2013-14	12	7	19	29	13	42
2014-15	13	4	17	33	7	40
2015-16	16	0	16	47	0	47
2016-17	8	6	14	18	19	37
Average	11	4	15	30	8	38

Notes:

- ¹ Table 21 includes all storm events with a daily average sustained wind speed exceeding 15 kt (8 m/s) at Barrow Airport.
- ² The period of record extends from October 1st through February 28th/29th.

Notwithstanding the differences between the Beaufort and Chukchi in terms of wind and storm direction, the average numbers of storms and storm-days have been identical over the past eight years. Each basin has averaged 15 storms and 38 storm-days from October through February.

Unfortunately, data pertaining to storm events in the 1980's suitable for direct comparison with those in Tables 20 and 21 are not readily available. However, an indication of storm conditions in that era was developed by Dickins and Vaudrey (1994), who compiled mid-winter wind data (January through April) at Barrow for the 18-year period from 1977 through 1994. They defined a storm as having a sustained wind speed exceeding 15 kt (8 m/s) for a period exceeding 12 hr. The six winters from 1981 through 1986 were excerpted from this database in order to compare the mid-winter storm frequency in the early 1980s with that which occurred from 2010 through 2017.

The results of the comparison are shown in Figure 75. Whereas Dickins and Vaudrey computed an average of 8.5 storm events per mid-winter season in the early 1980s, the number has ranged from seven to 13 events in recent years. The average, 9.6 storms per winter, represents an increase of about 13%.

A cyclical trend in storm frequency is evident in the data compiled by Walsh and Eicken (2007), who tabulated the number of storm events at Barrow during the open-water and freeze-up seasons from 1950 through 2004 (Figure 76). The storm count during freeze-up increased from the mid-1950s to early 1960s, declined from the early 1960s to mid-1970s, rose again from the mid-1970s to early 1990s, and remained nearly static from the early 1990s to early 2000s. The criteria used to define storm events are not specified, but the data nevertheless indicate that: (1) the increase in storm frequency that began in the mid-1970s was sustained through the early 2000s and (2) the storm frequency was approximately 50% higher in the early 2000s than in the early 1980s. Although other wind characteristics such as direction and duration also influence ice dynamics, the rise in the number of storm events during freeze-up that has occurred since the mid-1970s could be causing an increase in wind-driven ice movement and deformation.

Trends: Since the early 1980s, the frequency of storm events during freeze-up has increased by about 50%. The frequency of mid-winter storms (January through April) also has increased, but only by about 13%.

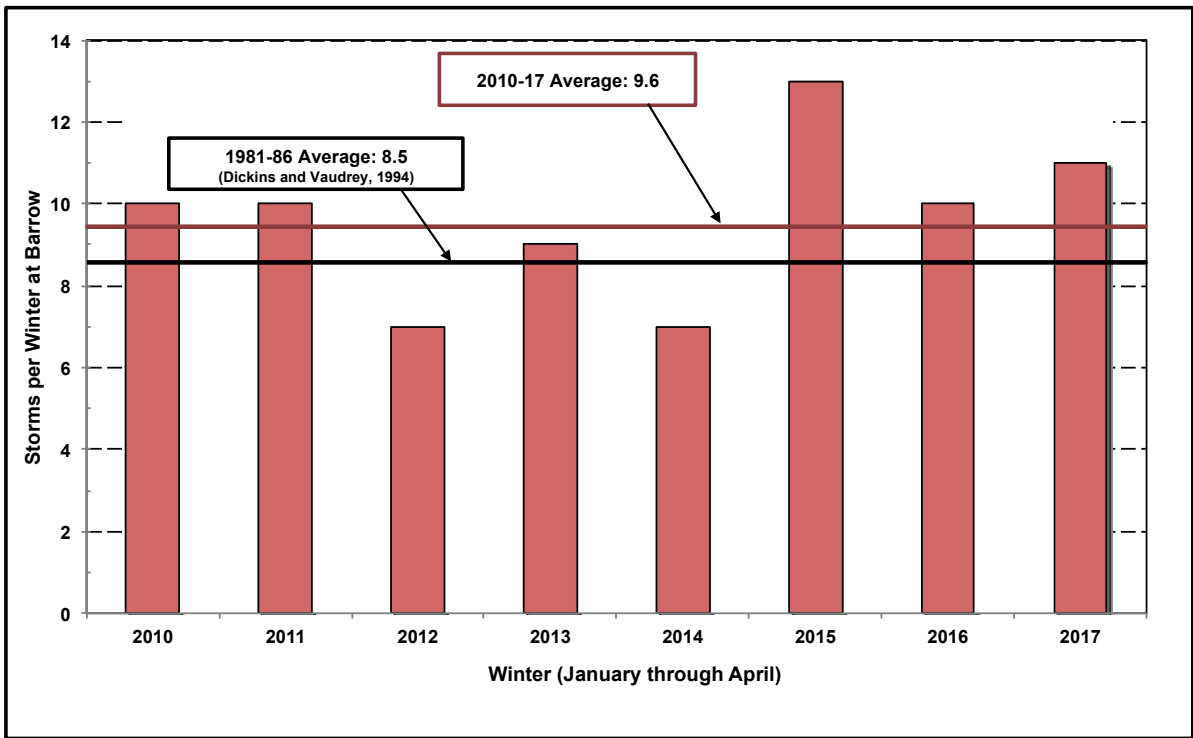


Figure 75. Storms per Winter at Barrow Airport, 2010-2017

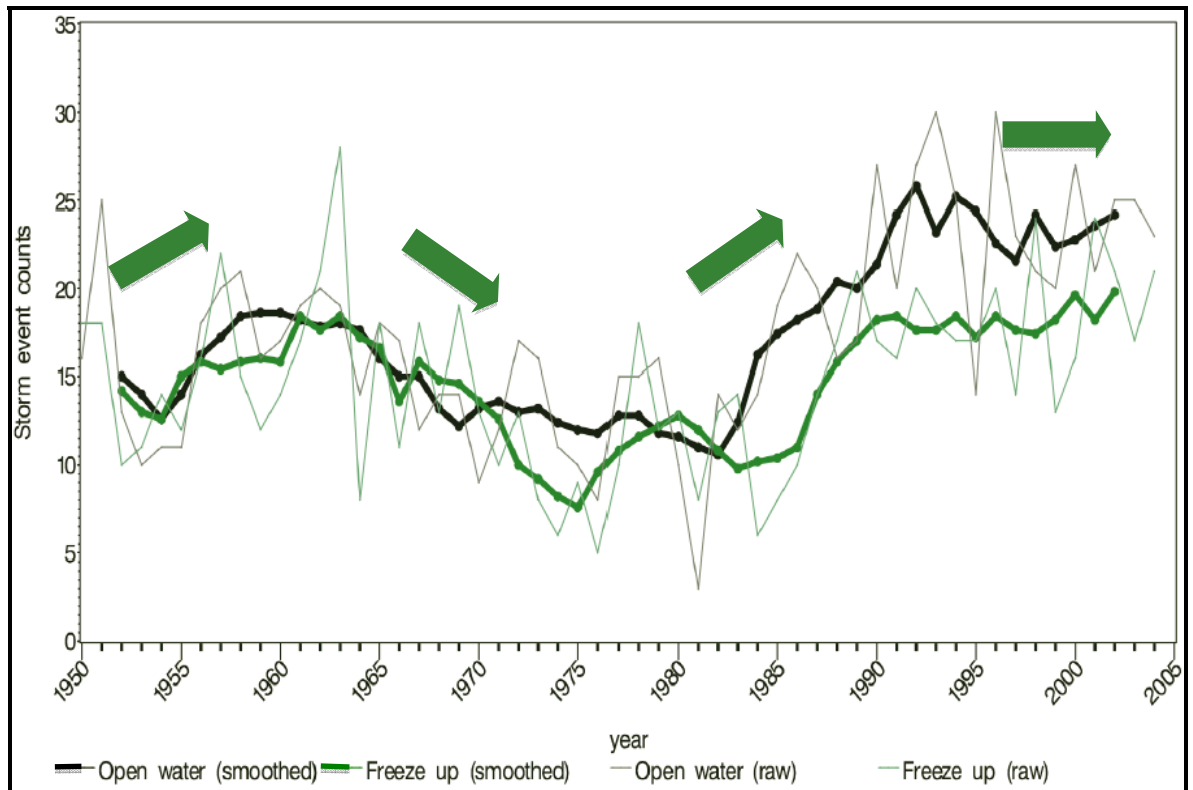


Figure 76. Yearly Storm Count at Barrow during Open-Water and Freeze-Up Seasons, 1950-2004 (after Walsh and Eicken, 2007)

6.3. Timing of Freeze-Up

As discussed in Section 6.1, the monthly average air temperatures at Barrow have exceeded the long-term averages for the period from 1971-72 through 1999-2000 by substantial margins in late summer and early autumn (3.2°F in September, 9.7°F in October, and 7.4°F in November; 1.8°, 5.4°, and 4.1°C, respectively; Figure 73). Based on an analysis conducted by Lindsay and Zhang (2005) using a coupled ice-ocean model, these warmer temperatures in late summer and early autumn have resulted from, and in turn contributed to, a decline in the extent and thickness of the pack ice and an increase in the temperature of the sea surface. The impact of this feedback loop, which is illustrated in Figure 77, has been a significant delay in the onset of freeze-up in the Beaufort and Chukchi Seas.

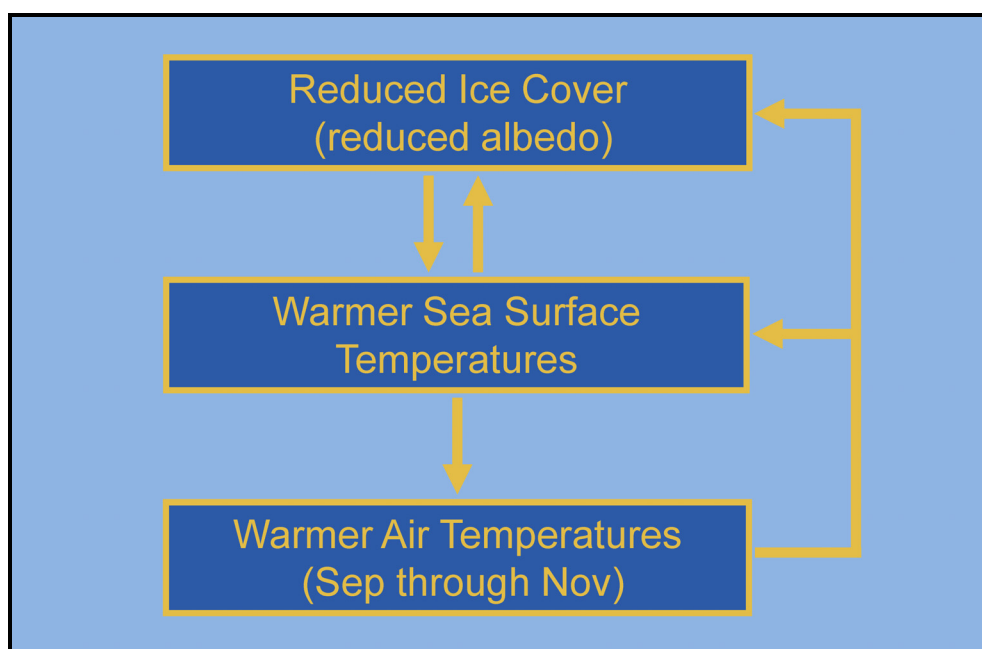


Figure 77. Feedback Loop Leading to Delay in Onset of Freeze-Up

Table 22 presents the timing of freeze-up in the Alaskan Beaufort Sea since 2009. The date of freeze-up in the nearshore region ranged from October 11th to November 7th, with the latter occurring in 2016. The average date, October 26th, is six days later than that from 2002 through 2006 (Vaudrey, 2007) and 22 days later than that derived from 11 years of on-site observations and satellite imagery acquired from 1980 through 1985 and 1987 through 1991 (Vaudrey, 1982a; 1983; 1984; 1985a; 1985b; 1986; 1988a; 1989a; 1990; 1991; 1992). The standard deviation during the past eight years was eight days. The number of accumulated freezing-degree days (FDD) at the time of nearshore freeze-up varied widely, from 80 to 363, with a mean value of 193 and a standard deviation of 97.

Table 22. Timing of Freeze-Up in Alaskan Beaufort Sea, 2009 through 2016

Year	First Ice ¹		Nearshore Freeze-Up ²		Complete Freeze-Up ³	
	Date	FDD	Date	FDD	Date	FDD
2009	Sep 28	15	Oct 22	106	Nov 9	412
2010	Oct 4	19	Oct 11	80	Nov 2	305
2011	Oct 12	14	Oct 26	102	Nov 1	201
2012	Oct 15	51	Nov 5	363	Nov 12	508
2013	Sep 24	19	Oct 26	197	Nov 20	678
2014	Oct 2	1	Oct 30	193	Nov 5	319
2015	Sep 21	0	Oct 26	219	Oct 31	318
2016	Oct 15	2	Nov 7	280	Nov 23	563
Average	Oct 3	15	Oct 26	193	Nov 9	413
Std. Dev.	9 days	17	8 days	97	9 days	159

Notes:

- ¹ “First Ice” refers to the date on which ice began to form in protected waters (excluding ice that formed but subsequently melted before freeze-up began in earnest).
- ² “Nearshore Freeze-Up” refers to the date on which ice covered that portion of the Alaskan Beaufort Sea typically occupied by landfast ice.
- ³ “Complete Freeze-Up” refers to the date on which ice covered the entire Alaskan Beaufort Sea.

Complete freeze-up in the Alaskan Beaufort Sea took place between October 31st and November 23rd. As in the case of nearshore freeze-up, the latest date occurred in 2016. The average date over the past eight years was November 9th, with a standard deviation of nine days. The number of FDD at complete freeze-up varied widely over the period of record, from 201 to 678. The average value was 413, with a standard deviation of 159. This outcome confirms the finding of previous freeze-up studies (*e.g.*, Coastal Frontiers and Vaudrey, 2014; 2016) that air temperature alone cannot be used to predict the date of freeze-up, and that other factors such as the sea surface temperature, wind conditions, and salinity must be taken into account.

Freeze-up dates in the Chukchi Sea during the past eight years are presented in Table 23. Nearshore freeze-up occurred between November 4th and December 10th. Once again, the latest freeze-up took place in 2016. The average was November 23rd, with a standard deviation of 12 days. Based on an assessment of landfast ice formation performed by Mahoney, *et al.* (2007), this date is more than one month later than in the mid-1970s. A

Table 23. Timing of Freeze-Up in Chukchi Sea, 2009 through 2016

Year	First Ice ¹		Nearshore Freeze-Up ²		Complete Freeze-Up ³	
	Date	FDD	Date	FDD	Date	FDD
2009	Oct 9	17	Nov 16	535	Nov 29	949
2010	Oct 7	16	Nov 4	265	Dec 7	959
2011	Oct 6	24	Nov 20	601	Nov 30	1,022
2012	Oct 13	4	Nov 15	322	Nov 28	722
2013	Oct 2	39	Nov 26	697	Dec 14	1,104
2014	Oct 7	14	Nov 28	751	Dec 17	1,472
2015	Oct 13	54	Dec 5	1,271	Dec 12	1,576
2016	Oct 15	0	Dec 10	878	Dec 27	1,282
Average	Oct 9	21	Nov 23	665	Dec 9	1,136
Std. Dev.	4 days	18	12 days	321	10 days	288

Notes:

- ¹ “First Ice” refers to the date on which ice began to form in protected waters (excluding ice that formed but subsequently melted before freeze-up began in earnest).
- ² “Nearshore Freeze-Up” refers to the date on which ice covered the region south of Point Barrow and east of the 163°W meridian.
- ³ “Complete Freeze-Up” refers to the date on which ice covered the entire Chukchi Sea north of Cape Lisburne.

significant delay in the occurrence of freeze-up also is implied by the research of Rodrigues (2009), who found that the length of the ice-free season off the coast between Point Barrow and Point Lay has increased from approximately 30 days in the late 1970s to 125 days at present. The number of accumulated FDD at the time of nearshore freeze-up varied widely during the past eight years, ranging from 265 to 1,271. The average was 665, while the standard deviation was 321.

Complete freeze-up in the Chukchi Sea north of Cape Lisburne took place between November 28th and December 27th. In keeping with the findings reported above, the latest date occurred in 2016. The mean value over the eight-year period was December 9th, with a standard deviation of ten days. Not surprisingly, the number of accumulated FDD at the time of complete freeze-up varied over a wide range, from 722 to 1,576, with an average value of 1,136 and a standard deviation of 288.

Figure 78 compares the timing of nearshore freeze-up in the Alaska Beaufort and Chukchi Seas during the past eight years. The dates have trended later at exceptionally high rates: 2.3 days/yr in the case of the former and 4.3 days/year in the case of the latter. If this pattern continues, the current four-week difference between nearshore freeze-up in the Beaufort and Chukchi will expand to five weeks within four years.

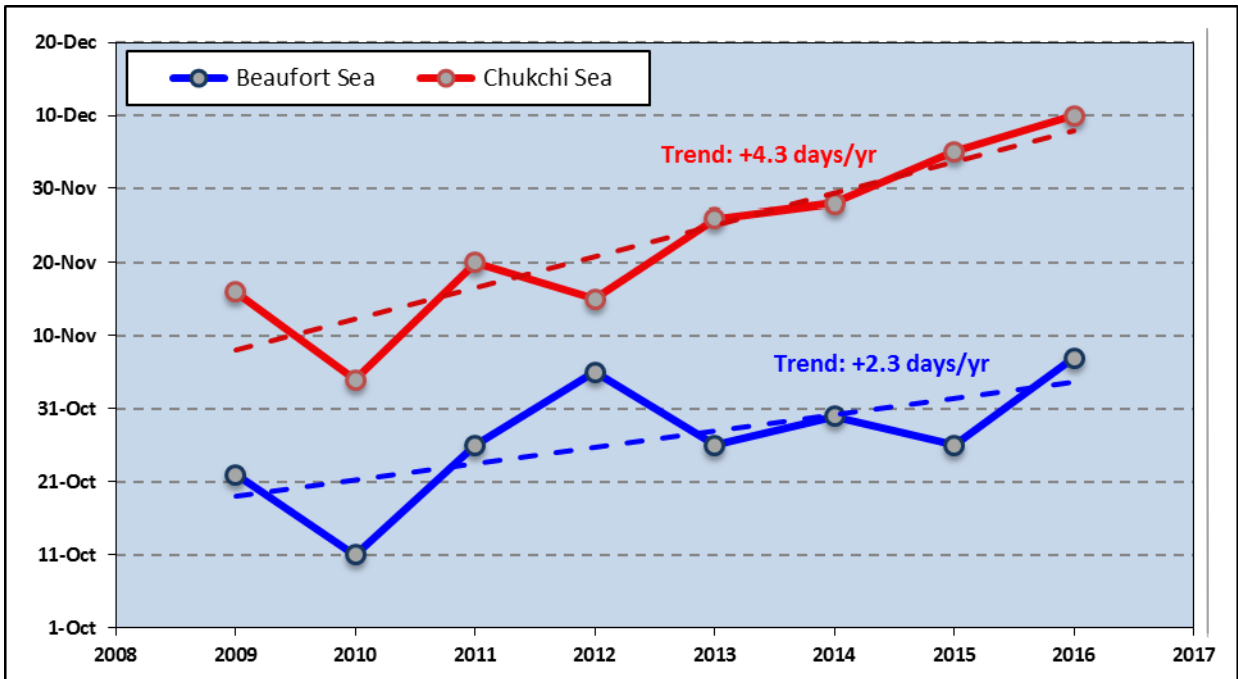


Figure 78. Timing of Nearshore Freeze-Up in Alaskan Beaufort and Chukchi Seas, 2009-2016

Trend: Freeze-up in the nearshore region of the Alaskan Beaufort Sea currently tends to occur during the fourth week in October, about three weeks later than in the 1980s. The rate of change has accelerated in recent years, with the date of freeze-up currently trending later by 2.3 days/yr. In the northeastern Chukchi, nearshore freeze-up tends to occur during the fourth week in November, more than a month later than in the 1970s. Once again, the rate of change has accelerated; the date of freeze-up currently is trending later by 4.3 days/yr. These high rates of change imply that the length of the open-water season will increase substantially in the years ahead.

6.4. Duration of Freeze-Up

Table 24 chronicles the progression of freeze-up from first ice to complete cover in the Alaskan Beaufort Sea during the past eight years (2009-2016). The period from the first appearance of ice along the coast to nearshore freeze-up averaged 23 days, while that from

Table 24. Duration of Freeze-Up in Alaskan Beaufort Sea, 2009 through 2016

Year	First Ice to Nearshore Freeze-Up^{1,2} (Days)	Nearshore to Complete Freeze-Up^{2,3} (Days)	First Ice to Complete Freeze-Up^{1,3}
2009	24	18	42
2010	7	22	29
2011	14	6	20
2012	21	7	28
2013	32	25	57
2014	28	6	34
2015	35	5	40
2016	23	16	39
Average	23	13	36
Std. Dev.	9	8	11

Notes:

- ¹ “First Ice” refers to the date on which ice began to form in protected waters (excluding ice that formed but subsequently melted before freeze-up began in earnest).
- ² “Nearshore Freeze-Up” refers to the date on which ice covered that portion of the Alaskan Beaufort Sea typically occupied by landfast ice.
- ³ “Complete Freeze-Up” refers to the date on which ice covered the entire Alaskan Beaufort Sea.

nearshore freeze-up to complete freeze-up averaged 13 days. Combining these two phases yields an average of duration of 36 days from first ice to complete freeze-up, with a standard deviation of 11 days.

Table 25 presents comparable information for the Chukchi Sea. The period from first ice to nearshore freeze-up averaged 45 days over the past eight years, while that from nearshore freeze-up to complete freeze-up averaged 17 days. These values produce an average duration of 62 days from first ice to complete freeze-up, with a standard deviation of ten days.

The duration of freeze-up in the two basins is compared in Figure 79, which illustrates the total time from first ice to complete freeze-up. Notwithstanding significant interannual variations, the data indicate that the duration of freeze-up is not only considerably longer in the Chukchi, but also increasing at a faster rate: 2.3 days/yr in the Chukchi versus 1.3 days/yr in the Beaufort.

Table 25. Duration of Freeze-Up in Chukchi Sea, 2009 through 2016

Year	First Ice to Nearshore Freeze-Up ^{1,2} (Days)	Nearshore to Complete Freeze-Up ^{2,3} (Days)	First Ice to Complete Freeze-Up ^{1,3}
2009	38	18	56
2010	28	33	61
2011	45	10	55
2012	33	13	46
2013	55	18	73
2014	52	19	71
2015	53	7	60
2016	56	17	73
Average	45	17	62
Std. Dev.	11	8	10

Notes:

- ¹ “First Ice” refers to the date on which ice began to form in protected waters (excluding ice that formed but subsequently melted before freeze-up began in earnest).
- ² “Nearshore Freeze-Up” refers to the date on which ice covered the region south of Point Barrow and east of the 163°W meridian.
- ³ “Complete Freeze-Up” refers to the date on which ice covered the entire Chukchi Sea north of Cape Lisburne.

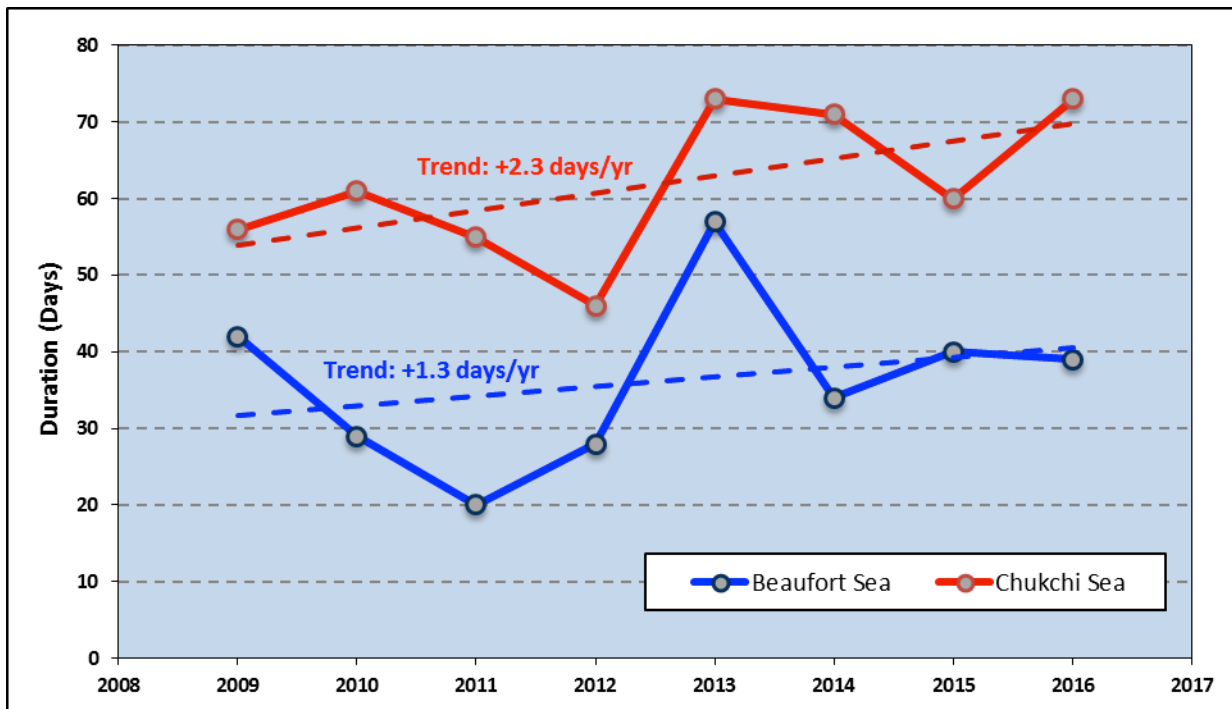


Figure 79. Duration of Freeze-Up in Alaskan Beaufort and Chukchi Seas, 2009-2016

Trend: The duration of freeze-up in the Alaskan Beaufort Sea, from first ice to complete cover, currently averages 36 days with a standard deviation of 11 days. In the Chukchi, the duration is substantially longer, averaging 62 days with a standard deviation of ten days. The duration in the Beaufort is increasing at a rate of 1.3 days/yr, while that in the Chukchi is increasing at 2.3 days/yr.

6.5 First-Year Ice Growth

As discussed in Section 4.1, the growth of undeformed first-year ice can be estimated on the basis of freezing-degree days (FDD) using the relationship of Lebedev (Bilello, 1960). Table 26 presents the computed ice thickness on a monthly basis for each winter season from 1970-71 through 2016-17. The results were obtained using the FDD data for Barrow Airport compiled in Table 17, and are presented in a comparable format with the highest ranking (No. 1) assigned to the lowest predicted ice thickness and lowest ranking (No. 47) assigned to the highest ice thickness.

In keeping with the air temperature data discussed in Section 6.1, the computed thickness of first-year ice in the Chukchi Sea at the end of the 2016-17 winter season was the lowest in the entire 47-year period of record by a wide margin: 134 cm versus the prior minimum of 143 cm in 2013-14. Of the remaining six winters covered by the current round of freeze-up studies, four produced ice thicknesses that ranked among the ten lowest in the period of record. The maximum thickness during this period, 167 cm, occurred in 2011-12. Notwithstanding this comparative outlier, the average thickness over the past eight years, 150 cm, was 21 cm less than that computed for the six-year period from 1980-81 through 1985-86.

Additional perspective on the diminishing growth of first-year ice is provided by Figure 80, which compares the computed thickness of undeformed first-year ice at the end of each month in each of the past eight winter seasons with the corresponding average value for the period from 1970-71 through 1989-90. Even in 2011-12, the ice failed to attain the average thickness that prevailed in the 1970s and 1980s. During the most recent winter, the ice thickness remained below the prior envelope of values for each month from November through May.

The reduction in ice thickness attributable to warmer air temperatures may be exacerbated by an increase in the depth of the snow cover. To quantify the relative importance of these and other factors, Brown and Cote (1992) investigated the interannual variability in the maximum ice thickness at four sites in the Canadian High Arctic between

Table 26. Computed Ice Thickness (cm) at Barrow, 1970-71 through 2016-17

Year	Sep	Oct	Nov	Dec	Jan	Feb	Mar	Apr	May	47-yr Rank
1970-71	16	52	77	102	127	150	169	182	186	46
1971-72	3	33	61	90	115	137	158	171	176	42
1972-73	7	24	55	79	105	125	148	161	165	24
1973-74	3	26	50	78	102	129	151	166	170	34
1974-75	5	43	73	108	135	152	167	180	183	45
1975-76	18	48	79	110	134	155	173	184	189	47
1976-77	4	34	60	92	113	133	156	169	173	40
1977-78	0	24	60	87	107	127	145	157	162	19
1978-79	5	42	63	93	110	133	153	165	169	31
1979-80	0	26	48	81	107	126	144	158	163	20
1980-81	15	37	67	97	114	134	151	163	165	24
1981-82	14	37	64	90	113	129	148	160	165	24
1982-83	7	43	75	99	125	143	161	172	176	42
1983-84	17	47	69	89	114	142	161	176	181	44
1984-85	0	29	65	94	114	135	153	167	170	34
1985-86	10	40	63	89	114	131	152	166	170	34
1986-87	4	31	59	85	110	132	150	164	167	29
1987-88	9	23	59	87	110	130	149	160	164	22
1988-89	9	48	81	104	131	139	155	164	169	31
1989-90	0	29	68	94	122	144	161	170	171	38
1990-91	6	30	65	95	118	139	159	169	169	31
1991-92	6	30	65	95	121	143	159	170	173	40
1992-93	17	41	67	93	116	134	152	161	164	22
Average	8	36	65	93	116	137	155	168	171	
Std. Dev.	6	9	8	8	9	8	8	7	7	
Year	Sep	Oct	Nov	Dec	Jan	Feb	Mar	Apr	May	47-yr Rank
1993-94	6	21	49	79	102	121	143	155	159	15
1994-95	10	42	73	102	123	143	162	170	171	38
1995-96	0	27	54	85	106	128	144	156	157	14
1996-97	13	46	64	87	114	133	152	162	166	28
1997-98	2	25	46	79	106	126	141	149	151	5
1998-99	0	16	52	83	110	129	149	162	165	24
1999-00	5	29	59	91	115	135	153	164	170	34
2000-01	7	30	59	84	107	122	143	154	161	17
2001-02	8	40	66	91	117	137	150	161	163	20
2002-03	0	19	47	73	98	120	139	147	151	5
2003-04	0	18	50	79	102	127	147	158	161	17
2004-05	3	23	53	82	104	124	141	152	155	11
2005-06	3	22	56	81	105	123	145	158	160	16
2006-07	0	14	45	72	101	120	140	149	154	9
2007-08	0	18	39	66	96	122	143	152	155	11
2008-09	2	20	50	73	100	117	139	150	152	8
2009-10	3	15	51	77	105	123	142	150	154	9
2010-11	3	20	43	76	100	117	135	148	151	5
2011-12	2	19	53	83	112	132	154	164	167	29
2012-13	0	12	44	76	100	123	140	152	155	11
2013-14	7	18	45	72	96	114	131	142	143	2
2014-15	0	22	46	76	100	118	137	147	148	4
2015-16	3	24	53	84	101	118	136	144	145	3
2016-17	0	7	34	62	83	103	122	132	134	1
Average	3	23	51	80	104	124	143	153	156	
Std. Dev.	4	9	9	8	8	8	8	8	9	

Note: Ice thicknesses were calculated using the corresponding FDD values in Table 17.

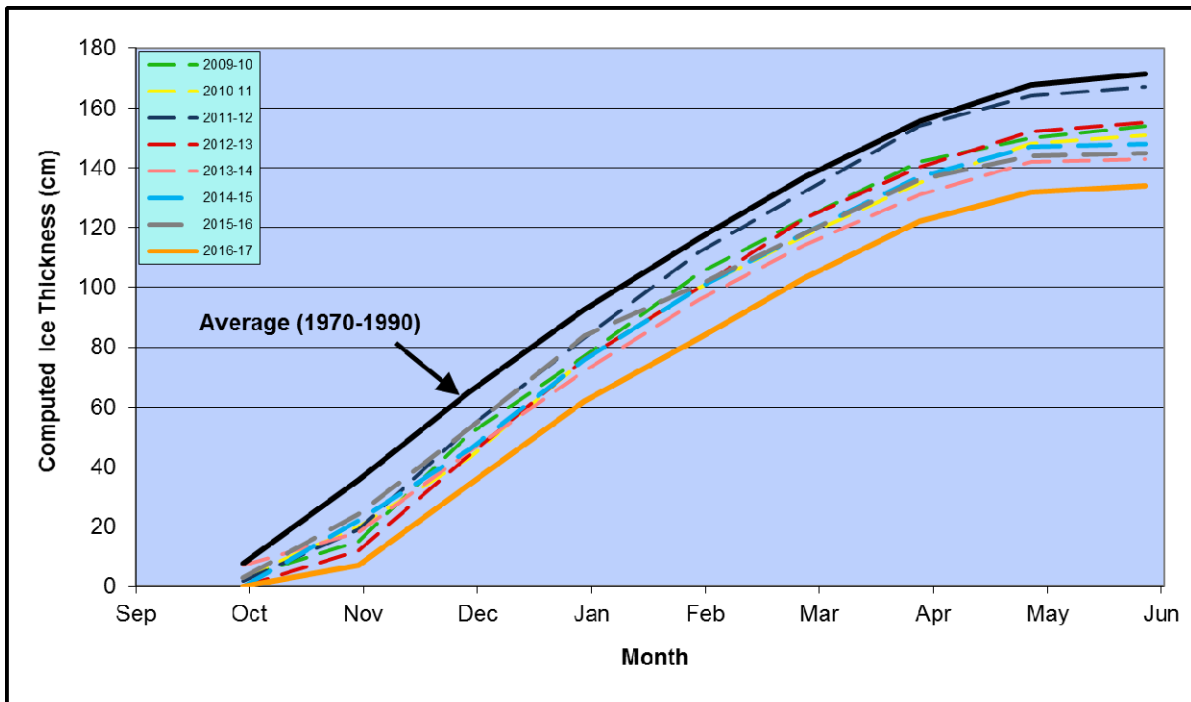


Figure 80. Computed Ice Thickness: Recent Winters vs. 1970s and 1980s

1950 and 1989 using a one-dimensional model of ice growth based on heat transfer. The depth of the snow cover was found to be the most important factor, explaining 30% to 60% of the variance in the maximum first-year ice thickness due to its insulating effect. Density fluctuations in the snow cover were estimated to account for an additional 15% to 30% of the variance. In contrast, annual variations in air temperature accounted for less than 4% of the variance in the maximum first-year ice thickness.

The average snowfall at Barrow during the five-month period from October through February has increased dramatically, from 30 cm in the 1980s to 57 cm in the 1990s and 88 cm in the 2000s (Figure 81). Despite the relatively small accumulations that occurred in each of the past four freeze-up seasons – 85, 82, 62, and 58 cm, respectively – the snowfall over the past eight years has averaged 93 cm, more than three times larger than in the 1980s. Over the entire 47-year period of record (1970-71 through 2016-17), snowfall during the freeze-up season has increased at an average rate of 1.7 cm/year.

In addition to reducing ice thickness, higher air temperatures tend to prolong the existence of leads and retard the production of new ice in those leads. Furthermore, higher temperatures and the insulating effect of heavier snowfall tend to decrease the degree of consolidation that occurs in ridges and rubble fields and reduce the overall strength of the ice canopy.

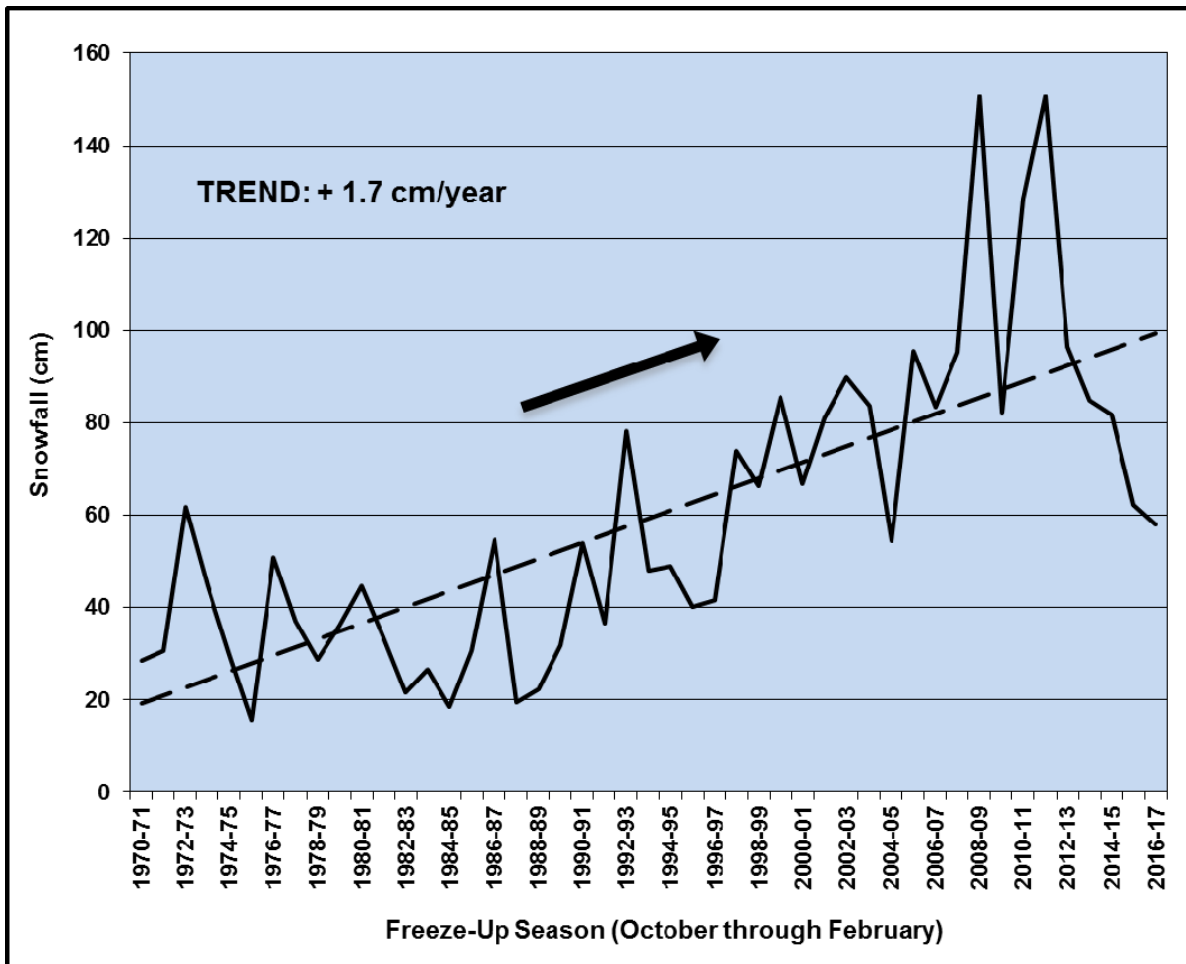


Figure 81. Annual Snowfall at Barrow during Freeze-Up (October – February), 1970-71 through 2016-17

Trend: Based on air temperature alone, the thickness of undeformed first-year ice attained during an average winter has decreased by 21 cm (12.3%) since the early 1980s. However, a significant increase in snowfall may be causing an even greater reduction in the ice thickness due to its insulating effect. Other temperature-related factors, including reduced ice production in leads, decreased consolidation of ridges and rubble fields, and reduced ice strength, serve to amplify the impact of reduced thickness on ice dynamics.

6.6. Landfast Ice

Personal observations and data presented by investigators that include Barry, *et al.* (1979), Eicken, *et al.* (2006), and Mahoney, *et al.* (2012), indicate that characteristic patterns and features of the ice cover tend to recur on an annual basis. Such patterns include the evolution of the landfast ice zone and the distribution of leads and polynyas over the course of the winter. Factors that contribute to these recurring patterns include the seasonal

cycles of meteorological and oceanographic conditions, the orientation of the shoreline and bathymetric contours, and the presence or absence of shoals.

Beaufort Sea: The wind, which tends to be coast-parallel in the Alaskan Beaufort Sea, constitutes the dominant driving force for ice movement. Easterlies produce westerly ice motion with an onshore component, creating a stable landfast ice zone that ultimately extends to the vicinity of the 20-m isobath (Mahoney, *et al.*, 2012). The western Beaufort between Point Barrow and Prudhoe Bay contains numerous shoals that are located up to 25 nm (46 km) offshore. The most prominent are Weller Bank, which lies off Harrison Bay, and Stamukhi Shoal, which lies off Pingok Island (Figure 3). The large grounded rubble piles that typically form on these shoals serve as anchor points for a relatively wide expanse of landfast ice. In contrast, water depths to the east of Prudhoe Bay increase more rapidly off the barrier islands from Cross to Flaxman, and off the coast in the vicinity of Barter Island. In these areas, the landfast ice zone typically remains less than 5 nm (9 km) wide. An exception occurs in Camden Bay, where landfast ice can extend more than 10 nm (19 km) offshore.

In the early 1980s, a well-grounded shear zone tended to form in the region west of Prudhoe Bay by mid-November. During the past eight freeze-up seasons, however, this process has been delayed by the warm air temperatures that have prevailed in September, October, and November (Section 6.1). The landfast ice has tended to remain poorly-grounded and subject to breakout events until much later in the freeze-up season, with the attainment of stability ranging from early December in 2015-16 (Coastal Frontiers and Vaudrey, 2016) to late February in 2016-17 (Section 4.1), and early March in 2014-15 (Coastal Frontiers and Vaudrey, 2015). An even greater departure from the 1980s occurred in 2010-11, when the formation of a securely-grounded shear zone was inhibited by a paucity of easterly storms and sustained easterly winds. As a result, the landfast ice zone remained relatively narrow and unstable through mid-winter (Coastal Frontiers and Vaudrey, 2011).

To the east of Prudhoe Bay, the contrast between the 1980s and recent years has encompassed not only the timing but also the extent of landfast ice development. A well-established, firmly-grounded shear zone formed off the barrier islands during five of the six freeze-up periods monitored in the 1980s. In five of the past eight years, though, the ice in part or all of this region has remained poorly-grounded and mobile throughout freeze-up and early winter.

Chukchi Sea: As discussed in Section 5, easterly (offshore) winds and relatively steep slopes in the nearshore area limit the extent of the landfast ice in the Chukchi Sea to a

narrow strip along the shoreline. The offshore edge typically lies within 5 to 10 nm (9 to 19 km) of the coast, but can retreat to the coast itself during breakout events triggered by easterly storms. Such an event occurred off Skull Cliff in February 2016 (Coastal Frontiers and Vaudrey, 2016). Exceptions to this pattern often occur in the semi-protected areas to the east of Icy Cape and Point Franklin, where the landfast ice tends to be wider and more stable.

Due to its dynamic nature, particularly with respect to breakout events, the landfast ice zone in the Chukchi fails to exhibit the progressive expansion over the course of the freeze-up season typically seen in the Beaufort. As a result, its maximum seaward extent is poorly correlated with water depth (Mahoney, *et al.*, 2012). In addition, the dynamic nature of the landfast ice zone increases the potential for ridge and rubble formation in the nearshore region, and for pile-ups at the shoreline.

A narrow, ephemeral landfast ice zone was observed in the northeast Chukchi Sea during a significant portion of each of the past eight freeze-up seasons. Instability was particularly prevalent in 2010-11, 2012-13, and 2015-16; in each instance, a continuous strip of landfast ice failed to materialize throughout freeze-up and early winter (Coastal Frontiers and Vaudrey, 2011; 2013; 2016).

Trend: In the Alaskan Beaufort Sea, the extent of the landfast ice zone to the west of Prudhoe Bay is similar to that observed in the 1980s but the landfast ice develops more slowly. To the east of Prudhoe Bay, a stable, well-grounded shear zone is less likely to develop during freeze-up and early winter, and develops more slowly in those years when it does occur. In the Chukchi, the narrow, ephemeral nature of the landfast ice zone noted in the 1980s continues to prevail today.

6.7. Coastal Flaw Lead

Seaward of the landfast ice zone in the northeast Chukchi Sea, the ice is driven offshore during periods of easterly winds. The resulting flaw lead separates the mobile pack ice from the stationary landfast ice, and generates new ice throughout the winter as it experiences repeated cycles of opening, expanding, and either closing or refreezing. A recent study by Hirano, *et al.* (2016) suggests that upwelling of relatively warm, dense water from Barrow Canyon also contributes to the formation and maintenance of the lead. Once again, easterly winds serve as the driving force. The width of the lead can vary substantially, depending on the duration, direction, and intensity of the winds.

Based on the trends identified in the preceding subsections, including warmer air temperatures, increased storminess, and slower ice growth during freeze-up, it was hypothesized that the ice canopy might be more prone to displacement, and therefore that the flaw lead might occur more frequently, than in the 1980s (Coastal Frontiers and Vaudrey, 2013). However, an assessment of the period from December through April for the 21 winters from 1993-94 through 2013-14 found that the frequency of occurrence has not changed appreciably (Ward, *et al.*, 2015). Specifically, the flaw lead was present 51% of the time during the first ten winters and 49% during the next 11. The frequency with which the lead extends to the northeast of Point Barrow also appears to have remained constant; the extended flaw lead was present 35% of the time during first ten winters in the period-of-record, and 37% during the next 11.

Trend: Notwithstanding trends toward warmer air temperatures, increased storminess, and slower ice growth during freeze-up, the frequencies with which the flaw lead and extended flaw lead occur off the Chukchi Sea coast have remained unchanged since the 1990s.

6.8. Multi-Year Ice

Two types of multi-year ice can occur in the Beaufort and Chukchi Seas: (1) true multi-year floes from the permanent polar pack in the Arctic Ocean (“pack floes”), and (2) second-year floes that develop when grounded fragments of thick first-year features survive the summer months due to a combination of cold air temperatures, mild winds, and/or a preponderance of northerly or westerly winds. The first-year features consist of ridges and rubble fields formed off the coast of the Beaufort Sea and in the Canadian Arctic Archipelago. Second-year floes can be distinguished from pack floes by their more jagged appearance, with many embedded ridges, and by their greater thickness (6 to 9 m for second-year floes versus 3 to 5 m for pack floes). Henceforth, the term “multi-year ice floes” will be used to refer to both pack floes and second-year floes.

Beaufort Sea: When the initial round of freeze-up studies was conducted in the 1980s, large multi-year ice floes were present in the nearshore region of the Alaskan Beaufort Sea during three of the six freeze-up seasons: 1980-81, 1983-84, and 1985-86 (Vaudrey, 1981a; 1981b; 1982a; 1983; 1984; 1985a; 1986). Grounded multi-year fragments with diameters as large as 120 m were observed during the other three seasons (1981-82, 1982-83, and 1984-85).

In the nine years that preceded the resumption of freeze-up studies in 2009-10, large multi-year floes invaded the nearshore region on only one occasion: 2001-02, when a low

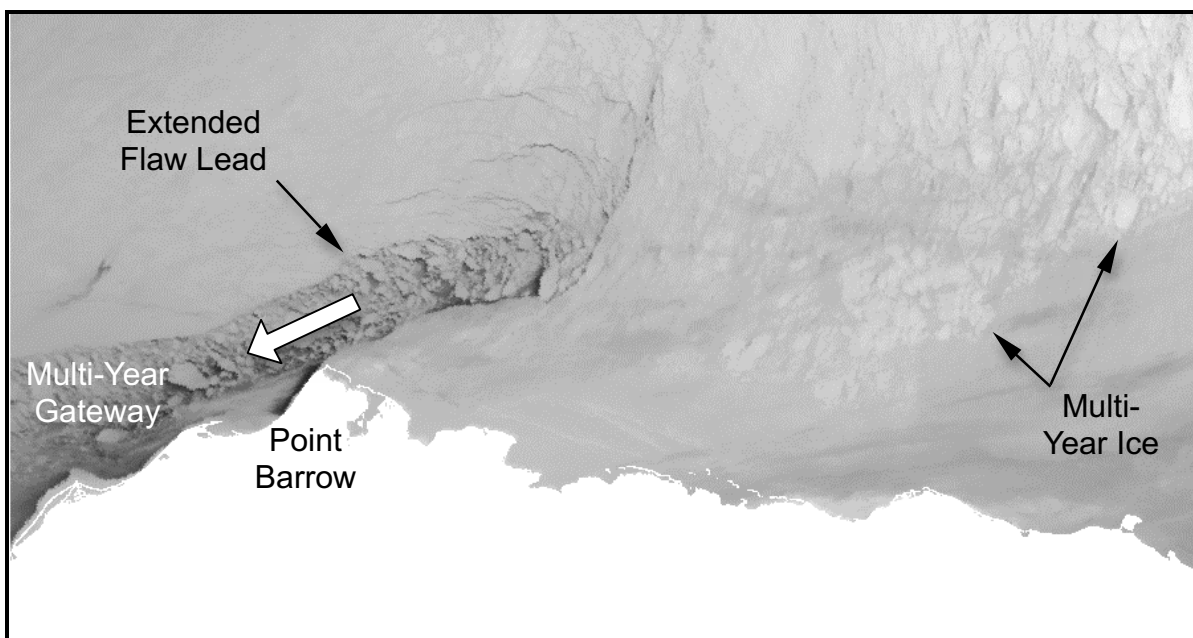
concentration approached the coast in the western Beaufort during the initial stages of freeze-up. The next invasion occurred in 2009-10, when a high concentration of massive floes with embedded ridges entered the nearshore region of the Alaskan Beaufort from Canada, moved west to Point Barrow, and split into northern and southern branches in the Chukchi (Coastal Frontiers and Vaudrey, 2010). Although small, grounded fragments of second-year ice were observed on and around the barrier islands in 2010-11 and 2015-16 (Coastal Frontiers and Vaudrey, 2011; 2016), and two small patches of second-year ice drifted away from Point Barrow in October 2016 (Section 4.3.1), large multi-year floes have remained absent from southern portion of the Alaskan Beaufort Sea since 2009-10. Hence, during the past 17 years, such floes have entered the nearshore region on only two occasions.

Chukchi Sea: Multi-year ice was present in the Chukchi Sea during each of the three freeze-up seasons from 1983-84 through 1985-86 (Vaudrey, 1984; 1985a; 1986) and also during the midwinter season of 1987 (Vaudrey, 1987a). The invasions were characterized by concentrations as high as 70%, and southerly limits between 71°N and 70°30'N.

In nine of the seventeen winters from 2000-01 through 2016-17, an extended flaw lead channeled large multi-year floes into the region south and west of Point Barrow: 2000-01, 2001-02, 2003-2004, 2005-2006, 2008-09, 2009-10, 2011-12, 2013-14, and 2015-16 (Ward, *et al.*, 2015). The invasions all followed a similar pattern, which involves four phases:

- ***Flaw Lead:*** a flaw lead develops off the northeast coast of the Chukchi Sea in response to sustained easterly winds.
- ***Extended Flaw Lead:*** an extended flaw lead results when the flaw lead stretches to the north and east of Point Barrow. As discussed by Eicken, *et al.* (2006), this northward extension (the “Barrow Arch”) is caused by westward movement of the Beaufort Sea pack ice, which in turn is caused by easterly winds.
- ***Multi-Year Ice in Extended Flaw Lead:*** multi-year floes can enter the extended flaw lead if it extends sufficiently far north to intersect the southern boundary of this ice. Because the floes lose confinement in the lead, they can travel to the southwest at much higher speeds than those embedded in the pack ice.
- ***Multi-Year Gateway:*** a “Multi-Year Gateway” forms when multi-year floes that have entered the extended flaw lead move into the region south and west of Point Barrow. A representative example of the Gateway that occurred in March 2001 is provided in Figure 82.

While the Multi-Year Gateway represents the primary means by which multi-year ice enters into the Chukchi Sea, an alternate mechanism (“Early-Season Entry”) has been noted



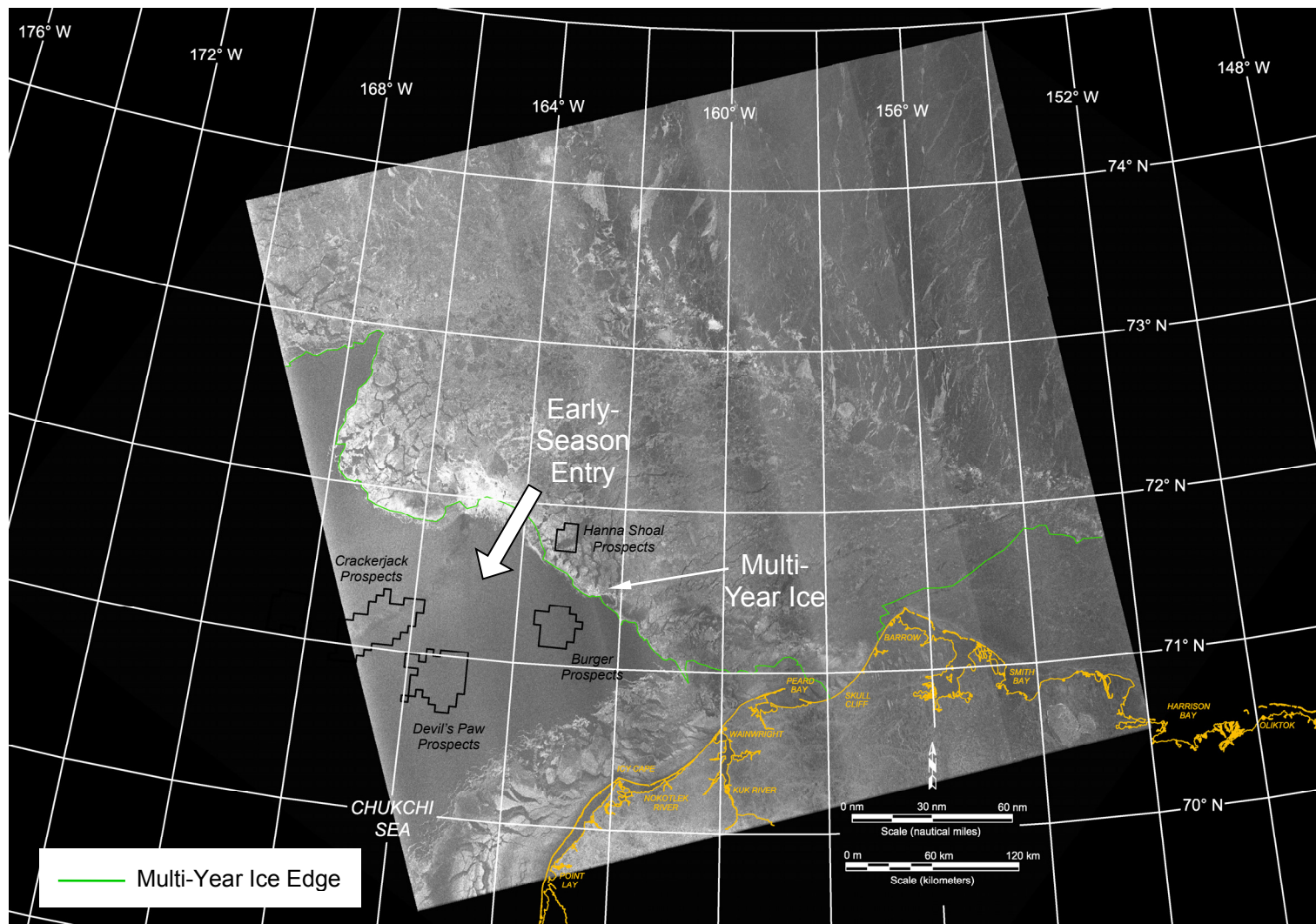
After Eicken, *et al.*, 2006

Figure 82. AVHRR Image Acquired on March 12, 2001 Illustrating Multi-Year Gateway

on three occasions: November 2010 (Ward, *et al.*, 2015), November 2014 (Coastal Frontiers and Vaudrey, 2015), and November 2015 (Coastal Frontiers and Vaudrey, 2016). In each case, the floes began to move into the region south and west of Point Barrow when the ice canopy was in an early stage of development. The Early-Season Entry that occurred in 2015 is illustrated in Figure 83, which shows the multi-year ice edge adjoining open water in the region between the Hanna Shoal and Burger Prospects. Although the Multi-Year Gateway and Early-Season Entry are distinctly different phenomena, they share a key characteristic: a loss of confinement that allows multi-year ice floes to move to the southwest at relatively high speeds.

Together, the Multi-Year Gateway and Early-Season Entry have caused multi-year ice to invade the region south and west of Point Barrow in 11 of the past 17 freeze-up seasons. The invasions resulted from the Multi-Year Gateway alone in eight seasons, Early Season Entry alone in two seasons, and both phenomena in 2015-16.

Trend: The probability of large multi-year ice floes invading the nearshore portion of the Alaskan Beaufort Sea in any given year is substantially less than in the 1980s. This trend may be explained in part by a reduction in the amount of multi-year ice comprising the permanent polar pack (Perovich, *et al.*, 2013) and in part by an increase in the northerly retreat of the ice edge during the summer months, both of which have reduced the opportunities for pack floes to enter the nearshore area. In addition, warmer air temperatures,



Source: RADARSAT-2 Data and Products © MacDonald Dettwiler and Associates Ltd., 2015 – All Rights Reserved

Figure 83. RADARSAT-2 Image Acquired on November 16, 2015, Illustrating Early-Season Entry

longer open-water seasons, and increased storminess have decreased the likelihood that first-year ridges and rubble will survive the summer melt season to become second-year floes of any consequence. Nevertheless, as demonstrated in 2009-10, the possibility of multi-year ice encounters cannot be ruled out in the nearshore region of the Beaufort. Furthermore, small fragments of second-year ice analogous to those observed in 2010-11 and 2015-16 can be present even if large multi-year floes remain well offshore.

The probability of multi-year ice entering the Chukchi Sea to the south and west of Barrow also has decreased since the 1980s, but to a lesser extent than in the Beaufort. Although the factors that have reduced the probability of invasions in the Beaufort apply to the Chukchi as well, their impact has been mitigated by the ability of the Multi-Year Gateway and Early-Season Entry to divert multi-year floes to the southwest.

7. SUMMARY AND CONCLUSIONS

7.1. Milestones

Freeze-up in 2016-17 was distinguished by exceptionally warm air temperatures, stunted ice growth, uncharacteristically high frequencies of westerly winds, and an absence of multi-year ice. Phenomena that exceeded the ranges established during the seven prior freeze-up seasons are summarized below:

Beaufort Sea

- Highest frequency of westerly winds during the five-month study period (October-February; 64%);
- Lowest number of easterly storms (7, tied with 2011-12) and storm-days (12) during the five-month study period;
- Lowest number of total storm-days during the five-month study period (31, tied with 2009-10);
- Latest occurrence of first ice (October 15th), nearshore freeze-up (November 7th), and complete freeze-up (November 23rd);
- Smallest computed thickness of undeformed first-year ice at the end of winter (148 cm, tied with 2014-15 and 2015-16).

Chukchi Sea

- Lowest number of FDD during the winter season (5,194);
- Largest deviation from the long-term average air temperature in a single month during the five-month study period (+15.5°F or +8.6°C in October 2016);
- Largest deviation from the long-term average air temperature for the nine-month period from September through May (+9.4°F; +5.2°C);
- Smallest computed thickness for undeformed first-year ice at the end of winter (134 cm);
- Highest frequency of westerly winds during the five-month study period (39%, tied with 2013-14);
- Highest number of westerly storm-days (19) during the five-month study period;
- Latest occurrence of first ice (October 15th), nearshore freeze-up (December 10th), and complete freeze-up (December 27th);

- Longest duration of freeze-up (73 days from first ice to complete freeze-up; tied with 2013);
- Lowest snowfall (58 cm) during the five-month study period.

7.2. Detailed Findings

Entire Study Area

1. **Air Temperatures:** For the fourth consecutive year, the air temperatures during the 2016-17 winter season were exceptionally warm. Those recorded at Barrow Airport were the highest in the past 47 years by a wide margin, while those at Deadhorse Airport ranked a close second among those recorded in the past eight years.
2. **First-Year Ice Growth:** The computed thickness of undeformed first-year ice at the end of the 2016-17 winter season was 148 cm in the Alaskan Beaufort Sea and 134 cm in the Chukchi Sea, based on accumulations of 6,144 and 5,194 FDD at Deadhorse and Barrow Airports, respectively. The thickness in the Beaufort tied that in 2014-15 and 2015-16 as the lowest value in the past eight years, while that in the Chukchi was 9 cm less than the prior minimum of 143 cm in 2013-14. The highest values in recent years, 176 cm in the Beaufort and 167 cm in the Chukchi, occurred in 2011-12.

Beaufort Sea

1. **Late Summer:** The ice cover in the Alaskan Beaufort Sea diminished slowly in June, July, and early August, reflecting the prevalence of cloudy skies and reduced solar insolation. The pace quickened appreciably in late August and early September, creating a large expanse of open water off the coast. The minimum ice extent, which occurred on September 10th, tied that in 2007 as the second lowest on record since the acquisition of satellite-based data began in 1979.
2. **Timing of Freeze-Up:** Freeze-up began in mid-October with the formation of ice in the semi-protected waters adjacent to the coast. Complete ice coverage in the nearshore region occurred on November 7th, followed by complete coverage in the entire Alaskan Beaufort Sea on November 23rd. During the past eight years, the average date for the occurrence of nearshore freeze-up has been October 26th with a standard deviation of eight days. The average date for the occurrence of basin-wide freeze-up has been November 9th with a standard deviation of nine days.
3. **Duration of Freeze-Up:** The duration of freeze-up was 39 days, consisting of 23 days from first ice to nearshore freeze-up and an additional 16 days from nearshore freeze-up to complete freeze-up in the basin. During the past eight years, the duration has averaged 36 days with a standard deviation of 11 days.

4. **Wind Regime:** Based on the daily average wind directions recorded at Deadhorse Airport, easterlies prevailed 65% of the time in October. Westerlies predominated in the four months that followed, with frequencies ranging from 65% in December to 77% in January. Over the entire five-month study period (October through February), westerlies outnumbered easterlies by a ratio of 64% to 36%, representing the highest frequency of westerly winds in the past eight years. The highest monthly average wind speed, a modest 12 kt (6 m/s), occurred in both January and February.
5. **Storm Events:** Storm events with daily average wind speeds exceeding 15 kt (8 m/s) occurred on 13 occasions encompassing 31 days. Seven of the events were easterlies, while six were westerlies. The westerly storms tended to be of longer duration, averaging 3.2 days/event versus 1.7 days/event for the easterlies. The total number of storm-days tied that in 2009-2010 as the lowest in the past eight years.
6. **Landfast Ice:** Landfast ice began to develop during the last week in October, and expanded to cover all of the coastal lagoons and a significant portion of Harrison Bay over the course of November. The expansion stalled in December, with gains during the first half of the month erased by losses during the second. The next major advance occurred in late January, when easterly winds propelled the ice edge to the vicinity of the 11-m isobath. After another period of minimal change, the ice edge moved to the 18-m isobath in late February in response to a strong easterly storm. This advance marked the first occasion during the 2016-17 freeze-up season when the ice reached its customary anchor points on Weller Bank and Stamukhi Shoal.
7. **Ice Pile-Ups:** Thirty-eight ice pile-ups formed in the central portion of the Alaskan Beaufort Sea during the 2016-17 freeze-up season. One was located on the Oooguruk Offshore Drillsite (ODS), one on the Spy Island Drillsite (SID), one on Northstar Production Island, two on Thetis Island (a natural barrier island in Harrison Bay), and 33 on natural barrier islands and shoals to the east of Prudhoe Bay. The dimensions of the pile-ups tended to be unexceptional by historical standards, with heights of 1 to 8 m, encroachment distances of 0 to 12 m, and block thicknesses of 20 to 40 cm. Several of the features extended alongshore for substantial distances, however, including a maximum length of 5.9 km on a spit that emanates from Point Brownlow.
8. **Multi-Year Ice:** With the exception of two small patches of second-year ice that drifted away from Point Barrow in October, multi-year ice remained absent from the nearshore region of the Alaskan Beaufort Sea throughout the five-month study period. The minimum separation between the ice and the coast, 170 nm (315 km), occurred off Barter Island at the end of February.

Chukchi Sea

- 1. *Timing of Freeze-Up:*** Ice began to form in Kasegaluk Lagoon, the Kuk River Inlet, and Peard Bay during the third week in October, but freeze-up proceeded slowly in the weeks that followed due to air temperatures that hovered near freezing. Complete coverage of these semi-enclosed basins and initial ice formation in the nearshore region occurred in early November. The pack ice, after advancing rapidly to the south during the first week in November, reached the vicinity of Point Barrow during the second week and began to coalesce with the nascent strip of coastal ice. On or about December 7th, a flash-freeze created an isolated patch of ice centered approximately 150 nm (278 km) west of Icy Cape. Freeze-up in the nearshore region took place three days later, on December 10th, in response to a cold spell that brought five days of air temperatures below -10°F (-23°C). Freeze-up in the entire Chukchi Sea north of Cape Lisburne followed on December 27th. During the past eight years, the average date for the occurrence of nearshore freeze-up has been November 23rd with a standard deviation of 12 days. The average date for the occurrence of basin-wide freeze-up has been December 9th with a standard deviation of ten days.
- 2. *Duration of Freeze-Up:*** The duration of freeze-up was 73 days, consisting of 56 days from first ice to nearshore freeze-up and an additional 17 days from nearshore freeze-up to complete freeze-up in the basin. During the past eight years, the duration has averaged 62 days with a standard deviation of nine days.
- 3. *Wind Regime:*** Easterly winds predominated in October, November, and December, with frequencies ranging from 58% to 77%. This pattern changed in January and February, when westerlies prevailed by narrow margins. Over the entire five-month period, easterlies outpaced westerlies by a margin of 61% to 39%. The highest average monthly speed, 12 kt (6 m/s), occurred in October and January.
- 4. *Storm Events:*** Fourteen storm events took place from October through February, consisting of eight easterlies and six westerlies. The easterlies produced 18 storm-days, for an average duration of 2.3 days/event. The westerlies produced 19 storm-days, averaging 3.2 days/event.
- 5. *Landfast Ice:*** The landfast ice zone reflected the influence of the wind regime, with stunted growth in November and December followed by substantial growth in January and early February. Landfast ice first appeared at the end of October, but remained narrow and discontinuous for the next two months in response to the predominance of easterly winds. The situation changed in January, when an increased frequency of westerly winds coupled with several westerly storms produced a continuous band of ice up to 10 nm (19 km) wide off Skull Cliff and 8 nm (15 km) wide between Icy Cape and Point Lay. During the second half of January, the ice grounded on Blossom Shoals, its

customary anchor point off Icy Cape. Additional expansion followed in early February, resulting in the maximum width observed during the study period, 20 nm (37 km) between Wainwright and the Nokotlek River mouth. Subsequently, at the end of February, a strong easterly storm dislodged the newly-accumulated ice and caused the landfast ice edge to retreat to the location it had occupied at the beginning of the month.

6. **Coastal Flaw Lead:** From December 2016 through February 2017, the distinctive flaw lead that forms off the Chukchi Sea coast in response to easterly winds opened on nine different occasions. The frequency of occurrence, which averaged 51% over the three-month period, increased from 42% in December to 52% in January and 61% in February. The maximum width, 50 nm (93 km), and maximum length, 250 nm (463 km), both occurred during a single event that began in late January and continued into early February. The lead persisted for periods that ranged from one to 15 days.
7. **Offshore Ice Cover:** When a reconnaissance flight was performed at the end of February, the ice on the west side of the flaw lead was found to be relatively uniform, consisting of first-year floes typically ranging from less than 500 m to 1 km in diameter. Deformation was modest relative to that noted in prior years, with ridge and rubble heights typically varying from 1 to 2 m and occasionally reaching 3 m.
8. **Ice Pile-Ups:** Sixty-three ice pile-ups occurred on the shoreline between Barrow and Point Lay during the 2016-17 freeze-up season. Fifty-two were located to the south of Point Belcher, while 11 were located to the north. Their dimensions were relatively small compared to those observed in past years, with heights of 1 to 5 m, encroachment distances of 0 to 10 m, and alongshore lengths of 50 m to 4 km. The block thicknesses were estimated to vary from 30 to 40 cm.
9. **Multi-Year Ice:** With the exception of the two small patches of second-year ice that drifted away from Point Barrow in October (discussed above for the Beaufort Sea), multi-year ice remained completely absent from the Chukchi Sea study area during the five-month study period.

Trends

1. **Air Temperatures:** Since the 1970s, progressively warmer winter seasons have caused the number of accumulated freezing-degree days at Barrow to decline at an average rate of 49 per year. The rate of warming has accelerated, with the greatest increase in temperature occurring during the early portion of freeze-up.
2. **Winds:** Since the early 1980s, the frequency of storm events during freeze-up has increased by about 50%. The frequency of mid-winter storms (January through April) also has increased, but only by about 13%.

3. **Timing of Freeze-Up:** Freeze-up in the nearshore region currently tends to occur during the fourth week in October in the Alaskan Beaufort Sea, and the fourth week in November in the northeastern Chukchi Sea. The former is about three weeks later than in the 1980s, while the latter is more than one month later than in the 1970s. The rate of change has accelerated in recent years, with the date of freeze-up currently trending later by 2.3 days/yr in the Beaufort and 4.3 days/year in the Chukchi. These high rates of change imply that the length of the open-water season will increase substantially in the years ahead.
4. **Duration of Freeze-Up:** The duration of freeze-up in the Alaskan Beaufort Sea, from first ice to complete cover, currently averages 36 days with a standard deviation of 11 days. In the Chukchi, the duration is substantially longer, averaging 62 days with a standard deviation of ten days. The duration in the Beaufort is increasing at a rate of 1.3 days/yr, while that in the Chukchi is increasing at 2.3 days/yr.
5. **First-Year Ice Growth:** Based on air temperature alone, the thickness of undeformed first-year ice attained during an average winter has decreased by 21 cm (12.3%) since the early 1980s. However, a significant increase in snowfall may be causing an even greater reduction in the ice thickness due to its insulating effect. Other temperature-related factors, including reduced ice production in leads, decreased consolidation of ridges and rubble fields, and reduced ice strength, serve to amplify the impact of reduced thickness on ice dynamics.
6. **Landfast Ice Development and Stability:** In the Alaskan Beaufort Sea, the extent of the landfast ice zone to the west of Prudhoe Bay is similar to that observed in the 1980s but the landfast ice develops more slowly. To the east of Prudhoe Bay, a stable, well-grounded shear zone is less likely to develop during freeze-up and early winter, and develops more slowly in those years when it does occur. In the Chukchi, the narrow, ephemeral nature of the landfast ice zone noted in the 1980s continues to prevail today.
7. **Coastal Flaw Lead:** Notwithstanding trends toward warmer air temperatures, increased storminess, and slower ice growth during freeze-up, the frequencies with which the flaw lead and extended flaw lead occur off the Chukchi Sea coast have remained unchanged since the 1990s.
8. **Multi-Year Ice in the Alaskan Beaufort Sea:** The probability of large multi-year ice floes invading the nearshore portion of the Alaskan Beaufort Sea is substantially less than in the 1980s. This change has resulted in part from a reduction in the amount of multi-year ice comprising the permanent polar pack and in part from an increase in the northerly retreat of the ice edge during the summer months, both of which have reduced the opportunities for pack floes to enter the nearshore area. In addition, warmer air temperatures, longer open-water seasons, and increased storminess have decreased the

likelihood that first-year ridges and rubble will survive the summer melt season to become second-year floes of any consequence. Nevertheless, as demonstrated in 2009-10, the possibility of multi-year ice invasions cannot be ruled out in the nearshore region of the Beaufort. The probability of an invasion currently is about 12% in any given freeze-up season, based on two such occurrences in the past 17 years.

9. ***Multi-Year Ice in the Chukchi Sea:*** The probability of multi-year ice entering the Chukchi Sea to the south and west of Point Barrow also has decreased since the 1980s, but to a lesser extent than in the Beaufort. Although the factors that have reduced the probability of invasions in the Beaufort apply to the Chukchi as well, their impact has been mitigated by the ability of the Multi-Year Gateway and Early-Season Entry to divert multi-year ice floes to the southwest. The probability of an invasion currently is about 65% in any given freeze-up season, based on 11 invasions in the past 17 years.

8. REFERENCES

- Arguez, A., I. Durre, S. Applequist, M. Squires, R. Vose, X. Yin, and R. Bilotta, 2010, "NOAA's U.S. Climate Normals (1981-2010)", NOAA National Climatic Data Center, 2015, <http://www.ncdc.noaa.gov/cdo-web/datatools/normals>.
- Barrett, S.A. and W.J. Stringer, 1978, "Growth Mechanisms of Katie's Floeberg", *Arctic and Alpine Research*, Vol. 10, No. 4, pp.775-783.
- Barry, R.G., R.E. Moritz, and J.C. Rogers, 1979, "The Fast Ice Regimes of the Beaufort and Chukchi Sea Coasts", *Cold Regions Science and Technology*, Vol. 1, pp. 129-152.
- Bilello, M., 1960, "Formation, Growth, and Decay of Sea Ice in the Canadian Arctic Archipelago", SIPRE Research Report 65, Hanover, New Hampshire.
- Brown, R. and P. Cote, 1992, "Interannual Variability of Landfast Ice Thickness in the Canadian High Arctic 1950-89", *Arctic*, Vol. 45, No. 3, pp. 273-284.
- Canadian Ice Service, 2016 and 2017, <http://www.ec.gc.ca/glaces-ice>.
- Coastal Frontiers Corporation and Vaudrey and Associates, Inc., 2010, "2009-10 Freeze-Up Study of the Alaskan Beaufort and Chukchi Seas", Joint Industry Project performed for Shell International Exploration and Production, Inc., and the U.S. Minerals Management Service, Chatsworth, California, 100 pp. + appen.
- Coastal Frontiers Corporation and Vaudrey and Associates, Inc., 2011, "2010-11 Freeze-Up Study of the Alaskan Beaufort and Chukchi Seas", Joint Industry Project performed for Shell Offshore, Inc., and Bureau of Ocean Energy Management, Regulation, and Enforcement, U.S. Dept. of the Interior, Chatsworth, California, 149 pp. + appen.
- Coastal Frontiers Corporation and Vaudrey and Associates, Inc., 2012a, "2011-12 Freeze-Up Study of the Alaskan Beaufort and Chukchi Seas", Joint Industry Project performed for Shell International Exploration and Production, Inc., and Bureau of Safety and Environmental Enforcement, U.S. Dept. of the Interior, Chatsworth, California, 182 pp. + appen.
- Coastal Frontiers Corporation and Vaudrey and Associates, Inc., 2012b, "Ice Encroachment in the Alaskan Beaufort and Chukchi Seas", Joint Industry Project performed for Shell Exploration and Production Company, and Bureau of Safety and Environmental Enforcement, U.S. Dept. of the Interior, Chatsworth, California, 78 pp. + appen.

- Coastal Frontiers Corporation and Vaudrey and Associates, Inc., 2013 (revised January 2014), “2012-13 Freeze-Up Study of the Alaskan Beaufort and Chukchi Seas”, Joint Industry Project performed for Shell Gulf of Mexico Inc. and Shell Offshore Inc., Statoil Petroleum AS, and Bureau of Safety and Environmental Enforcement, U.S. Dept. of the Interior, Moorpark, California, 175 pp. + appen.
- Coastal Frontiers Corporation and Vaudrey and Associates, Inc., 2014, “2013-14 Freeze-Up Study of the Alaskan Beaufort and Chukchi Seas”, Joint Industry Project performed for Shell Gulf of Mexico Inc. and Shell Offshore Inc., and Bureau of Safety and Environmental Enforcement, U.S. Dept. of the Interior, Moorpark, California, 185 pp. + appen.
- Coastal Frontiers Corporation and Vaudrey and Associates, Inc., 2015, “2014-15 Freeze-Up Study of the Alaskan Beaufort and Chukchi Seas”, Joint Industry Project performed for Shell Offshore Inc. and Bureau of Safety and Environmental Enforcement, U.S. Dept. of the Interior, Moorpark, California, 200 pp. + appen.
- Coastal Frontiers Corporation and Vaudrey and Associates, Inc., 2016, “2015-16 Freeze-Up Study of the Alaskan Beaufort and Chukchi Seas”, Joint Industry Project performed for Shell Offshore Inc. and Bureau of Safety and Environmental Enforcement, U.S. Dept. of the Interior, Moorpark, California, 203 pp. + appen.
- Dickins, D. and K. Vaudrey, 1994, “Phase III Ice Conditions, ANS Gas Commercialization Study: Marine Export Facilities”, prepared for Arco Alaska Inc., BP Exploration (Alaska) Inc., and Exxon Company, USA, prepared by DF Dickins Associates Ltd., Salt Spring Island, British Columbia, and Vaudrey & Associates Inc., San Luis Obispo, California.
- Eicken, H., L. Shapiro, A. Gaylord, A. Mahoney, and P. Cotter, 2006, “Mapping and Characteristics of Recurring Spring Leads and Landfast Ice in the Beaufort and Chukchi Seas”, OCS Study MMS 2005-068, U.S. Department of the Interior, Mineral Management Service, Alaska Outer Continental Shelf Region, Anchorage, Alaska.
- Hirano, D., Y. Fukamaci, E. Watanabe, K. Ohshima, K. Iwamoto, A.R. Mahoney, H. Eicken, D. Simizu, and T. Tamura, 2016, “A Wind-Driven, Hybrid Latent and Sensible Heat Coastal Polynya off Barrow, Alaska”, *Journal of Geophysical Research: Oceans*, 121, doi:10.1002/2015JC011318, 18 pp.
- Iowa Environmental Mesonet, Iowa State University, 2017, <https://www.mesonet.agron.iastate.edu>.
- Kovacs, A., A. Gow, and W. Dehn, 1976, “Islands of Grounded Sea Ice”, CRREL Report 76-4, Hanover, New Hampshire.

Lindsay, R.W. and J. Zhang, 2005, “The Thinning of Arctic Sea Ice, 1988-2003: Have We Passed a Tipping Point?”, *Journal of Climate*, Vol. 18, November 15, 2005, pp. 4879-4894.

MacDonald, Dettwiler and Associates Ltd., 2015-2017, <http://gs.mdacorporation.com>.

Mahoney, A., H. Eicken, A. Gaylord, and L. Shapiro, 2007, “Alaska Landfast Sea Ice: Links with Bathymetry and Atmospheric Circulation”, *Journal of Geophysical Research*, Vol. 112, C02001.

Mahoney, A., H. Eicken, L. Shapiro, R. Gens, T. Heinrichs, F. Meyer, and A. Graves, 2012, “Mapping and Characterization of Recurring Spring Leads and Landfast Ice in the Beaufort and Chukchi Seas”, Final Report, OCS Study BOEM 2012-067, University of Alaska Fairbanks, Fairbanks, Alaska, 154 pp.

Melling, H. and D. Riedel, 2005, “Trends in the Draft and Extent of Seasonal Pack Ice, Canadian Beaufort Sea”, *Geophysical Research Letters*, Vol. 32, L24501.

NASA, 2016 and 2017a, <https://earthdata.nasa.gov/earth-observation-data/near-real-time/rapid-response/modis-subsets>.

NASA, 2017b, “Arctic Sea Ice Minimum”, <http://climate.nasa.gov/vital-signs/arctic-sea-ice>.

National Ice Center, 2016 and 2017, <http://www.natice.noaa.gov/products>.

National Ocean Service, 2017, <http://tidesandcurrents.noaa.gov>.

National Snow and Ice Data Center, 2016, “2016 ties with 2007 for second lowest Arctic sea ice minimum”, Arctic Sea Ice News and Analysis, September 15, 2016, <http://nsidc.org/arcticseaicenews/2016/09/2016-ties-with-2007-for-second-lowest-arctic-sea-ice-minimum>.

National Weather Service, Alaska Region Headquarters, 2016 and 2017, <http://aawu.arh.noaa.gov/poes.php>.

NOAA, 2017, “The Global Drifter Program”, Atlantic Oceanographic & Meteorological Laboratory, <http://www.aoml.noaa.gov/phod/dac/index.php>.

Perovich, D., S. Gerland, S. Hendricks, W. Meier, M. Nicolaus, J. Richter-Menge, and M. Tschudi, 2013, “Arctic Report Card, Update for 2013”, Sea Ice, NOAA, http://www.arctic.noaa.gov/reportcard/sea_ice.html.

Polar Science Center, 2017a, “UpTempO: Measuring the Upper layer Temperature of the Polar Oceans”, Applied Physics Laboratory, University of Washington, <http://psc.apl.washington.edu/UpTempO/UpTempO.php>.

- Polar Science Center, 2017b, “International Arctic Buoy Programme”, Applied Physics Laboratory, University of Washington, <http://iabp.apl.washington.edu>.
- Reece, A.M., 2009, personal communication, Shell International Exploration and Production, Inc., Houston, Texas.
- Rigor, I. G., 2017 (compiled by Polar Science Center), *IABP Drifting Buoy Pressure, Temperature, Position, and Interpolated Ice Velocity, Version 1*. Boulder, Colorado, doi: <http://dx.doi.org/10.7265/N53X84K7>.
- Rodrigues, J., 2009, “The Increase in the Length of the Ice-Free Season in the Arctic”, *Cold Regions Science and Technology*, Vol. 59, pp. 78-101.
- Stringer, W. and S. Barrett, 1975, “Ice Motion in the Vicinity of a Grounded Floeberg”, *Proceedings POAC-75*, Fairbanks, Alaska.
- Toimil, L. and A. Grantz, 1976, “Origin of a Bergfield in the Northeastern Chukchi Sea and its Influence on the Sedimentary Environment”, *AIDJEX Bulletin 34*, December, 1976.
- Vaudrey, K.D., 1981a, “1980 Freezeup Study of the Barrier Island Chain and Harrison Bay”, AOGA Project No. 129, Vaudrey & Associates, Inc., Missouri City, Texas, 32 pp. + appen.
- Vaudrey, K. D., 1981b, “Beaufort Sea Multiyear Ice Features Survey, Volume I: Field Study”, AOGA Project No. 139, Vaudrey & Associates, Inc., Missouri City, Texas, 36 pp. + appen.
- Vaudrey, K.D., 1982a, “1981 Freezeup Study of the Barrier Island Chain and Harrison Bay”, AOGA Project No. 160, Vaudrey & Associates, Inc., Missouri City, Texas, 30 pp. + appen.
- Vaudrey, K.D., 1982b, “Ice Cracking in Stefansson Sound during the Winter of 1981-82”, Memorandum prepared for ARCO Alaska and Shell Oil Company, San Luis Obispo, California.
- Vaudrey, K.D., 1983, “1982 Freezeup Study of the Barrier Island Chain and Harrison Bay Region”, AOGA Project No. 200, Vaudrey & Associates, Inc., San Luis Obispo, California, 32 pp. + appen.
- Vaudrey, K.D., 1984, “1983 Freezeup Study of the Beaufort and Upper Chukchi Seas”, AOGA Project No. 246, Vaudrey & Associates, Inc., San Luis Obispo, California, 48 pp. + appen.

- Vaudrey, K.D., 1985a, “1984 Freezeup Study of the Beaufort and Upper Chukchi Seas”, AOGA Project No. 282, Vaudrey & Associates, Inc., San Luis Obispo, California, 44 pp. + appen.
- Vaudrey, K.D., 1985b, “Historical Summary of the 1980-82 Freezeup Seasons and 1981-83 Breakup Seasons (Volume 1 of 2)”, AOGA Project No. 275, Vaudrey & Associates, Inc., San Luis Obispo, California, 79 pp.
- Vaudrey, K.D., 1986, “1985 Freezeup Study of the Beaufort and Upper Chukchi Seas”, AOGA Project No. 327, Vaudrey & Associates, Inc., San Luis Obispo, California, 49 pp + appen.
- Vaudrey, K.D., 1987a, “1986-87 Chukchi Sea Ice Conditions”, AOGA Project No. 346, Vaudrey & Associates, Inc., San Luis Obispo, California, 68 pp + appen.
- Vaudrey, K., 1988a, “1987 Summer and Freeze-Up Ice Conditions in the Beaufort and Chukchi Seas Developed from Satellite Imagery”, AOGA Project No. 360, Vaudrey & Associates, Inc., San Luis Obispo, California.
- Vaudrey, K., 1989a, “1988 Summer and Freeze-Up Ice Conditions in the Beaufort and Chukchi Seas Developed from Satellite Imagery”, AOGA Project No. 370, Vaudrey & Associates, Inc., San Luis Obispo, California.
- Vaudrey, K., 1990, “1989 Summer and Freeze-Up Ice Conditions in the Beaufort and Chukchi Seas Developed from Satellite Imagery”, AOGA Project No. 372, Vaudrey & Associates, Inc., San Luis Obispo, California.
- Vaudrey, K., 1991, “1990 Summer and Freeze-Up Ice Conditions in the Beaufort and Chukchi Seas Developed from Satellite Imagery”, AOGA Project No. 381, Vaudrey & Associates, Inc., San Luis Obispo, California.
- Vaudrey, K., 1992, “1991 Summer and Freeze-Up Ice Conditions in the Beaufort and Chukchi Seas Developed from Satellite Imagery”, AOGA Project No. 386, Vaudrey & Associates, Inc., San Luis Obispo, California.
- Vaudrey, K., 2007, “Effects of Recent Climate Change on Sea Ice Conditions in the Alaskan Beaufort and Chukchi Seas”, prepared for Shell International Exploration and Production, Inc., prepared by Vaudrey & Associates, Inc., San Luis Obispo, California.
- Vaudrey, K. and B. Thomas, 1981, “Katie’s Floeberg – 1980”, report prepared for the Kopanoar Partners by Gulf Research and Development Company, Houston, Texas.

Walsh, J. and H. Eicken, 2007, "Sea Ice Changes Affecting Alaska: Offshore Transportation, Coastal Communities, Marine Ecosystems", presented at Symposium on the Impact of an Ice-Diminishing Arctic on Naval and Maritime Operations, sponsored by National Ice Center and U.S. Arctic Research Commission, 10-12 July 2007, Washington, D.C.

Ward, E.G., C. Leidersdorf, J. Coogan, and K. Vaudrey, 2015, "Multi-Year Ice Incursions into the Chukchi Sea", OTC 25476, *Proc. 2015 Arctic Technology Conference*, Copenhagen, Denmark, 13 pp.

Weather Underground, 2016 and 2017, <http://www.wunderground.com>.